# Contributions to Optimal Detection in OTDM and OCDMA Optical Receivers

*PhD Dissertation*

By

**Arash Yazdani**

PhD Program on Network Engineering

Network Engineering Department

Universitat Politècnica de Catalunya

Advisors:
Prof. Sebastià Sallent Ribes
Assoc. Prof. David Rincón Rivera

Castelldefels, Barcelona, Spain, June 2016

**Abstract**

Recent developments in optical communication systems have increased the performance of optical networks. Low attenuation fiber optics, high spectral purity lasers and optical amplifiers, among others, are systems that have allowed to transport terabits per second across thousands of kilometers, in a more reliable, secure and efficient manner, when compared to radiofrequency (RF) systems. New optical access network technologies such as EPON and GPON are also providing Gbits connectivity to customers in both the enterprise and consumer markets. This transport capacity provides enough data for the growing demand of new communication services.

The main goal of the researchers in optical networks is to provide higher-speed data transmission by exploiting the intrinsically fast behavior of the optical domain. Optical signal processing is a key technology for constructing flexible and ultra high-speed photonic networks. In this context, it will be possible to build ultra-high speed, simple and reliable optical networks, at low operational expenses, regardless of the format of the information [1].

Before these technologies enter into commercial operation, some obstacles should be removed, such as the problem of obtaining extremely precise synchronization the network without any optical-electrical conversion. Also synchronization-related problem appear at the receiver for some systems such as OTDM and OCDMA, where even the fastest photo-detectors are not able to separate the data of the desired user from the signals of the adjacent users. This means that detection of ultrashort pulses in the presence of the multiple access interference (MAI) is an important in these systems. Therefore, it is vital to apply an all-optical signal processing on the received optical signal before the photo-detection [2]. In most of the ultra-high-speed light-wave communication systems, it is an effective technique to use an optical time gating at the receiver side in order to extract the desired user's signal from the received signal. This approach requires an optical clock recovery procedure. But by increasing the data rate in optical networks the accuracy of the optical clock recovery decreases [3] because of increasing jitter and MAI and consequently the system performance is degraded. Currently the only approach is to use a clock signal that has the same pulse-width as the data, and when the jitter is large, this technique fails to properly capture the main part of the data signal and collects more interference instead. So these techniques have to lower the data-rate to avoid large BER. Our proposed technique can achieve larger signal to noise ratio versus the fixed pulse-width clock.

The main goal of this work is to discuss the characteristics of the current transmission technologies, including OTDM and OCDMA, providing a detailed analytical model and proposing a solution for improving the performance of optical receivers. We use a nonlinear media (Four Wave Mixing) as a combiner in the receivers. We have modeled analytically the relationship between the input and the output of the nonlinear media systems in these techniques using nonlinear Schrödinger equations. Then, we solved these equations by Volterra series. Our aim is to develop analytical models of the response of the optical receiver, and validate them with simulations. Also we consider the effect of variation of the bandwidth of the clock in the performance of receivers with presence of jitter. We obtain the optimum value of the clock's bandwidth and compare theory and simulation results together. Using our proposed technique, the data-rate of the optical systems can be increased and we can achieve lower BER for the same jitter. The goal of these efforts is the improvement of the overall performance of the network, in terms of transmission speed, bit error rate (BER), reliability and cost. The results could be applied to next-generation optical networks, in both the backbone and access scenarios.

# Contents

# List of Figures

# List of Tables

# Acronyms

**2D** . . . . . Two Dimensional
**APD** . . . . . Avalanche Photo Diode
**ASE** . . . . . Amplified Spontaneous Emission
**BER** . . . . . Bit Error Rate
**B-PONs** . . . . . Broadband Passive Optical Networks
**CDMA** . . . . . Code Division Multiple Access
**DFWM** . . . . . Degenerate Four Wave Mixing
**DSSS** . . . . . Direct Sequence Spread Spectrum
**EDFA** . . . . . Erbium Doped Fiber Amplifier
**EOM** . . . . . Electro Optical Modulator
**EPON** . . . . . Ethernet Passive Optical Network
**FPF** . . . . . Fabry Perot Filter
**FWHM** . . . . . Full width at Half Maximum
**FWM** . . . . . Four Wave Mixing
**G-PONs** . . . . . Gigabit Capable Passive Optical Networks
**Gbps** . . . . . Gigabits per second
**GE-PONs** . . . . Gigabit Ethernet Passive Optical Networks
**GF** . . . . . Galois Field
**GVM** . . . . . Group Velocity Mismatch
**JJEC** . . . . . Joint Jitter Estimator and Canceller
**LAN** . . . . . Local Area Network
**LPF** . . . . . Low Pass Filter
**MAI** . . . . . Multiple Access Interference
**MML** . . . . . TMode Lock Laser
**MUI** . . . . . Multi User Interference
**MZ** . . . . . Mach Zehnder
**NGA-PONs** . . Next Generation Access Passive Optical Networks
**NLS** . . . . . Nonlinear Schrodinger
**NOLM** . . . . . Nonlinear Optical Loop Mirrors
**OCDMA** . . . . Optical Code Division Multiple Access
**OFDM** . . . . . Orthogonal Frequency Division Multiplexing
**OOC** . . . . . Optical Orthogonal Codes
**O-OFDM** . . . . Optical Orthogonal Frequency Division Multiplexing
**OOK** . . . . . On Off Keying
**OTDM** . . . . . Optical Time Division Multiplexing
**PN** . . . . . Pseudo Noise
**PON** . . . . . Passive Optical Network
**PPLN** . . . . . Periodically Poled Lithium Niobate
**QOS** . . . . . Quality of Service
**RF** . . . . . Radio Frequency

**SAC** . . . . . Spectral Amplitude Coding
**SDH** . . . . . Synchronous Digital Hierarchy
**SHG** . . . . . Second Harmonic Generator
**SIR** . . . . . Signal to Interference Ratio
**SNR** . . . . . Signal Noise Ratio
**SOA** . . . . . Semiconductor Optical Amplifier
**SONET** . . . . . Synchronous Optical Networking
**SPC** . . . . . Spectral Phase Coding
**SPE** . . . . . Spectral Phase Encoding
**SPM** . . . . . Self Phase Modulation
**TDM** . . . . . Time Division Multiplexing
**Th** . . . . . Threshold
**TOAD** . . . . . Terahertz Optical Asymmetric Demultiplexer
**TPA** . . . . . Two Photon Absorption
**TPC** . . . . . Temporal Phase Code
**WDM** . . . . . Wavelength Division Multiplexing
**XPM** . . . . . Cross Phase Modulation

Chapter 1

# Introduction

This chapter has the following organization. The motivation of this Ph.D is presented in section 1.1. Section 1.2 enumerates the main results and contributions of the research work presented in this document. Finally, section 1.3 describes the structure of the document.

## 1.1 Motivation

In recent decades, when optical networks were identified as the main highways of telecommunications for transporting high volumes of information, the requirement for all-optical multi-access networking became important. An all-optical multi-access network is an access optical network which interconnects end-users with core networks sharing common optical resources. This network can be seen as a collection of multiple nodes interconnected via single- or multi-mode fiber optics, executing all their essential signal processing requirements such as multiplexing/demultiplexing, add-drop, switching and amplification in the optical domain. Optical CDMA, TDM and OFDM medium access mechanism are one possible way that permit multiple users to access the same optical channel optimizing the use of the physical resources, improving the quality of service (QOS) requirements (low access delay, bandwidth, losses,...) and maximizing the efficiency.

The main goal of the researchers in optical networks is to provide reliable higher-speed data transmission by exploiting the intrinsic fast behavior of the optical domain. Optical signal processing is a key technology for constructing flexible and ultra high-speed photonic networks. In optical networks, which use ultra-short light pulses for data transmission, even the fastest photo-detectors are not able to separate the data of the desired user from the signals of the adjacent users. Therefore, it is vital to apply an all-optical signal processing on the received optical signal before the photo-detection. In these systems, it is an effective technique to use optical time gating at the receiver side in order to extract the desired user's signal from

the received signal. This approach requires an optical clock recovery procedure. But by increasing the data rate in optical networks the accuracy of the optical clock recovery decreases and consequently the system performance is degraded. This model could be applied to the multiple access technologies (OTDM, OCDMA or O-OFDM).

The main goal of our research is to optimize the key parameters of optical access networks (specifically, of the optical receivers) and to apply some signal processing techniques, in order to increase the overall performance of the optical links (in terms of data transmission rate and other operational parameters). Specifically, we will obtain approximate (but accurate enough for our goals) relationship between the input and output of nonlinear systems that are used in OTDM and OCDMA receivers networks. For this purpose, a system model is proposed to describe nonlinearity for nonlinear media in receivers. We will use Schrödinger nonlinear (NLS) coupled equations and will analytically solve these equations, while maintaining the BER in order to optimize these systems by decreasing the BER for a certain data rate and/or increasing the data rate.

## 1.2 Main Research Contributions

The major contributions of this PhD dissertation are as follows:

- Definition of a model for optical receivers of OTDM and OCDMA systems and optimize the systems in order to decrease BER.
- Development of analytical tools for solving nonlinear Schrodinger equations with application to nonlinear optical systems using Volterra series. These tools are later used in modeling and analysis of receivers in high-speed OTDM and OCDMA systems.
- Finding the significant Volterra kernels and truncating the Volterra series representation of the nonlinear system solution. This simplifies the analysis of the optical communication systems in the presence of nonlinearity and makes it possible to present a closed-form solution.
- Introducing a new technique to minimize the effect of non-ideal synchronization in the detection of signals in ultra-fast OTDM networks.
- Obtaining an analysis and simulation of the effect of the clock signal's pulse width on the bit error rate (BER) at the OTDM receiver in presence of jitter.
- Calculation of the optimum value of the clock signal's pulse width that minimizes the BER in OTDM and OCDMA receivers.

- Development of an analytical model for describing nonlinear receivers that are used for in multi-user OCDMA networks. In this model optical orthogonal codes (OOC) are assumed to be used by users and the correlation is employed at the receiver to separate the desired signal.

- Evaluation of the influence of the pulse-width of codes in OCDMA networks for decreasing BER and increasing speed of transfer of data in optical communication.

## 1.3 Thesis Outline

The thesis is organized in six chapters and five appendixes. Background materials and the context for the contributions is provided in the first three chapters. Our results and the novel contributions of the author are presented in Chapter 4 and Chapter 5. The detail of mathematical analysis results in general are given in the appendixes. The organization of this document is shown next.

After introducing our goal in Chapter 1, Chapter 2 provides an overview on different multiple access techniques on optical networks such as OTDM, WDM and OCDM. Also in this chapter we consider to the auto and cross correlation of coding methods and several coding schemes in OCDMA techniques and compare them together.

Chapter 3 focused on the application of nonlinear techniques in optical communication. We review the application of the FWM (Four Wave Mixing) as a nonlinear media in optical receivers. Also we model FWM by helping nonlinear Schrödinger equations and using the Volttera series for solving these nonlinear equations. In the end of this chapter we review the application of FWM as optical AND gate, wavelength convertor and phase conjugation.

Chapter 4 studied the case of OTDM networks. In this chapter we focus on clock recovery techniques at the receivers. The model is developed by applying FWM as optical time gate. We show that the pulse width of the clock signal can be optimized to achieve a minimum bit error rate. The effect of jitter is also considered as a noise in the system, finding the optimal values of the clock pulse width to minimize the BER. Simulation results are also presented to evaluate the accuracy of the analytical expressions.

Chapter 5 presents an analytical model of receivers in optical CDMA networks. We study the performance of all-optical AND gates based on the FWM process, for application in the receivers of the time spreading multiplexing techniques because of its simplicity and low cost. The performance of AND gating receiver in time spreading OCDMA systems is analysed by modeling Schrödinger equations and using Volterra series for solving these equations. Finally, a comparison between simulation and analytical models is performed.

Chapter 6 summarizes the main concluding remarks from this PhD and points out future work directions.

Appendixes A, B, C and E present the analytical model for calculations of relationship between the optical detector current and Fourier transfer of optical field, Volterra series terms, characteristic Fourier transform of stationary random processing and mean and variance of current in the output of optical detector, respectively. Appendix D shows the complete solution of the NLS equations for optical AND gate using Volterra series.

Chapter 2

# Division Multiplexing Techniques in Optical Networks

Multiple access techniques are needed to fulfill the demand for high-speed and large capacity communications in optical networks, which permit multiple users to share the huge fibre bandwidth in base band. There are two major classic methods of multiple access: each user is assigned a specific time slot in time-division multiple-access (TDMA), or a specific frequency (wavelength) slot in wavelength division multiple-access (WDMA). Both techniques have been extensively studied and utilized in optical communication systems.

Alternatively, optical code-division multiple-access (OCDMA) has been considered because of its potential for improved information security, simplified and decentralized network control, enhanced spectral efficiency, and increased flexibility in the granularity of bandwidth that can be provisioned. In OCDMA, signals of different users may be overlapped both in time and frequency sharing a common communications medium, and multiple-access is achieved by allocation of minimally interfering code sequences to different transmitters, which must subsequently be detected in the presence of multiple access interference (MAI) from other users.

Another method to increase capacity is optical orthogonal frequency division multiplexing (O-OFDM), where data is transmitted over multiple subcariers. Recently, OFDM has received interest as a means of spectral shaping, reducing the guard band requirement between neighboring channels and therefore, it increases bandwidth utilization and spectral efficiency.

This chapter has the goal of presenting the OTDM, WDM, OCDMA and OFDM techniques, considering their specific characteristics, peculiarities, technical challenges and state of the art. Therefore, first we introduce to TDM and OTDM techniques and then we revise the classical CDMA mechanism, pointing out the fundamentals of spread spectrum and the orthogonal codes that cause the spectrum to be spread. Next

we explain how CDMA can be implemented in optical communication. Finally, we consider several types of OCDMA systems and compare them and study the optical signal processing and OCDMA codes and methods for decrease of interference in OCDMA.

## 2.1 Optical Time Division Multiplexing

Time division multiplexing (TDM) is a technique where several optical signals are combined, transmitted together, and separated again based on different arrival times. Fig. 2.1-a shows an example of the TDM technique applied to four signals. In this technique, each signal transmits one bit at a time. So, in the situation shown in Fig. 2.1-a, the output signal has a throughput four times greater than that of each input signal. The input signals should be synchronized with the output signal as for the characteristic of time division. The receivers should also be synchronized in order to recover the information sent to each one of them.

In recent decades, most optical communication services used TDM, but the multiplexing was realized electrically and the transmission devices processed a single bit stream. SDH and SONET were examples for electronic TDM transmitted over a single optical carrier. Researches have allowed to transmit data at a rate up to 160 Gbps with optical processing. Due to the high bit rate, some of these works had focused on routing and synchronization technologies for faster signals [2]. Getting to rates of 160 Gbps per channel was possible to reach either greater throughput, or fewer transmitters and fibers could be used, as shown in Fig. 2.1-b.

Due to the disponibility of erbium doped fiber amplifiers (EDFA), OTDM systems usually use the third optical window (1.55 $\mu$m). These devices permit long distance links to be viable using shifted dispersion fibers, thus minimizing the chromatic dispersion problem [5]. Execution methods for OTDM systems have been proposed using fibers with special manufacturing characteristics [6], combination of time-delayed pulses

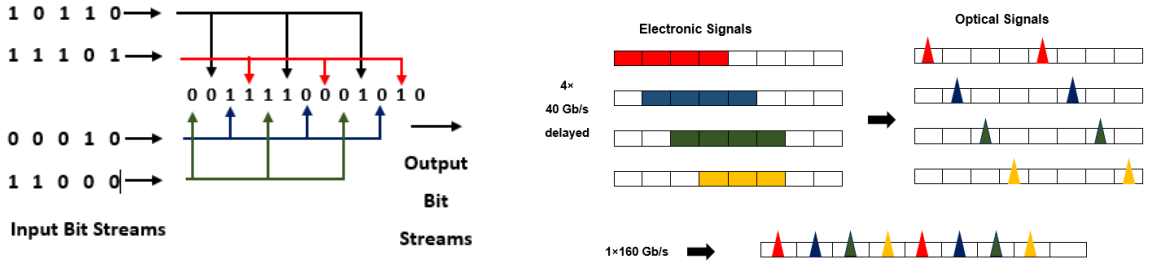


(a) (b)

Figure 2.1: (a) Time Division Multiplexing (TDM) (b) Transmission bit rate optimization using OTDM.

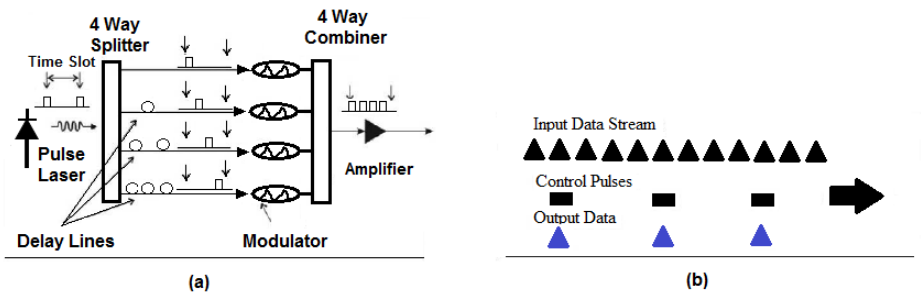


Figure 2.2: (a) OTDM configuration using splitters and delay lines to multiplex 4 independent streams (b) Extraction of one channel in an OTDM stream using control pulses.

by fibers with different lengths [7] or solitons [8].

Fig. 2.2-a illustrates another procedure for OTDM, proposed in [7]. In this method, each time slot is divided in four time intervals with RZ (return to zero)-coded bits. This way, at the beginning of each time slot, the laser generates a pulse during 1/8 of a period of that slot. The signal produced in the laser passes through a 1:4 power splitter. Three of the signals are delayed by fibers with different physical lengths. Afterward, the pulses are modulated separately with the respective information and are then recombined and amplified for transmission. In this way, only one transmitter is used.

In order to avoid electronic limitations, the demultiplexing process should be realized optically. The optical extraction of data can be built using Nonlinear Optical Loop Mirrors (NOLM). By means of control pulses, this device works as an AND logical gate that selects every $n^{th}$ pulse, as is shown in Fig. 2.2-b. An Add/Drop type of multiplexer is able to receive or substitute a particular channel, intercalated in time, without interfering with the other signals. The challenges in the OTDM demultiplexing process are 1) the synchronization between the receiver and the input signal, 2) a trade-off between using bandwidth versus signal to noise ratio (SNR) and this technique need the ultrafast optical switching, the ultrafast signal processing and the optical buffering [9].

## 2.2 Wavelength Division Multiplexing

Wavelength division multiplexing (WDM) is another multiplexing technique for obtaining high capacity in long-haul transmission systems. In this technology, a number of optical carrier signals are multiplexed onto a single optical fiber by using different wavelengths of laser light in fiber-optic communications. This technique enables bidirectional communications over one strand of fiber, as well as addition of capacity. WDM has the

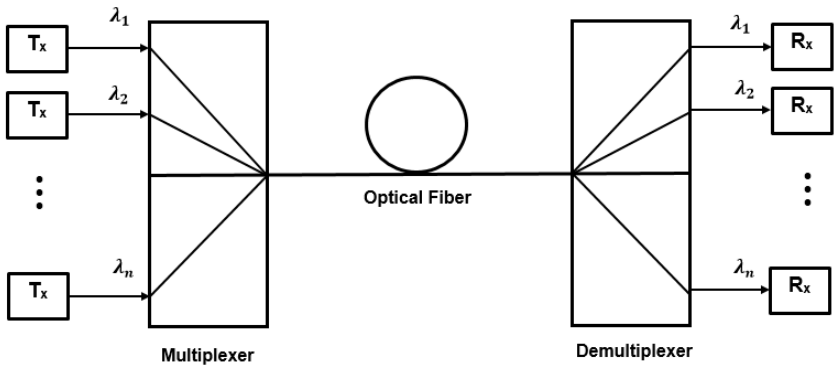


Figure 2.3: Multichannel point-to-point fiber link. Separate transmitter-receiver pairs are used to send and receive the signal at different wavelengths.

potential for utilizing the large bandwidth offered by optical fibers.

For long-haul fiber links forming the backbone or the core of a telecommunication network, the role of WDM is to increase the total bit rate. Fig. 2.3 illustrates schematically such a point-to-point, high-capacity, WDM link. The output of several transmitters with their own special carrier frequency (or wavelength) is multiplexed together. The multiplexed signal is passed into the optical fiber to the other end, where a demultiplexer sends each channel to its own receiver. With this method, the system capacity is enhanced in proportion to number of multiplexed signals. For instance, Coarse WDM (CWDM) provides up to 16 channels across multiple transmission windows of silica fibers. Dense WDM (DWDM) uses the C-Band transmission window but with denser channel spacing. Channel plans vary, but a typical DWDM system would use 40 channels at 100 GHz spacing or 80 channels with 50 GHz spacing.

In the DWDM technique, one of the motivations for the flexible grid is to allow a mixed bit rate or mixed modulation format transmission system to allocate frequency slots with different widths so that they can be

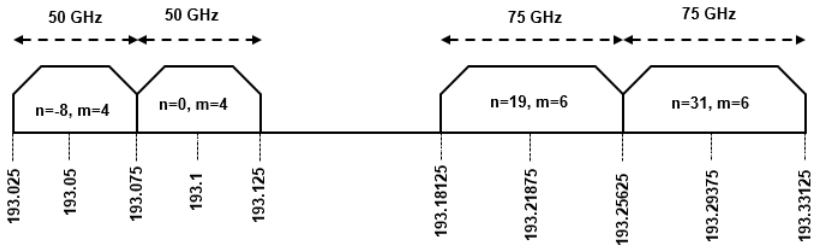


Figure 2.4: An example of the use of the flexible grid. For the flexible DWDM grid, the allowed frequency slots have a nominal central frequency (in THz) defined by: $193.1 + n \times 0.00625$ where n is a positive or negative integer including 0 and 0.00625 is the nominal central frequency granularity in THz. A slot width defined by: $12.5 \times m$ where m is a positive integer and 12.5 is the slot width granularity in GHz.

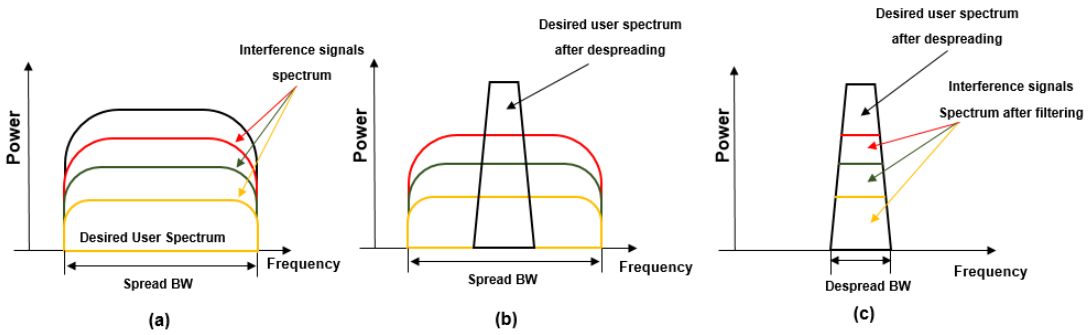


Figure 2.5: CDMA technique. (a) Signals from four users, spread by the use of the spreading code, in the same frequency band; (b) Desired signal is despread; (c) Signals after filtering.

optimized for the bandwidth requirements of particular bit rate and modulation scheme of the individual channels. An example use of the flexible DWDM grid is shown in Fig. 2.4, where two 50 GHz slots are shown together with two 75 GHz slots [10].

## 2.3 Optical Code Division Multiple Access

Optical Code Division Multiplexing (OCDMA) is a process by which communication channel is identified by a specific optical code rather than a wavelength, as in WDM, or a time slot, as in OTDM. The spread spectrum technique is the basic principle used in Code Division Multiple Access (CDMA). Each user's transceiver in the system uses a different spreading code. To visualize the basic process used in CDMA, consider a system with four users transmitting signals in the same frequency band, as shown in Fig. 2.5. The signals are transmitted with the same power, even though they are presented one above the other in the figure. If there where no time multiplexing, all users would transmit at the same time. To make this possible, a special code is designated to each user (signal), and this code distinguishes one signal from the others. The receiver recovers the desired signal by means of correlation between the received signal and the code that is applied at the transmitter. The desired signal is then filtered and decoded and the other signals, now with lower power, appear to the receiver as noise [11]. A spread spectrum signal must have two special characteristics: the bandwidth is much bigger than the bandwidth of the signal that contains the information; and it is generated from an independent modulation signal, that has to be known by the receiver in order to be recovered. This independent signal, in the CDMA case, is each user's individual spreading code [12].

### 2.3.1 Effects Derived from Spectrum Spreading

The transmission capacity, $C$, of a channel is obtained by the Shannon-Hartly law, expressed as

$$C = B \cdot log_2(1 + \frac{P}{N}), \tag{2.1}$$

where $B$ and $P$, respectively, are the bandwidth and signal power, and $N$ is the noise power. Thus, fixing the power and increasing the signal bandwidth, the channel capacity also increases. In CDMA, the system capacity is determined by choosing the demanded Signal/Noise power, P/N, for each user or by the spreading gain, i.e., by an increase of the bandwidth B in equation 2.1. The noise signals to be considered include thermal noise, interference due to multiple access and, most importantly, interference from other users. Originally proposed for military purposes, spectral spreading was used initially for confidential communications, since spread signals have excellent rejection to intentional jamming. On the other hand, the use of pseudo-random codes to generate the transmitted signal makes the information recovery process more complex. The reason is that, in order to decode the signal, it is necessary to apply the same code used on the transmitted signal. Among the advantages of the use of spectrum spreading are: improvement in the transmitted signals immunity against multipath distortion; rejection to strong narrow-band interference; low transmitting power (low energy consumption); and simpler service planning, since all users use the same transmitting and the same receiving frequency. This type of transmission technique has been used successfully in radio communications. In optical systems, it is expected to use CDMA in a shared optical medium local network (LAN), and in local access networks based on next generation PON's [7].

### 2.3.2 Direct Sequence Spread Spectrum (DSSS)

Consider the information to be transmitted, $m(t)$, to be a train of random pulses as in

$$m(t) = \sum_{k=-\infty}^{\infty} a_k P(t - kT_b - \alpha), 0 \leq \alpha \leq T_b, \tag{2.2}$$

where $T_b$ is the width of each pulse, delayed by $kT_b$ seconds, $a_k$ is a random weighting variable and $\alpha$ is phase shift respect to the origin, Fig. 2.6-a. This signal's spectrum is shown in Fig. 2.6-b. The information signals spectrum spreading by means of the use of the Direct Sequence Spread Spectrum (DSSS) technique consists in multiplying m(t) by a signal of the same shape as m(t), but at a much higher bit rate. The signal with these characteristics is called Pseudorandom (PN) sequence (Fig. 2.7-a). Fig. 2.7-b compares the spectrum of m(t) and the PN sequence, respectively, $S_m(\omega)$ and $S_G(\omega)$. One can observe that $S_G(\omega)$ has a

much wider bandwidth than the information's spectrum. The bits in the PN sequence are called chips. The ratio between the bit rate of the information signal and the chip rate is defined as the spreading ratio, or the processing gain. In optical systems, on-off modulation of the PN sequence can be realized by means of an XOR (exclusive OR) operation of the signal and the data pulse train. This new sequence can modulate an optical carrier, as shown in Fig. 2.8-a, b. Despreading is obtained by multiplying the receiver signal by the same PN sequence used in the generation of the spread signal, delayed by a period of $T_d$ seconds, relative to the delay suffered by the signal propagation in the communication channel. Therefore, it is essential to maintain a synchronisation between transmitters and receivers.

### 2.3.3 Optical CDMA

In Optical CDMA (OCDMA) we use the CDMA method to transfer information in fiber optic links. At first, OCDMA or fiber optic CDMA (FO-CDMA) was considered, due to the fact that the optical fiber has an available bandwidth in the order of 25 THz for information transmission. However, the processing capacity of electronic devices used in the electric-optic-electric conversion reduces the throughput of data in an optical network. This problem can be minimized if both signal spreading and correlation are realized in the optical domain. Having this as a goal, research on OCDMA has been focused on the development of compatible pseudo-random sequences and on device projects able to process optically those sequences. In this sense, Salehi proposes a class of optical orthogonal codes (OOC) [4, 13]. The basic difference between OOC and codes used in RF systems is in the polarity of the PN sequences. Bipolar signals, levels +1 or -1, used in conventional spread spectrum systems are unrealizable in optical systems.

The On-Off keying (OOK) technique is the simplest form of modulating light in order to generate OOC

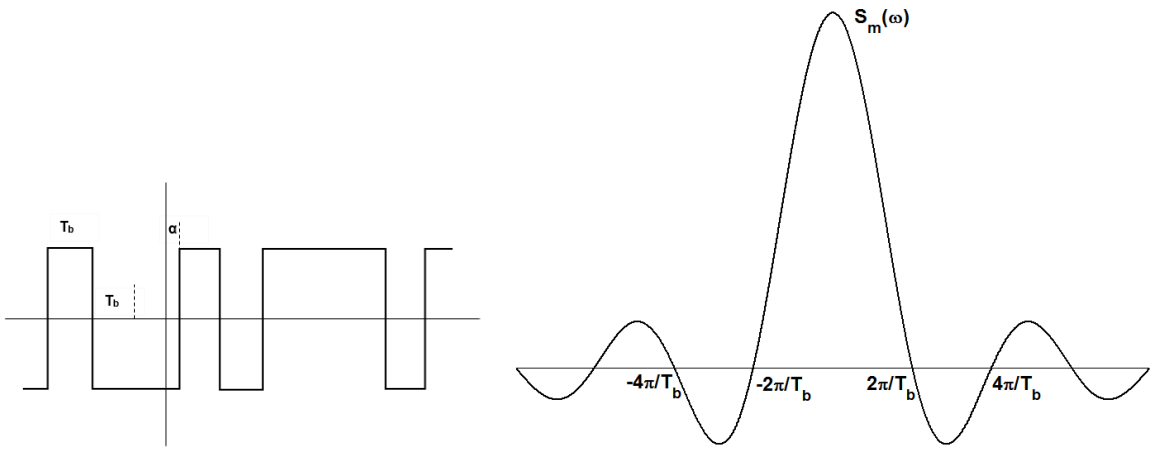


Figure 2.6: (a) Pulse train (bits) of a signal m(t) as defined in Equation (2.2). (b) Spectrum of the signal.

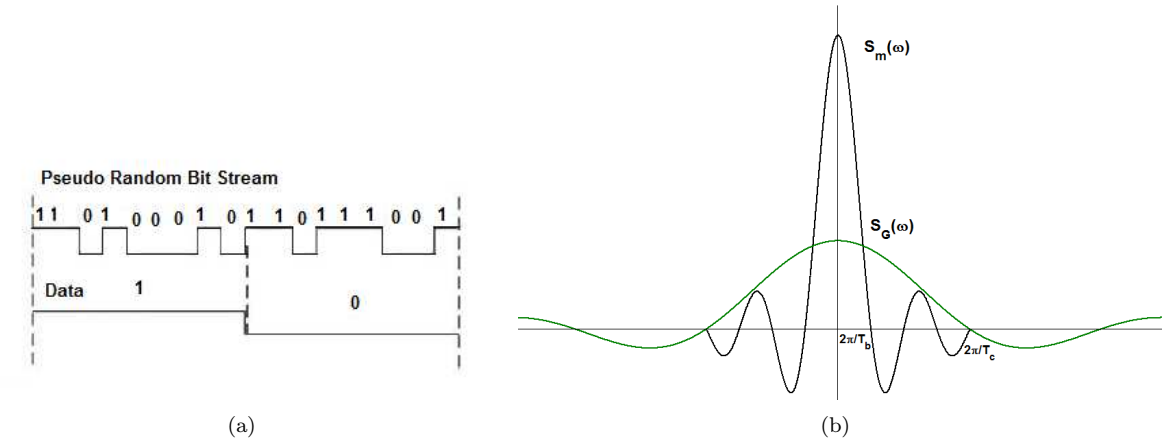


(a) (b)

Figure 2.7: (a) Pseudo-noise sequence used in DSSS to spread a signal intended for transmission. (b) The spectrum of a PN sequence $S_G(\omega)$ whose chip rate is much higher than other signal's bit rate m(t), has a much wider bandwidth.

codes. Fig. 2.8-b shows an optical code with 32 chips per bit and 4 active chips. Alternatively, this code can be shown by means of an optical disc as illustrated in Fig. 2.9-a, in which the disc perimeter is equivalent to a bit period ($T_b$) and each chip period ($T_c$) corresponds to a disc sector equal to $2\pi T_c/T_b$ [4]. This demonstration is useful to build an analogy to maximum autocorrelation values, Fig. 2.9-b, and with sequence shifting, by rotating the disc, Fig. 2.9-c. If many users are simultaneously connected, the use of OOC minimizes the interference caused by multiple signals on the desired signal along with a non-linearity optical limiter. This method can improve the performance of the optical system and with constant BER, a number up to five times greater of users can access the system [13].

In relation to optical processing devices, some models are proposed as transmitter and receiver architecture that work for bipolar OCDMA systems. At the transmitter, a laser generates ultra-fast pulses that are split and sent through distinct paths. At the receiver end, the pulses are recombined and transformed in elec-

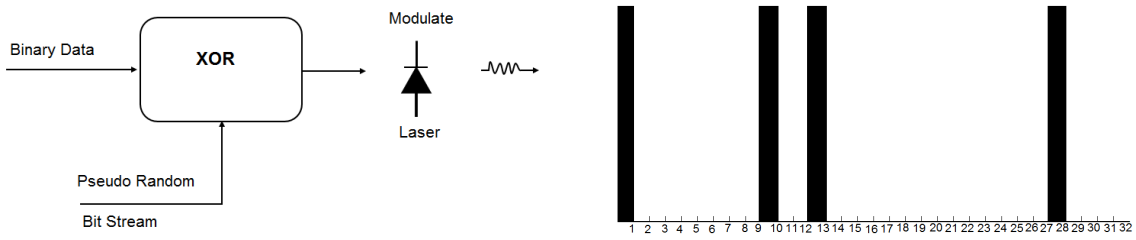


(a) (b)

Figure 2.8: (a) Basic CDMA transmitter diagram, in which the spread signal modulates a laser source and XOR is exclusive OR (b) Optical code represented by light pulses in the chip positions 1, 10, 13 and 28.

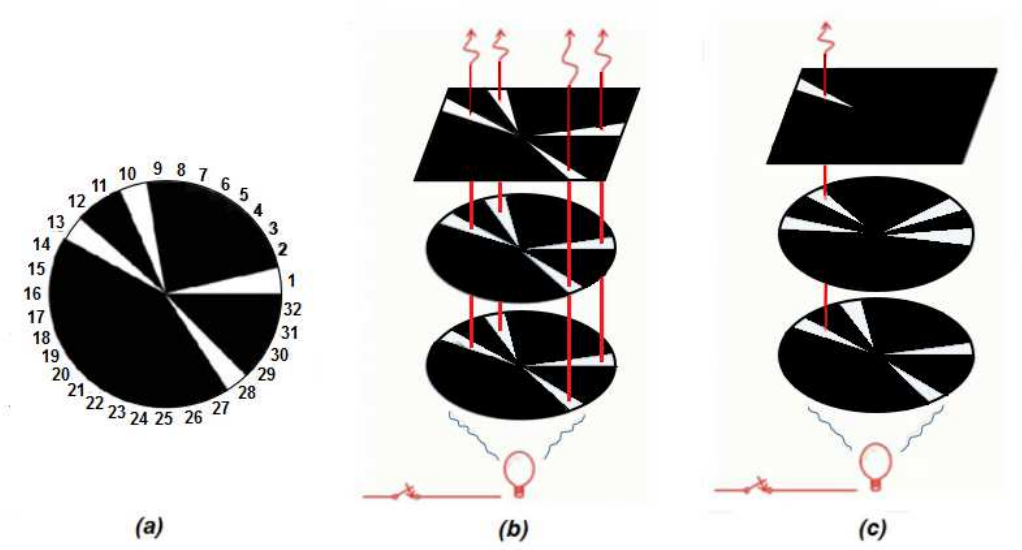


Figure 2.9: (a) Alternative representation of Fig.2.7-b optical code. Autocorrelation demonstration of a disk representing an optical PN sequence. (b) peak value. (c) autocorrelation with some shifting in the sequence [4].

trical pulses. Although it uses optical processing, this method has a limitation due to the noise introduced in the optical-to-electrical conversion in the final decision stage of the receiver.

A particularly interesting characteristic of the CDMA technique is efficiency asynchronous transmission. In the case of local area networks (LAN), that use a mechanism of bursty transmissions in a shared medium, the OCDMA technique permits the performance of access to these LANs at high bit rates and with a better cost-benefit relationship. This could open the way to use OCDMA in optical access networks such as next generation EPON (Ethernet Passive Optical Network) [7].

### 2.3.4 Classification of CDMA Techniques in Optical Communications

Coding schemes can be classified based on different choices of optical sources (e.g., coherent vs. incoherent, narrowband vs. broadband), detection schemes (e.g. coherent vs. incoherent) and coding techniques (e.g., time vs. wavelength, amplitude vs. phase) into six main categories: (I) pulse-amplitude-coding, (II) pulse-phase-coding, (III) Spectral-amplitude coding (SAC), (IV) Spectral phase coding (SPC), (V) Spatial coding and (VI) Wavelength-hopping time-spreading coding.

In the first two techniques coding is performed in the time domain and the schemes are based on incoherent processing with fiber optic delay lines and incoherent optical sources [14, 15]. These schemes are very simple to implement and require the use of unipolar pseudoorthogonal codes, such as optical orthogonal codes (OOCs) and prime codes, with nonzero cross-correlation functions. The plans in pulse-phase-coding utilize

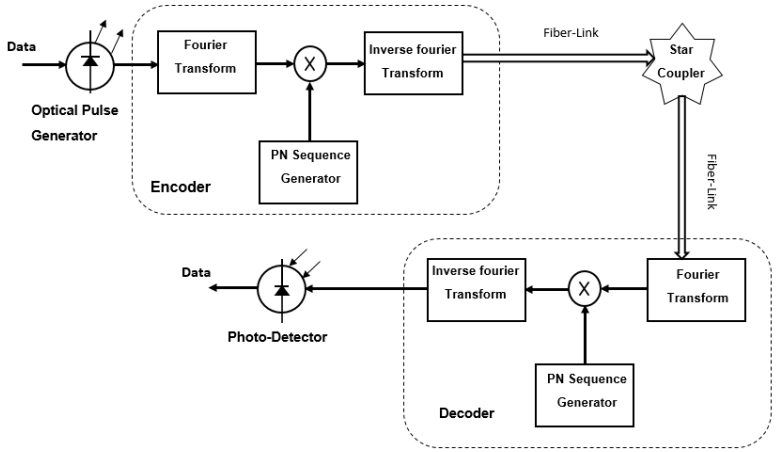


(a)

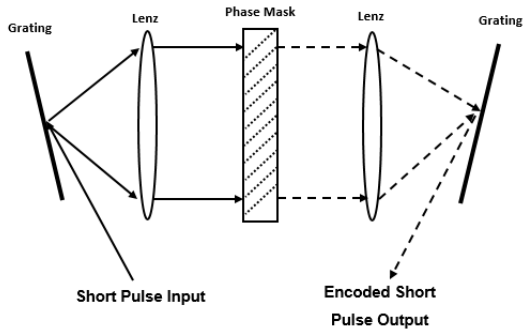


(b)

Figure 2.10: (a) Principle of SPC-OCDMA. (b) Structure of optical Fourier transform and SPC.

optical field by using phase modulator within fiber optic delay-lines for introducing 0° or 180° phase shift to pulses in a code sequence [16]. We can use bipolar orthogonal codes using coherent processing, such as maximal-length sequences and Walsh codes [17], with close to zero cross-correlation functions, thus reducing multiple access interference (MAI) and resulting in better code performance. Nevertheless, these two time-domain techniques are not inherently suitable for dense, high-speed, long-span optical networks because ultrashort pulses are required, making the systems sensitive to fiber dispersion and nonlinearities.

Coding is performed in the wavelength domain in spectral-amplitude coding and spectral phase coding [18]. The spectral nature of codes is decoupled from the temporal nature of the data so that code length is now independent of data rate. On the condition that coded spectra should be aligned to a common wavelength reference plane, spectral OCDMA systems are code-synchronous. An ultrashort pulse is first dispersed in multiple wavelengths by a grating in free space, spectral coding is performed by passing spectral components of pulse through a phase or amplitude mask, and the coded spectral components are finally recombined by another grating to form a code sequence. The length of the code sequence is determined by

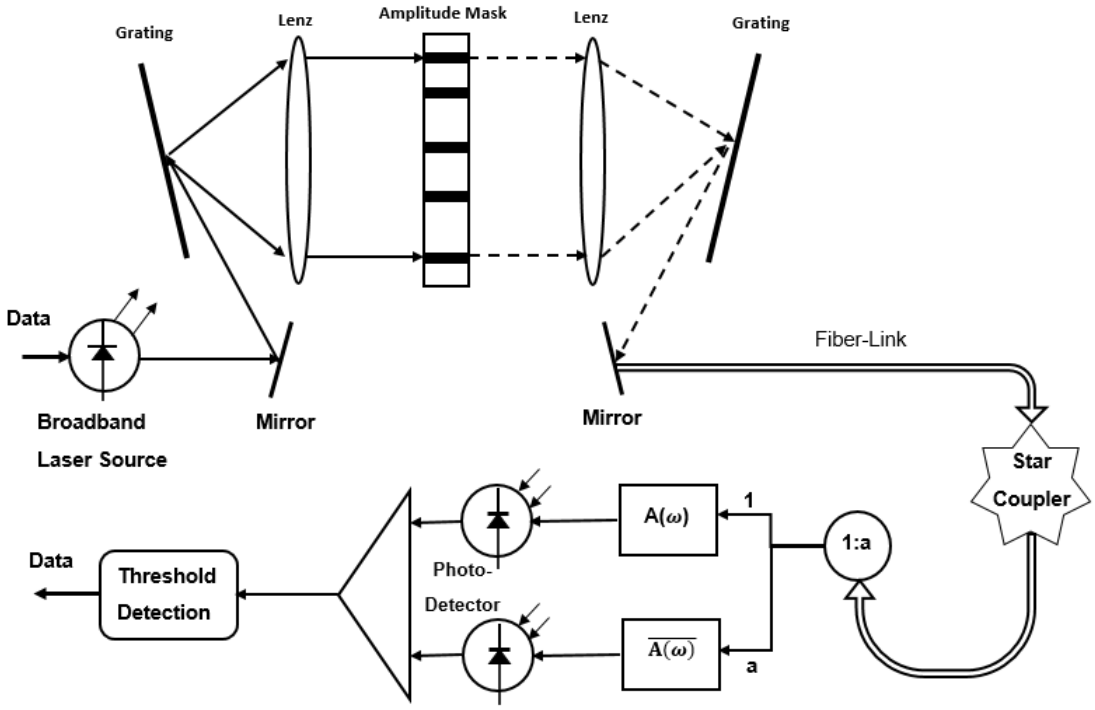


Figure 2.11: Principle of the SAC-OCDMA scheme.

the resolution of the gratings and masks. Bipolar orthogonal codes, such as maximal-length sequence and Walsh codes, are used for minimizing MAI.

Fig. 2.10-a shows an encoder and decoder for the spectral phase encoding system (SPC-OCDMA). The information source modulates very short laser pulses. The pulses are Fourier transformed and the spectral components are multiplied by the code corresponding to a phase shift of 0 or $\pi$. Fourier transform can be implemented by the grating and lens pair, as shown in Figure Fig. 2.10-b. In spectral amplitude coding optical code division access (SAC-OCDMA), the frequency components of the signal from a broadband optical source are encoded by selectively blocking or transmitting them in accordance with a signature code. Fig. 2.11 shows the principle structure of a SAC-OCDMA system. Compared to SPC-OCDMA, SAC-OCDMA is less expensive due to incoherent optical source. For the access networks environment, where cost is one of the most decisive factors, the SAC-OCDMA seems therefore to be a promising candidate.

Spatial coding requires the use of multiple fibers or multicore fibers with two-dimensional (2D) optical codes in the time and space domains simultaneously [19]. Similarly, the wavelength-time schemes in wavelength-hopping time-spreading coding require 2D coding in the time and wavelength domains [20]. The wavelength-time schemes provide lower the probability of interception and offers scalability and flexibility.

Probability of interception is converted because the pulse of each code sequence are transmitted in different wavelengths, thus increasing the security against eavesdropping. Where encryption delay is critical, this feature in physical layer can be useful for time-sensitive secure transmissions, such as in strategic or military systems. In addition, with 2D codes, the requirement of ultrashort pulses is lessened and wavelength-time systems are less vulnerable to fiber dispersion than coherent-spectral-coding systems, although some degrees of fiber-dispersion management strategy may still be employed.

### 2.3.5 Optical Spreading Codes

The main purpose of OCDMA systems is to recognize the intended user's signals in the presence of other user's signals, while maximizing the number of users in the system. In this case, the suitable optical sequence codes with the best orthogonal characteristics must be utilized. In terms of the correlation properties, spreading sequences are selected with the features of maximum autocorrelation and minimum cross-correlation in order to optimize the differentiation between the desired signal and interference. Optical orthogonal codes and the family of prime codes are considered in this section.

#### 2.3.5.1 Optical Orthogonal Codes (OOC)

OOC is one of the most important types of temporal codes that have been proposed for intensity modulation Direct Detection OCDMA systems. Because the code weight is very low (meaning that the code is very sparse), there are limits to the efficiency in practical coding and decoding. Moreover, the number of codes that can be supported is very low when compared to code sets with the same length used in RF communications (PN -pseudo noise-codes for example). We need to increase the length of the code for getting more codes, demanding the use of very short pulse optical sources having pulse width much smaller than the bit duration [4]. The required temporal OCDMA codes must satisfy the following conditions (OOC properties):

**a)** The peak autocorrelation function of the code should be maximized.

**b)** The side lobes of the autocorrelation function of the code should be minimized.

**c)** The cross-correlation between any two codes should be minimized.

Conditions a) and c) imply that the MAI is minimized, while condition b) simplifies the synchronization process at the receiver. If synchronous optical CDMA is used, then condition b) makes it possible to use one code for all users, which may reduce the coding and decoding complexity. The correlation $R_{C_iC_j}(\tau)$ of

two signature signals $C_i(t)$ and $C_j(t)$ is defined as

$$R_{C_iC_j}(\tau) = \int_{-\infty}^{\infty} C_i(t)C_j(t+\tau)dt, \qquad \text{for } i,j = 1,2,\ldots \tag{2.3}$$

where the signature signal $C_k(t)$ is defined as,

$$C_k(t) = \sum_{n=-\infty}^{\infty} c_k(n)P_{T_c}(t-nT_c), \qquad \text{for } k = 1,2,\ldots \tag{2.4}$$

where $P_{T_c}$ is pulse function with bandwidth of $T_c$ and $c_k(n) \in \{0,1\}$ is a periodic sequence of period N. The discrete correlation function $R_{c_ic_j}(m)$ between any two sequences $c_i(n)$ and $c_j(n)$ is given by,

$$R_{c_ic_j}(m) = \sum_{n=0}^{N-1} c_i(n)c_j(n+m), \qquad \forall m = \ldots -1,0,1,2,\ldots \tag{2.5}$$

The sum in the argument of $c_j(n+m)$ is calculated modulo N and we represent this operation from now on as $[x]_y$, which reads x modulo y. In the discrete form, the above conditions are rewritten as:

**I)** The number of ones in the zero-shift discrete autocorrelation function should be maximized.

**II)** The number of coincidences of the non-zero shift discrete autocorrelation function should be minimized.

**III)** The number of coincidences of the discrete cross-correlation function should be minimized.

An OOC is usually depicted by a quadruple, $(F,K,\lambda_a,\lambda_c)$, where F is the sequence length, K is the sequence weight (number of ones), $\lambda_a$ is the upper bound on the autocorrelation for non-zero shift and $\lambda_c$ is the upper

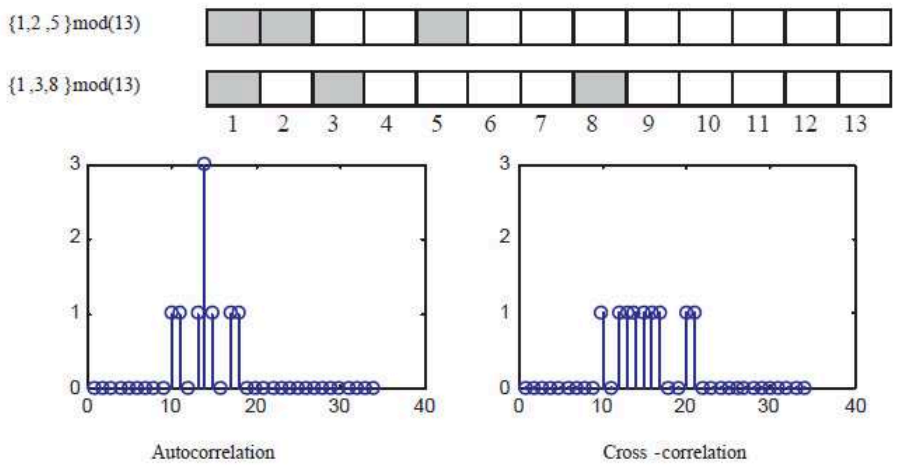


Figure 2.12: Two (13,3,3,1) OOC's and their autocorrelation and cross-correlation.

bound on cross-correlation. The conditions for optical orthogonal codes are:

$$R_{c_i c_i}(m) = \sum_{n=0}^{F-1} c_i(n)c_i(n+m) \leq \lambda_a, \qquad [m]_F \neq 0 \tag{2.6}$$

$$R_{c_i c_j}(m) = \sum_{n=0}^{F-1} c_i(n)c_j(n+m) \leq \lambda_c, \qquad \forall m, i \neq j \tag{2.7}$$

An example of a strict OOC (13,3,3,1) code set is C = 1100100000000, 1010000100000, plotted in Fig. 2.12. It is clear from the figure that the peak autocorrelation is equal to the code weight of 3, and the non-zero shift autocorrelation and the cross-correlation is less than or equal to one. The same code set C can be represented using the set notation as $C = [1, 2, 5], [1, 3, 8]$ mod(13), where the elements in the set represent the position of the pulses in the code.

#### 2.3.5.2 Prime Codes (PC)

The OOCs presented in last section lack the availability of a systematic way of code construction that can be used at both ends of the communication links. Codes have to be constructed beforehand (using iterative random search, combinatorial techniques, etc.) and some sort of lookup table is needed for each user. On the other hand, the OOC is a highly sparse code and the number of supported users can be very low. Another important type of codes proposed for OCDMA are the Prime codes. The prime code has a higher correlation value as compared to the OOC but it can support more users. Furthermore, the ease of generation of prime codes makes them a good candidate for OCDMA networks.

The Prime code consists of many blocks each containing a single pulse. For any prime number q, a code comprises q blocks of length q. A set of code sequences of length $N = q^2$, derived from prime sequences of length q, where q is a prime number, was derived in [21]. The procedure for code generation starts with the Galois Field, $GF(q) = 0, 1, \ldots, j, \ldots, q-1$, then a prime sequence $S_k = (S_{k0}, S_{k1}, \ldots, S_{kj}, \ldots, S_{k(q-1)})$ is evaluated by multiplying each element j of the GF(q) by an element k of GF(q) modulo q. q distinct prime sequences can thus be obtained which are mapped into a time-mapped binary code $c_k = (c_k(0), c_k(1), \ldots, c_k(j), \ldots, c_k(N-1))$ according to,

$$c_n(k) = \begin{cases} 1 & \text{for } n = s_{kj} + jq, s_{kj} = k \bigodot j, \\ 0 & otherwise. \end{cases}$$

where $j = 0, \ldots, q-1$ and $\bigodot$ means modulo q multiplication. Fig. 2.13 shows the q = 5 prime code in

mark position set format along with the autocorrelation of $c_3$ and crosscorrelation between $c_3$ and $c_4$. It is known that the peak autocorrelation of prime sequences is q, non-zero shift maximum autocorrelation of q-1, and maximum cross-correlation of 2, thus prime sequences can be considered as an OOC with $(F = q^2, K = q, \lambda_a = q - 1, \lambda_c = 2)$. The high non-zero shift autocorrelation of prime codes make the synchronization much more difficult at the receiving end. On the other hand, more users can be addressed using prime codes than with OOC of the same length and weight. Additionally, the prime codes can be generated more efficiently using a parallel serial network of delay lines and switches [22].

## 2.4 Optical Orthogonal Frequency Division Multiplexing

Another method to increase capacity of transmissions of data is optical orthogonal frequency division multiplexing (O-OFDM). Recently, O-OFDM has found interest in optical fiber transmission as a means of spectral shaping, reducing the guard band requirement between neighboring channels, and therefore increasing bandwidth utilization and spectral efficiency. We can express the transmitted signal as [23]

$$X(t) = \sum_{n=-\lfloor \frac{N_c}{2} \rfloor}^{\lceil \frac{N_c}{2} \rceil - 1} \sum_{m=-\infty}^{\infty} X_{n,m} p(t - nT_s) exp(j\omega_m t) \tag{2.8}$$

where $X_{n,m}$ is a two-dimensional complex valued symbol transmitted at the $m^{th}$ subcarrier in the $n^{th}$ symbol period, $\omega_m$ is the frequency of the $m$th subcarrier (relative to the channel's carrier frequency), $T_s$ is

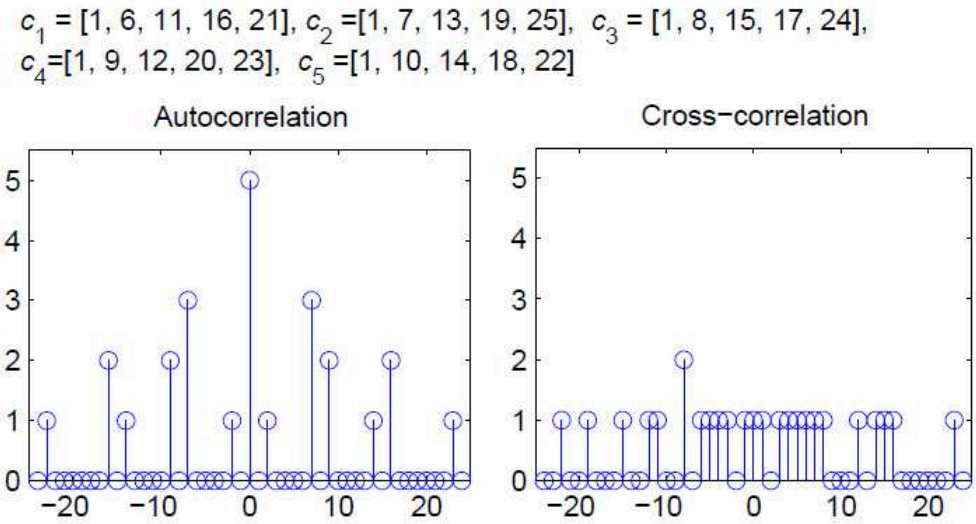


Figure 2.13: Autocorrelation and cross-correlation of prime sequence with q=5.

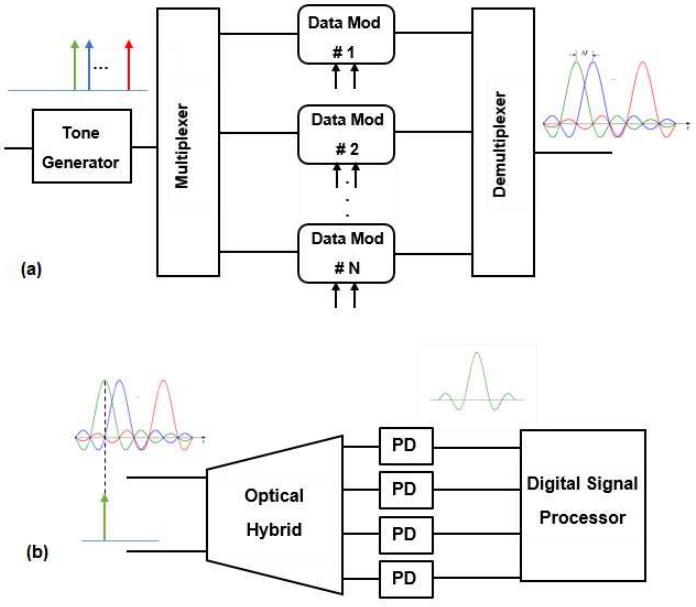


Figure 2.14: O-OFDM (a) transmitther and (b) receiver, where PD is a photo detector.

the symbol period, and p(t) is the pulse shape. In the OFDM technique, $p(t) = rect(t/T_s)$ is a rectangular pulse with duration $T_s$, and the subcarrier frequencies are $\omega_m 2\pi m/T_s$ where $-\lfloor N_c/2 \leq m < \lceil N_c/2 \rceil - 1$, with $\lfloor x \rfloor$ and $\lceil x \rceil$ being the nearest integers above and below x. Then, it can be shown that the set of basis functions $\phi_m(t) = rec(t/T_s)exp(j2\pi(m/T_s)t)$ are orthogonal over any continuous time interval $\tau \leq t < \tau + T_s$ duration $T_s$.

Examples of an O-OFDM transmitter and receiver are shown in Fig. 2.14, where the transmitter has a tone generator, usually a pulsed laser or an overdriven MZ modulator, which produces phase-locked optical tones. Optical OFDM manipulates pulses in the frequency domain, in contrast with OTDM which manipulates them in the time domain. In the receiver, the phase-locked tones are first demultiplexed, followed by parallel data modulation, followed by recombining. There are two types of optical OFDM, being the first single carrier modulation on each optically generated subcarrier (O-OFDM/SC), where each user transmits and receives data stream with only one carrier at any time. The other type is electrical OFDM on each optically-generated subcarrier (O-OFDM/E-OFDM) [23].

## 2.5 Multi User Interference Rejection

In both the spectral phase coded OCDMA and temporal phase coded OCDMA systems, multiuser interference noise from undesired users is still present even after the signals have passed through the matched

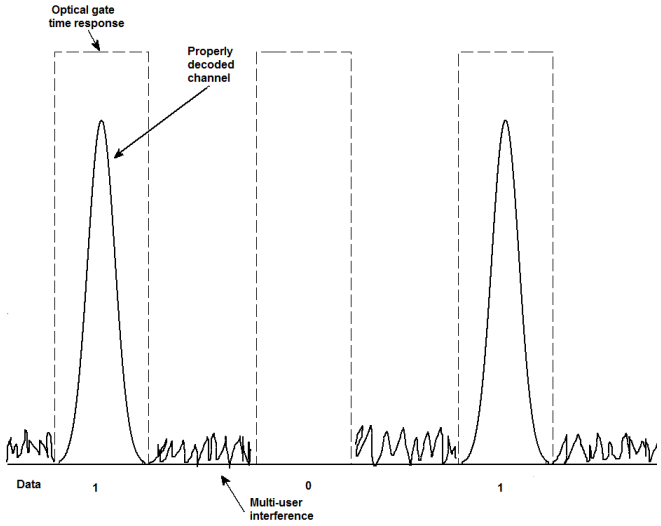


Figure 2.15: Illustration of optical time gating for multiuser interference rejection.

OCDMA decoder. In addition, since the optical signal energy present in both the decoded and undesired channels are similar in magnitude, both will appear essentially identical from the perspective of a typical photoreceiver that is band limited to the data bit rate, preventing the desired signal from being recovered correctly. Thus, further processing techniques are necessary in order to eliminate the interference. In principle, an ultrawide bandwidth optical photoreceiver could be used at the OCDMA receiver front-end, and the removal of interference could be performed in the electrical domain. However, given the bandwidth requirements of an OCDMA system, which is typically on the order of many tens or even hundreds of GHZ, this is likely to be impractical due to the need for ultrafast electronics. As a result, multiuser interference rejection is most commonly performed in the optical domain, where wideband optical processing can be performed relatively easily. Two categories of optical processing techniques for multiuser interference rejection are discussed here: optical time gating and optical thresholding.

### 2.5.1 Optical Time Gating

The basic concept of the application of optical time gating to exploit the decoded OCDMA signal is shown in Fig. 2.15. Through the proper selection of an appropriate code set for a synchronous coherent OCDMA system, it is possible to design the system such that the multiuser interference energy falls outside a time interval where the properly decoded signal pulse resides. Thus, by optically gating we have low loss within the desired time window for the composite signal. Besides, at the same time we would have high extinction outside that window, so only the properly decoded signal bit stream can be extracted.

For the purposes of application to coherent optical CDMA system, some of the more important perfor-

mance parameters for optical gating technologies include:

- Gate width
- Gate repetition rate
- Gate extinction rate
- Data pulse energy levels and dynamic range
- Gating control/clock pulse energy levels and dynamic range

As a result of these high efficiency requirements, relatively high-speed optical processing techniques should be applied, such as those used for all-optical demultiplexing. Although there are a wide variety of options, some of the technologies that have been demonstrated specifically for coherent OCDMA systems include:

- Nonlinear interferometers
- Four-wave mixing (FWM) techniques

#### 2.5.1.1 Semiconductor Optical Amplifier (SOA)-Based Nonlinear Interferometers for Optical Time Gating

The nonlinear phase change required in the nonlinear optical loop mirror (NOLM) can be implemented by using of as a semiconductor optical amplifier (SOA), allowing for the potential of device integration. An interferometric architecture similar to the NOLM can be used, as illustrated in Fig. 2-16. When the SOA is offset from the center of loop by $\triangle x$, the device is referred to as Terahertz optical asymmetric demultiplexer (TOAD) [24].

When the clock pulse is not present, incoming data pulses reflect from the TOAD. By injecting a clock pulse, which is typically chosen to be on the order of 10 dB larger in amplitude than the data pulse intensity, gating can occur. The clock pulse saturates the SOA, thereby changing its effective index. The clock pulse, which travels only in the clockwise direction, is injected following the clockwise propagating data pulse to give the clockwise data pulse the opportunity to propagate through the SOA before the clock pulse saturates the SOA index. Since the SOA slowly recovers on the time scale of hundreds of picoseconds, counter-propagating data pulse that arrive immediately after the clock pulse event has occurred see the SOA in approximately the same relative state and do not experience a differential phase shift. The temporal duration of the gating window is set by the offset of the SOA, $\triangle x$, from the center of the loop. As the offset is reduced, the gating window width decreases until the actual length of the SOA needs to be taken into account. The nominal gate width is related to the offset by $\triangle t_{gate} = 2\triangle x l c_{fiber}$, where $c_{fiber}$ is the speed of light in fiber and $l$

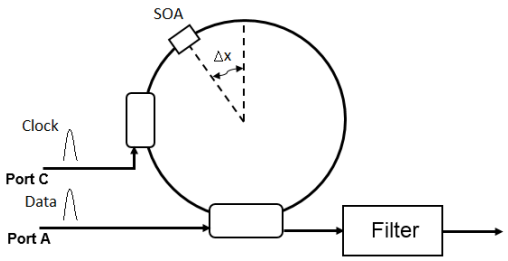


Figure 2.16: Illustration of terahertz optical asymmetric (TOAD) time gate.

is length of the ring. The TOAD optical time gate has been successfully applied to an implementation of SPC-OCDMA [25].

#### 2.5.1.2 Four Wave Mixing (FWM) Optical Time Gating

Another method in optical time gating is Four Wave Mixing (FWM). FWM is a third-order nonlinearity, similar to intermodulation distortion in the electrical domain. In FWM, the nonlinear beating between the data signal and a control signal at a different wavelength generates new optical tones as sidebands. FWM-based gating can be performed in optical fiber or in waveguide devices such as semiconductor optical amplifiers (SOAs).

In SOAs, FWM occurs through carrier density modulation. Two copolarized optical signals are coupled into the SOA. One is the control signal at frequency $f_c$ and typically has a much higher intensity than the other input signal (data) to be wavelength converted, which is at ferequency $f_d$. The two copropagating signals mix and, through carrier density modulation, form an index grating off which signals can be scattered. The scattering of the control signal from this grating generates two waves, one at the data frequency and one at a new frequency, $f_{converted} = 2f_c - f_d$. This is the useful wavelength-converted signal. Also, data signal scattering generates two much weaker waves, one at the control frequency and one at a new frequency, $f_{satellite} = 2f_c - f_d$. This is called the satellite wave and is generally not used.


Figure 2.17: Illustration of the four-wave mixing (FWM) time gate .

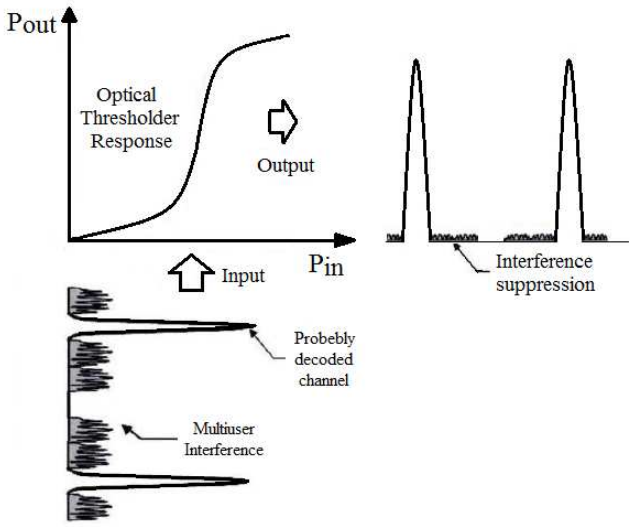


Figure 2.18: Illustration of optical thresholding for multiuser interference rejection.

By injecting a short optical control pulse along with the incoming OCDMA signal into the SOA as illustrated in Fig. 2.17, it is possible to create an optical time gate by filtering out the resulting wavelength converted signal. The clock pulse is temporally aligned to the correct position relative to the desired OCDMA pulse, and an optical bandpass filter is placed at the output of the SOA in order to extract the FWM signal only. The FWM optical time gate has been successfully applied in TPC-OCDMA [26].

### 2.5.2 Optical Thresholding

Another method for OCDMA multiuser interference rejection is nonlinear optical thresholding. The basic concept is based on a device that has a nonlinear power-transfer response, as illustrated in Fig. 2-18. The pulses for the properly decoded pulses are of large peak amplitude and therefore pass through the device with low relative loss. On the other hand, the undesired channels, that are of low peak intensity since they have been spread in time, are effectively suppressed. One of the advantages of optical thresholding over optical time gating is in eliminating the need for a synchronizing clock pulse.

There are various alternatives to implementing an all-optical thresholding device. Two methods that have been specifically applied to OCDMA systems include:

- Nonlinear Optical loop mirrors (NOLM)
- Second harmonic generation (SHG) in periodically poled lithium niobate (PPLN)

#### 2.5.2.1 NOLM-Based Thresholding

The NOLM used for all-optical nonlinear thresholding are very similar in construction to the NOLMs used for optical time gating without the clock pulse and its associated input port. Also, rather than using a 50:50 coupler to create the loop, an asymmetric coupling ratio is used, such as 70:30. By introducing this asymmetry, the nonlinear phase shift experienced by the two counter-propagating pulses of large amplitude is also different, and can result in the incoming pulse to be sent to the output port rather than get reflected. On the other hand, for low amplitude pulses, the nonlinear phase shift is not large for either and the pulses are primarily reflected as in the standard loop mirror configuration. NOLM-based thresholding has been used in phase-coded OCDMA systems both as a stand-alone device [27], as well as in conjunction with optical time gating [28].

#### 2.5.2.2 PPLN-Based Thresholding

Periodically poled lithium niobate (PPLN) devices can be used for nonlinear second harmonic generation. Since the output power is strongly dependent on the input signal intensity, they can be used as nonlinear thresholding devices. PPLN-based optical thresholding has been successfully applied in wideband SPC-OCDMA systems [29], using waveguide-based devices.

### 2.5.3 Second Harmonic Generation (SHG)

Approximately all of dielectric materials have nonlinear response to a strong optical field. This nonlinear effect is due to uncoordinated movement of electrons at the border under the influence of the applied field. As a result, induced polarization, P, follows nonlinear relationship with the electric field, E, that can be expressed as follows [30]:

$$P = \epsilon_0(\chi^{(1)}.E + \chi^{(2)} : EE + \chi^{(3)}\vdots EEE + \ldots) \tag{2.9}$$

where $\epsilon_0$ is the permittivity of vacuum and $\chi^{(j)}$ $j = 1, 2, \ldots$ is the susceptibility of $j$th order. Generally, $\chi^{(j)}$ is a tensor of order $j+1$th. Linear susceptibility, $\chi^{(1)}$, then compared to other order susceptibility is bigger. $\chi^{(2)}$ is known the second order nonlinear effect that SHG is due to this property. This index for materials such as glass, which has a molecular symmetry, is zero. Therefore, optical fiber generally do not have any second order nonlinear effect. For this reason, we should use materials that have Asymmetric molecular for generating second harmonics, as shown in Fig 2.19.

In the second harmonic generation process, photons with frequency $\omega$ that will interact with nonlinear materials, are combined together and new photons are produced with double energy. As a result, these new photons have a frequency twice the previous frequency (Fig. 2.20).

Now we describe how to reduce the multiple interference effect with SHG. A nonlinear threshold detector using second harmonic generation is shown in Fig. 2.21 [31]. A crystal for generating the SHG decode signals is placed between the photo-detector and the decoder. In this technique, the electric field of the input signal gets squared by the first stage and is applied to the input of a filter with a rectangular impulse response. The output is the electric field of the second-harmonic (SH) signal. After the crystal, a rectangular impulse response filter is used to remove the effects of the Group Velocity Mismatch (GVM) between the main signal and the SHG signal. The response of this filter are modeled as rectangular with length, $T_L$, and amplitude, $1/T_L$, where $T_L = L|\alpha|$, $L$ is length of nonlinear crystal and $\alpha = \frac{1}{v_{g1}} - \frac{1}{v_{g2}}$ is group velocity mismatch [32].

When the nonlinear crystal used is thin, $T_L$ is much smaller than the pulse duration, the filter response is Dirac signal, and the filtering effect can be ignored. But when the crystal is thick, $T_L$ is bigger than the pulse duration, the SHG signal is broadened in the time domain and is bandpass filtered in the frequency domain. Furthermore, for SHG receiver use thin crystal.

According to the optical carrier signal is twice by nonlinear crystal, So we need to get the signal to a photo detector at a wavelength equal to half the wavelength of the main signal. When by the desired sender is sent bit of "1", the energy of the second harmonic signal with a short pulse signal decoding is much stronger than the lower range of MUI. Thus, output of photo detector is quite different for the two bits "0" and "1".

### 2.5.4 Two Photon Absorption (TPA)

Two-photon absorption (TPA) is the simultaneous absorption of two photons of identical or different frequencies in order to excite a molecule from one state (usually the ground state) to a higher energy electronic state. The energy difference between the involved lower and upper states of the molecule is equal to the sum of the energies of the two photons. Two-photon absorption is a third-order process several orders of magnitude weaker than linear absorption at low light intensities. It differs from linear absorption in that the atomic transition rate due to TPA depends on the square of the light intensity, thus it is a nonlinear optical

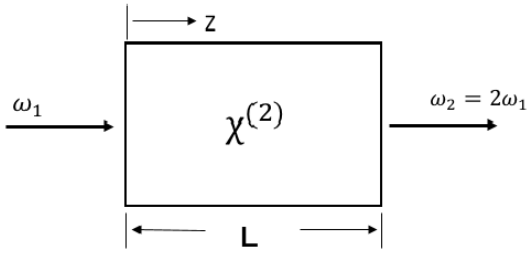


Figure 2.19: Nonlinear crystal for second harmonic generation.

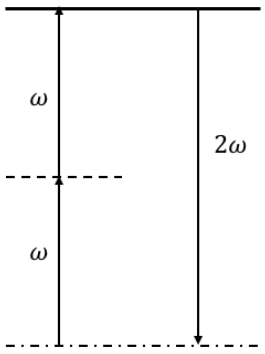


Figure 2.20: The second harmonic generation.

process, and can dominate over linear absorption at high intensities.

In the TPA process shown in Fig. 2.22, two identical photons, whose their energy is less than the energy of the distance of two band and more than half of its energy band, generate a pair of electrons and proton at the same time attracting. So for photo-detectors where the distance between the energy bands is larger than incoming photons, the current of photoelectrons generation can be expressed as follow:

$$\frac{dN}{dt} = \frac{\alpha}{h\upsilon} I(t) + \frac{\beta}{2h\upsilon} I(t)^2 \tag{2.10}$$

where I is the intensity of received light, $h$ is the Plank constant ($h = 6.624 \times 10^{-34}$), $\upsilon$ is the frequency of received light, $\alpha$ is one photon absorption coefficient and $\beta$ is the TPA coefficient. In fact, two photon absorption is proportional to the square of the incident light intensity and increases rapidly by increasing the light intensity. So the number of generations of photoelectrons in the duration of $[0, \Delta t]$ is :

$$N = \int_0^{\Delta t} \left( \frac{\alpha}{h\upsilon} I(t) + \frac{\beta}{2h\upsilon} I(t)^2 \right) dt \tag{2.11}$$

The operation of the TPA receivers is studied in [33] and [34]. In TPA receivers, it is assumed that one

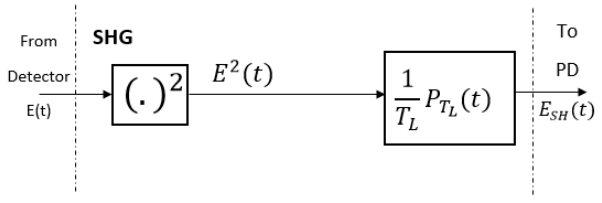


Figure 2.21: Nonlinear thershold detector using SHG.

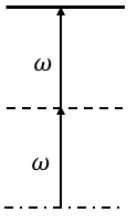


Figure 2.22: Two photon absorption process.

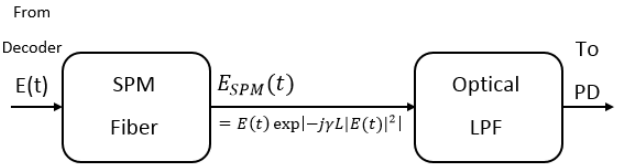


Figure 2.23: Structure of nonlinear threshold detector using the SPM technique.

photon absorption is zero ($\alpha = 0$).

### 2.5.5 Self-Phase Modulation (SPM)

The intensity dependence of the refractive index leads to a large number of interesting nonlinear effects, the two most widely studied are self-phase modulation (SPM) and cross-phase modulation (XPM). Self-phase modulation refers to the self-induced phase shift experienced by an optical field during its propagation in optical fibers. The value of induction phase is calculated as follows:[35]

$$\phi = \tilde{n}k_0L = (n + n_2|E|^2)k_0L \tag{2.12}$$

where $k_0 = 2\pi/\lambda$, $L$ is the length of the nonlinear environment, and $n$ is the linear refractive index. We can obtain the value of phase nonlinearity as follows:

$$\phi_{NL} = (n_2|E|^2)k_0L \tag{2.13}$$

where $\phi_{NL}$ is in effect of SPM. Thus, because of SPM, we observe the spectral broadening of the input signal that is proportional to the light intensity changes. The spectral deviation is:

$$\Delta\omega(t) = -\frac{d(\phi_{NL})}{dt} = -n_2k_0L\frac{\partial|E(t)|^2}{\partial t} \tag{2.14}$$

where the SPM coefficient is defined as $\gamma = n_2 k_0$, and (2.14) would become:

$$\Delta\omega(t) == -\gamma L \frac{\partial |E(t)|^2}{\partial t} \tag{2.15}$$

From (2.15), it can be seen that the frequency has changed over time. This time-dependent frequency variation is also called frequency chirping, which broadens the signal's spectrum. According after decoder time changing of the pulse amplitude of the main user is much larger than signal due to interference of other users, So using SPM is good solution for reducing interference effect. Because SPM effect has considerable broadening on the spectral main pulse, while the low intensity MAI signal's spectrum is broadened much less. The structure of the SPM-based nonlinear thresholder is shown in Fig. 2.23 [31]. When a bit "1" is transmitted, the rapid variation of the power of the recovered short pulse creates a strong broadening of the spectrum. Therefore, a considerable amount of energy can pass through the optical low-pass filter (LPF) that follows the SPM fiber. We assume that cutoff frequency low-pass filter is designed so that all the energy of the original signal passes through the filter to be removed. While SPM on the signal due to interference of other users have less effect and spectral widening on it is lower than main pulse. So much less of interference signal pass from filter. Furthermore, the value of received energy by photo-detector in cases "0" and "1" will be largely different.

## 2.6 Conclusions

In this chapter we studied the state of the art of the technologies related to the multiple access mechanisms applied to optical communications. The aim of this chapter was to consider the methods and techniques used in optical transmission. For this purpose, we introduced the different techniques used in the division multiplexing in optical networks: OTDM, WDM and OCDM. We follow our discussion by classification of the OCDMA techniques based on sources, detection and coding methods. After considering of different coding approaches we describe optical processing techniques and different methods for mitigating the effect of interference. In the end of this chapter, we comment several applications of nonlinear optical techniques in optical transmission and specifically application of time-gating in the OTDM and the OCDM receivers.

Chapter 3

# Application of Nonlinear Techniques in optical communications

The field of nonlinear optics has grown enormously in recent years and has evolved into many different branches. The growth of research in nonlinear optics has contributed to the rapid technological advances related to fiber optics and optical communications. On the one hand, the nonlinear response of optical fibers create impairments in the signal transmission quality in long-haul fiber optics links. On the other hand, fiber nonlinearity can be exploited for against the dispersion, fiber losses and scattering phenomena. Optical fibers can be used as a linear transmission medium and have basic properties such as: (1) optical power does not have an effect on the refractive index; (2) the superposition principle for multi independent optical signals holds; (3) optical wavelength or carrier frequency do not change in the length of fiber in the effect of power; (4) the light signal does not interact with any other light signal. When optical power or bit rates are low we can have these assumptions. However, when we have high optical power and optical amplifier and simultaneously several optical signals together (as is the case in the WDM), optical fiber behaves as a nonlinear medium with completely different properties. These properties are not good for optical transmission but, for some special cases they can be used for increasing the transmission capabilities of the fiber [36].

Nonlinearity in optical fiber is proportional to the intensity of the electromagnetic field of the propagating optical signal. The nonlinearity effect in optical fibers occurs due to a change in the refractive index of the medium caused by optical intensity and scattering phenomenon. The power dependence of the refractive index is responsible for the Kerr effect whereas scattering phenomena are responsible for Brillouin and Ramon effects [37]. Depending of the type of input signal, Kerr nonlinearity has three different effects: self phase

modulation (SPM), cross phase modulation (XPM) and Four Wave Mixing (FWM) [36]. These effects has been explained in the chapter 2.

FWM is one the most popular applications of nonlinear optical processing. FWM is a nonlinear effect that occurs in optical fibers during the propagation of a composite multichannel optical signal. The power dependence of the refractive index in optical fibers will not only shift the phases of the signals in individual channels is mentioned above $\omega$, but will also give a rise to new optical signals through the process known as Four Wave Mixing. The Four wave mixing is related to the fact that if there are three optical signals with different carrier frequencies that propagate through the fiber, a new optical frequency will be generated. In fact, FWM acts like a mixer in the electronic domain but for optical signals. We also mentioned the low response rate of the electronic equipment for modulating and switching of the information, then we need to use all-optical signal processing.

Accordingly, in this chapter our goal is to model the result of applying FWM to a signal. In order to accomplish that, we obtain the response of the nonlinear system by solving the nonlinear equations, thus obtaining the relationship between input and output optical signals. An important aspect, in order to take profit of any phenomenon (in our case, nonlinearity) is its correct characterization or modeling. We solve these equations bt using Volterra series and the results will be applied in Chapter 4 and Chapter 5, where we investigate the performance of FWM used as an AND optical gate for application in OTDM and OCDMA receivers.

## 3.1 Nonlinearities in Optical Fibers

As we mentioned in the introduction of this chapter, we must consider the theory of electromagnetic wave propagation in dispersive nonlinear media in order to understand the nonlinear phenomena in optical fibers. We want to obtain the basic equation of a nonlinear system by solving Maxwell's equations and apply effect of the linear and nonlinear parts of the induced polarization. Therefore, we can express the induced polarization $P(r,t) = P_L(r,t) + P_{NL}(r,t)$ where the linear part $P_L$ and the nonlinear part $P_{NL}$ are related to the electric field. Regarding the nonlinear part, nonlinear effects appears to short pulses with widths from $10ns$ to $10fs$ when they propagate through the fiber. Both dispersive and nonlinear effects influence their shapes and spectra. We can write relation between the electrical field and the induced polarization as follows:

$$\nabla^2 E - \frac{1}{c^2}\frac{\partial^2 E}{\partial t^2} = \mu_0 \frac{\partial^2 P_L}{\partial t^2} + \mu_0 \frac{\partial^2 P_{NL}}{\partial t^2} \tag{3.1}$$

The origin of all nonlinear optical phenomena lies in the nonlinear response of the material to an electromagnetic field. In fact, the polarization induced in the material does not have a linear relationship with the applied magnetic field and includes a series of nonlinear terms. The relationship between the induced nonlinear electric polarization, P, and electric field, E, is [38]:

$$P = \varepsilon_0(\chi^{(1)}.E + \chi^{(2)} : EE + \chi^{(3)}\vdots EEE + \ldots) \tag{3.2}$$

where $\varepsilon_0$is the vacuum permittivity and $\chi^{(1)}$, $\chi^{(2)}$, $\chi^{(3)}$ are the first, second and third order nonlinear susceptibility and " . ", " : " and " $\vdots$ " are the expansion of order tensor multiplication in the subject matter. The linear susceptibility $\chi^{(1)}$ represents the dominant contribution to $P$, that has influence in the refractive index $n$. Nonlinear effects such as second-harmonic generation and sum-frequency generation are due to the second-order susceptibility $\chi^{(2)}$ that it is nonzero only for media that lacks an inversion symmetry at the molecular level. However, for a symmetric molecule such as silica glasses ($SiO_2$), is zero. All third-order nonlinear effects such as FWM, third-harmonic generation and parametric amplification are due to the third-order of the nonlinear magnetization, $\chi^{(3)}$. Indeed, FWM in optical fibers was studied according to its ability for generating new wavelengths. The main features of FWM can be understood from the third-order polarization term in (3.2),

$$P_{NL} = \varepsilon_0\chi^{3}\vdots EEE, \tag{3.3}$$

Consider four continuous wave (CW) waves oscillating at frequencies $\omega_1$, $\omega_2$, $\omega_3$ and $\omega_4$, linearly polarized along the same axis $Z$. The electric field can be written as [39]:

$$E = \frac{1}{2}\hat{\chi}\sum_{m=1}^{4} E_m e^{j(k_m z-\omega_m t)} + c.c \tag{3.4}$$

where $k_m$ is the propagation constant ($k_m = n_m\omega_m/c$), $n_m$ is the mode index in $\omega_m$, $E_m$ is the amplitude of electric field of the m$th$ wave ($1 \leq m \leq 4$), $\hat{\chi}$ indicates that the polarization is along the $x$ axis, and the abbreviation c.c stands for complex conjugate. By substituting (3.4) in (3.3), $P_{NL}$ can be written as:

$$P_{NL} = \frac{1}{2}\hat{\chi}\sum_{m=1}^{4} P_m e^{j(k_m z-\omega_m t)} + c.c \tag{3.5}$$

$P_m$ consists of $E_1$, $E_2$, $E_3$ and $E_4$. For example, $P_4$ can be expressed as

$$P_4 = \frac{3\varepsilon_0}{4}\chi^{(3)}_{xxxx}[|E_4|^2E_4 + 2(|E_1|^2 + |E_2|^2 + |E_3|^2)E_4 + 2E_1E_2E_3e^{j\theta_+} + 2E_1E_2E_3^*e^{j\theta_-} + \cdots] \tag{3.6}$$

where $\chi^{(3)}_{xxxx}$ is the fourth rank tensor that is on contributes to the refractive index [35] and $\theta_+$ and $\theta_-$ are defined as

$$\theta_+ = (k_1 + k_2 + k_3 - k_4)z - (\omega_1 + \omega_2 + \omega_3 - \omega_4)t \tag{3.7}$$

$$\theta_- = (k_1 + k_2 - k_3 - k_4)z - (\omega_1 + \omega_2 - \omega_3 - \omega_4)t \tag{3.8}$$

The first four terms containing $E_4$ in Eq. (3.6) are responsible for the SPM and XPM effects, but the remaining terms result from the frequency combinations (sum or difference) of all four waves. Many of these are effective during a FWM process depending on the phase mismatch between $E_4$ and $P_4$ governed by $\theta_+$, $\theta_-$, or a similar quantity. Significant FWM occurs only if the phase mismatch nearly vanishes. This requires matching of the frequencies as well as of the wave vectors. The latter requirement is often referred to as phase matching. In other words, FWM occurs when photons from one or more waves are annihilated and new photons are created at different frequencies such that the net energy and momentum are conserved during the parametric interaction.

Usually we are interested in the sixth term of (3.6). Then, the phase matching condition becomes:

$$k_1 + k_2 - k_3 - k_4 = 0 \tag{3.9}$$

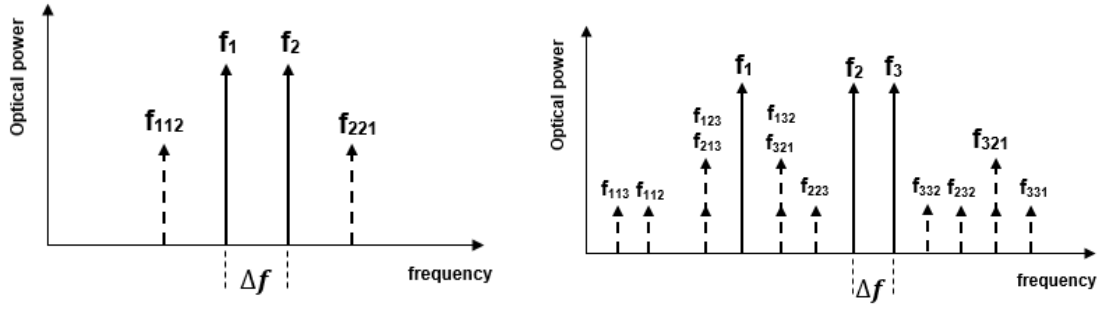


Figure 3.1: Four-wave mixing (a) Degeneration case, and (b) Non-degeneration case.

$$\omega_1 + \omega_2 - \omega_3 - \omega_4 = 0 \tag{3.10}$$

If we define $\Delta k$ as the wave vector mismatch, the matching condition fulfills $\Delta k = 0$. We can rewrite the aforementioned two conditions as:

$$\Delta k = n_1\omega_1 + n_2\omega_2 - n_3\omega_3 - n_4\omega_4 = 0 \tag{3.11}$$

$$\omega_4 = \omega_1 + \omega_2 - \omega_3 \tag{3.12}$$

The special case, in which $\omega_1 = \omega_2$ (degenerate case), is interesting because FWM can be initiated with a single pump beam. This degenerate case is often useful for optical fibers. This practical matching occurs when Group Velocity Dispersion (GVD) is very low and the channel spacing is narrow. In Fig. 3.1a, b, the generation of new optical frequencies due to FWM for two cases with two and three interacting optical channels are shown. As illustrated in the figure, if we have two optical channels with frequency $f_1$ and $f_2$, we would have two more optical frequencies both in $f_{112} = f_1 - \Delta f$ and $f_{221} = f_2 + \Delta f$. If there are three optical channels with frequencies $f_1$, $f_2$ and $f_3$, eight more optical frequencies are created (where $f_{ijk}$ is $f_i + f_j - f_k$).

## 3.2 Coupled FWM Equations

In order to obtain the coupled FWM equations we suppose that nonlinear environment factors do not have significant effect on the fiber modes. Therefore we can write the optical field $E_j(r,t)$, where r is axis vector and t is time, as follow:

$$E_j(r,t) = F_j(x,y)a_j(t,z)exp(ik_{0j}z) \tag{3.13}$$

where $F_j(x,y)$ is the fiber mode distribution, $a_j(t,z)$ is the $j$th amplitude signal and $k_{0j}$ is the propagation factor at carrier frequency $\omega_j$. So, according to section 3.1, the coupled FWM equations would be [30]:

$$\frac{\partial a_1(t,z)}{\partial z} = -\frac{\alpha_0}{2}a_1(t,z) - \sum_{k=1}^{\infty}\frac{\beta_k j^k}{k!} \times \frac{\partial^k a_1(t,z)}{\partial t^k} + \frac{jn^{'}\omega_1}{c} \times \left[\left(f_{11}|a_1(t,z)|^2 + 2\sum_{k\neq 1} f_{1k}|a_k(t,z)|^2\right)a_1(t,z) + 2f_{1234}a_2^*(t,z)a_3(t,z)a_4(t,z)e^{j\Delta kz}\right] \tag{3.14}$$

$$\frac{\partial a_2(t,z)}{\partial z} = -\frac{\alpha_0}{2}a_2(t,z) - \sum_{k=1}^{\infty}\frac{\beta_k j^k}{k!}\times\frac{\partial^k a_2(t,z)}{\partial t^k} + \frac{jn^{'}\omega_2}{c}\times\left[\left(f_{22}|a_2(t,z)|^2 + 2\sum_{k\neq 2} f_{2k}|a_k(t,z)|^2\right)a_2(t,z) + 2f_{2134}a_1^*(t,z)a_3(t,z)a_4(t,z)e^{j\Delta kz}\right] \tag{3.15}$$

$$\frac{\partial a_3(t,z)}{\partial z} = -\frac{\alpha_0}{2}a_3(t,z) - \sum_{k=1}^{\infty}\frac{\beta_k j^k}{k!}\times\frac{\partial^k a_3(t,z)}{\partial t^k} + \frac{jn^{'}\omega_3}{c}\times\left[\left(f_{33}|a_3(t,z)|^2 + 2\sum_{k\neq 3} f_{3k}|a_k(t,z)|^2\right)a_3(t,z) + 2f_{3412}a_1(t,z)a_2(t,z)a_4^*(t,z)e^{-j\Delta kz}\right] \tag{3.16}$$

$$\frac{\partial a_4(t,z)}{\partial z} = -\frac{\alpha_0}{2}a_4(t,z) - \sum_{k=1}^{\infty}\frac{\beta_k j^k}{k!}\times\frac{\partial^k a_4(t,z)}{\partial t^k} + \frac{jn^{'}\omega_4}{c}\times\left[\left(f_{44}|a_4(t,z)|^2 + 2\sum_{k\neq 4} f_{4k}|a_k(t,z)|^2\right)a_4(t,z) + 2f_{4312}a_1(t,z)a_2(t,z)a_3^*(t,z)e^{-j\Delta kz}\right] \tag{3.17}$$

where $\alpha_0$ is the attenuation constant in nonlinear environment, $\beta_k$ is the $n$th order dispersion, $\Delta k$ is the wave vector mismatch and $n'$ is the nonlinear refractive index, that can be calculated [35] as:

$$n' = \frac{3}{8n}Re\left(\chi^3_{zzzz}\right) \tag{3.18}$$

and the overlap integrals $f_{ij}$ and $f_{ijkl}$ are defined as follows:

$$f_{jk} = \frac{\iint |F_j(x,y)|^2|F_k(x,y)|^2dxdy}{\left(\iint |F_j(x,y)|^2dxdy\right)\left(\iint |F_k(x,y)|^2dxdy\right)} \tag{3.19}$$

$$f_{ijkl} = \frac{\langle F_i^* F_j^* F_l F_k\rangle}{\left[\langle |F_i|^2|F_j|^2|F_k|^2|F_l|^2\rangle\right]^{1/2}} \tag{3.20}$$

where angle brackets ($\langle\rangle$)denote integration over the transverse coordinates $x$ and $y$ and $f_{jk}$, $f_{ijkl}$ are the coefficients of the spatial distribution of the fiber mode. For the degeneration FWM case, where $\omega_1 = \omega_2$,

we have:

$$a_1(t,z) = a_2(t,z) = a_P(t,z)$$
$$a_3(t,z) = a_S(t,z)$$
$$a_4(t,z) = a_O(t,z) \tag{3.21}$$

We define $a_P(t,z)$ as a pump (clock) signal, $a_S(t,z)$ as the received signal in a nonlinear system and $a_O(t,z)$ as the output signal. Then, the coupled FWM equations are:

$$\frac{\partial a_P(t,z)}{\partial z} = -\frac{\alpha_0}{2}a_P(t,z) - \sum_{k=1}^{\infty}\frac{\beta_k j^k}{k!}\times\frac{\partial^k a_P(t,z)}{\partial t^k} + \frac{jn^{'}\omega_p}{c}\times\Bigg[\Bigg(2f_{pp}|a_P(t,z)|^2 + 2f_{ps}|a_S(t,z)|^2 + 2f_{po}|a_O(t,z)|^2\Bigg)a_P(t,z) + 2f_{pso}a_S(t,z)a_O(t,z)a_P^*(t,z)e^{j\Delta kz}\Bigg] \tag{3.22}$$

$$\frac{\partial a_O(t,z)}{\partial z} = -\frac{\alpha_0}{2}a_O(t,z) - \sum_{k=1}^{\infty}\frac{\beta_k j^k}{k!}\times\frac{\partial^k a_O(t,z)}{\partial t^k} + \frac{jn^{'}\omega_o}{c}\times\Bigg[\Bigg(2f_{oo}|a_O(t,z)|^2 + 2f_{os}|a_S(t,z)|^2 + 4f_{op}|a_P(t,z)|^2\Bigg)a_O(t,z) + 2f_{osp}a_S^*(t,z)a_P^2(t,z)e^{-j\Delta kz}\Bigg] \tag{3.23}$$

$$\frac{\partial a_S(t,z)}{\partial z} = -\frac{\alpha_0}{2}a_S(t,z) - \sum_{k=1}^{\infty}\frac{\beta_k j^k}{k!}\times\frac{\partial^k a_S(t,z)}{\partial t^k} + \frac{jn^{'}\omega_s}{c}\times\Bigg[\Bigg(2f_{ss}|a_S(t,z)|^2 + 2f_{so}|a_O(t,z)|^2 + 4f_{sp}|a_P(t,z)|^2\Bigg)a_S(t,z) + 2f_{sop}a_O^*(t,z)a_P^2(t,z)e^{-j\Delta kz}\Bigg] \tag{3.24}$$

These equations are nonlinear Schrödinger equations (NLS). For simplicity we define the nonlinear parameters as follows:

$$\gamma_{ij} = f_{ij}\frac{n'\omega_i}{c}; \qquad i,j\epsilon\{S,O,P\}$$
$$\gamma_{ijk} = f_{ijk}\frac{n'\omega_i}{c}; \qquad i,j,k\epsilon\{S,O,P\}$$

For the sake of simplicity, the coupled equations can be expressed in the frequency domain. If we suppose

that $A(\omega, z)$ is the Fourier transform of $a(t, z)$

$$A(\omega, z) = \int_{-\infty}^{\infty} a(t, z) e^{-j\omega t} dt$$

then, the coupled equations for $A_P(\omega, z)$, $A_O(\omega, z)$ and $A_S(\omega, z)$ are:

$$\begin{aligned}
\frac{\partial A_P(\omega, z)}{\partial z} =& -\frac{\alpha_0(\omega)}{2} A_P(\omega, z) - j\Delta(\omega) A_P(\omega, z) \\
&+ j \Bigg[ 2\gamma_{pp} \iint A_P(\omega_1, z) A_P^*(\omega_2, z) A_P(\omega - \omega_1 + \omega_2, z) d\omega_1 d\omega_2 \\
&+ 2\gamma_{ps} \iint A_S(\omega_1, z) A_S^*(\omega_2, z) A_P(\omega - \omega_1 + \omega_2, z) d\omega_1 d\omega_2 \\
&+ 2\gamma_{po} \iint A_O(\omega_1, z) A_O^*(\omega_2, z) A_P(\omega - \omega_1 + \omega_2, z) d\omega_1 d\omega_2 \\
&+ 2\gamma_{pso} e^{j\Delta kz} \iint A_P^*(\omega_2, z) A_S^*(\omega_1, z) A_O(\omega - \omega_1 + \omega_2, z) d\omega_1 d\omega_2 \Bigg]
\end{aligned} \tag{3.25}$$

$$\begin{aligned}
\frac{\partial A_O(\omega, z)}{\partial z} =& -\frac{\alpha_0(\omega)}{2} A_O(\omega, z) - j\Delta(\omega) A_O(\omega, z) \\
&+ j \Bigg[ \gamma_{oo} \iint A_O(\omega_1, z) A_O^*(\omega_2, z) A_O(\omega - \omega_1 + \omega_2, z) d\omega_1 d\omega_2 \\
&+ 2\gamma_{os} \iint A_S(\omega_1, z) A_S^*(\omega_2, z) A_O(\omega - \omega_1 + \omega_2, z) d\omega_1 d\omega_2 \\
&+ 4\gamma_{op} \iint A_P(\omega_1, z) A_P^*(\omega_2, z) A_O(\omega - \omega_1 + \omega_2, z) d\omega_1 d\omega_2 \\
&+ 2\gamma_{osp} e^{-j\Delta kz} \iint A_S^*(\omega_2, z) A_P^*(\omega_1, z) A_P(\omega - \omega_1 + \omega_2, z) d\omega_1 d\omega_2 \Bigg]
\end{aligned} \tag{3.26}$$

$$\begin{aligned}\frac{\partial A_S(\omega,z)}{\partial z} =& -\frac{\alpha_0(\omega)}{2}A_S(\omega,z) - j\Delta(\omega)A_S(\omega,z) \\ &+ j\Bigg[\gamma_{ss}\iint A_S(\omega_1,z)A_S^*(\omega_2,z)A_S(\omega-\omega_1+\omega_2,z)d\omega_1 d\omega_2 \\ &+ 2\gamma_{so}\iint A_O(\omega_1,z)A_O^*(\omega_2,z)A_S(\omega-\omega_1+\omega_2,z)d\omega_1 d\omega_2 \\ &+ 4\gamma_{sp}\iint A_P(\omega_1,z)A_P^*(\omega_2,z)A_S(\omega-\omega_1+\omega_2,z)d\omega_1 d\omega_2 \\ &+ 2\gamma_{sop}e^{-j\Delta kz}\iint A_O^*(\omega_2,z)A_P^*(\omega_1,z)A_P(\omega-\omega_1+\omega_2,z)d\omega_1 d\omega_2\Bigg] \end{aligned} \tag{3.27}$$

where $\alpha_0(\omega)$ is the attenuation factor of fiber and $\Delta(\omega)$ is the linear dispersion in fiber, that is defined as

$$\Delta(\omega) = \sum_{k=1}^{\infty}\beta_k\frac{\omega^k}{k!}$$

## 3.3 Solving the FWM Equations by Volterra Series

The NLS equations are a set of nonlinear partial differential equations whose exact analytical solution generally is very difficult to obtain except for some specific cases. A large number of approximate analytical and numerical methods have been developed to solve the NLS equations. One of the most powerful methods for describing the nonlinear system is Volterra series. This method is similar to the Taylor series, but it is able to capture memory effects. The Taylor series can be used to approximate the response of a nonlinear system to a given input if the output of this system depends strictly on the input at that particular time. While Volterra series are capable of capturing the response os a system whose current state depends on previous, current and future state. Expanding the first three terms of the Volterra series provides a good approximation of the solution of the NLS equations.

### 3.3.1 Volterra Series

Volterra theory and series were mentioned for first time in 1877 by Vito Volterra. The main benefit of Volterra series in compare of other series is, the output of the nonlinear system depends on the input to the system at all the times. The Volterra series of a system with input $x(t)$ and output $y(t)$ can be expressed as

[40], [41]:

$$y(t) = k_0 + \sum_{n=1}^{\infty} \frac{1}{n!} \int_{-\infty}^{\infty} \dots \int_{-\infty}^{\infty} k_n(s_1, s_2, \dots, s_n) x(t-s_1) x(t-s_2) \dots \times x(t-s_n) ds_1 ds_2 \dots ds_n \quad (3.28)$$

where $k_n$ is the $n$th Volterra kernel, which can be considered as the impulse response of higher order of the system. The Fourier transform of (3.28) can be written as:

$$Y(\omega) = \sum_{n=1}^{\infty} \int \dots \int H_n(\omega_1, \dots, \omega_{n-1}, \omega - \omega_1 - \dots \omega_{n-1}) X(\omega_1) \dots X(\omega_{n-1})$$
$$\times X(\omega - \omega_1 - \dots \omega_{n-1}) d\omega_1 \dots d\omega_{n-1} \quad (3.29)$$

where $X(\omega)$, $Y(\omega)$ are the Fourier transforms of $x(t)$, $y(t)$, respectively.

As an example, we now solve with the Volterra series the following nonlinear equation.

$$\frac{\partial a(t,z)}{\partial z} = -\frac{\alpha_0}{2} a(t,z) - \beta_1 \frac{\partial a(t,z)}{\partial t} - \frac{j}{2} \beta_2 \frac{\partial^2 a(t,z)}{\partial t^2} + j\gamma |a(t,z)|^2 a(t,z) \quad (3.30)$$

If the input is $a(t,0)$ and the output is $a(t,z)$ we have:

$$Y(\omega) = A(\omega, z)$$
$$X(\omega) = A(\omega,0) = A(\omega) \quad (3.31)$$

By substituting (3.31) in (3.30), we can write the two first terms of the response as follows:

$$A(\omega, z) = H_1(\omega, z) A(\omega) + \iint H_3(\omega_1, \omega_2, \omega - \omega_1 + \omega_2, z) A(\omega_1) A^*(\omega_2) A(\omega - \omega_1 + \omega_2) d\omega_1 d\omega_2 \quad (3.32)$$

Supposing that $G_1(\omega) = -\alpha(\omega) + j\Delta(\omega)$ and $G_3(\omega) = j\gamma$, we obtain [42]:

$$H_1(\omega, z) = e^{G_1(\omega) z} = e^{(-\alpha(\omega) - j\Delta(\omega)) z} \quad (3.33)$$

$$H_3(\omega_1, \omega_2, \omega_3, z) = G_3 \frac{e^{(G_1(\omega_1) + G_1^*(\omega_2) + G_1(\omega_3)) z} - e^{G_1(\omega_1 - \omega_2 + \omega_3) z}}{G_1(\omega_1) + G_1^*(\omega_2) + G_1(\omega_3) - G_1(\omega_1 - \omega_2 + \omega_3)} \quad (3.34)$$

Considering now a system with different inputs, $x_1(t)$, $x_2(t)$, ..., $x_k(t)$ and an output, $y(t)$, we can express Volterra series as follows:

$$\begin{aligned} y(t) = k_0 + \sum_{i_1=1}^{\infty}\sum_{i_2=1}^{\infty}\dots\sum_{i_k=1}^{\infty}\frac{1}{n!}\int_{-\infty}^{\infty}\dots\int_{-\infty}^{\infty}\Bigg[ & k_{i_1,i_2,\dots i_k}(s_1,s_2,...,s_n) \\ & \times x_1(t-s_1)...x_1(t-s_{i_1}) \\ & \times x_2(t-s_{(1+i_1)})...x_2(t-s_{(i_1+i_2)}) \\ & \times ... \\ & \times x_k(t-s_{(1+i_1+\dots+i_{k-1})})...x_k(t-s_n)\Bigg] ds_1 ds_2 ... ds_n \end{aligned} \tag{3.35}$$

where $i_1 + i_2 + ... + i_k = n$. In frequency domain we have:

$$\begin{aligned} Y(\omega) = \sum_{i_1=0}^{\infty}\sum_{i_2=0}^{\infty}\dots\sum_{i_k=0}^{\infty}\int_{-\infty}^{\infty}\dots\int_{-\infty}^{\infty}\Bigg[ & H_{i_1,i_2,\dots,i_k}(\omega_1,...,\omega_{n-1},\omega-\omega_1-...\omega_{n-1}) \\ & \times X_1(\omega_1)...X_1(\omega_{i_1}) \\ & \times X_2(\omega_{i_1+1})...X_2(i_1+i_2) \\ & \times ... \\ & \times X_k(\omega_{1+i_1+\dots+i_{k-1}})...X_k(\omega-\omega_1-...\omega_{n-1})\Bigg] d\omega_1 d\omega_2 ... d\omega_{n-1} \end{aligned} \tag{3.36}$$

### 3.3.2 Solving NLS equations by Volterra series

Regarding to expressed equations in last section, we consider FWM in degenerate state for a system with inputs, $A_s(\omega,0)$, $A_p(\omega,0)$ and for outputs $A_o(\omega,z)$, $A_s(\omega,z)$. The relation between inputs and outputs are described by (3.25), (3.26), (3.27). For simplicity, we suppose that in these equations in the length of the nonlinear environment $A_s(\omega,z)$, $A_o(\omega,z)$ do not have any influence on pump signal (clock), $A_p(\omega,z)$. Mentioned to (3.36), Volterra series for this system are as follows [43]:

$$\begin{aligned} A_p(\omega,z) = \sum_{\substack{k=1 \\ k:odd}}^{\infty}\int\dots\int H_{p_k}(\omega_1,\dots,\omega_{k-1},\omega-\omega_1+...+\omega_{k-1},z) \\ \times A_p(\omega_1)A_p^*(\omega_2)...A_p^*(\omega_{k-1})A_p(\omega-\omega_1+...+\omega_{k-1})d\omega_1 d\omega_2 ... d\omega_{k-1} \end{aligned} \tag{3.37}$$

where we can assume that since the pump signal $A_p$ has a much bigger amplitude (in the order 10-100 times) than $A_s$ and $A_o$, we can neglect the terms related to $A_s$ and $A_o$.

$$
\begin{aligned}
A_s(\omega,z) = & \sum_{\binom{k=1}{k:odd}}^{\infty} \int \dots \int H_{s_k}(\omega_1,\dots,\omega_{k-1},\omega-\omega_1+\dots+\omega_{k-1},z) \\
& \times A_s(\omega_1)A_s^*(\omega_2)\dots A_s^*(\omega_{k-1})A_s(\omega-\omega_1+\dots+\omega_{k-1})d\omega_1 d\omega_2\dots d\omega_{k-1} \\
& + \sum_{\binom{l=1}{l:odd}}^{\infty}\sum_{\binom{k=2}{k:even}}^{\infty} \int \dots \int H_{s_{l,k}}(\omega_1,\dots,\omega_{k+l-1},\omega-\omega_1+\dots+\omega_{k+l-1},z) \\
& \times A_p(\omega_1)A_p^*(\omega_2)\dots A_p(\omega_{k-1})A_p^*(\omega_k) \\
& \times A_s(\omega_{k+1})A_s^*(\omega_{k+2})\dots A_s^*(\omega_{k+l-2})A_s^*(\omega_{k+l-1}) \\
& \times A_s(\omega-\omega_1+\dots+\omega_{k+l-1})d\omega_1 d\dots d\omega_{k+l-1} \\
& + \sum_{\binom{l=1}{l:odd}}^{\infty}\sum_{\binom{k=2}{k:even}}^{\infty} \int \dots \int H'_{s_{l,k}}(\omega_1,\dots,\omega_{k+l-1},\omega-\omega_1+\dots+\omega_{k+l-1},z) \\
& \times A_p(\omega_1)A_p^*(\omega_2)\dots A_p^*(\omega_{k-2})A_p(\omega_{k-1}) \\
& \times A_s^*(\omega_k)A_s(\omega_{k+1})\dots A_s(\omega_{k+l-2})A_s^*(\omega_{k+l-1}) \\
& \times A_p(\omega-\omega_1+\dots+\omega_{k+l-1})d\omega_1\dots d\omega_{k+l-1}
\end{aligned}
\tag{3.38}
$$

$$
\begin{aligned}
A_o(\omega,z) = & \sum_{\binom{k=3}{k:odd}}^{\infty} \int \dots \int H_{o_k}(\omega_1,\dots,\omega_{k-1},\omega-\omega_1+\dots+\omega_{k-1},z) \\
& \times A_s(\omega_1)A_s^*(\omega_2)\dots A_s^*(\omega_{k-1})A_s(\omega-\omega_1+\dots+\omega_{k-1})d\omega_1 d\omega_2\dots d\omega_{k-1} \\
& + \sum_{\binom{l=1}{l:odd}}^{\infty}\sum_{\binom{k=4}{k:even}}^{\infty} \int \dots \int H_{o_{l,k}}(\omega_1,\dots,\omega_{k+l-1},\omega-\omega_1+\dots+\omega_{k+l-1},z) \\
& \times A_p(\omega_1)A_p^*(\omega_2)\dots A_p(\omega_{k-1})A_p^*(\omega_k) \\
& \times A_s(\omega_{k+1})A_s^*(\omega_{k+2})\dots A_s^*(\omega_{k+l-2})A_s(\omega_{k+l-1}) \\
& \times A_s(\omega-\omega_1+\dots+\omega_{k+l-1})d\omega_1\dots d\omega_{k+l-1} \\
& + \sum_{\binom{l=1}{l:odd}}^{\infty}\sum_{\binom{k=2}{k:even}}^{\infty} \int \dots \int H'_{o_{l,k}}(\omega_1,\dots,\omega_{k+l-1},\omega-\omega_1+\dots+\omega_{k+l-1},z) \\
& \times A_p(\omega_1)A_p^*(\omega_2)\dots A_p^*(\omega_{k-2})A_p(\omega_{k-1}) \\
& \times A_s^*(\omega_k)A_s(\omega_{k+1})\dots A_s(\omega_{k+l-2})A_s^*(\omega_{k+l-1}) \\
& \times A_p(\omega-\omega_1+\dots+\omega_{k+l-1})d\omega_1 d\dots d\omega_{k+l-1}
\end{aligned}
\tag{3.39}
$$

For obtaining the polynomial of Volterra series for $A_o(\omega,z)$ and $A_s(\omega,z)$, we substitute equations (3.36), (3.37), (3.38) in (3.25), (3.26), (3.27), obtaining:

$$\frac{\partial H_{p_k}(\omega_1,...,\omega_k,z)}{\partial z} = G_1(\omega_1-\omega_2+...+\omega_k)H_{p_k}(\omega_1,...,\omega_k,z)$$
$$+ j2\gamma_{pp}\sum_{\binom{l,m,n}{l+m+n=k}} H_{p_l}(\omega_1,...,\omega_k,z)H^*_{p_m}(\omega_{l+1},...,\omega_{l+m},z)H_{p_n}(\omega_{l+m+1},...,\omega_k,z) \tag{3.40}$$

$$\frac{\partial H_{s_k}(\omega_1,...,\omega_k,z)}{\partial z} = G_1(\omega_1-\omega_2+...+\omega_k)H_{s_k}(\omega_1,...,\omega_k,z)$$
$$+ j2\gamma_{ss}\sum_{\binom{l,m,n}{l+m+n=k}} H_{s_l}(\omega_1,...,\omega_k,z)H^*_{s_m}(\omega_{l+1},...,\omega_{l+m},z)H_{s_n}(\omega_{l+m+1},...,\omega_k,z) \tag{3.41}$$

$$\frac{\partial H_{s_{l,k}}(\omega_1,...,\omega_{k+l},z)}{\partial z} = G_1(\omega_1-\omega_2+...+\omega_{k+l})H_{s_{l,k}}(\omega_1,...,\omega_{k+l},z) + j2\gamma_{ss}\sum_{\binom{p,m,n}{p+m+n=l}}$$
$$\sum_{\binom{h,i,j}{h+i+j=k}}\left[H_{s_{p,h}}(\omega_1,...,\omega_{p+h},z)H^*_{s_{m,i}}(\omega_{p+h+1},...,\omega_{p+h+m+i},z)H_{s_{n,j}}(\omega_{p+h+m+i+1},...,\omega_{k+l},z)\right]$$
$$j2\gamma_{so}\sum_{\binom{\binom{p,m,n}{p,m\geq 3}}{p+m+n=l}}\sum_{\binom{h,i,j}{h+i+j=k}}\left[H_{o_{p,h}}(\omega_1,...,\omega_{p+h},z)H^*_{o_{m,i}}(\omega_{p+h+1},...,\omega_{p+h+m+i},z)H_{s_{n,j}}(\omega_{p+h+m+i+1},...,\omega_{k+l},z)\right]$$
$$+ j4\gamma_{sp}\sum_{m,n}H_{p_m}(\omega_1,...,\omega_m,z)H^*_{p_n}(\omega_{m+1},...,\omega_{m+n},z)H_{s_{l,(k-m-n)}}(\omega_{m+n+1},...,\omega_{k+l},z)$$
$$+ j2\gamma_{sop}e^{-j\Delta kz}\sum_{m,n}H_{p_m}(\omega_1,...,\omega_m,z)H^{'*}_{o_{l,(k-m-n)}}(\omega_{m+1},...,\omega_{k-n+l},z)H_{p_n}(\omega_{k-n+l+1},...,\omega_{k+l},z) \tag{3.42}$$

$$\frac{\partial H^{'}_{s_{l,k}}(\omega_1,...,\omega_{k+l},z)}{\partial z} = G_1(\omega_1-\omega_2+...+\omega_{k+l})H^{'}_{s_{l,k}}(\omega_1,...,\omega_{k+l},z) + j2\gamma_{ss}\sum_{\binom{p,m,n}{p+m+n=l}}$$
$$\sum_{\binom{h,i,j}{h+i+j=k}}\left[H^{'}_{s_{p,h}}(\omega_1,...,\omega_{p+h},z)H^{'*}_{s_{m,i}}(\omega_{p+h+1},...,\omega_{p+h+m+i},z)H^{'}_{s_{n,j}}(\omega_{p+h+m+i+1},...,\omega_{k+l},z)\right]$$
$$j2\gamma_{so}\sum_{\binom{\binom{p,m,n}{p,m\geq 3}}{p+m+n=l}}\sum_{\binom{h,i,j}{h+i+j=k}}\left[H^{'}_{o_{p,h}}(\omega_1,...,\omega_{p+h},z)H^{'*}_{o_{m,i}}(\omega_{p+h+1},...,\omega_{p+h+m+i},z)H^{'}_{s_{n,j}}(\omega_{p+h+m+i+1},...,\omega_{k+l},z)\right]$$
$$+ j4\gamma_{sp}\sum_{m,n}H_{p_m}(\omega_1,...,\omega_m,z)H^*_{p_n}(\omega_{m+1},...,\omega_{m+n},z)H^{'}_{s_{l,(k-m-n)}}(\omega_{m+n+1},...,\omega_{k+l},z)$$
$$+ j2\gamma_{sop}e^{-j\Delta kz}\sum_{m,n}H_{p_m}(\omega_1,...,\omega_m,z)H^*_{o_{l,(k-m-n)}}(\omega_{m+1},...,\omega_{k-n+l},z)H_{p_n}(\omega_{k-n+l+1},...,\omega_{k+l},z) \tag{3.43}$$

$$\frac{\partial H_{o_{l,k}}(\omega_1,...,\omega_{k+l},z)}{\partial z} = G_1(\omega_1-\omega_2+...+\omega_{k+l})H_{o_{l,k}}(\omega_1,...,\omega_{k+l},z) + j2\gamma_{oo}\sum_{\binom{p,m,n}{p+m+n=l}}$$
$$\sum_{\binom{h,i,j}{h+i+j=k}}\left[H_{o_{p,h}}(\omega_1,...,\omega_{p+h},z)H^*_{o_{m,i}}(\omega_{p+h+1},...,\omega_{p+h+m+i},z)H_{o_{n,j}}(\omega_{p+h+m+i+1},...,\omega_{k+l},z)\right]$$
$$j2\gamma_{os}\sum_{\binom{\binom{p,m,n}{p,m\geq 3}}{p+m+n=l}}\sum_{\binom{h,i,j}{h+i+j=k}}\left[H_{s_{p,h}}(\omega_1,...,\omega_{p+h},z)H^*_{s_{m,i}}(\omega_{p+h+1},...,\omega_{p+h+m+i},z)H_{o_{n,j}}(\omega_{p+h+m+i+1},...,\omega_{k+l},z)\right]$$
$$+ j4\gamma_{op}\sum_{m,n}H_{p_m}(\omega_1,...,\omega_m,z)H^*_{p_n}(\omega_{m+1},...,\omega_{m+n},z)H_{o_{l,(k-m-n)}}(\omega_{m+n+1},...,\omega_{k+l},z)$$
$$+ j2\gamma_{osp}e^{-j\Delta kz}\sum_{m,n}H_{p_m}(\omega_1,...,\omega_m,z)H^{'*}_{s_{l,(k-m-n)}}(\omega_{m+1},...,\omega_{k-n+l},z)H_{p_n}(\omega_{k-n+l+1},...,\omega_{k+l},z) \quad (3.44)$$

$$\frac{\partial H^{'}_{o_{l,k}}(\omega_1,...,\omega_{k+l},z)}{\partial z} = G_1(\omega_1-\omega_2+...+\omega_{k+l})H^{'}_{o_{l,k}}(\omega_1,...,\omega_{k+l},z) + j2\gamma_{oo}\sum_{\binom{p,m,n}{p+m+n=l}}$$
$$\sum_{\binom{h,i,j}{h+i+j=k}}\left[H^{'}_{o_{p,h}}(\omega_1,...,\omega_{p+h},z)H^{'*}_{o_{m,i}}(\omega_{p+h+1},...,\omega_{p+h+m+i},z)H^{'}_{o_{n,j}}(\omega_{p+h+m+i+1},...,\omega_{k+l},z)\right]$$
$$j2\gamma_{os}\sum_{\binom{\binom{p,m,n}{p,m\geq 3}}{p+m+n=l}}\sum_{\binom{h,i,j}{h+i+j=k}}\left[H^{'}_{s_{p,h}}(\omega_1,...,\omega_{p+h},z)H^{'*}_{s_{m,i}}(\omega_{p+h+1},...,\omega_{p+h+m+i},z)H^{'}_{o_{n,j}}(\omega_{p+h+m+i+1},...,\omega_{k+l},z)\right]$$
$$+ j4\gamma_{op}\sum_{m,n}H_{p_m}(\omega_1,...,\omega_m,z)H^*_{p_n}(\omega_{m+1},...,\omega_{m+n},z)H^{'}_{o_{l,(k-m-n)}}(\omega_{m+n+1},...,\omega_{k+l},z)$$
$$+ j2\gamma_{osp}e^{-j\Delta kz}\sum_{m,n}H_{p_m}(\omega_1,...,\omega_m,z)H^*_{s_{l,(k-m-n)}}(\omega_{m+1},...,\omega_{k-n+l},z)H_{p_n}(\omega_{k-n+l+1},...,\omega_{k+l},z) \quad (3.45)$$

By definition, in above relationships we have:

$$H^{'}_{s_{m,o}}(\omega_1,...,\omega_m,z) = H_{s_{m,o}}(\omega_1,...,\omega_m,z) = H_{s_m}(\omega_1,...,\omega_m,z) \quad (3.46)$$

In these equations we suppose that $A_o(\omega,z)=0$ in $z=0$. Therefore with considering equation (3.38), all polynomials $H_{o_k}(\omega_1,...,\omega_k,z)$ are zero.

## 3.4 Application of FWM in Optical Systems

FWM has many applications in telecommunication systems as well as optical processing, including the ability to build optical gates, phase conjugation, wavelength conversion and real-time holographic imaging.

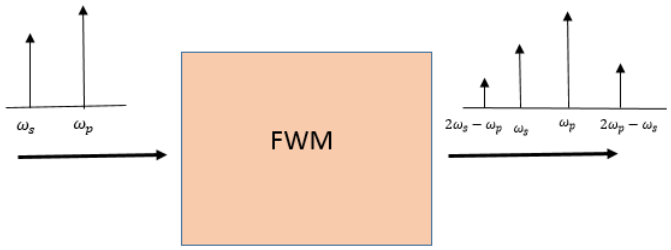


Figure 3.2: Degenerate Four Wave Mixing process with input and output frequencies.

### 3.4.1 Optical AND Gate

AND gates have wide applications in optical systems. One of the most important use of all-optical AND gate is in the receivers of optical multiple access systems. For example, in OTDM systems we need to separate the desired signal from other adjacent signals in time domain. But because of the small bandwidth of light pulses, even the fastest electronic photo-detectors are not able to separate these signals. So it is necessary to use all-optical processing on the received optical signal before the electronic photo-detection.

In Fig. 3.2 we suppose that two signals with frequencies $\omega_s$ and $\omega_p$ enter a nonlinear device. Note that for this AND gate phase-matching conditions must be satisfied in order to obtain degenerate four wave mixing (DFWM). As described in section 3.1, the two input signal generate two additional frequencies at the output, called conjugate and satellite signals:

$$\begin{aligned} \omega_{conjugate} &= 2\omega_p - \omega_s \\ \omega_{satellite} &= 2\omega_s - \omega_p \end{aligned} \tag{3.47}$$

The structure of a time gate by using FWM is shown in Fig. 3.3. In this configuration a semiconductor optical amplifier (SOA) has been used as a nonlinear environment for obtaining the FWM process. In SOA, FWM is done by using carrier density modulation. Owning to the nonlinear interaction between the pump

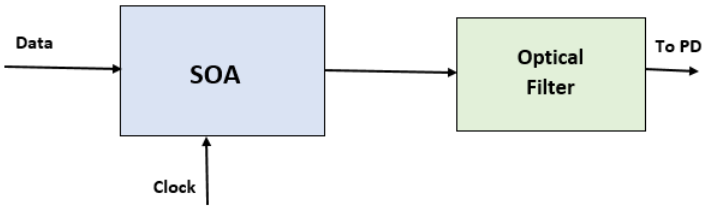


Figure 3.3: Using DFWM applied to an all-optical AND gate.

signal with carrier frequency $\omega_s$, a part of their energy has been transformed into a new signal with carrier frequency $(2\omega_p - \omega_s)$. If any of these two signals were zero then no energy will be transformed to the new frequency and the output signal will be zero. So this structure will acts just like an all optical AND gate. At the output of nonlinear media an optical filter separates the output signal with the central frequency $(2\omega_p - \omega_s)$ from the pump and input signals.

### 3.4.2 Wavelength Converter

Wavelength converters are used to change the frequency of the input signal. Transforming a wavelength to other wavelength has many applications in optical telecommunications, especially in switching and routing of optical carriers. There are several approaches to build wavelength converters and using FWM supposes two important benefits in comparison to other alternatives. First this method can be performed at high speed and a second one is its ability to convert signals of the same band frequency at the same time.

Again, we consider the case of degenerate FWM. We have a pump signal with frequency $\omega_p$ and an input signal with frequency $\omega_s$, obtaining frequency $2\omega_p - \omega_s$ at the output. We can adjust the output frequency by changing the frequency of the pump signal.

### 3.4.3 Phase Conjugation

Phase conjugation is a physical transformation of a wave field where the resulting field has a reversed propagation direction but keeps its amplitude and phase. In fact, It is possible, using nonlinear optical processes, to exactly reverse the propagation direction and phase variation of a beam of light. In other words, the wave seems to go back in time. It is useful when a signal through the heterogeneous environments has been distorted. Because by phase conjugation and pass signal from same path, distortion would be lost.

FWM can be used to perform phase conjugation on the input signal. Considering equations (3.14), (3.15),

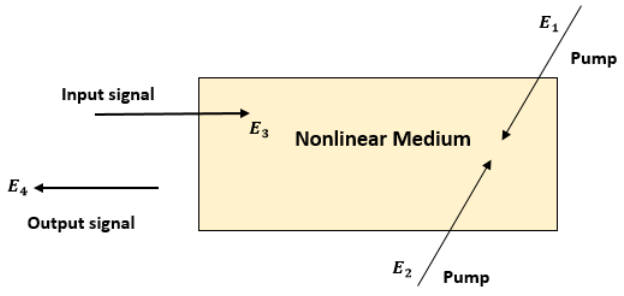


Figure 3.4: Phase conjugation by FWM.

(3.16), (3.17)and also with direction of wave propagation as shown in Fig. 3.4 can apply phase conjugation. If all signals are in the same frequency and in the degenerate FWM case and also mention to $E_1$, $E_2$ are opposite direction, output signal $E_4$ would be reversed propagation direct of $E_3$. So with phase matching condition, nonlinear media acts as a mirror phase conjugation for input signal. One of application of this phase conjugation is in lasers. With using this mirror in cavity of laser can eliminate the distortion due to lasing environment on the signals in cavity.

### 3.4.4 Conclusions

In this chapter, we have considered the application of nonlinear optical techniques in optical communications, focusing on FWM. According to the limiting response time of electrical parts in optical communications, it is necessary to use all-optical processing in receivers. FWM could be used as combiner (AND gate) in receivers of multiple access systems, reducing the effect of interference due to other users. We have described the mathematical model of FWM and the equations related to input, pump (clock) and output signals, (3-25), (3-26), (3-27). We have solved these equations using Volterra series. The chapter has described also some applications of FWM in the telecommunications field. For more details about the kernels of Volterra series and the detailed steps of the calculation, please refer to Appendix B.

Chapter 4

# Bit Detection in Optical TDM Networks

Optical networks are a promising technology in providing high-speed access (Tbps). Optical sources can generate sub-picosecond pulses and transmit the information at significantly high data-rates. An important goal in the area of optical communications is to provide high-speed data transmission by exploiting the intrinsically fast behaviour of the optical domain. Detecting these ultra-short pulses is a challenge in optical systems since commercially available detectors are not fast enough. Therefore, optical signal processing is a key technology for detection and signal recovery in ultra-fast optical networks.

One of the traditional techniques for implementing optical networks is optical time division multiplexing (OTDM). This is a powerful optical multiplexing technique that increases the channel usage in optical fibers and enables high capacity transmission of data over a single optical channel. Without applying multiplexing, exploiting the existing optical fiber bandwidth (Tb/s) is problematic since the effective usage of its maximum bandwidth depends on the capability of the electronics within the terminal and repeater equipment. Commercially available electronic components are limited a data-rate of around 50Gb/s, and hence, impose a bottleneck on high-speed communication. OTDM is a popular technique to overcome this bottleneck.

OTDM networks use ultra-short light pulses for data transmission, but even the fastest photo-detectors are unable to separate data from the desired user from signals produced by adjacent users. Therefore, it is vital to apply all-optical signal processing on the received optical signal before photo-detection [44]. In these systems, it is an effective technique to use optical time gating at the receiver side to extract the desired user signal from the received signal. This approach requires an optical clock recovery procedure. However, increasing the data rate in OTDM networks means the accuracy of the optical clock recovery decreases [3], [45] and the system performance is consequently degraded.

Different aspects of optical clock recovery have been studied by various researchers. For example, the effect of the pattern sequence length on optical clock recovery (OCR) using passive filtering is evaluated in [46]. The study is focused on the quality of the optical clock recovered with the passive filtering, and also on the relation between quality and data sequence length. An optoelectronic phase-locked loop (PLL) with three-wave mixing in a periodically poled lithium niobate (PPLN) for the phase comparator is presented in [47]. A simple all-optical clock recovery technique for short data packets at 160 Gb/s and beyond, based on the Fabry-Pérot filter (FPF) is suggested in [48]. The novel feature of the technique is the use of a highly nonlinear fiber followed by an optical bandpass filter (centered at the initial carrier wavelength) which acts as an ultrafast power limiter by removing the amplitude modulation of the FPFs output, as well as providing the clock signal. Although one of the questions to be answered in any clock recovery system is the optimum value of the clock pulse width, the aforementioned works did not address this topic.

In this chapter we analyse and simulate the effect of the clock signal's pulse width on the bit error rate (BER) in the receiver. We have considered a time jitter in the clock signal and the aim is to find an optimum value for the clock signal pulse width to minimise the BER of the receiver. The BER is calculated from the eye diagram for different parameters and plotted versus the pulse width of the clock signal. To the best of our knowledge, this is the first analytical study on the influence of the pulse width of the clock signal on the quality of the received signal.

## 4.1 Structure of Optical Clock Recovery in an OTDM Receiver

In high-speed OTDM networks, time gating in the optical domain is a very important issue for achieving a good performance in detecting the received data bits. Optical time gating requires optical clock recovery, which is an essential requirement for synchronising the clock signal with the received data signal. Fig. 4.1 shows the configuration of a typical optical clock recovery system [49]. As depicted, high-speed optical data and clock signals are combined and entered into an Erbium-doped fiber amplifier (EDFA) as a nonlinear

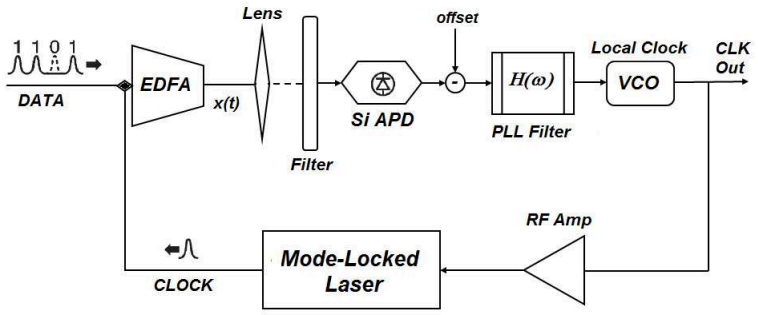


Figure 4.1: Configuration of the optical clock recovery in optical networks using a mode-locked laser.

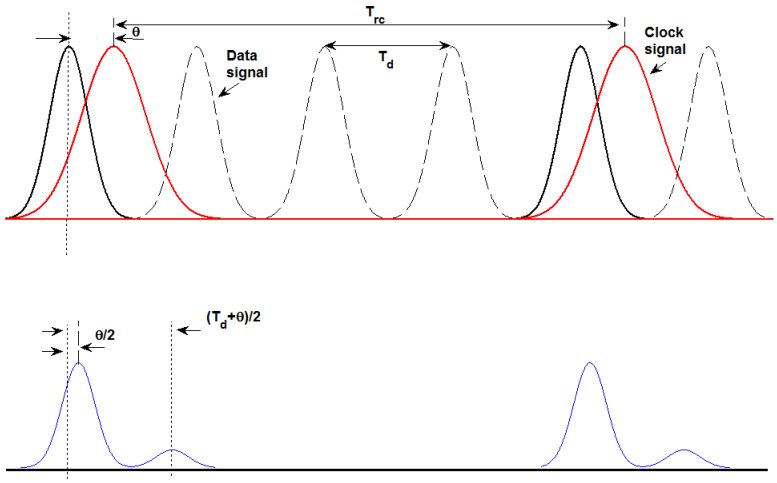


Figure 4.2: Data and clock signals and their generated output when there is jitter in the clock signal.

media and then focused on the surface of a silicon avalanche photodiode (APD). The combination of the EDFA and the filter can be considered as an optical AND gate [50]. The optical clock signal is generated by a mode-locked semiconductor laser diode driven by a voltage-controlled microwave oscillator. The low-pass filter shown in the diagram is used to block any short wavelengths that would otherwise generate a linear photocurrent. The loop filter, $H(\omega)$, is designed so that the closed-loop transfer function has the desired bandwidth.

In high-speed communication systems, the accuracy of the clock recovery decreases because of the shorter duration of the pulses, and consequently, a time jitter appears in the clock signal. This time jitter can cause errors in the detection of the desired user data, as shown in Fig. 4.2. In this work, we have assumed the jitter to be the main limiting factor at the receiver and so the effects of amplified spontaneous emission (ASE) [51], thermal, shot and beat noises and nonlinear phenomena such as Raman and Brillouin scattering are not considered in order to simplify the analysis.

Moreover, by widening the pulse width of the clock signal, the receiver's performance can be improved. This manipulation can be helpful in the detection of a larger portion of the data pulse. As shown in Fig. 4.3, by increasing the pulse width of the clock signal, a part of the pulses from adjacent users will also be gathered by the detector. This effect generates another error source at the output signal and this error becomes larger when increasing the pulse width of the clock. By widening the pulse width, the greatest error occurs when the desired signal is zero and the adjacent bit is "1", since the clock will be mixed with them and the detector may detect a one instead of a zero. This effect is shown in Fig. 4.4. Considering the trade-off between the two error sources, we hypothesize that there is an optimum value for the clock signal

pulse width, for which the BER is minimized.

One of the most important characteristics of optical clock sources is their flexility regarding the manipulation of the clock signal. For example, [52] proposes an approach for synchronizing the mode locked laser (MLL) with a second fiber laser via an intracavity electro-optic modulator (EOM), while [53] presents a method to alter the pulse-width of the laser by manipulating the grating bandwidth, utilizing electro-optic modulation. Using these two techniques the pulse-width an appropriate frequency of the clock signal can be set to the desired values.

## 4.2 Calculation of the Bit Error Rate

In this section we analyze the bit error rate (BER) by considering the phase error in the optical clock recovery system. We only consider the jitter of the clock signal as the noise source, and ignore other noises. The scheme of a receiver using time gating in OTDM networks is shown in Fig. 4.5.

The output of the EDFA can be approximated [54] as

$$x(t) = \eta_F e^{-\alpha L}(gL)^2 a_c^2(t-\tau)a_d(t), \tag{4.1}$$

where $\tau$ is the delay between clock and data signals, $a_c(t)$ and $a_d(t)$ are respectively the optical powers of

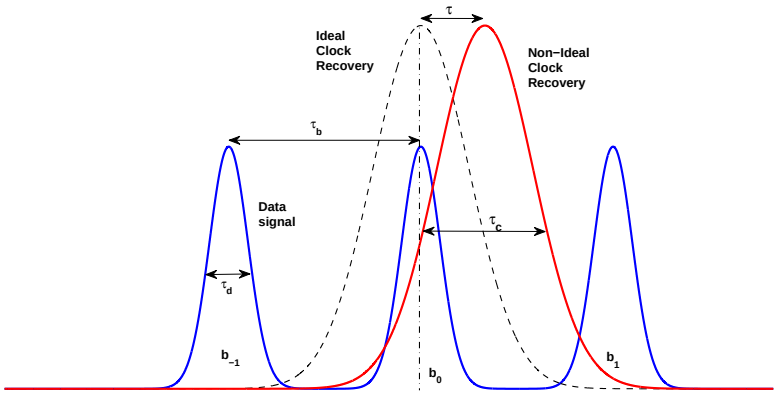


Figure 4.3: Non-ideal clock recovery and its time delay respect to the received data signal when the desired bit is one.

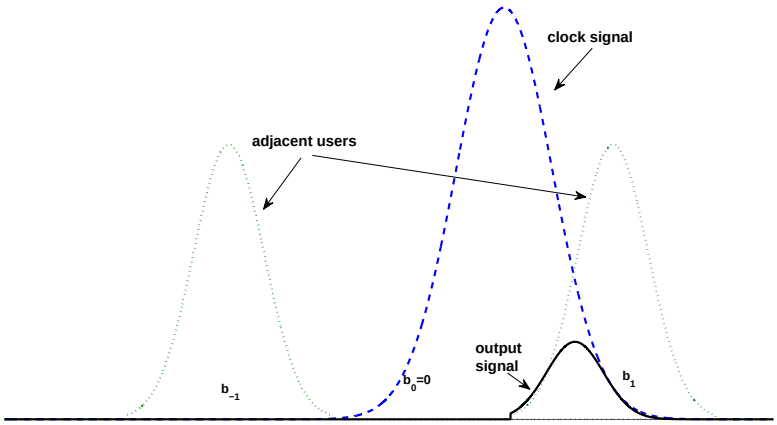


Figure 4.4: Non-ideal clock recovery and output signal when the desired bit is zero and the adjacent user's bit is one.

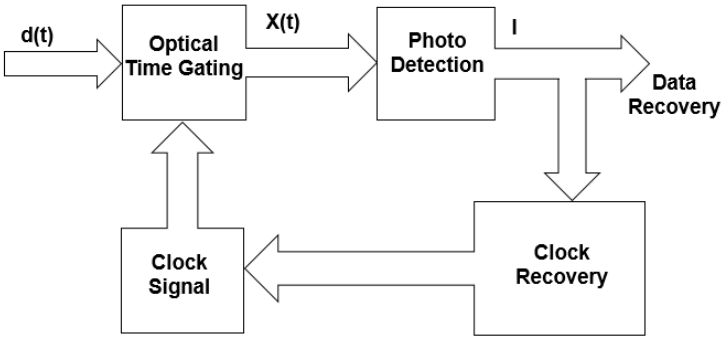


Figure 4.5: Diagram of the OTDM receiver based on optical time-gating.

the clock and data signals with peak powers of $P_c$ and $P_d$, $L$ is the length of the nonlinear medium, $\alpha$ is the loss of the nonlinear medium, $g$ is the third order susceptibility and $\eta_F$ is a measure of the four-wave mixing (FWM) defined [55] as

$$\eta_F = \left| \frac{1 - e^{-(\alpha + j\Delta k)L}}{(\alpha + j\Delta k)L} \right|^2 . \tag{4.2}$$

Here we assume that the mismatch factor, $\Delta k$, is zero. For simplicity, we define $\gamma = \eta_F e^{-\alpha L}(gL)^2$, as a coefficient that represents the strength of the nonlinearity of the EDFA, which only depends on the physical characteristics of the nonlinear medium and is assumed to be time invariant. We assume that $\tau$ is a zero

mean Gaussian random variable [56]. Moreover, we consider the clock and data signal in one bit period. The clock signal can then be written as

$$a_c(t) = P_c e^{-\frac{t^2}{2T_c^2}}, \tag{4.3}$$

where $T_c$ is the full width at half maximum (FWHM) of the clock pulse-width. We also suppose that the variation of the clock signal is small enough, so that we only consider the effect of the two adjacent user signals for evaluating the BER of the desired user. In these calculations we consider the data signal as follows

$$a_d(t) = P_d \left[ b_{-1} e^{-\frac{(t+T_b)^2}{2T_d^2}} + b_0 e^{-\frac{t^2}{2T_d^2}} + b_1 e^{-\frac{(t-T_b)^2}{2T_d^2}} \right], \tag{4.4}$$

where $b_0$ is the data bit of the desired user, $b_{-1}$ and $b_1$ are the data bits of the users before and after the desired user, $T_b$ is the bit period and $T_d$ is the FWHM of the data pulse. The Fourier transform of (4.1) can be expressed as [50]

$$X(\omega) = \int_{-\infty}^{\infty} \int_{-\infty}^{\infty} \gamma e^{-j\omega_1 \tau} A_c(\omega_1) e^{+j\omega_2 \tau} A_c^*(\omega_2) A_d(\omega - \omega_1 + \omega_2) d\omega_1 d\omega_2, \tag{4.5}$$

where $A_c(\omega)$ and $A_d(\omega)$ are the Fourier transforms of $a_c(t)$ and $a_d(t)$, respectively, and can be written as follows

$$A_c(\omega) = P_c T_c \sqrt{2\pi} e^{-\frac{\omega^2}{2} T_c^2}, \tag{4.6}$$

$$A_d(\omega) = P_d T_d \sqrt{2\pi} \left( b_{-1} e^{j\omega T_b} + b_0 + b_1 e^{-j\omega T_b} \right) e^{-\frac{\omega^2}{2} T_d^2}. \tag{4.7}$$

The integration time of the photo-detector is considered to be much greater than the pulse widths of the data and clock signals, and thus the output signal of the photo-detector can be calculated from the following equation:

$$I = R \int_{-\infty}^{\infty} x(t) dt = R X(\omega = 0). \tag{4.8}$$

In this formula $R$ is the responsivity of the photo-detector, which is defined as

$$R = \frac{\eta q_e}{h\upsilon}, \tag{4.9}$$

where $\eta$ is the quantum efficiency of the photo-detector, $q_e$ is the electron charge ($1.6 \times 10^{-19}C$), $h$ is the Planck's constant ($6.63 \times 10^{-34}J.s$) and $\upsilon$ is the optical carrier frequency.

The error probability can be calculated applying the law of total probability:

$$P_e = P(b=0)P(\text{error}|b=0) + P(b=1)P(\text{error}|b=1). \tag{4.10}$$

By considering an equally-probable binary transmission and Gaussian distribution for the output current, (4.10) becomes as follows

$$P_e = \frac{1}{2}\left[\mathrm{Q}\left(\frac{Th - m_0}{\sigma_0}\right) + \mathrm{Q}\left(\frac{m_1 - Th}{\sigma_1}\right)\right], \tag{4.11}$$

where $m_j$ and $\sigma_j^2$ $(j = 0, 1)$ are, respectively the mean and the variance of the output current when bit $j$ is sent, i.e., $(b_0 = j)$. $Th$ is the optimum threshold that minimizes the bit error rate (BER), and can be approximated [57] as

$$Th = \frac{m_1\sigma_0 + m_0\sigma_1}{\sigma_0 + \sigma_1}. \tag{4.12}$$

Substituting (4.12) in (4.11) gives us the following relation for $P_e$

$$P_e = \mathrm{Q}\left(\frac{m_1 - m_0}{\sigma_0 + \sigma_1}\right). \tag{4.13}$$

The mean, $m_I$, and variance, $\sigma_I^2$, of the output current can be derived from (4.8) as follows

$$m_I = RE\{X(\omega = 0)\}, \tag{4.14}$$

$$\sigma_I^2 = R^2E\{X^2(\omega = 0)\} - R^2E^2\{X(\omega = 0)\}. \tag{4.15}$$

Applying (4.5) in (4.14) and (4.15) we obtain

$$m_I = R\gamma \int_{-\infty}^{\infty}\int_{-\infty}^{\infty} \phi_\tau(\omega_1 - \omega_2)A_c(\omega_1)A_c^*(\omega_2)E\Big\{A_d(\omega_2 - \omega_1)\Big\}d\omega_1 d\omega_2, \tag{4.16}$$

$$\sigma_I^2 + m_I^2 = R^2\gamma^2 \iiiint_{-\infty}^{\infty} \phi_\tau(\omega_1 - \omega_2 - \nu_1 + \nu_2) A_c(\omega_1) A_c^*(\omega_2) \times E\left\{ A_d(\omega_2 - \omega_1) A_d^*(\nu_2 - \nu_1) \right\} A_c^*(\nu_1) A_c(\nu_2) d\omega_1 d\omega_2 d\nu_1 d\nu_2, \tag{4.17}$$

where $\phi_\tau(\omega)$ is the characteristic function of the random variable $\tau$ and is defined as $\phi_\tau(\omega) = E\{\exp(-j\omega\tau)\}$. As indicated in [56], the error in the clock recovery leads to an error in the timing synchronization between the data and the clock, which is indicated by $\tau$ in this paper, and is considered to be a Gaussian zero mean random variable with variance $\sigma_\tau^2$ and therefore its characteristic function is $\phi_\tau(\omega) = e^{-\frac{\omega^2}{4}\sigma_\tau^2}$. Substituting (4.6) and (4.7) in (4.16) yields

$$m_I = R\gamma P_c^2 P_d T_c^2 T_d 2\sqrt{2}\pi^{\frac{3}{2}} \int_{-\infty}^{\infty}\int_{-\infty}^{\infty} e^{-\frac{(\omega_1-\omega_2)^2}{4}\sigma_\tau^2} e^{-\frac{\omega_1^2+\omega_2^2}{2}T_C^2} e^{-\frac{(\omega_2-\omega_1)^2}{2}T_d^2} \times (b_0 + \cos((\omega_2 - \omega_1)T_b) d\omega_1 d\omega_2. \tag{4.18}$$

Setting $x = \omega_1 - \omega_2$, (4.18) can be simplified as

$$m_I = R\gamma P_c^2 P_d T_c^2 T_d 2\sqrt{2}\pi^{\frac{3}{2}} \int e^{-\frac{x^2}{4}(\sigma_\tau^2 + T^2)} \times (b_0 + \cos(xT_b))\, dx, \tag{4.19}$$

where $T$ is $\sqrt{T_c^2 + 2T_d^2}$. Using $\int_{-\infty}^{\infty} e^{-\alpha x^2} \cos\beta x dx = \sqrt{\frac{\pi}{\alpha}} e^{-\frac{\beta^2}{4\alpha}}$, (4.19) can be written as

$$m_I = R\gamma P_c^2 P_d T_c^2 T_d \pi^2 \frac{4\sqrt{2}}{\sqrt{\sigma_\tau^2 + T^2}} \left( b_0 + e^{-\frac{T_b^2}{\sigma_\tau^2 + T^2}} \right). \tag{4.20}$$

Similarly by defining $x = \omega_1 - \omega_2$ and $y = \nu_1 - \nu_2$, (4.17) becomes

$$\sigma_I^2 + m_I^2 = R^2\gamma^2 P_c^4 P_d^2 T_c^4 T_d^2 8\pi^3 \int_{-\infty}^{\infty}\int_{-\infty}^{\infty} e^{-\frac{x^2+y^2}{4}T^2} e^{-\frac{(x-y)^2}{4}\sigma_\tau^2} \times \left[ \left( b_0 + \cos(xT_b) \right) \left( b_0 + \cos(yT_b) \right) + \frac{1}{2}\cos((x-y)T_b) \right] dxdy, \tag{4.21}$$

and by calculating the integrations we have

$$\sigma_I^2 + m_I^2 = R^2\gamma^2 P_c^4 P_d^2 T_c^4 T_d^2 32\pi^4 \times \left[ \frac{b_0}{T\sqrt{T^2+2\sigma_\tau^2}} \left( 1 + 2e^{-\frac{T_b^2}{T^2+2\sigma_\tau^2}\left(1+\frac{\sigma_\tau^2}{T^2}\right)} \right) \right.$$
$$\left. + \frac{1}{T\sqrt{T^2+2\sigma_\tau^2}} e^{-\frac{2T_b^2}{T^2+2\sigma_\tau^2}} + \frac{2}{T\sqrt{T^2+2\sigma_\tau^2}} e^{-2\frac{T_b^2}{T^2}} \right]. \tag{4.22}$$

According to (4.20) and (4.22), these four parameters ($m_0$, $\sigma_0^2$, $m_1$ and $\sigma_1^2$) are as follows:

$$m_0 = R\gamma P_c^2 P_d T_c^2 T_d \pi^2 \frac{4\sqrt{2}}{\sqrt{\sigma_\tau^2+T^2}} e^{-\frac{T_b^2}{\sigma_\tau^2+T^2}}, \tag{4.23}$$

$$\sigma_0^2 = R^2\gamma^2 P_c^4 P_d^2 T_c^4 T_d^2 32\pi^4 \left[ \frac{e^{-\frac{2T_b^2}{T^2+2\sigma_\tau^2}} + 2e^{-\frac{2T_b^2}{T^2}}}{T\sqrt{T^2+2\sigma_\tau^2}} - \frac{e^{-\frac{2T_b^2}{\sigma_\tau^2+T^2}}}{\sigma_\tau^2+T^2} \right], \tag{4.24}$$

$$m_1 = R\gamma P_c^2 P_d T_c^2 T_d \pi^2 \frac{4\sqrt{2}}{\sqrt{\sigma_\tau^2+T^2}} \left( 1 + e^{-\frac{T_b^2}{\sigma_\tau^2+T^2}} \right), \tag{4.25}$$

$$\sigma_1^2 = R^2\gamma^2 P_c^4 P_d^2 T_c^4 T_d^2 32\pi^4 \times \left[ \frac{1}{T\sqrt{T^2+2\sigma_\tau^2}} \left( 1 + 2e^{-\frac{T_b^2}{T^2+2\sigma_\tau^2}\left(1+\frac{\sigma_\tau^2}{T^2}\right)} \right) \right.$$
$$\left. + e^{-\frac{2T_b^2}{T^2+2\sigma_\tau^2}} + 2e^{-\frac{2T_b^2}{T^2}} \right) - \frac{1}{\sigma_\tau^2+T^2} \left( 1 + e^{-\frac{T_b^2}{\sigma_\tau^2+T^2}} \right)^2 \right]. \tag{4.26}$$

Substituting (4.23)-(4.26) in (4.11) gives us the bit error probability of this system.

## 4.3 Simulation results

We have simulated and analyzed the effect of the clock pulse width on the SNR of the receiver in an OTDM system using MATLAB. First we generate an OTDM signal with random data from eight users. In the receiver we build a clock signal for the desired user that repeat in time period of desired user. Then the

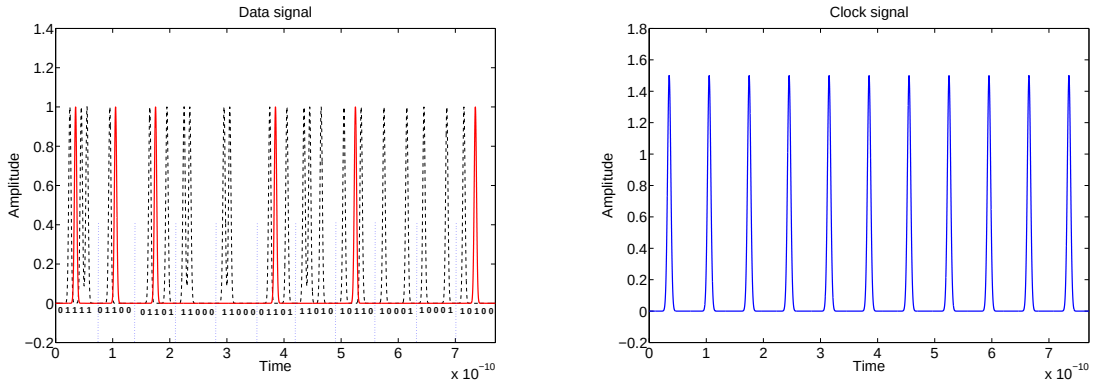


(a) (b)

Figure 4.6: (a) Example of data signal at the input of the OTDM receiver with 5 users, and 11 repetitions of the OTDM frame with $T_d$=1 ps. The desired signal is shown with red line in the figure. (b) Example of clock signal at the input of the receiver for 5 bit and 11 times repetition with $T_c$=2 ps.

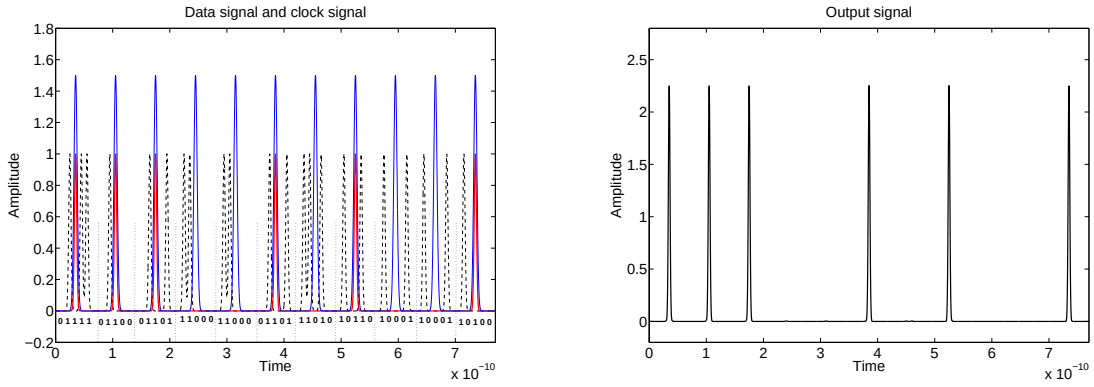


(a) (b)

Figure 4.7: (a) Example of the data and clock signals at the input of the receiver with 5 users and 11 repetition of the OTDM frame with $T_c$=2 ps and $T_d$=1 ps. The desired and clock signals are shown with red and blue lines respectively and the other adjacent bit are black and dashed. (b) Signal at the output of the receiver when there is no jitter in the clock and the bandwidth of the clock is bigger than the bandwidth of data.

clock signal and the received signal are multiplied. In the output of system, we obtain the integral of the signal duration of bit belong desired user. We can modify the values of several parameters such as different bandwidth of clock and data, or jitter. Each simulation has been repeated 1000 times for each value of the parameters and we obtain the eye diagram of the desired signal at the output. We plot the eye diagram for each case and calculate $m_1$, $m_0$, $\sigma_0$ and $\sigma_1$ from the eye pattern [58]. The BER is then obtained using (4.11). The simulation results are obtained for a bitrate of 10 Gb/s, and a data pulse width of 4 ps.

A simple example of simulations of the signals in the input, clock and output for a ideal OTDM receiver are shown in Figs. 4.6 and 4.7. In these figures the nonlinear effects of AND gate are not considered. We show 5 users that send information in 5 adjacent time slots, and the OTDM frame is repeated 11 times. We

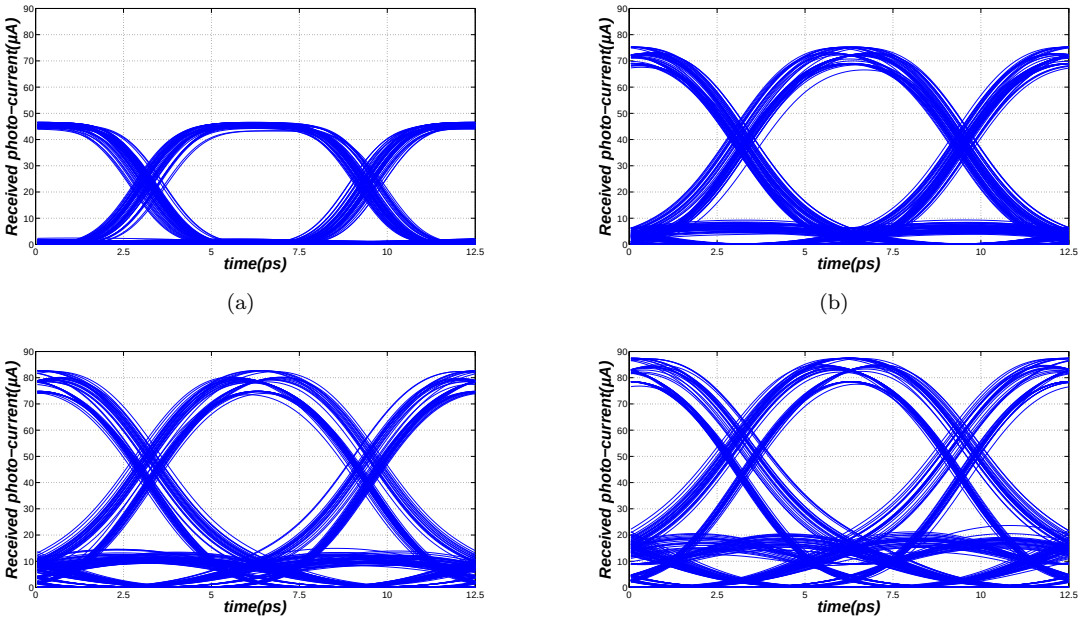


Figure 4.8: Examples of eye diagrams at the output of the receiver for $\tau$=0.5$T_d$, $T_d = 4ps$, $T_b = 12.5ps$ and different clock pulse-widths (a) $T_c$=4 ps, (b) $T_c$=8 ps, (c) $T_c$=10 ps and (d) $T_c$=12 ps.

assume that the bit duration of the data signal is 1 ps and the bit duration of the clock signal is 2 ps and

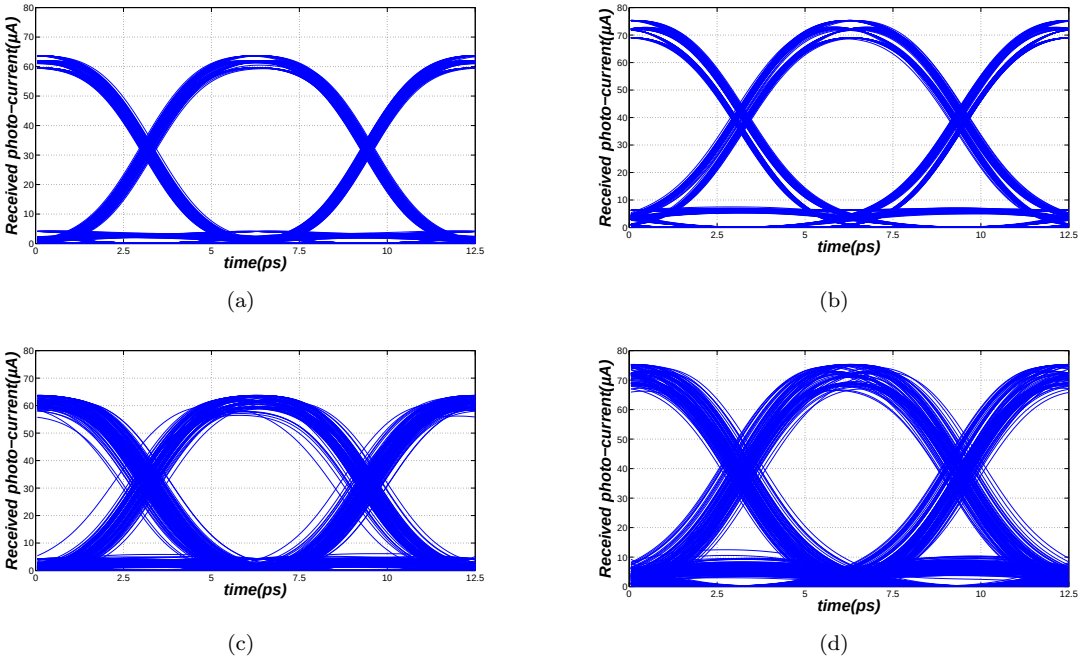


Figure 4.9: Examples of eye diagrams at the output of the receiver for $T_d = 4ps$, $T_b = 12.5ps$ (a) $\tau$=0.2$T_d$ and $T_c$=6 ps, (b) $\tau$=0.2$T_d$ and $T_c$=8 ps, (c) $\tau$=0.7$T_d$ and $T_c$=6 ps and (d) $\tau$=0.7$T_d$ and $T_c$=8 ps.

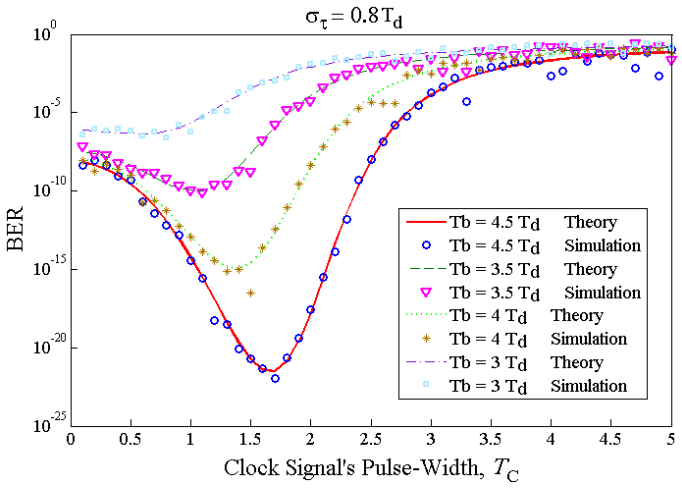


Figure 4.10: BER versus clock pulse-width for different data pulse-widths with $\tau$=0.8$T_d$, $T_b$ = 12.5$ps$, $T_d$ = 4$ps$ .

we do not have any jitter in the system. In figures of 4.6 and 4.7, the desired signals are depicted in red line, the clock signal is blue, and the adjacent users are in black-dash line. This figures shown how we can extract desired signal from received signal in a ideal OTDM system.

We now focus on the effect of jitter and widening effect of the clock signal in the performance of the system. In these results it has been considered that by widening the clock signal its peak power is decreased and so its total energy remains constant. In Fig. 4.8, four eye diagrams at the output of the receiver are depicted for $\sigma_\tau$= 0.5$T_d$ and different clock pulse widths. By increasing the clock pulse width the received energy increases, and the upper level of the eye diagram becomes larger because $I_{max}$ is increased. As can be seen, the best eye-diagram among the four depicted cases is for the second case, for which the clock pulse width is $T_c$=8 ps. Although the width of the eye diagram showing the variance is thicker for Fig. 4.8-b than Fig. 4.8-a, it has a lower BER since the received energy is much higher. In Fig. 4.8-a, since the pulse width of the clock signal is small, the signals from neighbouring users are not gathered by the photo-detector, and therefore the received signal for data bit "0" has a small variation. But for the data bit "1", due to the jitter of the clock signal, the photo-detector cannot integrate the entire data signal and thus the received signal has a variation in its amplitude. In Fig. 4.8-b the clock signal is widened and therefore the received signal for data-bit "1" is improved. Moreover, the overlap between the clock signal and signals of the neighbouring users is increased, and consequently, the variance of the received signal for data bit "0" becomes greater. Similarly, by increasing the width of the clock pulse in Fig. 4.8-c and Fig. 4.8-d the variance of the received signal increases for both data bits "1" and "0". Thus, by integrating more data signal and avoiding major interference from the adjacent signals we can obtain an optimum value for the pulse-width of the clock signal to minimize the BER.

Fig. 4.9 shows the effect of widening the clock signal on the receivers with different jitter amplitudes. Fig. 4.9-a and Fig. 4.9-b are for $\sigma_\tau = 0.2T_d$, and Fig. 4.9-c and Fig. 4.9-d are for $\sigma_\tau = 0.7T_d$. As we can see, for Fig. 4.9-a and Fig. 4.9-c the eye height (the distance between the upper and lower levels) are almost the same, but the width of the eye is thicker for the second example. The same effect holds for Fig. 4.9-b and Fig. 4.9-d.

Fig. 4.10 shows the BER of the receiver versus the pulse width of the clock signal for different bit-rates, plotting both the theoretical and simulated values. The analytical results are plotted using (4.11) by applying $m_0$, $m_1$, $\sigma_0$ and $\sigma_1$ as calculated from Eqs (4.23)-(4.26). In Fig. 4.10 the results are for $\sigma_\tau = 0.8T_d$ and $T_d = 4$ ps. By increasing the clock pulse width the gathered energy becomes larger. However, by widening the clock pulse, the portion of neighbouring users gathered by the receiver becomes larger. Hence there is an optimum point for which the ratio between the gathered energy and the variance reaches a maximum. The BER versus the pulse width of the clock signal for different bit-rates is plotted in Fig. 4.11 for $\sigma_\tau = 0.5T_d$. In both Fig. 4.10 and Fig. 4.11 the optimum clock pulse width is increased by increasing the data rate, which means that wider clock pulses are needed for higher bit-rates.

The BERs obtained with different jitter amplitudes have been plotted versus the clock pulse width in Fig. 4.12. The results show that by decreasing the time jitter of the clock signal, the performance of the receiver is improved. For a fixed bit-rate, the distance of the signals from two adjacent users is larger for shorter data signals, and therefore the interference probability on the desired user's signal is lower. There is an optimum value for the clock pulse width, which is the same for the different bit rates. Finally, Fig. 4.10, Fig. 4.11 and Fig. 4.12 show that simulated results match remarkably well with the analysis described in Section 3.

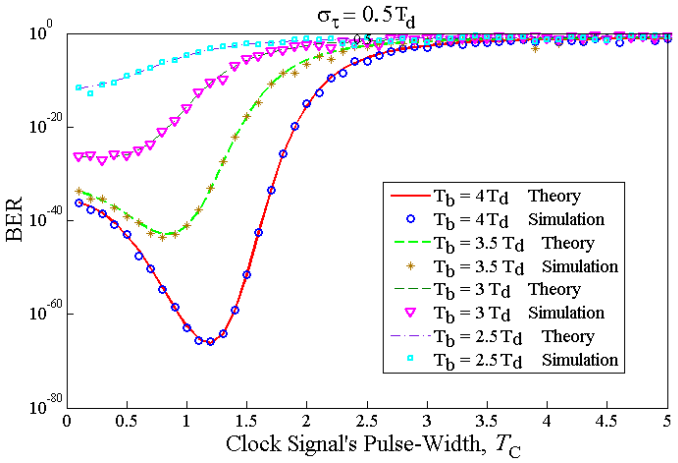


Figure 4.11: BER versus clock pulse-width for different data pulse-widths with $\sigma_\tau$=0.5$T_d$, $T_b = 12.5ps$, $T_d = 4ps$.

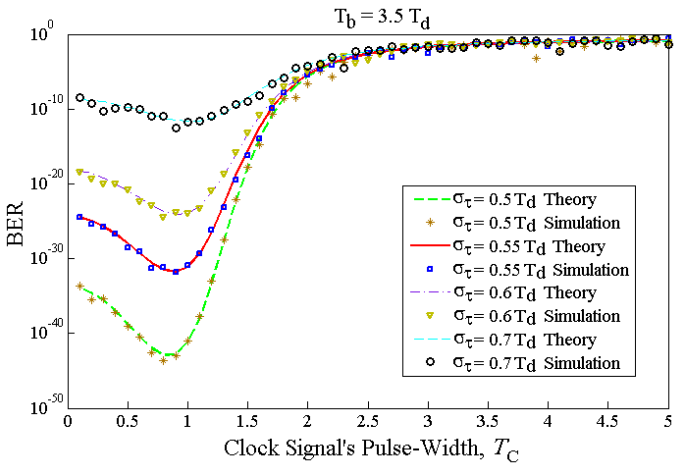


Figure 4.12: BER versus clock pulse-width for different jitter amplitudes, $T_b = 12.5ps$, $T_d = 4ps$.

## 4.4 Summary

Ultra-fast optical communication is the backbone of the high-speed global networking. OTDM is a popular technique for multiplexing the data of multiple simultaneous users on a single optical channel. In this chapter, the effects of the clock signal pulse width and different jitter amplitudes on the performance of the receiver are studied in an on-off modulated OTDM network using both analytical and simulated results. We assume that the optical clock signal used for time-gating has jitter, and therefore, there is a delay between the clock and data signals. We model this delay as a zero mean Gaussian random variable. Using the analytical results, an optimum clock signal width for obtaining the best performance of the receiver for different errors and time periods has been obtained. Moreover it has been shown that the minimum BER is not always obtained with $T_c = T_d$ and that the minimum can change depending on the variance of the error and bit duration. It has also been shown that there is an optimum value for the pulse width of the clock signal for which the BER is minimized. We can deduce that jitter amplitude is the key factor in determining the optimum value of the clock signal for a fixed bit rate. Simulation results are presented to evaluate the accuracy of the analytical expression. In this research we consider that the bandwidth of $T_c$ and $T_d$ are a portion of $T_b$, and therefore increasing the data rate and decreasing the bandwidth of $T_b$ would cause decrease the bandwidth of $T_d$ and $T_c$ in portion of $T_b$. Therefore, in order to improve the performance of the receiver and decrease the BER of the system, recievers should be able to tune the bandwith of $T_c$.

Chapter 5

# Bit Detection in Optical CDMA Networks

The growth in the demand for high-speed transmission of information has increased the need for high capacity optical networks. Multiple access techniques play a key role in accessing the bandwidth of multi-user data communication networks. Optical code division multiple access (OCDMA) systems are becoming more and more attractive in all-optical communications as multiple users can access the network asynchronously and simultaneously with a high level of security [59]. The main advantages of this approach are the flexibility in the allocation of channels, the ability to operate asynchronously and enhanced privacy and increased capacity. Direct detection OCDMA systems have been widely studied and applied to high-speed local area networks (LAN), because they allow multiple users to access network simultaneously [60].

Several coding schemes can be used depending on the available optical sources (coherent and incoherent), detection method (coherent and incoherent), encoding domain (time, wavelength or space), and encoding techniques (amplitude and phase), such as pulse-amplitude-coding, pulse-phase-coding, spectral-amplitude-coding, spectral-phase-coding [61], spatial-coding[62] and wavelength hopping time spreading coding [17], among others. One important aspect in OCDMA is the orthogonality of the code, a key property of the system [59]. Many researchers have proposed several codes such as prime code, optical orthogonal code [63].

In this chapter we focus on the time-spreading technique since, because of its simplicity and low cost, it is the most popular form of OCDMA, and we consider optical orthogonal codes (OOC) for the encoding method as they have good auto- and cross-correlation properties. In this case each receiver calculates the correlation between the received signal and a pre-assigned signature pattern, locally generated by the clock signal, and then makes a decision on the received data based on the output of the correlator. The correlation is usually calculated in the optical domain to increase efficiency [64]. The slow response of photo-detectors in time domain causes the integration time of electrical part to be much greater than the duration of the

ultrashort pulse, thus revealing the necessity of all-optical processing in the receivers [65].

In high-speed communication systems, increasing the number of simultaneous users is challenging since it increases the multiple access interference (MAI), which looks like a noise to receivers and makes signal detection difficult. At high data-rates (Tbps), the time width of the bits is small (in the order of femtoseconds) and any small time-mismatch (usually referred to as jitter [66]) between the clock and the received signal at the receiver will cause an error in the correlation receiver, leading to an increased bit-error-rate (BER). High speed OCDMA systems are usually contaminated by jitter at the receiver because of the short duration of the pulses, and consequently, the accuracy of the data recovery decreases with transmission speed.

The detection of the desired user's signal in the presence of the multiple access interference is an important problem in OCDMA systems. For a given system performance, the maximum number of users is limited by the the MAI-generated noise [67]. Different techniques have been proposed to reduce the effect of MAI in optical domain, including "time gating" and "optical thresholding" of the auto-correlation peak. Both techniques apply non-linear devices on the received signal to make MAI weaker. In nonlinear optical thresholding, a non-linear photonic device is used before the electrical detection step in order to increase the intensity difference between the main pulse and the interfering signals, without any need of exact synchronization with the received ultra-short pulse of the desired user. The optical non-linear thresholding has been successfully implemented using different non-linear optical effects such as second harmonic generation (SHG) [68], self-phase modulation (SPM) [31] and two-photon absorption (TPA) [33]. On the other hand, the time-gating method uses a control signal to separate the ultrashort pulse from its neighbourhood signals, and unlike the thresholding method it requires a proper synchronization between the control signal and the desired user's pulses. Two common configurations for constructing optical AND gates are nonlinear optical loop mirror and four-wave-mixing (FWM) processes [69].

Some researchers have proposed techniques for increasing the accuracy of the detection, and also different coding techniques for decreasing the BER, such as the use of OCDMA with optical orthogonal codes in [70], the performance analysis of nonlinear receivers in Asynchronous Spectral-Phase-Encoding in OCDMA Systems in [31], or the application of AND gates based on four-wave-mixing in OCDMA systems in [71], while [72] discusses the mitigation the effects of jitter and MAI in the BER by using a joint jitter estimator and canceller (JJEC). Also in [73] and [74] the authors propose a hybrid pulse position modulation/ultrashort light pulse CDMA (PPM/ULP-CDMA) system for ultrafast optical communications. In these papers the performance is improved of the system by increasing the effective the number chips and PPM symbols and by decreasing the duration bandwidth of the pulse using a time-space processor.

Our goal in this chapter is to use optical time gating to decrease the effect of MAI in the presence of jitter in time spreading OCDMA systems. In order to describe time gating as a nonlinear process we use

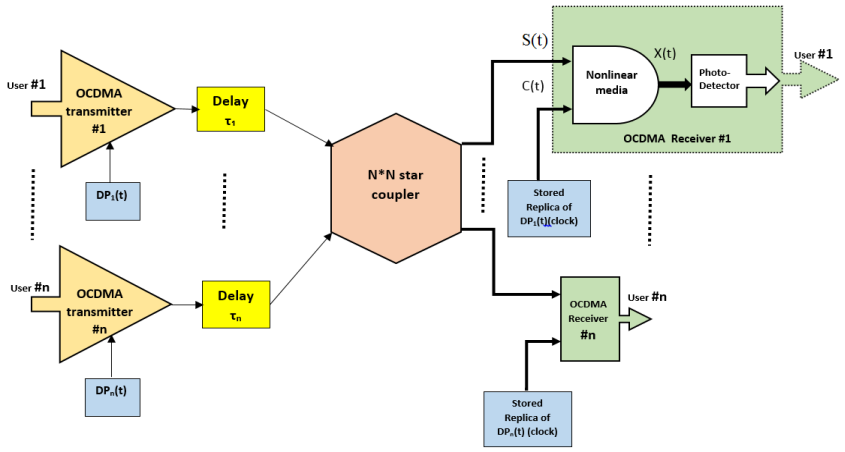


Figure 5.1: OCDMA architecture using a nonlinear device in the receiver. $\mathrm{DP}_n$ is the $n$th user's OOC, and $\tau_n$ is the delay associated with the $n$th signal.

nonlinear Schrödinger (NLS) equations, which are solved using Volterra series and numerical approach. We also consider fine-tuning the pulse-width of the clock as a technique to decrease the MAI so that the BER of the receiver is improved. We analyze and simulate the OCDMA receiver with discrete NLS equations using an optical orthogonal code (OOC) and evaluate the effect of the code pulse-width on the bit error rate (BER) of the receiver in the presence of jitter. Our results confirm that there is an optimum value for the pulse width of the code signal exists for which the BER is minimized. To the best of our knowledge, this is the first analytical study of the time-spreading OCDMA technique using NLS equation to describe nonlinear media and the influence of the pulse width of the codes in the quality of the received signal.

## 5.1 Structure of an OCDMA System with Optical Time Gating at the Receiver

### 5.1.1 OCDMA System

In a typical OCDMA communication network there are $N$ transmitter and receiver pairs (users), as shown in Fig. 5.1. We assume that the communication between the transmitters and receivers is pairwise, and communications between each $n$th $(1 < n < N)$ transmitter and receiver pair is continuous. All optical sources are incoherent. As a result, the optical light intensity of multiple users transmitting at the same time are added in intensity. Furthermore, all users have the same effective average optical power at each receiver so that one user could not overwhelm the others, and all users have identical bit rate and pulse shape. For each user, each bit of information data is codified by a signature sequence consisting of a number

of shorter time intervals called chips, encoded by a unique signature sequence called code-word. Then all the encoded data from all users are added together and are sent over an optical channel. At the receiver side, the same code-word for each user is used to decode the received signal. By correlating between the incoming signal and the stored copies of that user's unique sequence and comparing the output with a threshold level (TL), the information is recovered. The received bit is decoded as a "1" if the output of the correlator is bigger than TL and "0" otherwise. In OCDMA systems all users transmit their signals over a common medium, which makes detection of the desired signal hard as it is mixed with some interference. Therefore, it is important to use codes that cause smallest possible interference on each other in OCDMA system. In this work, we use optical orthogonal codes (OOC), which have small autocorrelation and small cross-correlation properties.

### 5.1.2 Four-Wave Mixing as a Time Gate

All OCDMA systems are primarily limited in their performance by MAI. The receiver's goal is to integrate over the desired user's short pulse without adding the MAI signal, but even the fastest photo-detectors have a response time longer than the decoded ultrashort optical pulse duration. This relatively slow response of the receiver's electrical part causes a fraction of the MAI signal to be collected by the photo-detector, and this severely degrades the signal-to-interference ratio (SIR) of the receiver. For this reason it is common in time-spread OCDMA receivers to use an optical non-linear device before the photo-detection to mitigate the MAI effect on the system performance, as shown in Fig. 5.1.

In the time-gating method, an all-optical AND gate is used to separate the ultrashort pulse from the MAI signal and to eliminate the interference signal. In Fig. 5.2 a nonlinear media (such as a silica fiber) is used for the FWM process. The input signal, with carrier frequency $\omega_r$, and the pump signal, with carrier frequency of $\omega_c$, enter the FWM device and with the nonlinear interaction between these signals, a part of their energy is transformed into a new signal with carrier frequency $2\omega_c - \omega_r$. This new signal will be zero if any of these two signals was zero. An optical filter in the output separates the new output signal from the pump and input signals. Globally, this mechanism acts as an optical AND gate. The synchronization of the pump signal (clock) with the received pulse (input signal) can be achieved with an optical phase locked loop based on the TPA technique [75]. Then, the random signal at the input of the nonlinear media in the OCDMA receiver is

$$s(t) = \sum_{n=1}^{N} b_n(t-\tau_n) DP_n(t-\tau_n) e^{j\varphi_n(t)} \tag{5.1}$$

where $b_n$ is the $n$th data sequence that takes values "0" or "1" (on-off keying), $DP_n(t)$ is the $n$th user's OOC

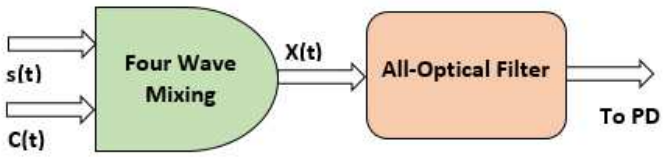


Figure 5.2: Nonlinear media: all-optical AND gate (FWM) and all-optical filter.

(signature sequence), $\tau$ is delay between the $n$th user and the desired user, and $\varphi_n$ is the phase shift of the $n$th user.

### 5.1.3 Jitter

In high-speed communication systems, the accuracy of the clock recovery decreases, as was reported in [76] for OTDM receivers, because of the shorter duration of the pulses and, consequently, a timing jitter appears in the clock signal. In this chapter we consider the effect of the timing jitter caused by long transmission distance, optical devices and limitations or errors in the synchronisation between the clock signal and the received signal. All these effects contribute cause decrease the signal interference ratio (SIR) at the output of the system. In fact, each bit in OCDMA system is divided into smaller parts (chips) and therefore timing jitter effects are increased. Since orthogonal codes have good distance properties between codes in each bit, by widening the pulse width of the codes, the receiver performance can be improved. This manipulation could be helpful in the detection of a bigger portion of the code pulse. On the other hand, by increasing the pulse width of the code, a part of the pulses from adjacent code or other users will be also gathered by detector. This effect generates another error in the code detection, and by increasing the pulse width of the codes, this error becomes larger. Given the trade-off between the two described error sources, we hypothesize that there exists an optimum value for the code's pulse width, so we can decrease effect of timing jitter in detection and therefore minimize BER.

## 5.2 Analytical Model of the OCDMA Receiver

In this section we analyze the nonlinear behaviour of optical correlators in OCDMA receivers using Nonlinear Schrödinger (NLS) equations, and we employ Volterra series to solve these equations. We consider the variations in the bandwidth of clock signal ($T_c$) and its effect in the output. For a more accurate response in the simulations, we obtain the discrete version of NLS equations. For the reader's convenience we summarize the parameters used in equations on Tables 5.1 and 5.2, together with some of the values used on the simulation and numerical results.

| Symbol | Description |
|---|---|
| $b_n$ | The nth data sequence |
| $DP_n(t)$ | The nth user's OOC (signature sequence) |
| $\varphi_n$ | Phase shift of nth user |
| $k$ | Weight of the code |
| $F$ | Number of chips |
| $T_b$ | Duration of bit |
| $T_c$ | Full width at half maximum (FWHM) of the clock pulse-width (code word) |
| $T_d$ | FWHM of the data pulse |
| $\sigma_\tau$ | jitter value |
| $S(t,z)$ | Received signal (input signal) |
| $C(t,z)$ | Clock signal (pump) |
| $X(t,z)$ | Output signal |
| $\lambda$ | Code autocorrelation |

Table 5.1: List of parameters used in the equations and the simulations.

| Symbol | Description Parameters | Magnitude |
|---|---|---|
| $\alpha_0$ | Attenuation constant | 0.2 dB/km |
| $\beta_1$ | First order dispersion | $2.3 \times 10^{-12} s/m$ |
| $\beta_2$ | Second order dispersion | $4.5 \times 10^{-26} s^2/m$ |
| $n^{'}$ | Refractive index | $5 \times 10^{-20}$ |
| $\omega_c$ | Clock signal frequency | $1.2161 \times 10^{15}$ Hz |
| $\omega_o$ | Output signal frequency | $1.2122 \times 10^{15}$ Hz |
| $\omega_r$ | Received signal frequency | $1.22 \times 10^{15}$ Hz |
| $f_{ijkl}$ | Spatial distribution of the fiber mode | $1.25 \times 10^{11}$ |
| $A_{eff}$ | Effective core area | $8\mu m^2$ |
| $\Delta k$ | Wave vector mismatch | 0 |
| $L$ | Length of nonlinear media | 30 m |
| $\Delta t$ | Duration of step in time domain | $10 \times 10^{-11}$ s |
| $\Delta z$ | Length of step in direct of fiber | 0.01 m |

Table 5.2: Parameter values used for Schrödinger equations and simulations.

### 5.2.1 Autocorrelation at the Input of the OCDMA Receiver

According to the calculation of the mean and variance of the current at the output of detector due to the interference signal, we need to calculate the output autocorrelation as shown in Appendix A. For this purpose, first we should obtain the input autocorrelation and then use it for the output autocorrelation. In order to calculate the autocorrelation of the received signal, we need to find the expected value of (5.1). To that end, we define the auto-correlation as

$$R_s(t, t+\Delta) = E[s(t)s^*(t+\Delta)] =$$

$$E_b\{E_\tau\{E_\varphi\{\sum_{n=0}^{N}\sum_{m=0}^{N} b_n(t-\tau_n)b_m(t-\tau_m+\Delta)DP_n(t-\tau_n)DP_m(t-\tau_m+\Delta)e^{j\varphi_n(t)}e^{-j\varphi_m(t+\Delta)}\}\}\} \qquad (5.2)$$

We can estimate the auto-correlation separately in terms of phase, data and code because these parameters are independent and they do not have any influence on each other. Therefore, we can obtain the phase autocorrelation by assuming $\Delta\varphi$ is also a zero-mean Gaussian random process with probability density function $P_{\Delta\varphi}(\Delta\varphi) = \frac{1}{\sqrt{2\pi}\sigma_{\Delta\varphi}} e^{-[(\Delta\varphi)^2/2\sigma^2_{\Delta\varphi}]}$ , where $\sigma^2_{\Delta\varphi}$ is the variance of the phase difference, which depends only on $\Delta$. Then, the autocorrelation of the phase shift is [77]:

$$\overline{e^{j\Delta\varphi(\Delta)}} \triangleq \int_{-\infty}^{+\infty} e^{j\Delta\varphi(\Delta)} P_{\Delta\varphi}(\Delta\varphi) d(\Delta\varphi) = e^{-(1/2)D_{\varphi(|\Delta|)}} \tag{5.3}$$

$$E_\varphi\{e^{j\varphi_n(t)} e^{-j\varphi_m(t+\Delta)}\} = \begin{cases} 0 & n \neq m \\ e^{-\frac{1}{2}D_\varphi(\Delta)} & n = m \end{cases} \tag{5.4}$$

where $D_\varphi(\Delta) \equiv \sigma^2_{\Delta\varphi}$. Then by applying (5.4) and (5.2), we obtain

$$R_r(t, t+\Delta) = e^{-\frac{1}{2}D_\varphi(\Delta)} \sum_{n=0}^{N} E_\tau\{E_b\{b_n(t-\tau_n) b_n(t-\tau_n+\Delta) DP_n(t-\tau_n) DP_n(t-\tau_n+\Delta)\} \tag{5.5}$$

Regarding the autocorrelation of the data, $R_b(t, t+\Delta) = E_b\{b_n(t) b_n(t+\Delta)\}$ and considering that $b_n(t) = \sum_{l=-\infty}^{+\infty} b_l^{(n)} P_{T_b}(t - lT_b)$, where $P_{T_b}(t - lT_b) = \begin{cases} 1 & lT_b < t < (l+1)T_b \\ 0 & \text{otherwise} \end{cases}$, we can obtain the autocorrelation function of the data using the power spectrum function as [78]:

$$S_x(\omega) = \frac{1}{T} s_b(e^{j\omega}) . |H(\omega)|^2 \tag{5.6}$$

where $s_b(e^{j\omega}) = \sum_{m=-\infty}^{\infty} R[m] e^{-jm\omega}$ is the discrete Fourier transform of autocorrelation of bit, $R[m]$, and $R[m] = E[b_{m+n} . b_n] = \begin{cases} m=0 & \rightarrow \quad E[b_n . b_n] = \frac{1}{2} \\ m \neq 0 & \rightarrow \quad E[b_{m+n} . b_n] = \frac{1}{4} \end{cases} = 1/4\delta[m] + 1/4$ so we have:

$$s_b(e^{j\omega}) = \sum_{m=-\infty}^{\infty} \Big[1/4\delta[m] + 1/4\Big] e^{-jm\omega} \tag{5.7}$$

On the other hand, we have $h(t) = P_T(t - l.T_b)$ then, $H(f) = T_b \frac{\sin \pi f T_b}{\pi f T_b}$ and with substituting in 5.6 we obtain:

$$S_x(f) = \frac{1}{T_b} \left( \sum_{m=-\infty}^{\infty} \Big[1/4\delta[m] + 1/4\Big] e^{-jm\omega} \right) \left( T_b \frac{\sin \pi f T_b}{\pi f T_b} \right)^2 \tag{5.8}$$

By simplifying and considering $\sum_{n=-\infty}^{\infty} e^{-jn\omega} = \frac{1}{T_b}\sum_{n=-\infty}^{\infty}\delta(f-\frac{n}{T_b})$ we obtain:

$$S_x(f) = \frac{T_b}{4}\left(\frac{\sin \pi f T_b}{\pi f T_b}\right)^2 + \frac{1}{4}\delta(f) \tag{5.9}$$

We can use the inverse Fourier transform of the power spectrum function, $S_x(f)$, and obtain the auto-correlation function as follow:

$$R(\tau) = F^{-1}\{S_x(f)\} = \frac{1}{4}triag(\frac{\tau}{2T_b}) + \frac{1}{8\pi} \tag{5.10}$$

where $triag(\frac{\tau}{2T_b}) = \left(\frac{\tau}{T_b}+1\right)\left(u\left(\frac{\tau}{T_b}+1\right) - u\left(\frac{\tau}{T_b}\right)\right) + \left(-\frac{\tau}{T_b}+1\right)\left(u\left(\frac{\tau}{T_b}\right) - u\left(\frac{\tau}{T_b}-1\right)\right)$. Finally, for the autocorrelation of the OOC code we consider $DP_n(t) = \sum_{j=-\infty}^{\infty} A_j^{(n)} P_{T_c}(t-jT_c)$ where $P_{T_c}(t-jT_c) = \{^{1 \quad jT_c<t<(j+1)T_c}_{0 \quad \text{otherwise}}$. By definition, the correlation between OOC codes are $R[l] = E[A_n A_{n\bigoplus l}] = \{^{\frac{\lambda}{F} \quad 1\le l\le F-1}_{\frac{K}{F} \quad l=0}$ where $\lambda$ is the code auto-correlation, and in the case of strict orthogonality would be zero. According to 5.6 we have:

$$s_{P_n}(e^{j\omega}) = \frac{1}{F}\sum_{l=0}^{F-1}\left[(K-\lambda_a)\delta[l]+\lambda_a\right]e^{-jl\omega} \tag{5.11}$$

Assume that the Dirac function of code is $h_2(t) = \text{Sinc}(\frac{t}{T_c})$, we have $H_2(\omega) = \frac{T_c}{\sqrt{2\pi}}rect(\frac{\omega T_c}{2\pi})$ and substituting in (5.11) we obtain:

$$S_{P_n}(f) = \frac{1}{T_c F}\sum_{l=0}^{F-1}\left[(K-\lambda_a)\delta[l]+\lambda_a\right]e^{-jl\omega}\left(\frac{T_c}{\sqrt{2\pi}}rect(\frac{\omega T_c}{2\pi})\right)^2 \tag{5.12}$$

Then, simplifying (5.12), we obtain:

$$S_{P_n}(f) = \frac{1}{T_c F}\left[(K-\lambda_a)\frac{T_c}{\pi}\left(\frac{T_c}{2}rect(\frac{\omega T_c}{2\pi})\right) + \lambda_a\sum_{l=0}^{F-1}e^{-jl\omega}\frac{T_c}{\pi}\left(\frac{T_c}{2}rect(\frac{\omega T_c}{2\pi})\right)\right] \tag{5.13}$$

Furthermore, the autocorrelation of the OOC can be expressed as:

$$R_{DP_n}(\tau) = \frac{1}{F\sqrt{\pi}}[(K-\lambda_a)(\mathrm{sinc}(\frac{2\tau}{\mathrm{T_c}})) + \lambda_{\mathrm{a}} \sum_{\mathrm{l}=0}^{\mathrm{F}-1}(\mathrm{sinc}(\frac{2(\tau-\mathrm{l})}{\mathrm{T_c}}))] \tag{5.14}$$

According to (5.5), (5.10) and (5.14), the autocorrelation for all parameters becomes

$$R_s(t,t+\Delta) = e^{-\frac{1}{2}D_\varphi(\Delta)}[\frac{1}{4}triag(\frac{\Delta}{2T_b}) + \frac{1}{8\pi}]\{\frac{1}{F\sqrt{\pi}}[(K-\lambda_a)(\mathrm{sinc}(\frac{2\Delta}{\mathrm{T_c}})) + \lambda_{\mathrm{a}} \sum_{\mathrm{l}=0}^{\mathrm{F}-1}(\mathrm{sinc}(\frac{2(\Delta-\mathrm{l})}{\mathrm{T_c}}))]\} \tag{5.15}$$

### 5.2.2 NLS Equation in a Nonlinear System

The NLS equations, which describe the propagation of optical pulses over fibers and are derived from Maxwell's equations, are the fundamental equations for describing a nonlinear system. The NLS equations for analyzing the FWM in a non-linear optical media (as shown in Fig. 2), considering (3.22), (3.23) and (3.24), can be written as [54]

$$\frac{\partial C(t,z)}{\partial z} = -\frac{\alpha_0}{2}C(t,z) - \sum_{k=1}^{\infty}\frac{\beta_k j^k}{k!} \times \frac{\partial^k C(t,z)}{\partial t^k} + \frac{jn^{'}\omega_C}{c} \times \Bigg[\Bigg(2f_{CC}|C(t,z)|^2 + 2f_{CS}|S(t,z)|^2 + 2f_{CX}|X(t,z)|^2\Bigg)C(t,z) + 2f_{CSX}S(t,z)X(t,z)C^*(t,z)e^{j\Delta kz}\Bigg] \tag{5.16}$$

$$\frac{\partial X(t,z)}{\partial z} = -\frac{\alpha_0}{2}X(t,z) - \sum_{k=1}^{\infty}\frac{\beta_k j^k}{k!} \times \frac{\partial^k X(t,z)}{\partial t^k} + \frac{jn^{'}\omega_X}{c} \times \Bigg[\Bigg(2f_{XX}|X(t,z)|^2 + 2f_{XS}|S(t,z)|^2 + 4f_{XC}|C(t,z)|^2\Bigg)X(t,z) + 2f_{XSC}S^*(t,z)C^2(t,z)e^{-j\Delta kz}\Bigg] \tag{5.17}$$

$$\frac{\partial S(t,z)}{\partial z} = -\frac{\alpha_0}{2}S(t,z) - \sum_{k=1}^{\infty}\frac{\beta_k j^k}{k!} \times \frac{\partial^k S(t,z)}{\partial t^k} + \frac{jn^{'}\omega_s}{c} \times \Bigg[\Bigg(2f_{SS}|S(t,z)|^2 + 2f_{SX}|X(t,z)|^2 + 4f_{SC}|C(t,z)|^2\Bigg)S(t,z) + 2f_{SXC}X^*(t,z)C^2(t,z)e^{-j\Delta kz}\Bigg] \tag{5.18}$$

where $\sum_{k=1}^{\infty}\beta_k j^k/k!$ represents the linear dispersion, $c$ is light speed and we assume that $X(t,z)$ and $S(t,z)$ have no influence on the clock signal and its variation is only due to the attenuation and dispersion.

### 5.2.3 Volterra Series

The NLS equations are a set of nonlinear partial differential equations whose exact analytical solution generally is very difficult to obtain except for some specific cases. There are a large number of approximate

analytical and numerical to solve the NLS equations. The Volterra series method is one of the most powerful methods to describe the nonlinear system. This method is able to capture memory effects. In the Volterra series the output of the nonlinear system depends on the input to the system at all other times. In this section we consider the first three terms of the Volterra series to provide a good approximation of the solution of the NLS equations [43]. Following this approach, and for simplicity of the calculations, the system output $X(\omega, z)$ in spectral domain can be evaluated as:

$$X(\omega, z) = X_1(\omega, z) + X_2(\omega, z) + X_3(\omega, z) \tag{5.19}$$

where $X_1(\omega, z)$, $X_2(\omega, z)$ and $X_3(\omega, z)$ are the first three terms output and $C(\omega)$, $S(\omega)$ are the clock and the received signal in spectral domain respectively. These terms are defined as follows:

$$X_1(\omega, z) = \iint H'_{O_{1,2}}(\omega_1, \omega_2, \omega - \omega_1 + \omega_2, z) C(\omega_1) S^*(\omega_2) C(\omega - \omega_1 + \omega_2) d\omega_1 d\omega_2 \tag{5.20}$$

$$\begin{aligned} X_2(\omega, z) = \iiiint & H'_{O_{3,2}}(\omega_1, \omega_2, \omega_3, \omega_4, \omega - \omega_1 + ... + \omega_4, z) C(\omega_1) S^*(\omega_2) S(\omega_3) S^*(\omega_4) \\ & \times C(\omega - \omega_1 + ... + \omega_4) d\omega_1 ... d\omega_4 \end{aligned} \tag{5.21}$$

$$\begin{aligned} X_3(\omega, z) = \iiiint & H'_{O_{1,4}}(\omega_1, \omega_2, \omega_3, \omega_4, \omega - \omega_1 + ... + \omega_4, z) C(\omega_1) C^*(\omega_2) C(\omega_3) S^*(\omega_4) \\ & \times C(\omega - \omega_1 + ... + \omega_4) d\omega_1 ... d\omega_4 \end{aligned} \tag{5.22}$$

We consider that the phase match condition has been satisfied and the phase mismatch, $\Delta K$, is zero. Then, Volterra kernels $H'_{O_{1,2}}$, $H'_{O_{3,2}}$ and $H'_{O_{1,4}}$ can be expressed as follows (more details in Appendix B and [71]):

$$H'_{O_{1,2}}(\omega_1, \omega_2, \omega - \omega_1 + \omega_2, z) = 2j f_{OSC} e^{G_1(\omega) z (\frac{1 - e^{-2\alpha z}}{2\alpha})} \tag{5.23}$$

$$H'_{O_{3,2}}(\omega_1, \omega_2, \omega_3, \omega_4, \omega - \omega_1 + ... + \omega_4, z) = 2 f_{OSC} (f_{SS} + 2 f_{OS}) e^{G_1(\omega) z (\frac{1 - e^{-2\alpha z}}{2\alpha})^2} \tag{5.24}$$

$$H'_{O_{1,4}}(\omega_1, \omega_2, \omega_3, \omega_4, \omega - \omega_1 + ... + \omega_4, z) = 8 f_{OSC} (f_{SC} + 2 f_{OC}) e^{G_1(\omega) z (\frac{1 - e^{-2\alpha z}}{2\alpha})^2} \tag{5.25}$$

where $f_{ijkl} \approx f_{ij} \approx \frac{n^{'}\omega}{cA_{eff}}$ are spatial distribution of the fiber modes whose parameters are defined in Table 5.2.

### 5.2.4 Solving the NLS Equations for a Nonlinear Media by Volterra Series

We will now obtain the output of the nonlinear system by solving NLS equations with Volterra series, as described in the previous section. Usually, optical signals are considered to follow a Gaussian shape but we would have complicated integrals for obtaining $X_1$, $X_2$ and $X_3$, so for simplicity we assume that the signals are Sinc-shaped. The received and clock signals in time and spectral domain are as follows:

$$c(t) = \sum_{m=1}^{k} A_c^{'} \text{sinc}(\frac{t - (C_m T_b/F)}{T_c}) \tag{5.26}$$

$$C(\omega) = F\{C(t)\} = A_c^{'} T_c \pi \prod (\frac{\omega T_c}{2}) \sum_{m=1}^{k} e^{-2\pi j C_m (T_b/F)\omega} \tag{5.27}$$

$$s(t) = b \sum_{m=1}^{k} A_d \text{sinc}(\frac{t - (C_m T_b/F)}{T_d}) \tag{5.28}$$

$$S(\omega) = F\{s(t)\} = b A_d T_d \pi \prod (\frac{\omega T_d}{2}) \sum_{m=1}^{k} e^{-2\pi j C_m (T_b/F)\omega} \tag{5.29}$$

where $c(t)$, $s(t)$ are the deterministic clock and the received signal in time domain and $C(\omega)$, $S(\omega)$ are the Fourier transform of the clock and received signal, $A_c^{'}, A_d$ are the amplitudes of the clock and the received signal, $C_m$ is the code number, b is value of bit "0" or "1" and $k$ is the weight of the code. The rest of parameters are described in Tables I and II. Using Volterra series, we can write the first three output response terms as follows:

$$\begin{aligned} X_1(\omega, z) = \iint 2j f_{OSC} e^{G_1(\omega) z (\frac{1-e^{-2\alpha z}}{2\alpha})} \times \{A_c^{'} T_c \pi \prod (\frac{\omega_1 T_c}{2}) \sum_{m=1}^{k} e^{-2\pi j C_m (T_b/F)\omega_1}\} \\ \times \{b A_d T_d \pi \prod (\frac{\omega_2 T_d}{2}) \sum_{m=1}^{k} e^{2\pi j C_m (T_b/F)\omega_2}\} \times \{A_c^{'} T_c \pi \prod (\frac{(\omega - \omega_1 + \omega_2) T_c}{2}) \\ \times \sum_{m=1}^{k} e^{-2\pi j C_m (T_b/F)(\omega - \omega_1 + \omega_2)}\} d\omega_1 d\omega_2 \end{aligned} \tag{5.30}$$

$$X_2(\omega,z)=\iiiint 2f_{OSC}(f_{SS}+2f_{OS})e^{G_1(\omega)z(\frac{1-e^{-2\alpha z}}{2\alpha})^2}\times\{A_c^{'}T_c\pi\prod(\frac{\omega_1T_c}{2})\sum_{m=1}^{k}e^{-2\pi jC_m(T_b/F)\omega_1}\}$$
$$\times\{bA_dT_d\pi\prod(\frac{\omega_2T_d}{2})\sum_{m=1}^{k}e^{2\pi jC_m(T_b/F).\omega_2}\}\times\{A_c^{'}T_c\pi\prod(\frac{\omega_3T_c}{2})\sum_{m=1}^{k}e^{-2\pi jC_m(T_b/F)\omega_3}\}$$
$$\times\{bA_dT_d\pi\prod(\frac{\omega_4T_d}{2})\sum_{m=1}^{k}e^{2\pi jC_m(T_b/F)\omega_4}\}\times\{A_c^{'}T_c\pi\prod(\frac{(\omega-\omega_1+...+\omega_4)T_c}{2})$$
$$\times\sum_{m=1}^{k}e^{-2\pi jC_m(T_b/F)(\omega-\omega_1+...+\omega_4)}\}d\omega_1...d\omega_4 \tag{5.31}$$

$$X_3(\omega,z)=\iiiint 8f_{OSC}(f_{SC}+2f_{OC})e^{G_1(\omega)z(\frac{1-e^{-2\alpha z}}{2\alpha})^2}\times\{A_c^{'}T_c\pi\prod(\frac{\omega_1T_c}{2})\sum_{m=1}^{k}e^{-2\pi jC_m(T_b/F)\omega_1}\}$$
$$\times\{A_c^{'}T_c\pi\prod(\frac{\omega_2T_c}{2})\sum_{m=1}^{k}e^{2\pi jC_m(T_b/F)\omega_2}\}\times\{A_c^{'}T_c\pi\prod(\frac{\omega_3T_c}{2})\sum_{m=1}^{k}e^{-2\pi jC_m(T_b/F)\omega_3}\}$$
$$\times\{bA_dT_d\pi\prod(\frac{\omega_4T_d}{2})\sum_{m=1}^{k}e^{2\pi jC_m(T_b/F)\omega_4}\}\times\{A_c^{'}T_c\pi\prod(\frac{(\omega-\omega_1+...+\omega_4)T_c}{2})$$
$$\times\sum_{m=1}^{k}e^{-2\pi jC_m(T_b/F)(\omega-\omega_1+...+\omega_4)}\}d\omega_1...d\omega_4 \tag{5.32}$$

By calculating the integrations in (5.30), (5.31) and (5.32), and depending on whether $T_c$ is larger than $T_d$ or not, we obtain different responses in different frequency ranges. By defining $f(x)$ and $E_1$ as:

$$f(x)=\frac{1}{2\pi j(T_b/F)}e^{-2\pi j\frac{T_b}{F}x},E_1=2\pi^3bjf_{OSC}e^{G_1(\omega)z(\frac{1-e^{-2\alpha z}}{2\alpha})}A_d(A_c^{'})^2T_dT_c^2 \tag{5.33}$$

then, for $T_d>T_c$, $X_1$ would be :

$$(1)For\quad \omega>\frac{2}{T_c}+\frac{1}{T_d},\quad \omega<-\frac{2}{T_c}-\frac{1}{T_d}\quad\Longrightarrow\quad X_1(\omega,z)=0 \tag{5.34}$$

$$(2)For\quad \frac{1}{T_d}<\omega<\frac{2}{T_c}+\frac{1}{T_d}$$
$$X_1(\omega,z)=E_1\sum_{m=1}^{k}\sum_{i=1}^{k}\sum_{l=1}^{k}\frac{1}{(C_l-C_m)}\frac{2\pi j\frac{T_b}{F}}{(C_i+C_m-2C_l)}f((C_l-C_i)\frac{2}{T_c})f((C_i-C_m-2C_l)\frac{1}{T_d})f(C_i\omega) \tag{5.35}$$

$$(3)For \quad \frac{1}{T_d}-\frac{2}{T_c}<\omega<\frac{1}{T_d}$$
$$X_1(\omega,z)=E_1\sum_{m=1}^{k}\sum_{i=1}^{k}\sum_{l=1}^{k}\frac{2\pi j\frac{T_b}{F}}{(C_l-C_m)}\{\frac{1}{(C_i-C_m)}f(C_i\omega)f((C_m-C_l)\frac{2}{T_c})f((C_m-C_i)\frac{1}{T_d})$$
$$+\frac{1}{(C_i+C_m-2C_l)}f((2C_l-C_i)\omega)f((C_m-C_l)\frac{2}{T_c})f((C_i+C_m-2C_l)\frac{1}{T_d})\} \tag{5.36}$$

$$(4)For \quad -\frac{1}{T_d}-\frac{2}{T_c}<\omega<\frac{1}{T_d}-\frac{2}{T_c}$$
$$X_1(\omega,z)=E_1\sum_{m=1}^{k}\sum_{i=1}^{k}\sum_{l=1}^{k}\frac{2\pi j\frac{T_b}{F}}{(C_l-C_m)}\frac{1}{(C_i-C_m)}f((2C_m-C_i)\omega)f((2C_m-C_l-C_i)\frac{2}{T_c})f((C_m-C_i)\frac{1}{T_d}). \tag{5.37}$$

When the pulse-width of the data is smaller than the pulse-width of clock ($T_d<T_c$) we have

$$(1)For \quad \omega>\frac{2}{T_c}+\frac{1}{T_d}, \quad \omega<-\frac{2}{T_c}-\frac{1}{T_d} \quad \Longrightarrow \quad X_1(\omega,z)=0 \tag{5.38}$$

$$(2)For \quad \frac{1}{T_d}<\omega<\frac{2}{T_c}+\frac{1}{T_d}$$
$$X_1(\omega,z)=E_1\sum_{m=1}^{k}\sum_{i=1}^{k}\sum_{l=1}^{k}\frac{1}{(C_l-C_m)}\frac{2\pi j\frac{T_b}{F}}{(C_i+C_m-2C_l)}f((C_l-C_i)\frac{2}{T_c})f((C_i-C_m-2C_l)\frac{1}{T_d})f(C_i\omega) \tag{5.39}$$

$$(3)For \quad -\frac{1}{T_d}+\frac{2}{T_c}<\omega<\frac{1}{T_d}$$
$$X_1(\omega,z)=E_1\sum_{m=1}^{k}\sum_{i=1}^{k}\sum_{l=1}^{k}\frac{1}{(C_l-C_m)}\{\frac{2\pi j\frac{T_b}{F}}{(C_i-C_m)}f(C_i\omega)f((C_m-C_l)\frac{2}{T_c})f((C_i-C_m)\frac{1}{T_d})$$
$$+\frac{1}{(C_i+C_m-2C_l)}f((C_m-2C_l)\omega)f((C_l-C_i)\frac{2}{T_c})\} \tag{5.40}$$

$$(4)For \quad \frac{1}{T_d}-\frac{2}{T_c}<\omega<-\frac{1}{T_d}+\frac{2}{T_c}$$
$$X_1(\omega,z)=E_1\sum_{m=1}^{k}\sum_{i=1}^{k}\sum_{l=1}^{k}\frac{2\pi j\frac{T_b}{F}}{(C_l-C_m)}\{\frac{1}{(C_i-C_m)}f(C_i\omega)f((C_m-C_l)\frac{2}{T_c})f((C_i-C_m)\frac{1}{T_d})$$
$$+\frac{1}{(C_i+C_m-2C_l)}f((2C_l-C_i)\omega)f((C_m-C_l)\frac{2}{T_c})f((2C_l+C_i-C_m)\frac{1}{T_d})\} \tag{5.41}$$

$$(5) For \quad -\frac{1}{T_d} < \omega < -\frac{2}{T_c} + \frac{1}{T_d}$$

$$X_1(\omega, z) = E_1 \sum_{m=1}^{k} \sum_{i=1}^{k} \sum_{l=1}^{k} \frac{1}{(C_l - C_m)} \{ \frac{1}{(C_i - C_m)} f(C_m \omega) f((C_l - C_i - 2C_m) \frac{2}{T_c}) +$$

$$\frac{2\pi j \frac{T_b}{F}}{(C_i + C_m - 2C_l)} f((2C_l - C_i)\omega) f((C_m - C_l)\frac{2}{T_c}) f((2C_l - C_i - C_m)\frac{1}{T_d}) \} \tag{5.42}$$

$$(6) For \quad -\frac{1}{T_d} - \frac{2}{T_c} < \omega < -\frac{1}{T_d}$$

$$X_1(\omega, z) = E_1 \sum_{m=1}^{k} \sum_{i=1}^{k} \sum_{l=1}^{k} \frac{2\pi j \frac{T_b}{F}}{(C_l - C_m)} \frac{1}{(C_i - C_m)} f((2C_m - C_i)\omega) f((2C_m - C_l - C_i)\frac{2}{T_c}) f((C_m - C_i)\frac{1}{T_d}) \tag{5.43}$$

For a detailed analysis of the responses of $X_2$ and $X_3$ refer to Appendix D.

### 5.2.5 Autocorrelation, Mean and Variance of the FWM Output

For obtaining the mean and the variance of the current of the photodetector we should calculate the output autocorrelation function of FWM's output MAI signal. As shown in Appendix E we can define the autocorrelation function of the four-wave mixer's output signal in frequency domain as follows:

$$R_X(\omega, \upsilon, z) = E\{X(\omega, z) X^*(\upsilon, z)\} = \sum_{m,n=1,2,3} E\{X_m(\omega, z) X_n^*(\upsilon, z)\} \tag{5.44}$$

Since parameter $H'_{O_{1,2}}$ is imaginary and both $H'_{O_{3,2}}$ and $H'_{O_{1,4}}$ are real, we can write (5.44) as:

$$R_X(\omega, \upsilon, z) = \sum_{m=1,2,3} E\{X_m(\omega, z) X_m^*(\upsilon, z)\} + 2E\{|X_2(\omega, z) X_3^\star(\upsilon, z)|\} \tag{5.45}$$

Now we can employ (5.45) for obtaining the autocorrelation of the MAI signal at the output of the four-wave mixer.

$$R_{MAI}(\omega, \upsilon, z) = \sum_{m=1,2,3} E\{X_{MAI_m}(\omega, z) X_{MAI_m}^*(\upsilon, z)\} + 2E\{|X_{MAI_2}(\omega, z) X_{MAI_3}^\star(\upsilon, z)|\} \tag{5.46}$$

$R_{MAI}(\omega, \upsilon, z)$ is composed of four terms. Considering [71] and comparing the amplitude of $R_{MAI_1}$, $R_{MAI_2}$, $R_{MAI_3}$ and $R_{MAI_4}$ we observe that the magnitude of $R_{MAI_1}$ is much greater than the other parts and

therefore $R_{MAI}$ can be approximated by $R_{MAI_1}(\omega, \upsilon, z)$. Thus,

$$R_{MAI}(\omega,\upsilon,z) = E\{X_{MAI_1}(\omega,z)X^*_{MAI_1}(\upsilon,z)\} = \int\int\int\int H'_{O_{1,2}}(\omega_1,\omega_2,\omega-\omega_1+\omega_2,z)$$
$$\times H'^*_{O_{1,2}}(\upsilon_1,\upsilon_2,\upsilon-\upsilon_1+\upsilon_2,z)\times C(\omega_1)C(\omega-\omega_1+\omega_2)\times C^*(\upsilon_1)C^*(\upsilon-\upsilon_1+\upsilon_2)$$
$$\times E\{S^*(\omega_2)S(\upsilon_2)\}d\omega_1 d\omega_2 d\upsilon_1 d\upsilon_2 \tag{5.47}$$

Furthermore, considering (5.47) and (5.15), the auto-correlation function of $R(\omega)$ is

$$R_S(\omega-\upsilon) = E\{S(\omega)S^*(\upsilon)\} = S_a(\omega)\delta(\omega-\upsilon) \tag{5.48}$$

where $S_a(\omega)$ is defined as

$$S_a(\omega) = \int_{-\infty}^{\infty} R_s(\tau)e^{-j\omega\tau}d\tau \tag{5.49}$$

Now we obtain the mean and variance of the photo-detector output current in the presence of MAI. The optical field that is collected by the photo-detector can be decomposed into two statistically independent parts, $A(\omega) = S(\omega)+A_{MAI}(\omega)+A_{FWM}(\omega)$. We neglect the effect of $A_{FWM}(\omega)$ (noise due to FWM) because its value is very small compared to the other terms. So, as shown the detail in Appendix E the mean at the output current can be rewritten as

$$\mu_{I,M,b} = E\{I|M,b\} = (\frac{1}{2\pi})^2\int_{-\infty}^{\infty}\int_{-\infty}^{\infty}[X(\omega)X^*(\upsilon)+R_{MAI}(\omega,\upsilon)]Sinc(\frac{(\omega-\upsilon)T}{2\pi})d\omega d\upsilon. \tag{5.50}$$

where I is the output current, M is the number of interfering users, and b is the value of the bit. Also the variance of the photo-detector current is

$$\sigma^2_{I,M,b} = E\{I^2\} - E^2\{I\} = (\frac{1}{2\pi})^4\int_{-\infty}^{\infty}\dots\int_{-\infty}^{\infty}[R_{MAI}(\omega_1,\upsilon_2)R_{MAI}(\omega_2,\upsilon_1)$$
$$+2X(\omega_2)X^*(\upsilon_1)R_{MAI}(\omega_2,\upsilon_1)]Sinc(\frac{(\omega_1-\upsilon_1)T}{2\pi})Sinc(\frac{(\omega_2-\upsilon_2)T}{2\pi})d\omega_1 d\upsilon_1 d\omega_2 d\upsilon_2 \tag{5.51}$$

Using the results of (5.50) and (5.51), the bit error probability expression can be evaluated by applying the total probability law:

$$P(Error) = (\frac{1}{2})^M\sum_{l=1}^{M}\binom{M}{l}\times\frac{1}{2}[Q(\frac{Th-\mu_{I,M,0}}{\sigma_{I,M,0}})+Q(\frac{\mu_{I,M,1}-Th}{\sigma_{I,M,1}})] \tag{5.52}$$

where $Th$ is the optimum threshold of the receiver for deciding on the received bit.

### 5.2.6 Numerical Approach for the NLS Equations

In order to check the accuracy of the presented analytical results, we use numerical approaches to find the solution for NLS equations. Some researchers have proposed different numerical methods for solving the NLS equations [79], [80], while [81] presents a time-splitting cosine-spectral (TS-Cosine) method when the nonzero far-field conditions are or can be reduced to homogeneous Neumann conditions. Our approach consists on discretizing the time and length of the fiber and replacing the continuous NLS equations (5.16), (5.17), (5.18) with their discrete form, as shown below:

$$C(t_m, z_{n+1}) = (1 - \frac{\Delta z \alpha_0}{2})C(t_m, z_n) - j\beta_1 \Delta z \frac{C(t_{m+1}, z_n) - C(t_m, z_n)}{\Delta t} + \frac{\beta_2}{2}\Delta z$$
$$\frac{C(t_{m+1}, z_n) - 2C(t_m, z_n) + C(t_{m-1}, z_n)}{(\Delta t)^2} + \frac{jn^{'}\omega_C \Delta z}{c}\Big[\Big(2f_{CC}|C(t_m, z_n)|^2 + 2f_{CS}|R(t_m, z_n)|^2$$
$$+ 2f_{CX}|X(t_m, z_n)|^2\Big)C(t_m, z_n) + 2f_{CSX}S(t_m, z_n)X(t_m, z_n)C^*(t_m, z_n)e^{j\Delta kz}\Big] \tag{5.53}$$

$$X(t_m, z_{n+1}) = (1 - \frac{\Delta z \alpha_0}{2})X(t_m, z_n) - j\beta_1 \Delta z \frac{X(t_{m+1}, z_n) - X(t_m, z_n)}{\Delta t} + \frac{\beta_2}{2}\Delta z$$
$$\frac{X(t_{m+1}, z_n) - 2X(t_m, z_n) + X(t_{m-1}, z_n)}{(\Delta t)^2} + \frac{jn^{'}\omega_X \Delta z}{c}\Big[\Big(2f_{XX}|X(t_m, z_n)|^2 + 2f_{XS}|S(t_m, z_n)|^2$$
$$+ 4f_{XC}|C(t_m, z_n)|^2\Big)X(t_m, z_n) + 2f_{XSC}S^*(t_m, z_n)C^2(t_m, z_n)e^{-j\Delta kz}\Big] \tag{5.54}$$

$$S(t_m, z_{n+1}) = (1 - \frac{\Delta z \alpha_0}{2})S(t_m, z_n) - j\beta_1 \Delta z \frac{S(t_{m+1}, z_n) - S(t_m, z_n)}{\Delta t} + \frac{\beta_2}{2}\Delta z$$
$$\frac{S(t_{m+1}, z_n) - 2S(t_m, z_n) + S(t_{m-1}, z_n)}{(\Delta t)^2} + \frac{jn^{'}\omega_S \Delta z}{c}\Big[\Big(2f_{SS}|S(t_m, z_n)|^2 + 2f_{SX}|X(t_m, z_n)|^2$$
$$+ 4f_{SC}|C(t_m, z_n)|^2\Big)S(t_m, z_n) + 2f_{SXC}X^*(t_m, z_n)C^2(t_m, z_n)e^{-j\Delta kz}\Big] \tag{5.55}$$

With these expression we can analyze the system step by step over fiber segments of length $\Delta z$.

## 5.3 Simulation Results

### 5.3.1 Simulation Environment

Based on the previous analytical model, we have simulated with Matlab and analyzed the effect of the pulse-width of the code on the BER of the receiver in an OCDMA system with six users using different OOC codes. We show the structure of typical optical correlator for extracting the data of a certain user in the receiver

of an OCDMA system in Fig. 5.3. In the time-gating method, a nonlinear media is used as an all-optical AND gate to separate the ultrashort pulse from the MAI signal, thus eliminating the interference signal. In fact the nonlinear media acts as a multiplier in electronic domain and for extracting of each user, the signal by code stored replica of each user is multiplied in received signal. We use NLS equations in discrete form (5.53), (5.54) and (5.55) to describe the nonlinear media so that we can simulate it numerically. After the detection we use the integrator to gather the obtained signal during the length of a bit. By sampling at the bit duration periods we can obtain the numerical value of the output.

The diagram of the simulation scenario is shown in Fig. 5.4. For this purpose, first we considered a bit for each users based on codes that defined on the Table 5.3, of course the signals used for chips are Sinc-shape. User's signals are randomly delayed in order to account for the fact that in real environments users are not synchronized. These user's signals gathered together and create the received signal. The distribution of bit values, "0" or "1", is uniform. We use a nonlinear fiber as a combiner, and with the combination of the received signal and the stored replica of each user code, the receiver extracts the desired user's signal. Fig. 5.4 shows an example with six users whose codewords are shown in Table 5.3. At the input of the receiver we have the sum of all the users for the duration of one bit. In all the simulations we assume that the duration of each bit, $T_b$, is 6300 ps (bit rate of 158.73 Mbit/s)and the duration of each chip is 100 ps (10 Gchip/s).

In order to generate the FWM effect we use a nonlinear fiber optic whose length is assumed to be 30 m and the power of the received and clock signal are 1 mW and 100 mW, respectively. The values of the other parameters used in the simulations are given in Table 5.2, based on [54]. In order to perform the simulations, we need information of the evolution of signals along the whole length of the fiber, during the whole period of the simulated time, thus the calculations are performed step by step in a recursive manner. In each step, at each $Z + \Delta z$ point we analyze the NLS equations (5.53), (5.54) and (5.55) from time 0 to $T$ in $\Delta t$ step sizes, and at the end of the line we obtain the output of the system. The bit encoding follows an OOC code

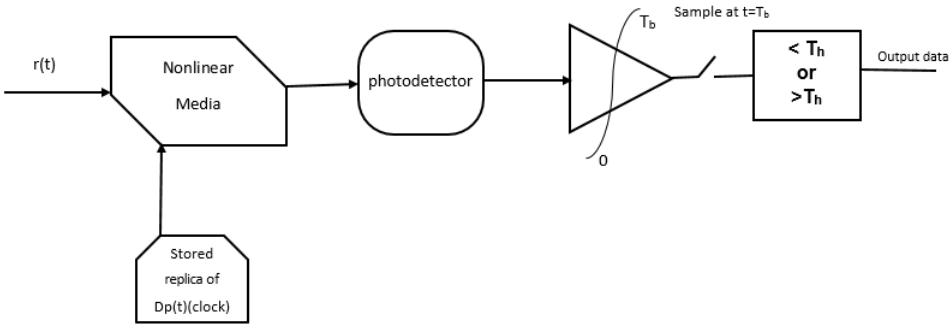


Figure 5.3: Ideal optical correlator using optical components.

with parameters ($F = 63, \lambda = 2, K = 9$), whose code words are listed in Table 5.3, where $F$ is number of division of at the duration of bit, chip, $K$ is the code weight (number of chips that are used for the code) and $\lambda$ is the autocorrelation between codes.

The output signal of the nonlinear media passes through the integrator and the sampler and, finally is compared with the threshold value (Th). If the value is bigger than $Th$ we decide that the sent bit was "1" and "0" otherwise. We calculate the BER by comparing the bit originally sent with the value decided at the output of the threshold module. Each simulation for each parameter is repeated until we achieve a confidence interval of 95% in the estimation of the BER.

### 5.3.2 Calculation of the Threshold

The optimum threshold (Th) for deciding if the bit was "0" or "1" is half of the output value when we simulate the system without any jitter, not delay between users and only one user, avoiding the interference from other users. We also assume that the bandwidth of the codes for the received signal is equal to the bandwidth of the codes in the clock signal, so we have maximum amplitude of the output. We only consider the effect of nonlinearity of the system. We obtain for each user, a different value of Th. In order to illustrate the process, Fig 5.5 shows waveform generated by six users using the codes define in table 5.3. The signal obtained at the receiver input, composed of the sum of the waveform, is shown in Fig 5.7. In Fig 5.9 we show the output signals when there is no jitter and users are synchronized (they start the communication simultaneously). We can obtain Th for each user by integrating of the waveforms during one bit period, Given the maximum value for the output of the integrator for each user, the $Th$ is half of these value.

### 5.3.3 Results

To confirm our hypothesis (the existence of an optimum value of the bandwidth of code pulse of clock signal for which the BER at the receiver is minimized) we have simulated the system and obtained the BER

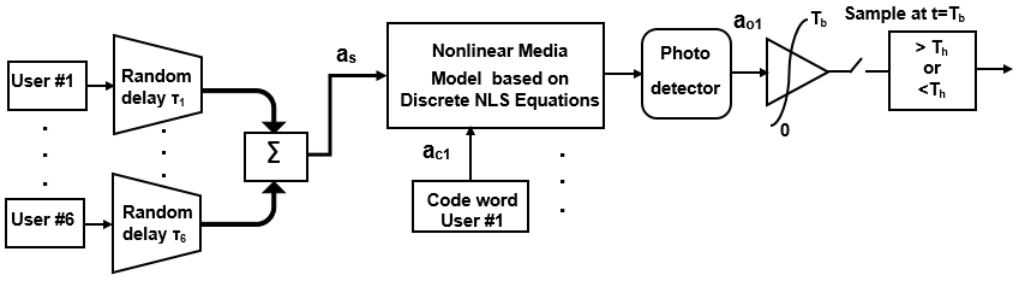


Figure 5.4: Block diagram of the Matlab simulation of an OCDMA receiver with six users.

for different values of jitter and delay between users. As we have seen in previous sections, jitter may be caused by long transmission distance, imprecision in the clocks used by optical devices, and errors in the synchronisation between the clock signal and the received signal. In our simulations, the range of variation of the jitter is up to 10% of the duration of chip or 20% of the duration of the clock period, which we think is plausible in real systems. In all our simulations we consider the power of the received signal to be 1 mW and power of the clock (pump) signal to be 100 mW. In real environments usually the power of pump is more than 100 times bigger than the received signal at the input of the receivers. In Fig 5.6 we show pump (clock) signal with code words that are the same as used to encode the user signals. One of the problems in OCDMA systems is the different delay between users, causing an increase in interference and depend of the cross-correlation between codes raise the BER in systems. Fig. 5.8 illustrates the six users with different delays. In comparison to Fig. 5.7 the signal has lost amplitude and has increased the interference.

We first simulate the system with synchronized users, and investigate the effect of changing the bandwidth of codes in the clock signal with presence of a random jitter in the clock signal. Fig. 5.10 shows the output signals, $a_o$, for each one of the six users when there is random jitter in the code pulse width (clock signal). As mentioned in section (5.1), by increasing the jitter in the code pulse width, MAI is increased and the error rate increases. In fact, this jitter can cause error in the detection of the desired user's data. By widening the code pulse width, the receiver performance can be improved. This manipulation could be helpful in the detection of a bigger portion of the data pulse. On the other hand, by increasing the pulse width of the clock signal, a part of the pulses from adjacent users will be also gathered by the detector. This effect generates another error source at the output signal, and by increasing the pulse width of the clock, this error becomes larger. Considering the trade-off the two described error sources, there exists an optimum value for the clock signal's pulse width, for which the BER is minimized.

In Figures 5.11, 5.12, the BER at the output of system has been plotted in terms of the ratio of the code signal's bandwidth, $T_c$, to the bandwidth of chip, $T_{chip}$, for a fixed code and power amplitude and different pulse-widths of the received signal, $T_d$, and different jitter, $\sigma_\tau$. In this case we assume that we have a perfect synchronization between the pump signal (clock signal) and the input signals in the four-wave mixer,

| User's No. | Codes | | | | | | | | |
|---|---|---|---|---|---|---|---|---|---|
| user1 | 1 | 5 | 8 | 18 | 28 | 31 | 35 | 40 | 59 |
| user2 | 2 | 7 | 10 | 16 | 17 | 36 | 55 | 56 | 62 |
| user3 | 3 | 11 | 24 | 25 | 27 | 29 | 30 | 43 | 51 |
| user4 | 4 | 9 | 14 | 20 | 32 | 34 | 47 | 49 | 61 |
| user5 | 6 | 22 | 23 | 39 | 48 | 50 | 54 | 58 | 60 |
| user6 | 12 | 15 | 33 | 37 | 44 | 45 | 46 | 53 | 57 |

Table 5.3: OOC codewords for 6 different users with $F = 63$, $K = 9$ and $\lambda = 2$, (63,9,2)

and the users are synchronized ( their delays are the same). As we see from the results, by increasing the code pulse-width the collected energy becomes larger. However, by widening the code pulse, portions of the neighboring codes are also collected and the interference caused by the other users gathered by the receiver becomes larger. Also, by decreasing the bandwidth of the code used in the clock signal, we lose some of the amplitude of the codes in the chips and BER increases. Hence, there is an optimum point for which the ratio between the gathered energy and reduction of interference due to other users. Of course reducing the bandwidth of the code in compare of bandwidth of the chip cause reducing the BER, but for this purpose we need to allocate more frequency bandwidth for transferring data in OCDMA, an approach that is not economically feasible. On the other hand, by increasing the data rate, the jitter of the code signal in the receiver will also increase and the performance of the receiver is degraded. So by selecting an optimum value for the code bandwidth in the receiver we can improve the SNR.

By increasing the number of users and introducing different delay between them causes the MAI to increase, thus degrading severely the receiver performance, while a stronger pump signal improves the performance of the receiver. We plot six users with different delay in Fig. 5.13 and the sum of these signals at the input of FWM in Fig. 5.8. For these series of simulations we introduce different delay between users and jitter on the clock signal. In realistic performance analysis, we have to consider an error in the synchronization of the pump and input signals in four-wave mixer, and therefore we have more MAI noise and more jitter noise in the system. This synchronization error can degrade the performance of this kind of receivers. The output signal for six users with different delay and jitter on the clock signal is shown in Fig. 5.14. As we see the original shape of codes is destroyed and regarding to arrange some of them reduce its amplitude, sometimes leading to errors in the detector. In general, errors in the detection of a “0” bit sent are high error than vice-verse, because of the interference of other users.

Figs. 5.15 and 5.16 show the BER of the receiver versus the ratio of the pulse width of the clock codes to the bandwidth of the chip for different jitter and random delay values. In Fig. 5.15 the results are for $T_d = 0.3T_{chip}$ and $T_{chip} = 100\ ps$ and in Fig. 5.16 for $T_d = 0.5T_{chip}$ and $T_{chip} = 100\ ps$ and different jitter values. The optimum bandwidth of the code signal (pump or clock) can vary with the transmitted power of users, the power of the pump signal and the number of interfering users. The figures have been caculated for a fixed pump power and different number of interfering users (in the simulation every user to multiply random number of “0” or “1” uniformly). As shown, the BER is increased for bandwidth smaller than the optimum one, because of the presence of MAI. For a bandwidth bigger than the optimal and increasing number of interfering users, a great part of the MAI signal is collected at the receiver and this degrades the SNR of the receiver (the BER is increased). In Figs. 5.17 and 5.18 we can see the BER has increased, compared to Fig. 5.11 and Fig. 5.12, because data is asynchronously transmitted.

Figs 5.17 and 5.18 show the BER the ratio of the bandwidth of codes in the clock signal and the bandwidth of the chip signal for different jitter, and bandwidth of codes in the data, the figure includes both the analytical and simulated results. The analytical results in Fig. 5.17, 5.18 are plotted using (5.52). Integrals in (5.50) and (5.51) are solved by numerical methods for different bandwidths of clock, data and jitter and by substituting the mean and variance in (5.52) we obtain the BER. As we see from the results, by increasing the code pulse-width the collected energy becomes larger. However, by widening the code pulse, portions of the neighboring codes are also collected and the interference caused by the other users gathered by the receiver becomes larger. Hence, there is an optimum point for which the ratio between the gathered energy and the variance reaches a maximum. On the other hand, by increasing the jitter of the code signal in the receiver, the performance of receiver is degraded.

Fig. 5.19 depicts the optimum bandwidth of the clock versus the number active users for a fixed jitter. We have used an OOC code with length $F = 70$, weight $w = 10$ and cross-correlation $\lambda = 3$. According to the Johnson bound [82], the maximum number of users is given by

$$\text{Maximum Number of Users} \leq \left\lfloor \frac{(F-1)(F-2)\cdots(F-\lambda)}{w(w-1)\cdots,(w-\lambda)} \right\rfloor.$$

Therefore, for this code the number of users is bounded by 62. We have used only 52 codewords from this code. The list of the codewords is provided in Table 5.4. These codes are generated using the algorithm introduced in [82]. Each row shows the position of the bits with value "1" in each codeword.

For each number of active users, we repeat the simulation to obtain the optimum bandwidth of clock signal for which the BER is minimized. The optimum bandwidth of the user's code receiver (clock) varies in terms of the number of interfering users. As shown in Fig. 5.19, by increasing the number of active users, the optimum bandwidth is smaller to avoid gathering the interference from other undesired users because of the increase of the MAI signal. On the other hand, for smaller number of active users we need a larger bandwidth for a better detection of desired signals. Therefore, by selecting an optimum value for the code bandwidth in the receiver we can improve the signal to noise ratio.

Here we consider the effect of the number active users in the BER of system and find the optimum bandwidth of the clock signal for different number of active users. For this purpose we simulate the system for a fixed jitter, 1 $ps$, and for each number of active users we repeat the simulation. We have used different OOC codes, whose weight (k) is defined in Table 5.4. Because of the higher number users and code weight, the autocorrelation between code of each user and crosscorrelation between codes of other undesired users are increased. In Fig. 5.20 the BER versus the number of active users is ploted. In this case the jitter is

| Code's No. | Codes | Code's No. | Codes |
|---|---|---|---|
| 1 | 10-66-69-39-4-16-23-52-1-3 | 27 | 3-6-37-38-42-48-49-52-56-69 |
| 2 | 28-37-29-45-42-19-70-1-62-11 | 28 | 4-5-7-16-29-35-49-57-59-64 |
| 3 | 17-13-57-52-62-8-12-7-31-64 | 29 | 2-18-29-35-43-45-50-55-56-59 |
| 4 | 34-3-10-57-2-14-42-11-51-48 | 30 | 17-21-22-34-40-44-45-47-53-60 |
| 5 | 43-5-57-1-64-61-45-55-18-60 | 31 | 7-11-28-29-30-34-49-52-58-68 |
| 6 | 25-6-53-40-42-64-5-7-55-51 | 32 | 3-10-34-35-40-54-57-58-67-68 |
| 7 | 9-27-55-1-22-61-42-5-57-50 | 33 | 1-3-5-11-17-21-33-38-50-58 |
| 8 | 30-48-19-53-12-43-57-60-24-70 | 34 | 11-23-29-34-39-42-44-51-56-64 |
| 9 | 1-2-9-23-27-29-38-49-51-67 | 35 | 4-18-21-27-30-49-50-52-57-61 |
| 10 | 1-6-8-13-20-34-35-38-54-59 | 36 | 4-12-28-29-38-45-57-59-66-70 |
| 11 | 2-11-26-34-37-43-44-48-57-69 | 37 | 6-11-12-33-40-48-49-50-59-67 |
| 12 | 2-3-15-24-28-50-53-56-60-67 | 38 | 1-17-18-32-39-47-49-58-67-68 |
| 13 | 1-7-9-10-13-26-29-33-37-63 | 39 | 3-6-37-38-42-48-49-52-56-69 |
| 14 | 4-5-15-16-22-29-31-39-44-49 | 40 | 4-5-7-16-29-35-49-57-59-64 |
| 15 | 2-18-19-23-28-32-45-48-58-59 | 41 | 17-25-28-33-38-39-43-45-47-57 |
| 16 | 1-5-6-12-19-28-37-46-47-53 | 42 | 4-6-16-17-23-42-57-58-65-70 |
| 17 | 1-12-16-26-31-34-35-49-57-65 | 43 | 8-9-18-19-20-31-36-39-44-64 |
| 18 | 1-2-8-9-14-19-32-33-42-47 | 44 | 2-13-14-17-33-39-42-48-58-67 |
| 19 | 5-9-18-19-27-33-39-48-49-68 | 45 | 5-6-7-9-23-31-57-61-62-65 |
| 20 | 4-7-13-14-15-22-27-29-38-49 | 46 | 5-20-22-38-40-50-51-53-61-67 |
| 21 | 10-16-23-27-34-41-50-57-63-64 | 47 | 4-6-20-22-24-27-34-39-54-61 |
| 22 | 7-11-19-26-30-35-37-48-67-69 | 48 | 11-15-28-35-54-56-59-62-63-64 |
| 23 | 1-2-10-11-23-30-36-40-56-68 | 49 | 6-7-16-21-24-43-47-64-68-69 |
| 24 | 1-3-4-20-28-31-33-41-51-55 | 50 | 2-7-15-16-19-25-27-63-66-68 |
| 25 | 4-13-15-19-27-35-56-57-59-70 | 51 | 1-8-17-26-50-51-52-59-66-67 |
| 26 | 3-4-13-36-37-46-58-59-63-67 | 52 | 17-25-28-33-38-39-43-45-47-57 |

Table 5.4: List of codewords for a $(70, 10, 3)$ OOC code.

constant and the bandwidth of codes for the clock and received signals are the same, and according to the increased number of users, there is more interference and so BER is increased. Simulation results show that for more number active users the BER curve would be destroyed and would not have significant changes, So the performance of receiver greatly reduced.

*A Rule for Choosing the Optimal Clock Pulse-Width:* Based on the simulation results, we have fitted the curves to obtain an approximate formula that gives the optimal clock signal's pulse-width in terms of the MAI, jitter, and the ratio of the data signal pulse-width to the chip interval, i.e., $T_d/T_{chip}$. For simplicity we assume $T_d/T_{chip} = \alpha$. Then, the optimal $T_c$ is

$$T_c \approx T_{chip} \frac{1.65\alpha^{1.71}(\beta^2 + 3.82\beta)}{(N_{act}\lambda^2/F)^{0.85}}$$

where $(N_{act}\lambda^2/F)$ is the MAI caused by interfering users, $N_{act}$ is the number of active users, and $\beta = \sigma/T_d$, with $\sigma$ being the standard deviation of the jitter. This equation is estimated by fitting a curve into numerical results and calculating the coefficients that minimize the mean squared error. As it is expected, by increasing

the jitter, $\sigma^2$, $T_c$ increases to make sure we capture correctly the main signal. Also, increasing the MAI forces $T_c$ to decrease to push the amount of the collected interference signal to a smaller value.

## 5.4 Conclusions

In this chapter we consider optical time gating OCDMA receiving using OOC codes and analyze the effect of the bandwidth of the code signal pulse in the receiver and also the effect of different jitter amplitudes on the performance of the receiver. First we model the FWM process using NLS equations and the first three terms of the Volterra expansion are used to solve it. We obtain the spectral autocorrelation function of the input and output signals at the FWM device and then we obtain the mean and variance of the photo-detector output current from the autocorrelation function. We analyze and simulate the optical nonlinear media in an OCDMA receiver system using NLS equations and calculate the BER at the output. The analytical results have been validated with a simulation using discrete NLS equations for describing the FWM in the receiver of the OCDMA system. These simulations have been performed for different cases, including variation in the delay of users and random jitter in the clock. Finally, we have corroborated our hypothesis about the existence of an optimum value for the pulse width of the code signal for which the BER is minimized, and based on simulation results we found a rule for choosing the optimal clock pulse width.

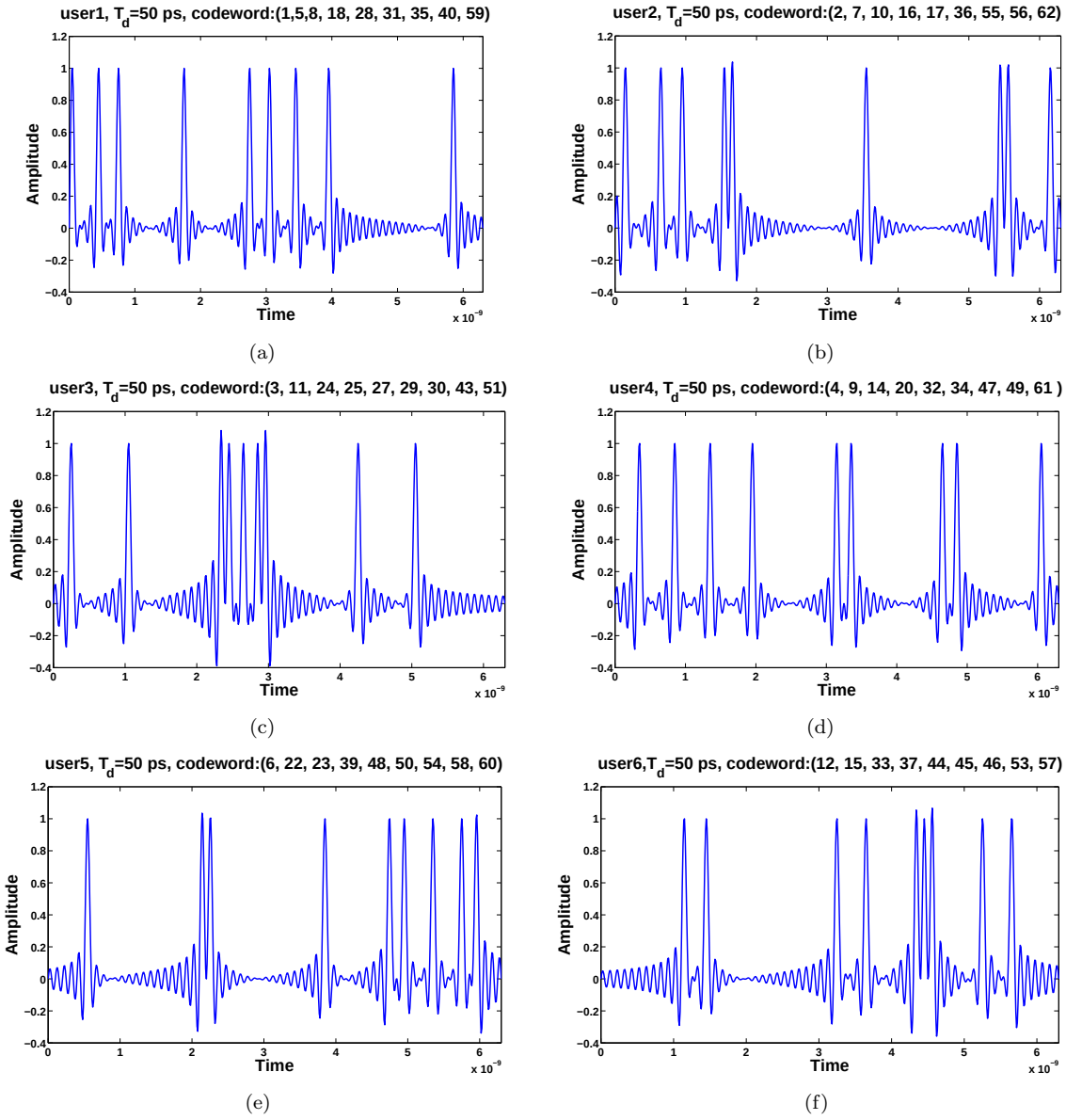


Figure 5.5: Waveform of the input signal of six users with different orthogonal codes, duration of bit = 6300 ps and duration of chip = 100 ps and signal power = 1 mW(a) $T_d = 50ps$, user code:( 1 5 8 18 28 31 35 40 59), (b) $T_d = 50ps$, user code:(2 7 10 16 17 36 55 56 62), (c) $T_d = 50ps$, user code:(3 11 24 25 27 29 30 43 51), (d) $T_d = 50ps$, user code:(4 9 14 20 32 34 47 49 61), (e) $T_d = 50ps$, user code:( 6 22 23 39 48 50 54 58 60) and (f) $T_d = 50ps$, user code:(12 15 33 37 44 45 46 53 57).

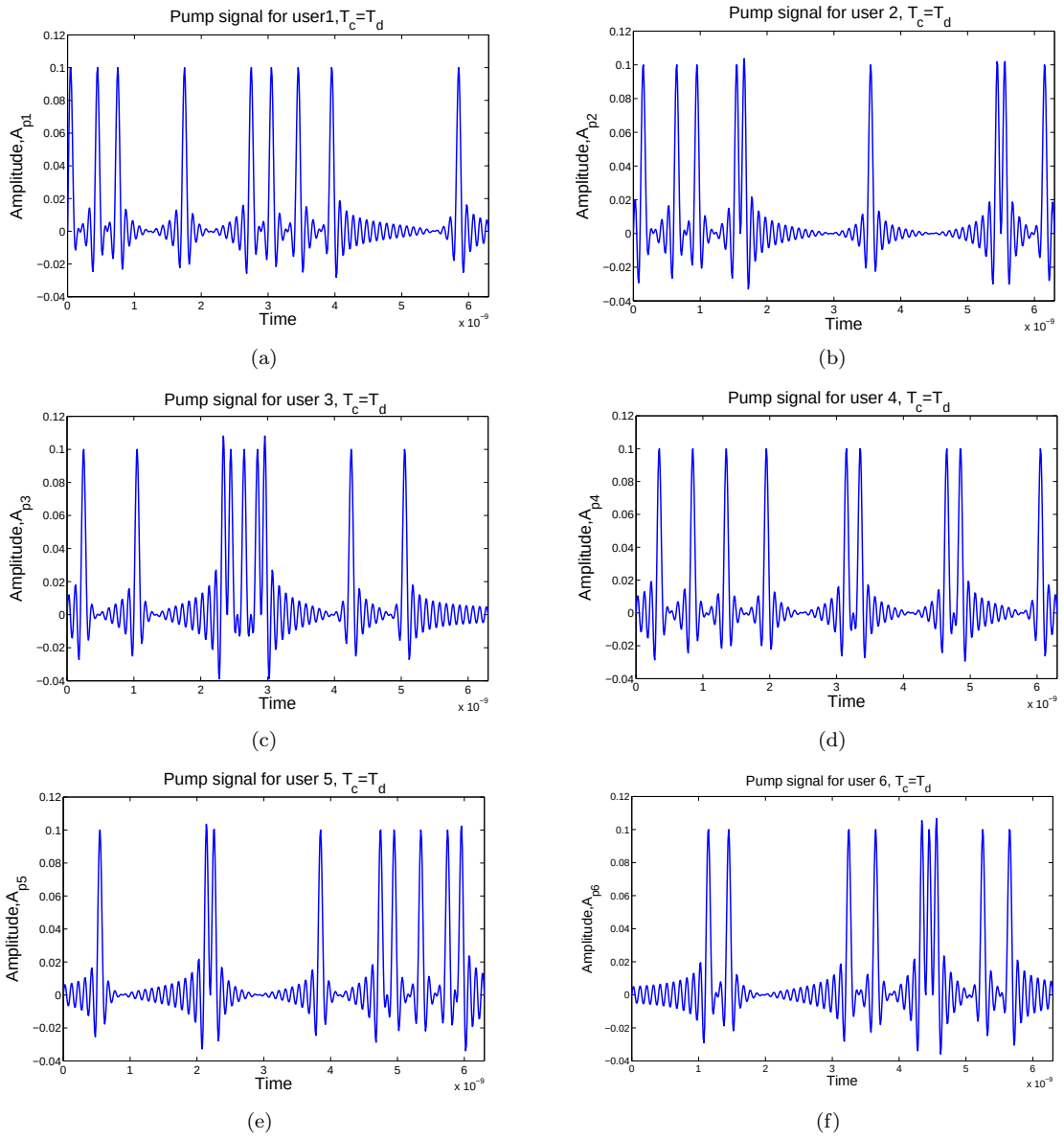


Figure 5.6: Waveform of the pump (clock) signal with the same codes used by users, duration of bit = 6300 ps, duration of chip = 100 ps, and power = 100 mW (a) $T_d = 50ps$, user code:( 1 5 8 18 28 31 35 40 59), (b) $T_d = 50ps$, user code:(2 7 10 16 17 36 55 56 62), (c) $T_d = 50ps$, user code:(3 11 24 25 27 29 30 43 51), (d) $T_d = 50ps$, user code:(4 9 14 20 32 34 47 49 61), (e) $T_d = 50ps$, user code:( 6 22 23 39 48 50 54 58 60) and (f) $T_d = 50ps$, user code:(12 15 33 37 44 45 46 53 57).

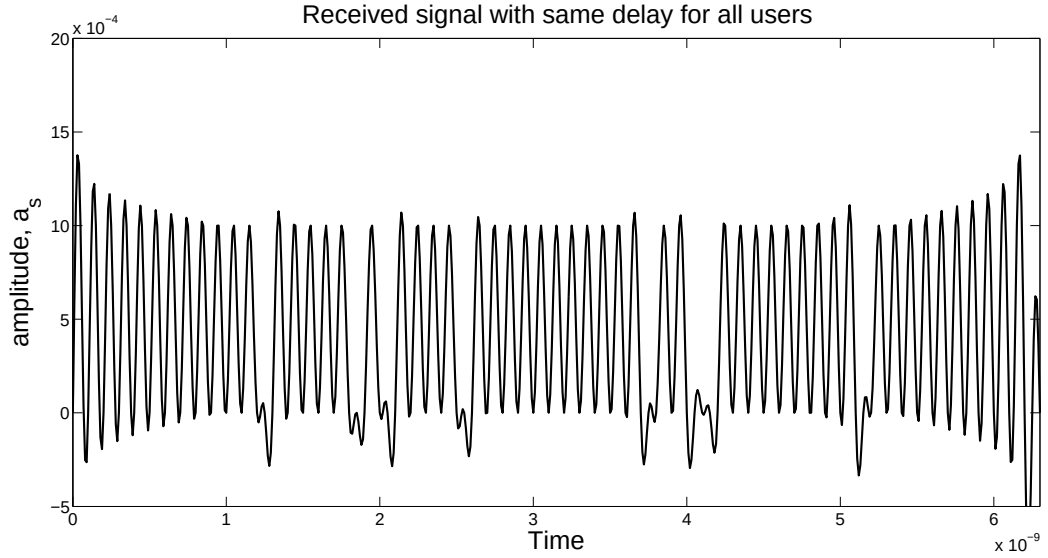


Figure 5.7: Signal at the input of the receiver, for six users, $a_s$, by assuming that all users have same delay.

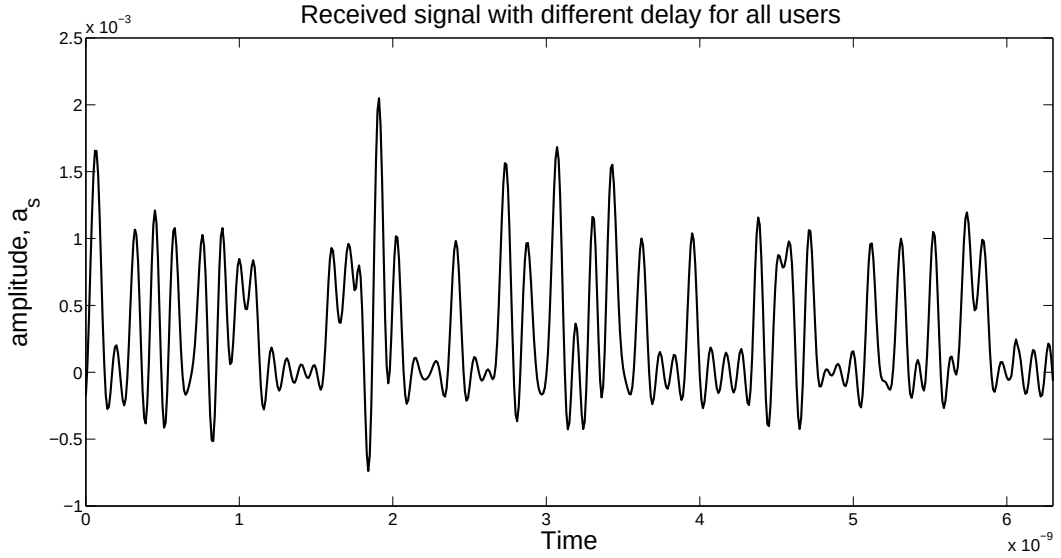


Figure 5.8: Signal at the input of the receiver, for six users, $a_s$, by assuming that all users have different delay.

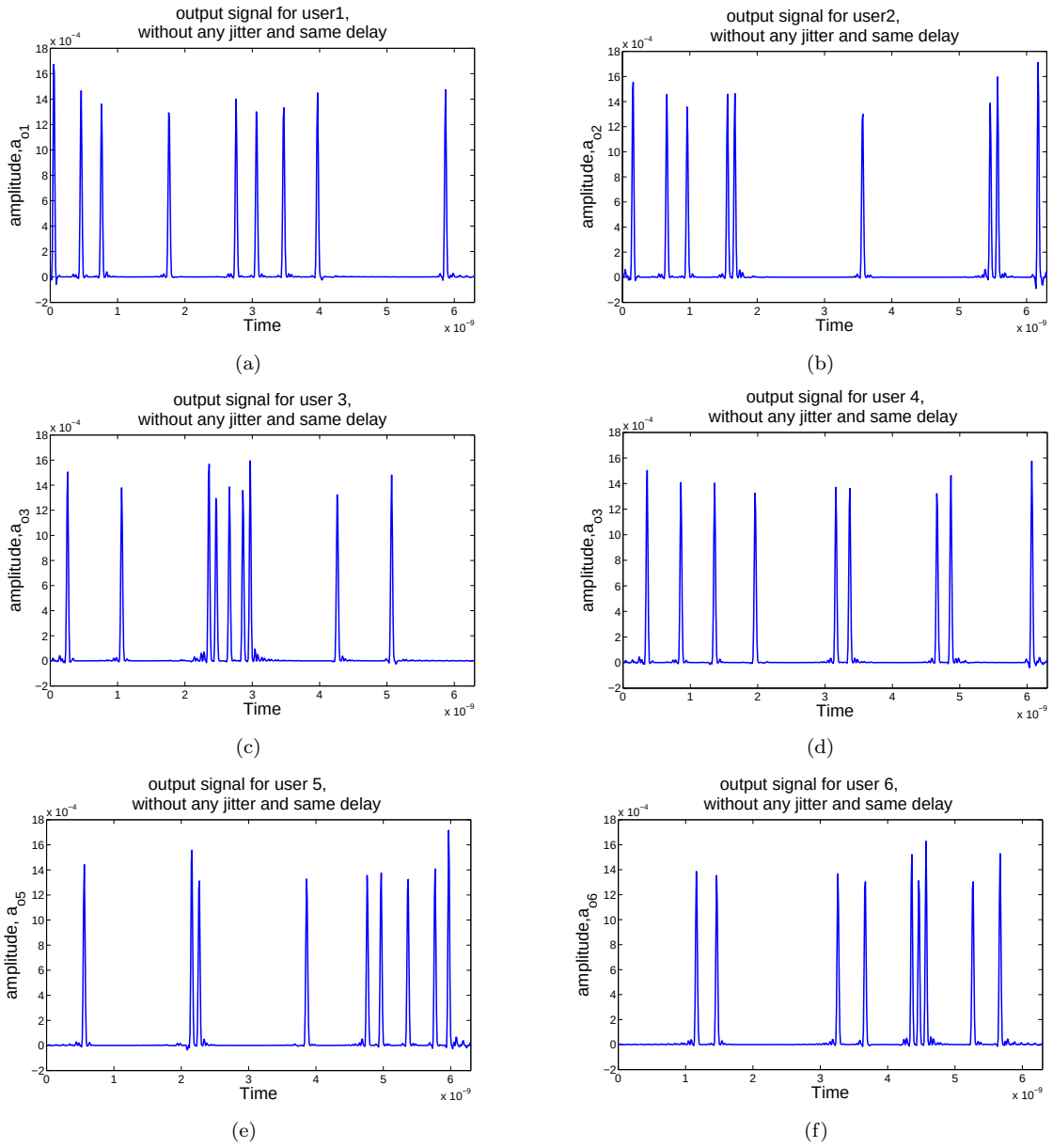


Figure 5.9: Signals of the different users at the output of the nonlinear media. There is no jitter and users are synchronized, $T_d = T_c = 50ps$. From a) to f), $a_{o_{1-6}}$ (users "1" for all).

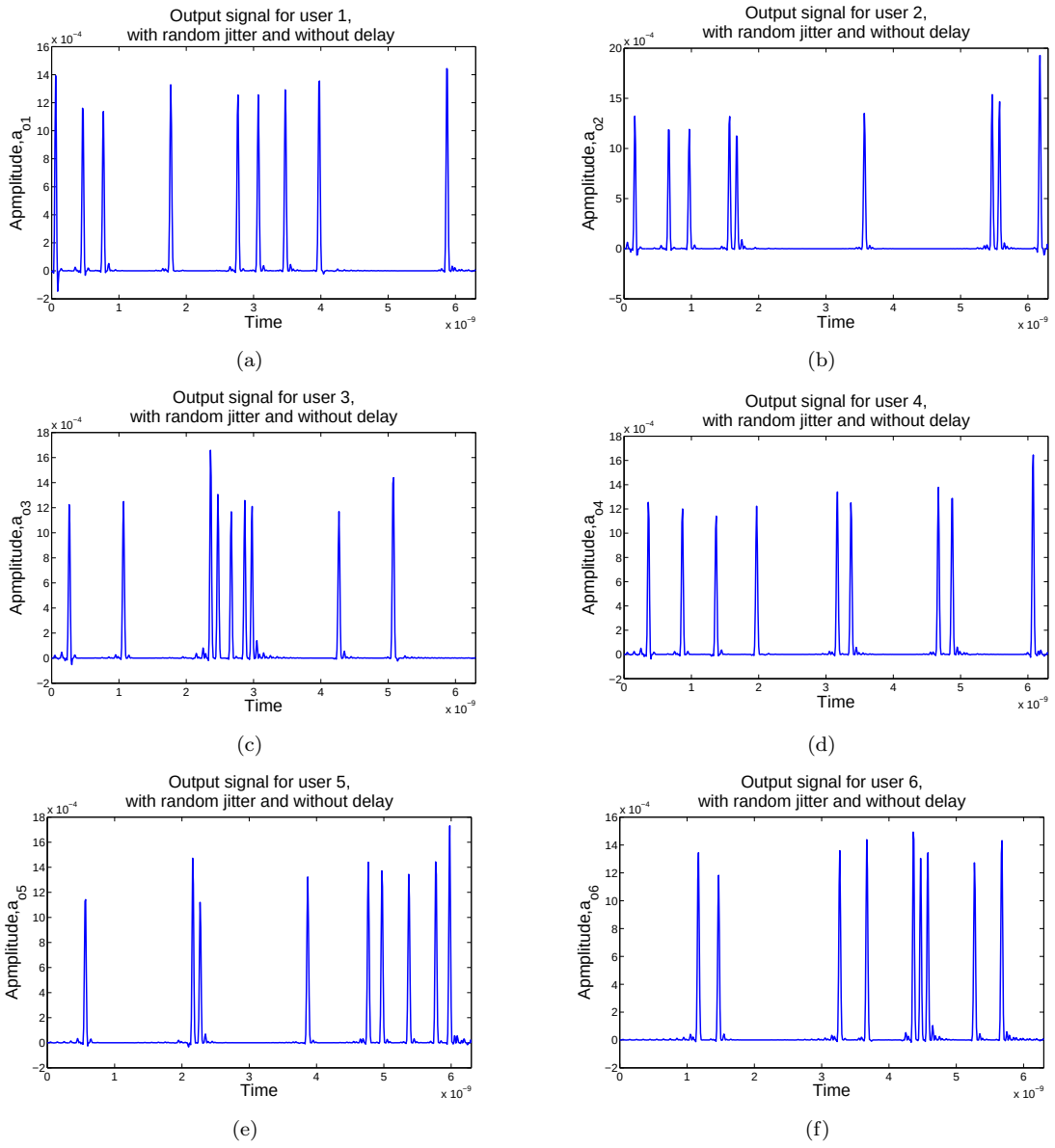


Figure 5.10: Signals of the different users at the output of the nonlinear media with random jitter on the pump signal, keeping the users synchronized, $T_d = T_c = 50ps$. From a) to f), $a_{o_{1-6}}$ (users "1" for all).

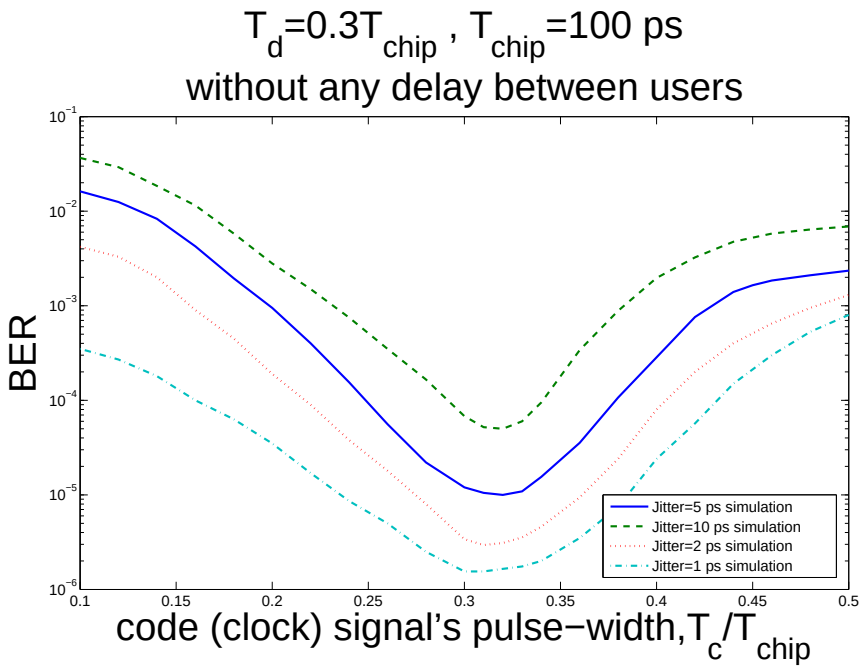


Figure 5.11: BER against the normalized clock bandwidth of user 1, $T_d = 30\ ps$ for different jitter amplitudes and same delay for all the users.

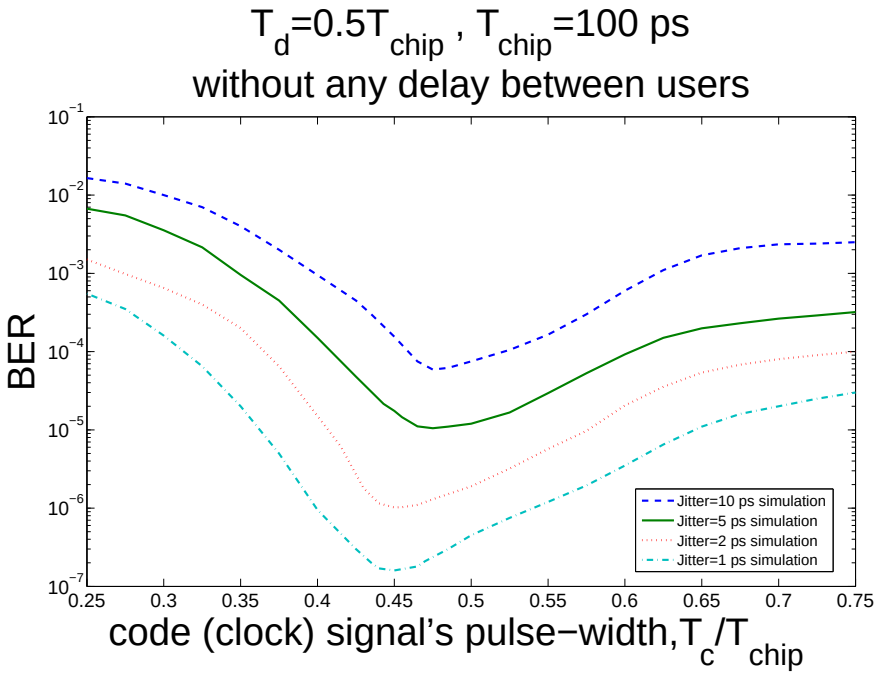


Figure 5.12: BER against the normalized clock bandwidth of user 1, $T_d = 50\ ps$ for different jitter amplitudes and same delay for all the users.

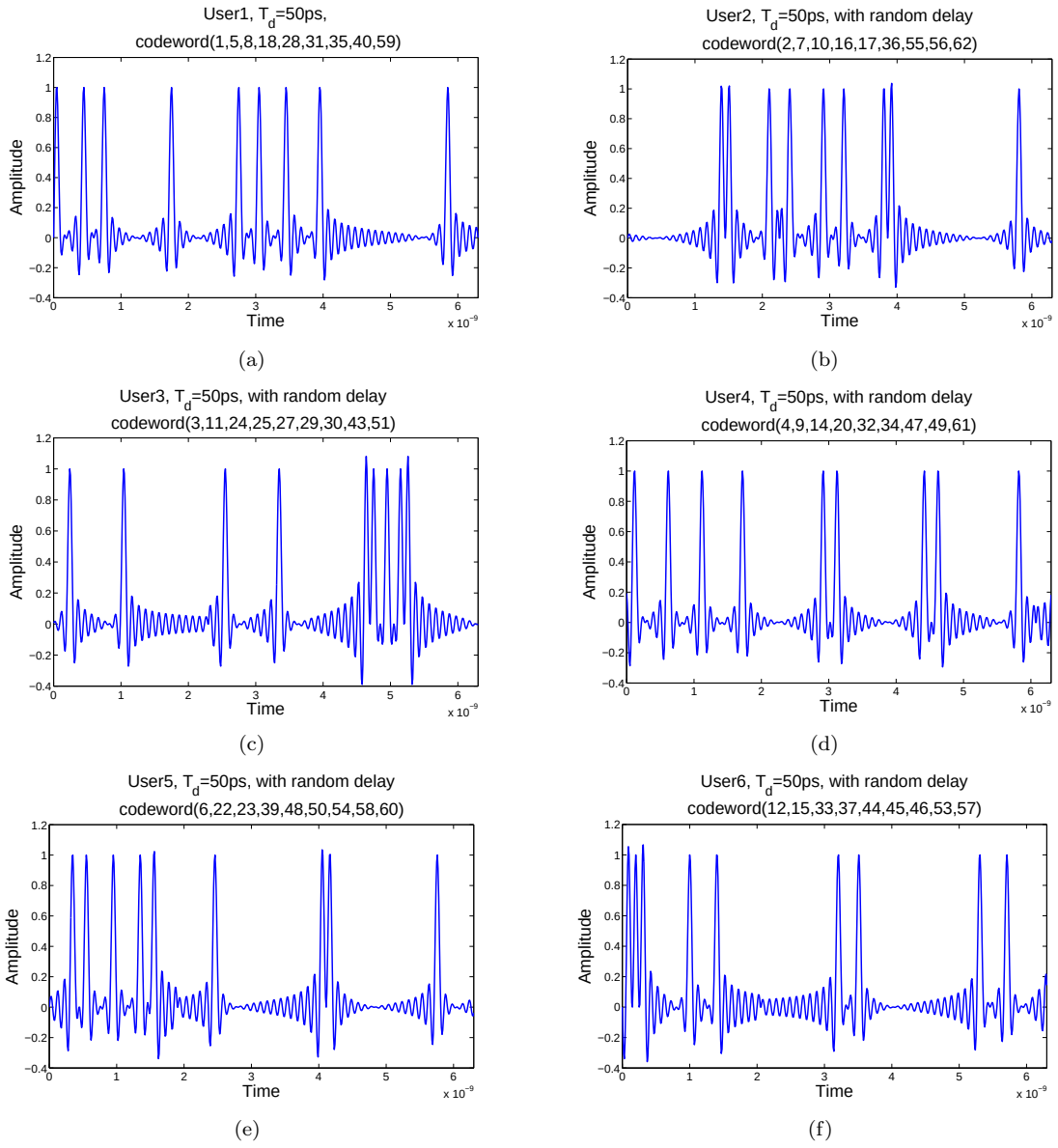


Figure 5.13: Input signals for different users with random delay for every user (a) user 1, (b) user 2, (c) user 3, (d) user 4, (e) user 5 and (f) user 6.

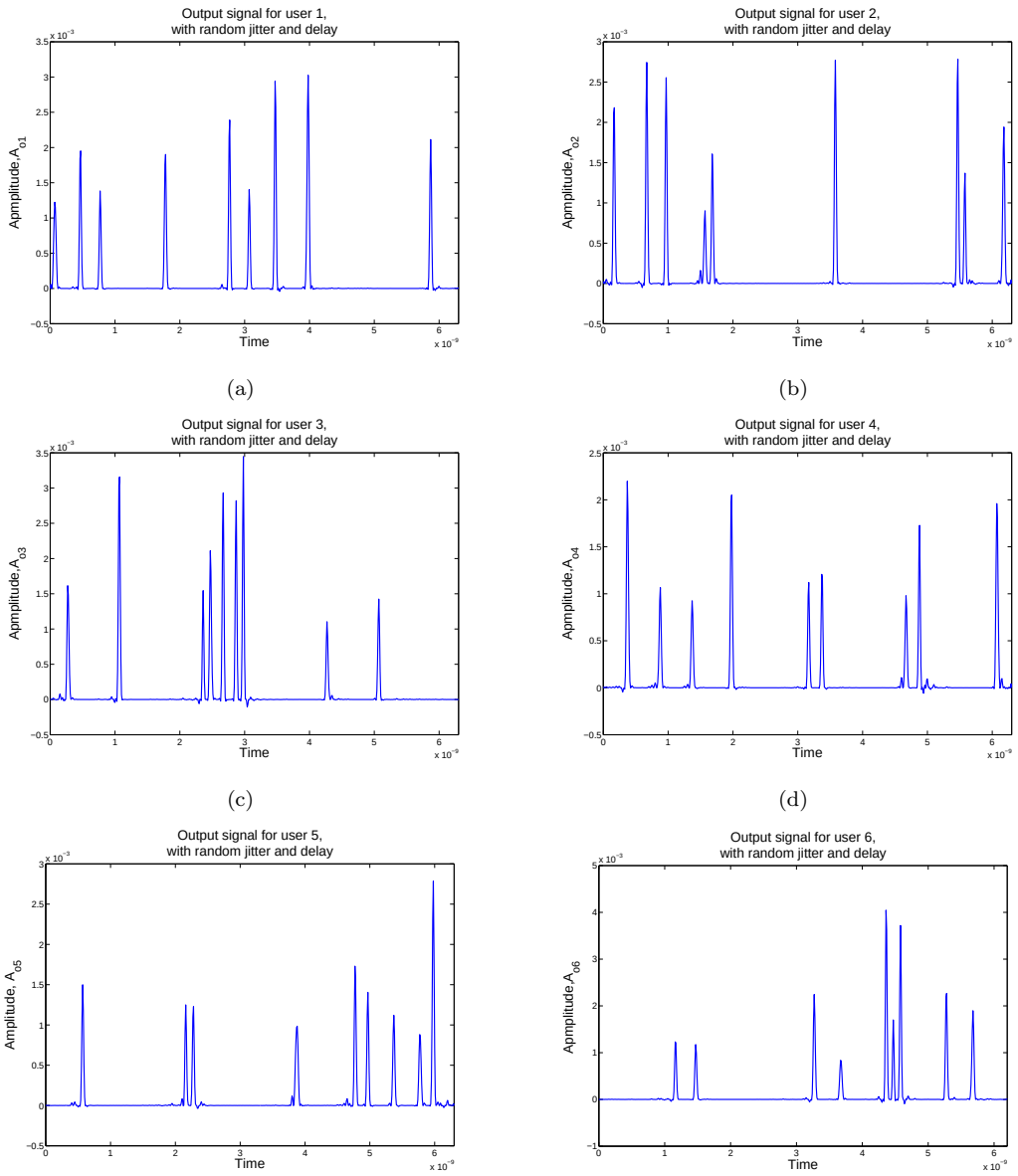


Figure 5.14: Signals for different users at the output of the nonlinear media, with random delay and random jitter with $T_d = T_c = 50\ ps$ (a) From a) to f), $a_{o_{1-6}}$ (users "1" for all).

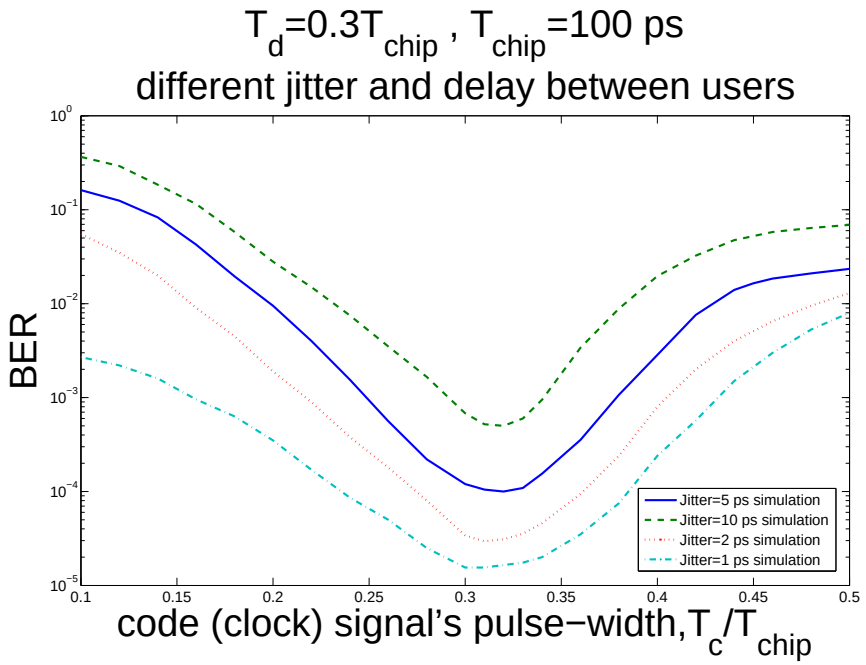


Figure 5.15: BER against the normalized clock bandwidth of user 1, $T_d = 30\ ps$ for different jitter amplitudes and random delay between users.

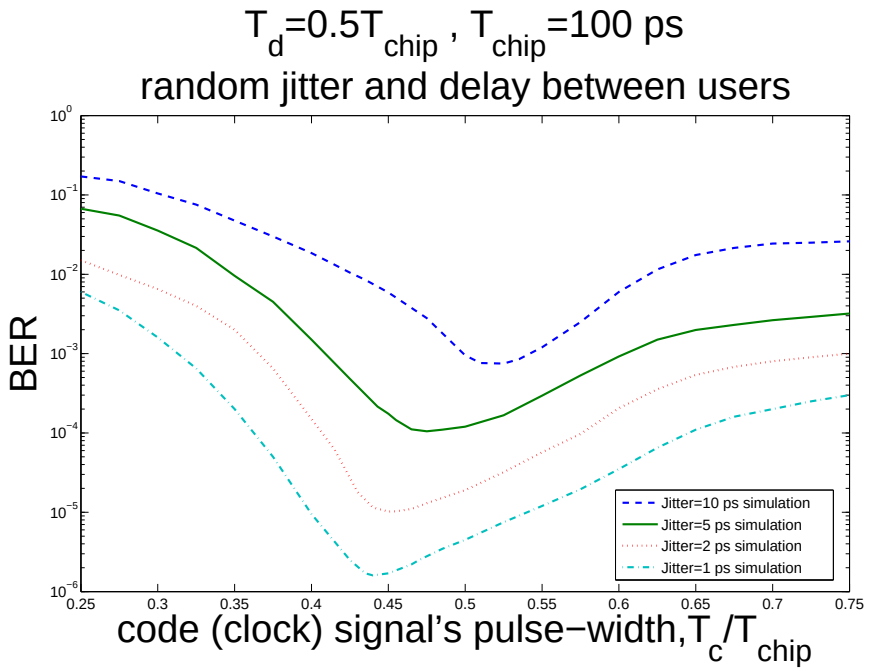


Figure 5.16: BER against the normalized clock bandwidth of user 1, $T_d = 50\ ps$ for different jitter amplitudes and random delay between users.

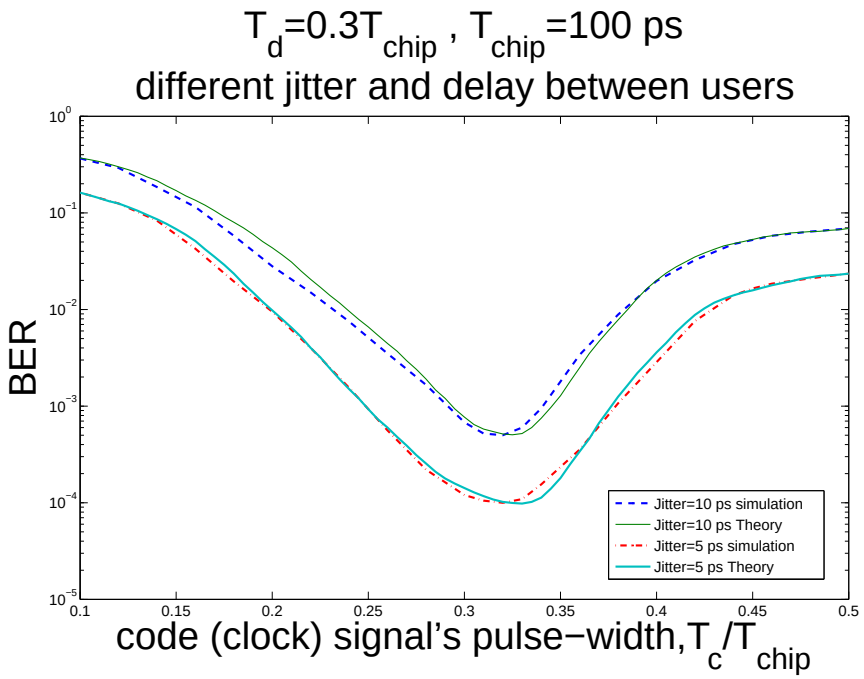


Figure 5.17: BER against the normalized clock bandwidth for user1, $T_d = 30\ ps$ and different jitter amplitudes and random delay for each user, (Both analytical and simulated results are shown).

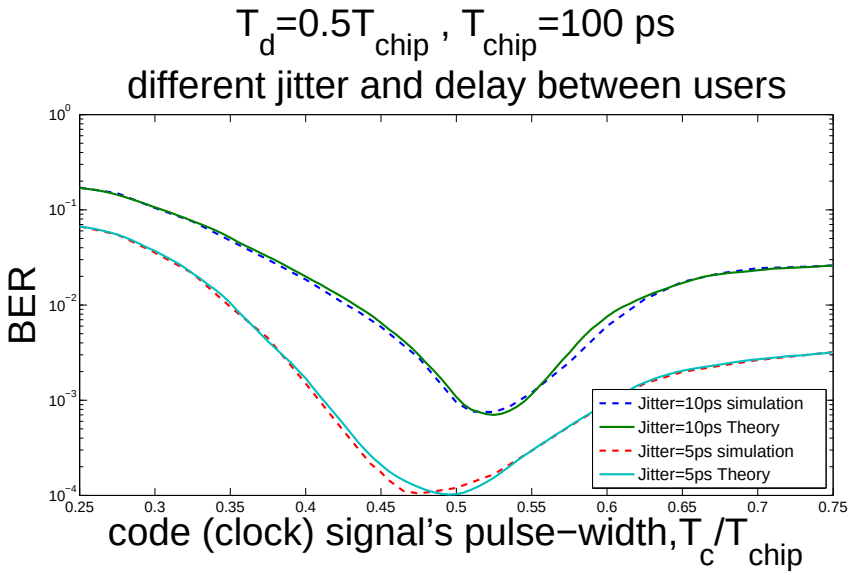


Figure 5.18: BER against the normalized clock bandwidth for user1, $T_d = 50ps$ and different jitter amplitudes and random delay for each user, (Both analytical and simulated results are shown).

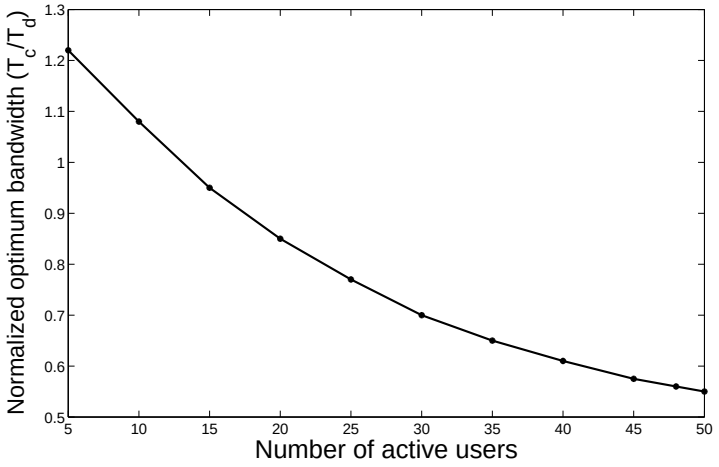


Figure 5.19: Normalized optimum pulse-width of the clock signal versus the number of active interfering users for OOC codes, $T_{chip} = 100\ ps$, $T_b = 6300\ ps$.

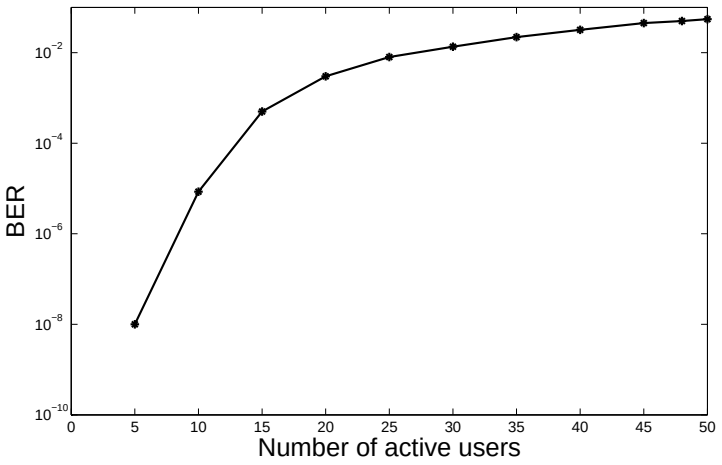


Figure 5.20: Simulated BER versus the number of active interfering users for OOC codes, $T_{chip} = 100\ ps$, $T_b = 6300\ ps$, jitter 1ps and optimal $T_c$ as calculated in Fig. 5.19.

Chapter 6

# Conclusions and Future Work

This chapter summarizes the main conclusion from the results obtained in our work together with a short discussion of future research lines.

## 6.1 Conclusions

This dissertation has focused on high speed OTDMA and OCDMA networks, and specifically on the application of nonlinear media on the optical receiver, with the goal of analyzing the effect of the jitter in performance of systems. We have proposed a new technique for analyzing nonlinearities in optical communication networks. For this purpose, we have reviewed the latest developments in optical multiple access techniques and different coding methods in the state of art. We classified and compared OCDMA techniques based on different choices of optical sources, detection schemes and coding techniques. In optical multiple access, because of the usage of ultra-short light pulses even the fastest electronic photo detectors are not able to separate the data of the desired user from signals of other users, and therefore optical signal processing on received signals is needed. We have studied multiple access interference cancellation techniques such as Optical Time Gating and Optical Thresholding. Related to the application of the fiber nonlinearity effect in these techniques for Multi User Interference Rejection we have considered different effects of nonlinearity such as Second Harmonic Generation (SHG), Two Photon Absorption (TPA), Self Phase Modulation (SPM), Cross Phase Modulation (XPM) and Four Wave Mixing (FWM).

Optical nonlinearities have many different effects in optical fibers. These effects can be disadvantageous in optical communications, but they also have many useful applications, especially for the implementation of all-optical processing in optical networks. In fact, nonlinear effects will be particularly important in the next generation of optical networks, which will rely on all-optical functions higher speeds and greater capacity.

All-optical devices and systems should permit the partial removal of optical-electronic-optical transformation in optical networks. In the third chapter we describe the application of nonlinear optical effects in optical communication such as the use of FWM as an AND gate. We consider fiber nonlinearities, the origin of FWM, and model FWM analytically using Schrödinger equations. We obtain the coupled FWM equations and solve these equations by Volterra series.

The application of nonlinear media as an AND gate on receivers of optical TDM and CDMA networks has been investigated in chapters 4 and 5. We have studied the structure of the receiver of an OTDM system that uses the optical time gating method. Optical time gating requires optical clock recovery, which is an essential requirement for synchronising the clock signal with the received data signal. When the bit-rate in optical transmission increases, duration of bit, and the accuracy of the clock recovery decreases because of the shorter duration of the pulses, and consequently, a time jitter appears in the clock signal. In Chapter 4, the effects of the clock signal pulse width and different jitter amplitudes on the performance of the receiver are studied. An analytical model of an on-off modulated OTDM system is analyzed using both approximate analytical model and simulated results. An optimum clock signal width for obtaining the best performance of the receiver and the minimum BER for different errors and bit length was obtained.

In Chapter 5 we have considered the case of optical CDMA system, and we focused on the time-spreading technique since, because of its simplicity and low cost, it is the most popular form of OCDMA, and we use optical orthogonal codes (OOC) as the encoding method as they have good auto- and cross-correlation properties. In high speed communication systems, increasing the number of simultaneous users is challenging since it increases the multiple access interference, which appears as a noise to receivers. On the other hand by decreasing the time width of the bits and chips causes an error in the correlation receivers due to the effect of small time mismatch between the clock and the received signal at the receiver and as a result bit error rate increases. In this chapter, the effect of the code signal pulse in the receiver and different jitter amplitudes on the performance of the receiver in time spreading OCDMA technique is considered. We have modeled analytically the nonlinearity of the optical nonlinear media in an OCDMA receiver system using nonlinear Schrödinger equations. We solved this model using Volterra series and we obtained the mean and variance of the photo-detector output current, and used it to evaluate the BER in the output. Finally, we have corroborated our hypothesis about the existence of an optimum value for the pulse width of the code signal for which the BER is minimized.

Throughout the document, we have simplified the details of the steps taken to solve the equations. The appendixes include a detailed version of the calculations. In Appendix A we considered to calculation of the relationship between the optical detector's current and the Fourier transform of the optical field for obtaining the mean and the variance of the detector's output current. The calculation of Volterra series

terms in Appendix B is needed in order to apply them to solving the NLS equations. Appendix C includes characteristics Fourier transform of stationary random processes and white noise needed to calculate the Fourier transform of the autocorrelation function. In Appendix D we have solved the NLS equations for a nonlinear media using Volterra series. Finally, in Appendix E we calculate the mean and the variance of the current in the output of optical detector, needed to calculate the BER in chapter 5.

## 6.2 Future Work

Optical fibers are known to have a nonlinear behavior in carrying signals in long haul systems [83], which can distort the data. In this work we only considered the nonlinearity in the optical receiver, and have ignored the nonlinearity of the optical channels and the dispersion effect induced by it. As a future work, it would be interesting to consider also these effects on the received signal and try to design a clock signal that can partially mitigate the issues caused by the optical channels. Combining these technique with different equalization approaches, such as zero-forcing [84] or minimum mean squared error (MMSE) [85] can lead to a huge gain in the data detection.

Multi-user detection systems can also be analyzed using a similar technique to that introduced in this thesis. In this scenario, each receiver is assumed to detect the signals of multiple users at a time using a joint detection system. While designing the clock signals for each one of the users' data can be a challenging problem, the joint detection of the data of multiple users can be helpful in removing the interference effect caused by each other.

Orthogonal frequency division multiplexing (OFDM) is a technique for encoding digital data on multiple carrier frequencies [86]. These systems use a large number of parallel narrow-band sub-carriers instead of a single wide-band carrier to transmit information. These narrow-band sub-carriers are equally spaced in spectral domain, and therefore, in a nonlinear environment new signals are generated. As a result, in a long haul fiber optic communication system, at the output of the link an interference is introduced on each subcarrier. This interference is the result of the fiber nonlinearity effects, such as self phase modulation (SPM), four-wave mixing (FWM) and cross-phase modulation (XPM). As discussed in this thesis, these nonlinearities are usually described by nonlinear Schrödinger (NLS) equations. Therefore, one can think of using Volterra series to solve these equations and calculate the statistical properties of the output signal of a sub-carrier in an optical OFDM system. This can be very interesting for the OFDM based standards that are being designed now, such as broadband passive optical networks (B-PONs), gigabit ethernet passive optical network (GE-PONs), gigabit capable passive optical networks (G-PONs) and next generation access passive optical network (NGA-PONs) [87].

Appendix A

# Calculation of the Relationship between the Photo-Detector Current and the Fourier Transform of the Amplitude of the Optical Field

In this appendix we want to obtain the relationship between the photo-detector's current and the amplitude of the optical field in the frequency domain. Then, by substituting the main interference and noise signals in these equations we can calculate the variance of the output current at the detector. The results of this appendix are used in (5.51). We know that the output of the optical detector is obtained from the integration of the optical received power.

$$I = \int_{-\frac{T}{2}}^{\frac{T}{2}} P(t)dt = \int_{-\frac{T}{2}}^{\frac{T}{2}} |A(t)|^2 dt \tag{A.1}$$

where $A(t)$ is the amplitude of the optical field. $A(\omega)$, the Fourier transform of $A(t)$, is defined as:

$$A(\omega) = \int_{-\infty}^{\infty} A(t)e^{-j\omega t}dt \tag{A.2}$$

So we have

$$P(t) = |A(t)|^2 = \left(\frac{1}{2\pi}\right)^2 \int_{-\infty}^{\infty}\int_{-\infty}^{\infty} A(\omega)A^*(\upsilon)e^{-j(\omega-\upsilon)t}d\omega d\upsilon \tag{A.3}$$

and therefore the mean of the detector current is:

$$E\{I\} = \left(\frac{1}{2\pi}\right)^2 \int_{-\frac{T}{2}}^{\frac{T}{2}}\int_{-\infty}^{\infty}\int_{-\infty}^{\infty} E\{A(\omega)A^*(\upsilon)\}e^{-j(\omega-\upsilon)t}d\omega d\upsilon dt \tag{A.4}$$

By simplifying the equation, we obtain

$$\begin{aligned} I =& \left(\frac{1}{2\pi}\right)^2 \int_{-\infty}^{\infty}\int_{-\infty}^{\infty} E\{A(\omega)A^*(\upsilon)\}\left[\int_{-\frac{T}{2}}^{\frac{T}{2}} e^{-j(\omega-\upsilon)t}dt\right]d\omega d\upsilon \\ =& \left(\frac{1}{2\pi}\right)^2 \int_{-\infty}^{\infty}\int_{-\infty}^{\infty} E\{A(\omega)A^*(\upsilon)\}Sinc\left(\frac{(\omega-\upsilon)T}{2\pi}\right)d\omega d\upsilon \end{aligned} \tag{A.5}$$

Now by substituting $A(\omega) = A_O(\omega) + A_{MAI}(\omega)$ in (A.5), where $A_O(\omega)$, $A_{MAI}(\omega)$ are the amplitude of the main signal and the interference signal,respectively we obtain:

$$I = \left(\frac{1}{2\pi}\right)^2 \int_{-\infty}^{\infty}\int_{-\infty}^{\infty} \left[A_O(\omega)A_O(\upsilon) + E\{A_{MAI}A^*_{MAI}(\upsilon)\}\right]Sinc\left(\frac{(\omega-\upsilon)T}{2\pi}\right)d\omega d\upsilon \tag{A.6}$$

We can write the variance of the output current as follows:

$$\begin{aligned} \sigma_I^2 = E\{I^2\} - E^2\{I\} =& \left(\frac{1}{2\pi}\right)^4 \iint\iint E\{A(\omega_1)A^*(\upsilon_1)A(\omega_2)A^*(\upsilon_2)\}Sinc\left(\frac{(\omega_1-\upsilon_1)T}{2\pi}\right) \\ \times Sinc&\left(\frac{(\omega_2-\upsilon_2)T}{2\pi}\right)d\omega_1 d\upsilon_1 d\omega_2 d\upsilon_2 - \left(\frac{1}{2\pi}\right)^4 \left[\int_{-\infty}^{\infty}\int_{-\infty}^{\infty} E\{A(\omega)A^*(\upsilon)\}Sinc\left(\frac{(\omega-\upsilon)T}{2\pi}\right)d\omega d\upsilon\right]^2 \end{aligned} \tag{A.7}$$

where by substituting $A(\omega) = A_O(\omega) + A_{MAI}(\omega)$ in (A.7), and assuming $A_{MAI}(\omega)$ follows a gaussian shape we obtain [78]:

$$\sigma_I^2 = \left(\frac{1}{2\pi}\right)^4 \iint\iint \Bigg[E\{A(\omega_1)A^*(\upsilon_1)\}E\{A(\omega_2)A^*(\upsilon_2)\} + E\{A_{MAI}(\omega_1)A^*_{MAI}(\upsilon_2)\}E\{A_{MAI}(\omega_2)A^*_{MAI}(\upsilon_1)\}$$
$$+ A_O(\omega_2)A^*_O(\upsilon_1)E\{A_{MAI}(\omega_1)A^*_{MAI}(\upsilon_2)\} + A_O(\omega_1)A^*_O(\upsilon_2)E\{A_{MAI}(\omega_2)A^*_{MAI}(\upsilon_1)\}\Bigg]$$
$$\times Sinc\left(\frac{(\omega_1-\upsilon_1)T}{2\pi}\right)Sinc\left(\frac{(\omega_2-\upsilon_2)T}{2\pi}\right)d\omega_1 d\upsilon_1 d\omega_2 d\upsilon_2$$
$$-\left(\frac{1}{2\pi}\right)^4\left[\int_{-\infty}^{\infty}\int_{-\infty}^{\infty} E\{A(\omega)A^*(\upsilon)\}Sinc\left(\frac{(\omega-\upsilon)T}{2\pi}\right)d\omega d\upsilon\right]^2 \tag{A.8}$$

With a small simplification we obtain:

$$\sigma_I^2 = \left(\frac{1}{2\pi}\right)^4 \iint E\{A(\omega_1)A^*(\upsilon_1)\}Sinc\left(\frac{(\omega_1-\upsilon_1)T}{2\pi}\right)d\omega_1 d\upsilon_1 \times \iint E\{A(\omega_2)A^*(\upsilon_2)\}Sinc\left(\frac{(\omega_2-\upsilon_2)T}{2\pi}\right)d\omega_2 d\upsilon_2$$
$$+\left(\frac{1}{2\pi}\right)^4 \iint\iint \Bigg[E\{A_{MAI}(\omega_1)A^*_{MAI}(\upsilon_2)\}E\{A_{MAI}(\omega_2)A^*_{MAI}(\upsilon_1)\}$$
$$+ A_O(\omega_2)A^*_O(\upsilon_1)E\{A_{MAI}(\omega_1)A^*_{MAI}(\upsilon_2)\} + A_O(\omega_1)A^*_O(\upsilon_2)E\{A_{MAI}(\omega_2)A^*_{MAI}(\upsilon_1)\}\Bigg]$$
$$\times Sinc\left(\frac{(\omega_1-\upsilon_1)T}{2\pi}\right)Sinc\left(\frac{(\omega_2-\upsilon_2)T}{2\pi}\right)d\omega_1 d\upsilon_1 d\omega_2 d\upsilon_2$$
$$-\left(\frac{1}{2\pi}\right)^4\left[\int_{-\infty}^{\infty}\int_{-\infty}^{\infty} E\{A(\omega)A^*(\upsilon)\}Sinc\left(\frac{(\omega-\upsilon)T}{2\pi}\right)d\omega d\upsilon\right]^2 \tag{A.9}$$

And finally:

$$\sigma_I^2 = \left(\frac{1}{2\pi}\right)^4 \iint\iint \Bigg[E\{A_{MAI}(\omega_1)A^*_{MAI}(\upsilon_2)\}E\{A_{MAI}(\omega_2)A^*_{MAI}(\upsilon_1)\}$$
$$+ 2A_O(\omega_2)A^*_O(\upsilon_1)E\{A_{MAI}(\omega_1)A^*_{MAI}(\upsilon_2)\}\Bigg]Sinc\left(\frac{(\omega_1-\upsilon_1)T}{2\pi}\right)Sinc\left(\frac{(\omega_2-\upsilon_2)T}{2\pi}\right)d\omega_1 d\upsilon_1 d\omega_2 d\upsilon_2 \tag{A.10}$$

Appendix B

# Calculation of Volterra Series Terms

Regarding to the application of Volterra series for solving nonlinear Schrödinger equations, in this appendix we obtain the kernels of Volterra series. For obtaining Volterra series terms in equations (3.36) and (3.37), we first write soem of the terms $A_O(\omega, z)$:

$$
\begin{aligned}
A_O(\omega,z) &= \iint H'_{O_{1,2}}(\omega_1,\omega_2,\omega-\omega_1+\omega_2,z)A_p(\omega_1)A_s^*(\omega_2)A_p(\omega-\omega_1+\omega_2)d\omega_1 d\omega_2 \\
&+ \iint\iint H'_{O_{1,2}}(\omega_1,\omega_2,\omega_3,\omega_4,\omega-\omega_1+\omega_2-\omega_3+\omega_4,z)A_p(\omega_1)A_s^*(\omega_2)A_s(\omega_3)A_s^*(\omega_4) \\
&\times A_p(\omega-\omega_1+\omega_2-\omega_3+\omega_4)d\omega_1 d\omega_2 + \iint\iint H'_{O_{1,4}}(\omega_1,\omega_2,\omega_3,\omega_4,\omega-\omega_1+\omega_2-\omega_3+\omega_4,z) \\
&\times A_p(\omega_1)A_p^*(\omega_2)A_p(\omega_3)A_s^*(\omega_4)A_p(\omega-\omega_1+\omega_2-\omega_3+\omega_4)d\omega_1 d\omega_2
\end{aligned}
\tag{B.1}
$$

By substituting these series in equations (3.25), (3.26) and (3.27), and considering results in Section (3.3.2), the equations of the volterra series factors become:

$$
\frac{\partial H'_{O_{1,2}}(\omega_1,\omega_2,\omega_3,z)}{\partial z} = G_1(\omega_1-\omega_2+\omega_3)H'_{O_{1,2}}(\omega_1,\omega_2,\omega_3,z) + j2\gamma_{osp}e^{-j\Delta kz}H_{p_1}(\omega_1,z)H^*_{s_1}(\omega_2,z)H_{p_1}(\omega_3,z)
\tag{B.2}
$$

$$
\begin{aligned}
&\frac{\partial H'_{O_{3,2}}(\omega_1,\omega_2,\omega_3,\omega_4,\omega_5,z)}{\partial z} = G_1(\omega_1-\omega_2+\omega_3-\omega_4+\omega_5)H'_{O_{3,2}}(\omega_1,\omega_2,\omega_3,\omega_4,\omega_5,z) \\
&+ j2\gamma_{osp}e^{-j\Delta kz}H_{p_1}(\omega_1,z)H^*_{s_3}(\omega_2,\omega_3,\omega_4,z)H_{p_1}(\omega_5,z) + j2\gamma_{os}H_{s_1}(\omega_1,z)H^*_{s_1}(\omega_2)H'_{o_{1,2}}(\omega_3,\omega_4,\omega_5,z)
\end{aligned}
\tag{B.3}
$$

$$\frac{\partial H'_{O_{1,4}}(\omega_1,\omega_2,\omega_3,\omega_4,\omega_5,z)}{\partial z} = G_1(\omega_1-\omega_2+\omega_3-\omega_4+\omega_5)H'_{O_{1,4}}(\omega_1,\omega_2,\omega_3,\omega_4,\omega_5,z)$$
$$+ j2\gamma_{osp}e^{-j\Delta kz}H_{p_1}(\omega_1,z)H^*_{s_{1,2}}(\omega_2,\omega_3,\omega_4,z)H_{p_1}(\omega_5,z) + j4\gamma_{op}H_{p_1}(\omega_1,z)H^*_{p_1}(\omega_2)H'_{o_{1,2}}(\omega_3,\omega_4,\omega_5,z) \tag{B.4}$$

Where $H_{s_1}(\omega_1,z)$,$H_{s_3}(\omega_1,\omega_2,\omega_3,z)$ and $H_{s_{1,2}}(\omega_1,\omega_2,\omega_3,z)$ are [43]:

$$H_{s_1}(\omega,z) = H_{p_1}(\omega,z) = e^{G_1(\omega)}z \tag{B.5}$$

$$H_{s_3}(\omega_1,\omega_2,\omega_3,z) = H_{p_3}(\omega_1,\omega_2,\omega_3,z) = j\gamma_{ss}\frac{e^{(G_1(\omega_1)+G_1^*(\omega_2)+G_1(\omega_3))z} - e^{G_1(\omega_1-\omega_2+\omega_3)z}}{G_1(\omega_1)+G_1^*(\omega_2)+G_1(\omega_3)-G_1(\omega_1-\omega_2+\omega_3)} \tag{B.6}$$

$$H_{s_{1,2}}(\omega_1,\omega_2,\omega_3,z) = j4\gamma_{sp}\frac{e^{G_1(\omega_1-\omega_2+\omega_3)z} - e^{(G_1(\omega_1)+G_1^*(\omega_2)+G_1(\omega_3))z}}{G_1(\omega_1-\omega_2+\omega_3)-G_1(\omega_1)-G_1^*(\omega_2)-G_1(\omega_3)} \tag{B.7}$$

In order to simplify the equations we suppose that $\Delta(\omega) = \beta_1\omega + \beta_2\omega^2/2$, then we obtain the following equations:

$$G_1(\omega_1-\omega_2) = -\alpha - j\left(\beta_1(\omega_1+\omega_2) + \frac{\beta_2(\omega_1+\omega_2)^2}{2}\right) = G_1(\omega_1)+G_1(\omega_2)+\alpha-j\beta_2\omega_1\omega_2$$

In general we have:

$$G_1(\omega_1+\omega_2+\ldots+\omega_k) = G_1(\omega_1)+G_1(\omega_2)+\ldots+G_1(\omega_k)+(k-1)\alpha - j\beta_2\sum_{\binom{m,n=1}{m\neq n}}^{k}\omega_m\omega_n \tag{B.8}$$

Then $H_{s_3}(\omega_1,\omega_2,\omega_3,z)$ and $H_{s_{1,2}}(\omega_1,\omega_2,\omega_3,z)$ would become:

$$H_{s_3}(\omega_1,\omega_2,\omega_3,z) = j\gamma_{ss}e^{G_1(\omega_1-\omega_2+\omega_3)z}\left(\frac{1-e^{-2\alpha z}e^{j\beta_2(\omega_2-\omega_3)(\omega_2-\omega_1)z}}{2\alpha - j\beta_2(\omega_2-\omega_3)(\omega_2-\omega_1)}\right) \tag{B.9}$$

$$H_{s_{1,2}}(\omega_1,\omega_2,\omega_3,z) = j4\gamma_{sp}e^{G_1(\omega_1-\omega_2+\omega_3)z}\left(\frac{1-e^{-2\alpha z}e^{j\beta_2(\omega_2-\omega_3)(\omega_2-\omega_1)z}}{2\alpha - j\beta_2(\omega_2-\omega_3)(\omega_2-\omega_1)}\right) \tag{B.10}$$

On the other hand, we know that the solution of the following equation:

$$\frac{dy}{dz} = ay + c_0 e^{az} + c_1 e^{b_1 z} + c_2 e^{b_2 z} + \ldots + c_m e^{b_m z}$$

is:

$$y(z) = c_0 z e^{az} + \left( \sum_{i=1}^{m} \frac{b_i}{a - c_i} \right) e^{az} + \frac{b_1}{c_1 - a} e^{b_1 z} + \frac{b_2}{c_2 - a} e^{b_2 z} + \ldots + \frac{b_m}{c_m - a} e^{b_m z}$$

Then, we obtain:

$$H'_{o_{1,2}}(\omega_1, \omega_2, \omega_3, z) = 2j\gamma_{osp} \frac{e^{(G_1(\omega_1 - \omega_2 + \omega_3)z} - e^{[G_1(\omega_1) + G_1^*(\omega_2) + G_1(\omega_3)]z} e^{-j\Delta k z}}{G_1(\omega_1 - \omega_2 + \omega_3) - [G_1(\omega_1) + G_1^*(\omega_2) + G_1(\omega_3)] + j\Delta k}$$
$$= 2j\gamma_{osp} e^{(G_1(\omega_1 - \omega_2 + \omega_3)z} \left( \frac{1 - e^{-2\alpha z} e^{j\beta_2(\omega_2 - \omega_3)(\omega_2 - \omega_1)z} e^{-j\Delta k z}}{2\alpha - j\beta_2(\omega_2 - \omega_3)(\omega_2 - \omega_1) + j\Delta k} \right) \tag{B.11}$$

$$H'_{s_{3,2}}(\omega_1, \omega_2, \omega_3, \omega_4, \omega_5, z) = 2 \frac{\gamma_{ss}\gamma_{osp}}{G_1^*(\omega_2) + G_1^(\omega_3) + G_1^*(\omega_4) - G_1^*(\omega_2 - \omega_3 + \omega_4)}$$
$$\times \left[ \frac{e^{G_1(\omega_1 - \omega_2 + \omega_3 - \omega_4 + \omega_5)z} - e^{(G_1(\omega_1) + G_1^*(\omega_2) + G_1(\omega_3) + G_1^*(\omega_4) + G_1(\omega_5))z}}{G_1(\omega_1 - \omega_2 + \omega_3 - \omega_4 + \omega_5) - \left( G_1(\omega_1) + G_1^*(\omega_2) + G_1(\omega_3) + G_1^*(\omega_4) + G_1(\omega_5) \right)} \right.$$
$$\left. - \frac{e^{G_1(\omega_1 - \omega_2 + \omega_3 - \omega_4 + \omega_5)z} - e^{(G_1(\omega_1) + G_1^*(\omega_2 - \omega_3 + \omega_4) + G_1(\omega_5))z}}{G_1(\omega_1 - \omega_2 + \omega_3 - \omega_4 + \omega_5) - \left( G_1(\omega_1) + G_1^*(\omega_2 - \omega_3 + \omega_4) + G_1(\omega_5) \right)} \right]$$
$$+ 2 \frac{2\gamma_{os}\gamma_{osp}}{2\alpha - j\beta_2(\omega_2 - \omega_3)(\omega_2 - \omega_1) + j\Delta k}$$
$$\times \left[ \frac{e^{G_1(\omega_1 - \omega_2 + \omega_3 - \omega_4 + \omega_5)z} - e^{(G_1(\omega_1) + G_1^*(\omega_2) + G_1(\omega_3 - \omega_4 + \omega_5))z}}{G_1(\omega_1 - \omega_2 + \omega_3 - \omega_4 + \omega_5) - \left( G_1(\omega_1) + G_1^*(\omega_2) + G_1(\omega_3 - \omega_4 + \omega_5) \right)} \right.$$
$$\left. - \frac{e^{G_1(\omega_1 - \omega_2 + \omega_3 - \omega_4 + \omega_5)z} - e^{[G_1(\omega_1) + G_1^*(\omega_2) + G_1(\omega_3) + G_1^*(\omega_4) + G_1(\omega_5)]z} e^{-j\Delta k z}}{G_1(\omega_1 - \omega_2 + \omega_3 - \omega_4 + \omega_5) - \left( G_1(\omega_1) + G_1^*(\omega_2) + G_1(\omega_3) + G_1^*(\omega_4) + G_1(\omega_5) \right) + j\Delta k} \right] \tag{B.12}$$

and considering (B.8), (B.12) we obtain:

$$
\begin{aligned}
H'_{s_{3,2}}(\omega_1,\omega_2,\omega_3,\omega_4,\omega_5,z) &= 2\frac{\gamma_{ss}\gamma_{osp}}{2\alpha+j\beta_2(\omega_2-\omega_3)(\omega_2-\omega_1)}e^{G_1(\omega_1-\omega_2+\omega_3-\omega_4+\omega_5)z} \\
&\times\left[\frac{1-e^{j\beta_2[(\omega_2-\omega_1)(\omega_2-\omega_3)+(\omega_4-\omega_5)(\omega_4-\omega_3)+(\omega_2-\omega_1)(\omega_4-\omega_5)]z}}{4\alpha-j\beta_2[(\omega_2-\omega_1)(\omega_2-\omega_3)+(\omega_4-\omega_5)(\omega_4-\omega_3)+(\omega_2-\omega_1)(\omega_4-\omega_5)]}\right. \\
&\left.-\frac{1-e^{j\beta_2(\omega_2-\omega_3+\omega_4-\omega_1)(\omega_2-\omega_3+\omega_4-\omega_5)z}}{2\alpha-j\beta_2(\omega_2-\omega_3+\omega_4-\omega_1)(\omega_2-\omega_3+\omega_4-\omega_5)}\right] \\
&+2\frac{2\gamma_{os}\gamma_{osp}}{2\alpha-j\beta_2(\omega_2-\omega_3)(\omega_2-\omega_1)+j\Delta k}e^{G_1(\omega_1-\omega_2+\omega_3-\omega_4+\omega_5)z} \\
&\times\left[\frac{1-e^{j\beta_2(\omega_2-\omega_1)(\omega_2-\omega_3+\omega_4-\omega_5)z}}{2\alpha-j\beta_2(\omega_2-\omega_1)(\omega_2-\omega_3+\omega_4-\omega_5)}\right. \\
&\left.-\frac{1-e^{j\beta_2[(\omega_2-\omega_1)(\omega_2-\omega_3)+(\omega_4-\omega_5)(\omega_4-\omega_3)+(\omega_2-\omega_1)(\omega_4-\omega_5)]z}e^{-j\Delta kz}}{4\alpha-j\beta_2[(\omega_2-\omega_1)(\omega_2-\omega_3)+(\omega_4-\omega_5)(\omega_4-\omega_3)+(\omega_2-\omega_1)(\omega_4-\omega_5)]+j\Delta k}\right]
\end{aligned}
\tag{B.13}
$$

Considering the similarity of $H'_{s_{3,2}}$ and $H'_{s_{1,4}}$, we would have:

$$
\begin{aligned}
H'_{o_{1,4}}(\omega_1,\omega_2,\omega_3,\omega_4,\omega_5,z) &= 8\frac{\gamma_{sp}\gamma_{osp}}{2\alpha+j\beta_2(\omega_2-\omega_3)(\omega_2-\omega_1)}e^{G_1(\omega_1-\omega_2+\omega_3-\omega_4+\omega_5)z} \\
&\times\left[\frac{1-e^{j\beta_2[(\omega_2-\omega_1)(\omega_2-\omega_3)+(\omega_4-\omega_5)(\omega_4-\omega_3)+(\omega_2-\omega_1)(\omega_4-\omega_5)]z}}{4\alpha-j\beta_2[(\omega_2-\omega_1)(\omega_2-\omega_3)+(\omega_4-\omega_5)(\omega_4-\omega_3)+(\omega_2-\omega_1)(\omega_4-\omega_5)]}\right. \\
&\left.-\frac{1-e^{j\beta_2(\omega_2-\omega_3+\omega_4-\omega_1)(\omega_2-\omega_3+\omega_4-\omega_5)z}}{2\alpha-j\beta_2(\omega_2-\omega_3+\omega_4-\omega_1)(\omega_2-\omega_3+\omega_4-\omega_5)}\right] \\
&+4\frac{2\gamma_{op}\gamma_{osp}}{2\alpha-j\beta_2(\omega_2-\omega_3)(\omega_2-\omega_1)+j\Delta k}e^{G_1(\omega_1-\omega_2+\omega_3-\omega_4+\omega_5)z} \\
&\times\left[\frac{1-e^{j\beta_2(\omega_2-\omega_1)(\omega_2-\omega_3+\omega_4-\omega_5)z}}{2\alpha-j\beta_2(\omega_2-\omega_1)(\omega_2-\omega_3+\omega_4-\omega_5)}\right. \\
&\left.-\frac{1-e^{j\beta_2[(\omega_2-\omega_1)(\omega_2-\omega_3)+(\omega_4-\omega_5)(\omega_4-\omega_3)+(\omega_2-\omega_1)(\omega_4-\omega_5)]z}e^{-j\Delta kz}}{4\alpha-j\beta_2[(\omega_2-\omega_1)(\omega_2-\omega_3)+(\omega_4-\omega_5)(\omega_4-\omega_3)+(\omega_2-\omega_1)(\omega_4-\omega_5)]+j\Delta k}\right]
\end{aligned}
\tag{B.14}
$$

Appendix C

# Characteristic Fourier Transform of Stationary Random Processes

Since the calculation of autocorrelation in time domain is difficult, in this appendix we obtain the output autocorrelation function in frequency domain by using the characteristics of Fourier transform of stationary random process. The results of this section are used in (5-49). We assume signal $a(t)$ is stationary random process, and the autocorrelation function is defined as follows:

$$R_a(t_1, t_2) = E\{a(t_1)a^*(t_2)\} = R_a(t_1 - t_2) \tag{C.1}$$

We also assume that the Fourier transform of signal $a(t)$ is defined as:

$$A(\omega) = \int_{-\infty}^{\infty} a(t)e^{-j\omega t}dt \tag{C.2}$$

We want to obtain the autocorrelation of $A(\omega)$. For definition of the autocorrelation function, we have:

$$R_A(\omega_1, \omega_2) = E\{A(\omega_1)A^*(\omega_2)\} \tag{C.3}$$

By subsubstituting (C.2) in (C.3) we obtain:

$$R_A(\omega_1,\omega_2) = E\Big\{\Big(\int_{-\infty}^{\infty} a(t_1)e^{-j\omega_1 t_1}dt_1\Big)\Big(\int_{-\infty}^{\infty} a^*(t_2)e^{+j\omega_2 t_2}dt_2\Big)\Big\} = E\Big\{\int_{-\infty}^{\infty}\int_{-\infty}^{\infty} a(t_1)a^*(t_2)e^{+j\omega_2 t_2}e^{-j\omega_1 t_1}dt_1dt_2\Big\}$$
$$= \int_{-\infty}^{\infty}\int_{-\infty}^{\infty} E\{a(t_1)a^*(t_2)\}e^{+j\omega_2 t_2}e^{-j\omega_1 t_1}dt_1dt_2 = \int_{-\infty}^{\infty}\int_{-\infty}^{\infty} R_a(t_1-t_2)\}e^{-j(\omega_1-\omega_2)t_2}e^{-j\omega_1(t_1-t_2)}dt_1dt_2 \tag{C.4}$$

By changing $\tau = t_1 - t_2$ we have:

$$R_A(\omega_1,\omega_2) = \int_{-\infty}^{\infty}\int_{-\infty}^{\infty} R_a(\tau)e^{-j(\omega_1-\omega_2)t_2}e^{-j\omega_1(\tau)}d\tau dt_2 = \Big(\int_{-\infty}^{\infty} e^{-j(\omega_1-\omega_2)t_2}dt_2\Big)\Big(\int_{-\infty}^{\infty} R_a(\tau)e^{-j\omega_1\tau}d\tau\Big)$$
$$= \delta(\omega_1-\omega_2)\Big(\int_{-\infty}^{\infty} R_a(\tau)e^{-j\omega_1\tau}d\tau\Big) \tag{C.5}$$

The power spectral density (PSD), $S_a(\omega)$ is defined as follow:

$$S_a(\omega) = \int_{-\infty}^{\infty} R_a(\tau)e^{-j\omega\tau}d\tau \tag{C.6}$$

Therefore, the autocorrelation function of $A(\omega)$ becomes:

$$R_A(\omega_1,\omega_2) = S_a(\omega_1)\delta(\omega_1-\omega_2) \tag{C.7}$$

From (C.7) we know that $A(\omega)$ is white noise. Now we assume that $a(t)$ has the following autocorrelation function:

$$R_a(t_1,t_2) = q(t_1)\delta(t_1-t_2) \tag{C.8}$$

By considering (C.4), the autocorrelation function becomes:

$$R_A(\omega_1,\omega_2) = \int_{-\infty}^{\infty}\int_{-\infty}^{\infty} R_a(t_1,t_2)e^{-j(\omega_1-\omega_2)t_2}e^{-j\omega_1(t_1-t_2)}dt_1dt_2$$
$$= \int_{-\infty}^{\infty}\int_{-\infty}^{\infty} q(t_1)\delta(t_1-t_2)e^{-j(\omega_1-\omega_2)t_2}e^{-j\omega_1(t_1-t_2)}dt_1dt_2$$
$$= \int_{-\infty}^{\infty} q(t_1)e^{-j(\omega_1-\omega_2)t_1} = Q(\omega_1-\omega_2) \tag{C.9}$$

where $Q(\omega)$ is the Fourier transform of $q(t)$. Therefore, $A(\omega)$ is a stationary random process.

Appendix D

# Solving NLS Equations for a Nonlinear Media using Volterra Series

Volterra series expansion is one of the most powerful methods for describing non-linear systems. We will now obtain the output of the nonlinear system by solving the NLS equations with Volterra series. If we consider the first 3 terms of the Volterra series we will have a good approximation of the solution of the NLS equation. Therefore $X_o(\omega, z)$ can be evaluated as:

$$X_o(\omega, z) = X_{o_1}(\omega, z) + X_{o_2}(\omega, z) + X_{o_3}(\omega, z) \tag{D.1}$$

where $X_{o_1}(\omega, z)$, $X_{o_2}(\omega, z)$ and $X_{o_3}(\omega, z)$ are defined as follows:

$$X_{o_1}(\omega, z) = \iint H'_{O_{1,2}}(\omega_1, \omega_2, \omega - \omega_1 + \omega_2, z) A_c(\omega_1) A_s^*(\omega_2) A_c(\omega - \omega_1 + \omega_2) d\omega_1 d\omega_2 \tag{D.2}$$

$$\begin{aligned} X_{o_2}(\omega, z) = \iiiint & H'_{O_{3,2}}(\omega_1, \omega_2, \omega_3, \omega_4, \omega - \omega_1 + ... + \omega_4, z) A_c(\omega_1) S^*(\omega_2) A_s(\omega_3) A_s^*(\omega_4) \\ & \times A_c(\omega - \omega_1 + ... + \omega_4) d\omega_1 ... d\omega_4 \end{aligned} \tag{D.3}$$

$$\begin{aligned} X_{o_3}(\omega, z) = \iiiint & H'_{O_{1,4}}(\omega_1, \omega_2, \omega_3, \omega_4, \omega - \omega_1 + ... + \omega_4, z) A_c(\omega_1) A_c^*(\omega_2) A_c(\omega_3) A_s^*(\omega_4) \\ & \times A_c(\omega - \omega_1 + ... + \omega_4) d\omega_1 ... d\omega_4 \end{aligned} \tag{D.4}$$

where $A_c(t)$, $A_s(t)$ are the clock and the received signal in time domain, $A_c(\omega)$, $A_s(\omega)$ are the Fourier transform of the clock and the received signal, and the Volterra kernels, $H^{'}_{O_{1,2}}$, $H^{'}_{O_{3,2}}$ and $H^{'}_{O_{1,4}}$are calculated as follows:

$$H^{'}_{O_{1,2}}(\omega_1, \omega_2, \omega - \omega_1 + \omega_2, z) = 2j\gamma_{OSC} e^{G_1(\omega)z(\frac{1-e^{-2\alpha z}}{2\alpha})} \tag{D.5}$$

$$H^{'}_{O_{3,2}}(\omega_1, \omega_2, \omega_3, \omega_4, \omega - \omega_1 + ... + \omega_4, z) = 2\gamma_{OSC}(\gamma_{SS} + 2\gamma_{OS}) e^{G_1(\omega)z(\frac{1-e^{-2\alpha z}}{2\alpha})^2} \tag{D.6}$$

$$H^{'}_{O_{1,4}}(\omega_1, \omega_2, \omega_3, \omega_4, \omega - \omega_1 + ... + \omega_4, z) = 8\gamma_{OSC}(\gamma_{SC} + 2\gamma_{OC}) e^{G_1(\omega)z(\frac{1-e^{-2\alpha z}}{2\alpha})^2} \tag{D.7}$$

where $\alpha$ is the linear attenuation constant, and $\gamma_{ijkl}$ is the spatial distribution of the fiber mode. For simplicity of the calculation we suppose that the received and the clock signals are Sinc-shaped. Therefore, we can express these signals in time and spectral domain as follows:

$$A_c(t) = \sum_{m=1}^{k} A^{'}_c \text{sinc}(\frac{t - (C_m T_b/F)}{T_c}) \tag{D.8}$$

$$A_c(\omega) = F\{A_c(t)\} = A^{'}_c T_c \pi \prod (\frac{\omega T_c}{2}) \sum_{m=1}^{k} e^{-2\pi j C_m (T_b/F)\omega} \tag{D.9}$$

$$A_s(t) = b \sum_{m=1}^{k} A_d \text{sinc}(\frac{t - (C_m T_b/F)}{T_d}) \tag{D.10}$$

$$A_s(\omega) = F\{A_s(t)\} = b A_d T_d \pi \prod (\frac{\omega T_d}{2}) \sum_{m=1}^{k} e^{-2\pi j C_m (T_b/F)\omega}, \tag{D.11}$$

where $A^{'}_c$, $A_d$ are the amplitudes of the clock and the received signals, $C_m$ is the code number, $k$ is the weight of the code, $T_d$, $T_c$ are the full width at half maximum (FWHM) of the data pulse and the clock pulse-width (code word) , $T_b$ is the duration of bit and $b$ is the bit value “0” or “1”. Then we can write the first three output response terms as follows:

$$X_{o_1}(\omega,z)=\iint 2j\gamma_{OSC}e^{G_1(\omega)z(\frac{1-e^{-2\alpha z}}{2\alpha})}\{A_c^{'}T_c\pi\prod(\frac{\omega_1T_c}{2})\sum_{m=1}^{k}e^{-2\pi jC_m(T_b/F)\omega_1}\}$$
$$\times\{bA_dT_d\pi\prod(\frac{\omega_2T_d}{2})\sum_{m=1}^{k}e^{-2\pi jC_m(T_b/F)\omega_2}\}\{A_c^{'}T_c\pi\prod(\frac{(\omega-\omega_1+\omega_2)T_c}{2})$$
$$\times\sum_{m=1}^{k}e^{-2\pi jC_m(T_b/F)(\omega-\omega_1+\omega_2)}\}d\omega_1d\omega_2 \tag{D.12}$$

$$X_{o_2}(\omega,z)=\iiiint 2\gamma_{OSC}(\gamma_{SS}+2\gamma_{OS})e^{G_1(\omega)z(\frac{1-e^{-2\alpha z}}{2\alpha})^2}\{A_c^{'}T_c\pi\prod(\frac{\omega_1T_c}{2})\sum_{m=1}^{k}e^{-2\pi jC_m(T_b/F)\omega_1}\}$$
$$\times\{bA_dT_d\pi\prod(\frac{\omega_2T_d}{2})\sum_{m=1}^{k}e^{-2\pi jC_m(T_b/F).\omega_2}\}\{A_c^{'}T_c\pi\prod(\frac{\omega_3T_c}{2})\sum_{m=1}^{k}e^{-2\pi jC_m(T_b/F)\omega_3}\}$$
$$\times\{bA_dT_d\pi\prod(\frac{\omega_4T_d}{2})\sum_{m=1}^{k}e^{-2\pi jC_m(T_b/F)\omega_4}\}\{A_c^{'}T_c\pi\prod(\frac{(\omega-\omega_1+...+\omega_4)T_c}{2})$$
$$\times\sum_{m=1}^{k}e^{-2\pi jC_m(T_b/F)(\omega-\omega_1+...+\omega_4)}\}d\omega_1...d\omega_4 \tag{D.13}$$

$$X_{o_3}(\omega,z)=\iiiint 8\gamma_{OSC}(\gamma_{SC}+2\gamma_{OC})e^{G_1(\omega)z(\frac{1-e^{-2\alpha z}}{2\alpha})^2}\{A_c^{'}T_c\pi\prod(\frac{\omega_1T_c}{2})\sum_{m=1}^{k}e^{-2\pi jC_m(T_b/F)\omega_1}\}$$
$$\times\{A_c^{'}T_c\pi\prod(\frac{\omega_2T_c}{2})\sum_{m=1}^{k}e^{-2\pi jC_m(T_b/F)\omega_2}\}\{A_c^{'}T_c\pi\prod(\frac{\omega_3T_c}{2})\sum_{m=1}^{k}e^{-2\pi jC_m(T_b/F)\omega_3}\}$$
$$\times\{bA_dT_d\pi\prod(\frac{\omega_4T_d}{2})\sum_{m=1}^{k}e^{-2\pi jC_m(T_b/F)\omega_4}\}\{A_c^{'}T_c\pi\prod(\frac{(\omega-\omega_1+...+\omega_4)T_c}{2})$$
$$\times\sum_{m=1}^{k}e^{-2\pi jC_m(T_b/F)(\omega-\omega_1+...+\omega_4)}\}d\omega_1...d\omega_4 \tag{D.14}$$

By calculating the integrations in (D.12), (D.13) and (D.14), and depending on whether $T_c$ is larger than $T_d$ or not, we obtain different responses in different frequency ranges. By defining $E_1$ as:

$$E_1=2\pi^3bjf_{OSC}e^{G_1(\omega)z(\frac{1-e^{-2\alpha z}}{2\alpha})}A_d(A_c^{'})^2T_dT_c^2 \tag{D.15}$$

then, for $T_d>T_c$, $X_{o_1}$ would be :

(1)$For\quad \omega>\frac{2}{T_c}+\frac{1}{T_d},\quad \omega<-\frac{2}{T_c}-\frac{1}{T_d}\quad\Rightarrow\quad X_{o_1}(\omega,z)=0$

$(2)For \quad \frac{1}{T_d} < \omega < \frac{2}{T_c} + \frac{1}{T_d}$

$X_{o_1}(\omega, z) = E_1 \sum_{m=1}^{k} \sum_{i=1}^{k} \sum_{l=1}^{k} \frac{1}{2\pi j \frac{T_b}{F}(C_l - C_m)} \frac{1}{2\pi j \frac{T_b}{F}(C_i + C_m - 2C_l)} e^{2\pi j \frac{T_b}{F}(C_i - C_l)\frac{2}{T_c}} e^{-2\pi j \frac{T_b}{F}(C_i - C_m - 2C_l)\frac{1}{T_d}}$
$e^{-2\pi j \frac{T_b}{F} C_i \omega}$

$(3)For \quad \frac{1}{T_d} - \frac{2}{T_c} < \omega < \frac{1}{T_d}$

$X_{o_1}(\omega, z) = E_1 \sum_{m=1}^{k} \sum_{i=1}^{k} \sum_{l=1}^{k} \frac{1}{2\pi j \frac{T_b}{F}(C_l - C_m)} \left\{ \frac{1}{2\pi j \frac{T_b}{F}(C_i - C_m)} e^{2\pi j \frac{T_b}{F}(C_l - C_m)\frac{2}{T_c}} e^{2\pi j \frac{T_b}{F}(C_i - C_m)\frac{1}{T_d}} e^{-2\pi j \frac{T_b}{F} C_i \omega} \right.$
$\left. + \frac{1}{2\pi j \frac{T_b}{F}(C_i + C_m - 2C_l)} e^{2\pi j \frac{T_b}{F}(C_m - C_l)\frac{2}{T_c}} e^{2\pi j \frac{T_b}{F}(C_i + C_m - 2C_l)\frac{1}{T_d}} e^{-2\pi j \frac{T_b}{F}(2C_l - C_i)\omega} \right\}$

$(4)For \quad -\frac{1}{T_d} - \frac{2}{T_c} < \omega < \frac{1}{T_d} - \frac{2}{T_c}$

$$X_{o_1}(\omega, z) = E_1 \sum_{m=1}^{k} \sum_{i=1}^{k} \sum_{l=1}^{k} \frac{1}{2\pi j \frac{T_b}{F}(C_l - C_m)} \frac{1}{2\pi j \frac{T_b}{F}(C_i - C_m)} e^{2\pi j \frac{T_b}{F}(C_i + C_l - 2C_m)\frac{2}{T_c}} e^{2\pi j \frac{T_b}{F}(C_i - C_m)\frac{1}{T_d}}$$
$$e^{-2\pi j \frac{T_b}{F}(2C_m - C_i)\omega} \tag{D.16}$$

When the pulse-width of the data is smaller than the pulse-width of clock ($T_d < T_c$) we have

$(1)For \quad \omega > \frac{2}{T_c} + \frac{1}{T_d}, \quad \omega < -\frac{2}{T_c} - \frac{1}{T_d} \quad \Rightarrow \quad X_{o_1}(\omega, z) = 0$

$(2)For \quad \frac{1}{T_d} < \omega < \frac{2}{T_c} + \frac{1}{T_d}$

$X_{o_1}(\omega, z) = E_1 \sum_{m=1}^{k} \sum_{i=1}^{k} \sum_{l=1}^{k} \frac{1}{2\pi j \frac{T_b}{F}(C_l - C_m)} \frac{1}{2\pi j \frac{T_b}{F}(C_i + C_m - 2C_l)} e^{2\pi j \frac{T_b}{F}(C_i - C_l)\frac{2}{T_c}} e^{-2\pi j \frac{T_b}{F}(C_i - C_m - 2C_l)\frac{1}{T_d}} e^{-2\pi j \frac{T_b}{F} C_i \omega}$

$(3)For \quad -\frac{1}{T_d} + \frac{2}{T_c} < \omega < \frac{1}{T_d}$

$X_{o_1}(\omega, z) = E_1 \sum_{m=1}^{k} \sum_{i=1}^{k} \sum_{l=1}^{k} \frac{1}{2\pi j \frac{T_b}{F}(C_l - C_m)} \left\{ \frac{1}{2\pi j \frac{T_b}{F}(C_i - C_m)} e^{2\pi j \frac{T_b}{F}(C_l - C_m)\frac{2}{T_c}} e^{2\pi j \frac{T_b}{F}(C_i - C_m)\frac{1}{T_d}} e^{-2\pi j \frac{T_b}{F} C_i \omega} \right.$
$\left. + \frac{1}{2\pi j \frac{T_b}{F}(C_i + C_m - 2C_l)} e^{-2\pi j \frac{T_b}{F}(C_i - C_l)\frac{2}{T_c}} e^{2\pi j \frac{T_b}{F}(2C_l - C_m)\omega} \right\}$

$(4)For \quad \frac{1}{T_d} - \frac{2}{T_c} < \omega < -\frac{1}{T_d} + \frac{2}{T_c}$

$X_{o_1}(\omega, z) = E_1 \sum_{m=1}^{k} \sum_{i=1}^{k} \sum_{l=1}^{k} \frac{1}{2\pi j \frac{T_b}{F}(C_l - C_m)} \left\{ \frac{1}{2\pi j \frac{T_b}{F}(C_i - C_m)} e^{2\pi j \frac{T_b}{F}(C_l - C_m)\frac{2}{T_c}} e^{2\pi j \frac{T_b}{F}(C_i - C_m)\frac{1}{T_d}} e^{-2\pi j \frac{T_b}{F} C_i \omega} \right.$
$\left. + \frac{1}{2\pi j \frac{T_b}{F}(C_i + C_m - 2C_l)} e^{-2\pi j \frac{T_b}{F}(C_m - C_l)\frac{2}{T_c}} e^{2\pi j \frac{T_b}{F}(C_i + C_m - 2C_l)\frac{1}{T_d}} e^{-2\pi j \frac{T_b}{F}(2C_l - C_i)\omega} \right\}$

$(5)For \quad -\frac{1}{T_d} < \omega < -\frac{2}{T_c} + \frac{1}{T_d}$

$X_{o_1}(\omega, z) = E_1 \sum_{m=1}^{k} \sum_{i=1}^{k} \sum_{l=1}^{k} \frac{1}{2\pi j \frac{T_b}{F}(C_l - C_m)} \left\{ \frac{1}{2\pi j \frac{T_b}{F}(C_i - C_m)} e^{-2\pi j \frac{T_b}{F}(C_l + C_i - 2C_m)\frac{2}{T_c}} e^{2\pi j \frac{T_b}{F} C_m \omega} \right.$
$\left. + \frac{1}{2\pi j \frac{T_b}{F}(C_i + C_m - 2C_l)} e^{-2\pi j \frac{T_b}{F}(C_m - C_l)\frac{2}{T_c}} e^{2\pi j \frac{T_b}{F}(C_i + C_m - 2C_l)\frac{1}{T_d}} e^{-2\pi j \frac{T_b}{F}(2C_l - C_i)\omega} \right\}$

$$(6)For \quad -\frac{1}{T_d}-\frac{2}{T_c}<\omega<-\frac{1}{T_d}$$

$$X_{o_1}(\omega,z)=E_1\sum_{m=1}^{k}\sum_{i=1}^{k}\sum_{l=1}^{k}\frac{1}{2\pi j\frac{T_b}{F}(C_l-C_m)}\frac{1}{2\pi j\frac{T_b}{F}(C_i-C_m)}e^{2\pi j\frac{T_b}{F}(C_i+C_l-2C_m)\frac{2}{T_c}}e^{2\pi j\frac{T_b}{F}(C_i-C_m)\frac{1}{T_d}}$$

$$e^{-2\pi j\frac{T_b}{F}(2C_m-C_i)\omega} \tag{D.17}$$

In order to calculate $X_{o_2}$ we define parameters $S$, $S_1$, $S_2$, $S_3$,$S_4$ and $E_2$ as follow:

$$E_2=2\pi^5A_c^3A_d^2T_c^3T_d^2b^2\gamma_{osc}(\gamma_{ss}+2\gamma_{os})e^{G_1(\omega)z}\left(\frac{1-e^{-2\alpha z}}{2\alpha}\right)^2, S=\frac{1}{2\pi j\frac{T_b}{F}(C_m-C_l)}$$

$$, S_1=\frac{1}{2\pi j\frac{T_b}{F}(C_m-C_p)}, S_2=\frac{1}{-2\pi j\frac{T_b}{F}(C_m+C_p-2C_l)}, S_3=\frac{1}{2\pi j\frac{T_b}{F}(C_n+C_p-2C_m)}, S_4=\frac{1}{2\pi j\frac{T_b}{F}(C_n-C_p)}$$

With these parameters, for $T_d>T_c$, $X_{o_2}$ would be:

$$(1)For \quad \omega>\tfrac{3}{T_c}+\tfrac{2}{T_d}, \quad \omega<-\tfrac{3}{T_c}-\tfrac{2}{T_d} \quad \Rightarrow \quad X_{o_2}(\omega,z)=0$$

$$(2)For \quad \tfrac{3}{T_c}<\omega<\tfrac{3}{T_c}+\tfrac{2}{T_d}$$

$$X_{o_2}(\omega,z)=E_2\textstyle\sum_{m=1}^{k}\sum_{n=1}^{k}\sum_{p=1}^{k}\sum_{i=1}^{k}\sum_{l=1}^{k}SS_1S_3\frac{1}{2\pi j\frac{T_b}{F}(C_i-C_n)}e^{2\pi j\frac{T_b}{F}(3C_i-2C_l-C_m)\frac{1}{T_c}}$$

$$\times e^{2\pi j\frac{T_b}{F}(2C_i-C_n+C_p-2C_m)\frac{1}{T_d}}e^{-2\pi j\frac{T_b}{F}C_i\omega}$$

$$(3)For \quad \tfrac{1}{T_c}+\tfrac{2}{T_d}<\omega<\tfrac{3}{T_c}$$

$$X_{o_2}(\omega,z)=E_2\textstyle\sum_{m=1}^{k}\sum_{n=1}^{k}\sum_{p=1}^{k}\sum_{i=1}^{k}\sum_{l=1}^{k}\frac{SS_1S_3}{2\pi j\frac{T_b}{F}(C_i+C_p-2C_m)}e^{2\pi j\frac{T_b}{F}(3C_i-2C_l-C_m)\frac{1}{T_c}}$$

$$\times e^{2\pi j\frac{T_b}{F}(C_i+C_n+2C_p-2C_m)\frac{1}{T_d}}e^{-2\pi j\frac{T_b}{F}C_i\omega}+\frac{SS_1S_3}{2\pi j\frac{T_b}{F}(C_i-C_n)}e^{2\pi j\frac{T_b}{F}(-3C_i+6C_n-2C_l-C_m)\frac{1}{T_c}}$$

$$\times e^{2\pi j\frac{T_b}{F}(2C_i-C_n+C_p-2C_m)\frac{1}{T_d}}e^{-2\pi j\frac{T_b}{F}(C_i-2C_n)\omega}$$

$$(4)For \quad \tfrac{3}{T_c}+\tfrac{2}{T_d}<\omega<\tfrac{1}{T_c}+\tfrac{2}{T_d}$$

$$X_{o_2}(\omega,z)=E_2\textstyle\sum_{m=1}^{k}\sum_{n=1}^{k}\sum_{p=1}^{k}\sum_{i=1}^{k}\sum_{l=1}^{k}SS_2S_4\frac{1}{2\pi j\frac{T_b}{F}(C_i-C_n)}e^{2\pi j\frac{T_b}{F}(C_i-C_m)\frac{1}{T_c}}$$

$$\times e^{2\pi j\frac{T_b}{F}(2C_i-C_n+C_p)\frac{1}{T_d}}e^{-2\pi j\frac{T_b}{F}C_i\omega}+SS_1S_3\Bigg\{\frac{1}{2\pi j\frac{T_b}{F}(C_i-C_n)}e^{2\pi j\frac{T_b}{F}(C_i+C_m-2C_l)\frac{1}{T_c}}$$

$$\times e^{2\pi j\frac{T_b}{F}(2C_i-C_n+C_p-2C_m)\frac{1}{T_d}}e^{-2\pi j\frac{T_b}{F}C_i\omega}+\frac{1}{2\pi j\frac{T_b}{F}(C_i-C_n+2C_p-4C_m)}e^{2\pi j\frac{T_b}{F}(C_i+3C_m-2C_l-2C_p)\frac{1}{T_c}}$$

$$\times e^{2\pi j\frac{T_b}{F}(2C_i+3C_n+5C_p-10C_m)\frac{1}{T_d}}e^{-2\pi j\frac{T_b}{F}C_i\omega}+\frac{1}{2\pi j\frac{T_b}{F}(C_n+C_p-2C_m)}e^{2\pi j\frac{T_b}{F}(C_m-C_p+2C_i-2C_l)\frac{1}{T_c}}$$

$$\times e^{2\pi j\frac{T_b}{F}(C_n-C_i)\frac{1}{T_d}}e^{-2\pi j\frac{T_b}{F}(C_p-2C_m)\omega}+\frac{1}{2\pi j\frac{T_b}{F}(C_i-C_n)}e^{2\pi j\frac{T_b}{F}(6C_n-C_m-3C_i-2C_l)\frac{1}{T_c}}$$

$$\times e^{2\pi j\frac{T_b}{F}(2C_i-C_n+C_p-2C_m)\frac{1}{T_d}}e^{-2\pi j\frac{T_b}{F}(C_i-2C_n)\omega}\Bigg\}$$

$$(5)For \quad \tfrac{1}{T_c}<\omega<\tfrac{3}{T_c}+\tfrac{2}{T_d}$$

$$X_{o_2}(\omega,z)=E_2\textstyle\sum_{m=1}^{k}\sum_{n=1}^{k}\sum_{p=1}^{k}\sum_{i=1}^{k}\sum_{l=1}^{k}SS_2S_4\frac{1}{2\pi j\frac{T_b}{F}(C_i-C_n)}e^{2\pi j\frac{T_b}{F}(C_i-C_m)\frac{1}{T_c}}$$

$$\times e^{2\pi j\frac{T_b}{F}(2C_i-C_n+C_p)\frac{1}{T_d}}e^{-2\pi j\frac{T_b}{F}C_i\omega}+SS_1S_3\Bigg\{\frac{1}{2\pi j\frac{T_b}{F}(C_i-C_n)}e^{2\pi j\frac{T_b}{F}(C_i+C_m-2C_l)\frac{1}{T_c}}$$
$$\times e^{2\pi j\frac{T_b}{F}(2C_i-C_n+C_p-2C_m)\frac{1}{T_d}}e^{-2\pi j\frac{T_b}{F}C_i\omega}+\frac{1}{2\pi j\frac{T_b}{F}(C_i-C_n+2C_p-4C_m)}e^{2\pi j\frac{T_b}{F}(C_i+3C_m-2C_l-2C_p)\frac{1}{T_c}}$$
$$\times e^{2\pi j\frac{T_b}{F}(2C_i+3C_n+5C_p-10C_m)\frac{1}{T_d}}e^{-2\pi j\frac{T_b}{F}C_i\omega}+\frac{1}{2\pi j\frac{T_b}{F}(C_n+C_p-2C_m)}e^{2\pi j\frac{T_b}{F}(7C_m-4C_p-C_i-2C_l)\frac{1}{T_c}}$$
$$\times e^{2\pi j\frac{T_b}{F}(C_n+C_p-2C_m)\frac{1}{T_d}}e^{-2\pi j\frac{T_b}{F}(2C_p-4C_m-C_i)\omega}\Bigg\}$$

$(6)For\quad \frac{-1}{T_c}+\frac{2}{T_d}<\omega<\frac{1}{T_c}$

$$X_{o_2}(\omega,z)=E_2\sum_{m=1}^{k}\sum_{n=1}^{k}\sum_{p=1}^{k}\sum_{i=1}^{k}\sum_{l=1}^{k}SS_2S_4\Bigg\{\frac{1}{2\pi j\frac{T_b}{F}(C_i-C_p)}e^{2\pi j\frac{T_b}{F}(C_i-C_m)\frac{1}{T_c}}e^{2\pi j\frac{T_b}{F}(2C_n-2C_p)\frac{1}{T_d}}$$
$$\times e^{-2\pi j\frac{T_b}{F}C_i\omega}+\frac{1}{2\pi j\frac{T_b}{F}(C_i-C_n)}e^{2\pi j\frac{T_b}{F}(C_i-C_m)\frac{1}{T_c}}e^{2\pi j\frac{T_b}{F}(2C_i-C_n-C_p)\frac{1}{T_d}}e^{-2\pi j\frac{T_b}{F}(C_i-2C_n)\omega}\Bigg\}$$
$$+SS_1S_3\Bigg\{\frac{1}{2\pi j\frac{T_b}{F}(C_i+C_p-2C_m)}e^{2\pi j\frac{T_b}{F}(C_i+C_m-2C_l)\frac{1}{T_c}}e^{2\pi j\frac{T_b}{F}(2C_p+2C_n-4C_m)\frac{1}{T_d}}e^{-2\pi j\frac{T_b}{F}C_i\omega}$$
$$+\frac{1}{2\pi j\frac{T_b}{F}(C_i-C_n)}e^{2\pi j\frac{T_b}{F}(2C_n-C_i+C_m-2C_l)\frac{1}{T_c}}e^{2\pi j\frac{T_b}{F}(2C_i+C_p-C_n-2C_m)\frac{1}{T_d}}e^{-2\pi j\frac{T_b}{F}(C_i-2C_n)\omega}$$
$$+\frac{1}{2\pi j\frac{T_b}{F}(C_i+C_n+2C_p-4C_m)}e^{2\pi j\frac{T_b}{F}(9C_m-C_n-C_i-2C_l-5C_p)\frac{1}{T_c}}e^{2\pi j\frac{T_b}{F}(2C_i+3C_n+5C_p-10C_m)\frac{1}{T_d}}$$
$$\times e^{-2\pi j\frac{T_b}{F}(C_i+2C_n+4C_p-8C_m)\omega}\Bigg\}$$

$(7)For\quad \frac{1}{T_c}+\frac{-2}{T_d}<\omega<\frac{-1}{T_c}+\frac{2}{T_d}$

$$X_{o_2}(\omega,z)=E_2\sum_{m=1}^{k}\sum_{n=1}^{k}\sum_{p=1}^{k}\sum_{i=1}^{k}\sum_{l=1}^{k}\frac{SS_1S_4}{2\pi j\frac{T_b}{F}(C_i-C_n)}e^{2\pi j\frac{T_b}{F}(5C_m-C_i-3C_p-2C_l)\frac{1}{T_c}}e^{2\pi j\frac{T_b}{F}(2C_i-C_n-C_p)\frac{1}{T_d}}$$
$$\times e^{-2\pi j\frac{T_b}{F}C_i\omega}+\frac{SS_2S_4}{2\pi j\frac{T_b}{F}(C_i+C_n-2C_p)}e^{2\pi j\frac{T_b}{F}(2C_p-C_i-C_m)\frac{1}{T_c}}e^{2\pi j\frac{T_b}{F}(2C_i+3C_n-5C_p)\frac{1}{T_d}}e^{-2\pi j\frac{T_b}{F}C_i\omega}$$
$$+\frac{SS_1S_3}{2\pi j\frac{T_b}{F}(C_i+C_n+2C_p-4C_m)}e^{2\pi j\frac{T_b}{F}(5C_m-C_i-2C_p-2C_l)\frac{1}{T_c}}e^{2\pi j\frac{T_b}{F}(5C_p+3C_n+2C_i-10C_m)\frac{1}{T_d}}e^{-2\pi j\frac{T_b}{F}C_i\omega}$$
$$+\frac{SS_2S_4}{2\pi j\frac{T_b}{F}(C_i-C_n)}e^{2\pi j\frac{T_b}{F}(2C_i-C_m-C_p)\frac{1}{T_c}}e^{2\pi j\frac{T_b}{F}(C_n-C_i)\frac{1}{T_d}}e^{-2\pi j\frac{T_b}{F}C_p\omega}$$
$$+\frac{SS_1S_3}{2\pi j\frac{T_b}{F}(C_i+C_p-2C_m)}e^{2\pi j\frac{T_b}{F}(2C_i+C_p-C_m-2C_l)\frac{1}{T_c}}e^{2\pi j\frac{T_b}{F}(2C_m+C_n-C_p-2C_i)\frac{1}{T_d}}e^{-2\pi j\frac{T_b}{F}(2C_m-C_p)\omega}$$
$$+\frac{SS_2S_4}{2\pi j\frac{T_b}{F}(C_i-C_n)}e^{2\pi j\frac{T_b}{F}(2C_n-C_m-C_i)\frac{1}{T_c}}e^{2\pi j\frac{T_b}{F}(2C_i-C_n-C_p)\frac{1}{T_d}}e^{-2\pi j\frac{T_b}{F}(C_i-2C_n)\omega}$$
$$+\frac{SS_1S_3}{2\pi j\frac{T_b}{F}(C_i+C_n-2C_m)}e^{2\pi j\frac{T_b}{F}(2C_n+C_m-C_i-2C_l)\frac{1}{T_c}}e^{2\pi j\frac{T_b}{F}(2C_i+C_p-C_n-2C_m)\frac{1}{T_d}}e^{-2\pi j\frac{T_b}{F}(C_i-2C_n)\omega}$$
$$+\frac{SS_1S_3}{2\pi j\frac{T_b}{F}(C_i+2C_p+C_n-4C_m)}e^{2\pi j\frac{T_b}{F}(11C_m-6C_p-2C_n-C_i-2C_l)\frac{1}{T_c}}e^{2\pi j\frac{T_b}{F}(2C_i+3C_n+5C_p-10C_m)\frac{1}{T_d}}$$
$$\times e^{-2\pi j\frac{T_b}{F}(C_i+2C_n+4C_p-8C_m)\omega}$$

$(8)For\quad \frac{-3}{T_c}+\frac{2}{T_d}<\omega<\frac{-1}{T_c}$

$$X_{o_2}(\omega,z)=E_2\sum_{m=1}^{k}\sum_{n=1}^{k}\sum_{p=1}^{k}\sum_{i=1}^{k}\sum_{l=1}^{k}\frac{SS_1S_4}{2\pi j\frac{T_b}{F}(C_i-C_n)}e^{2\pi j\frac{T_b}{F}(5C_m-C_i-3C_p-2C_l)\frac{1}{T_c}}e^{2\pi j\frac{T_b}{F}(2C_i-C_n-C_p)\frac{1}{T_d}}$$
$$\times e^{-2\pi j\frac{T_b}{F}C_i\omega}+\frac{SS_2S_4}{2\pi j\frac{T_b}{F}(C_i+C_n-2C_p)}e^{2\pi j\frac{T_b}{F}(2C_p-C_i-C_m)\frac{1}{T_c}}e^{2\pi j\frac{T_b}{F}(2C_i+3C_n-5C_p)\frac{1}{T_d}}e^{-2\pi j\frac{T_b}{F}C_i\omega}$$
$$+\frac{SS_1S_3}{2\pi j\frac{T_b}{F}(C_i+2C_p+C_n-4C_m)}e^{2\pi j\frac{T_b}{F}(5C_m-2C_p-C_i-2C_l)\frac{1}{T_c}}e^{2\pi j\frac{T_b}{F}(2C_i+3C_n+5C_p-10C_m)\frac{1}{T_d}}e^{-2\pi j\frac{T_b}{F}C_i\omega}$$
$$+\frac{SS_2S_4}{2\pi j\frac{T_b}{F}(C_i-C_n)}e^{2\pi j\frac{T_b}{F}(C_i-C_m)\frac{1}{T_c}}e^{2\pi j\frac{T_b}{F}(2C_n-2C_p)\frac{1}{T_d}}e^{-2\pi j\frac{T_b}{F}(C_i-2C_p)\omega}$$
$$+\frac{SS_1S_3}{2\pi j\frac{T_b}{F}(C_i+C_p-2C_m)}e^{2\pi j\frac{T_b}{F}(C_m+C_i-2C_l)\frac{1}{T_c}}e^{2\pi j\frac{T_b}{F}(2C_p+2C_n-4C_m)\frac{1}{T_d}}e^{-2\pi j\frac{T_b}{F}(C_i+2C_p-2C_m)\omega}$$

$(9)For\quad \frac{-3}{T_c}+\frac{2}{T_d}<\omega<\frac{-1}{T_c}$

$$X_{o_2}(\omega,z)=E_2\sum_{m=1}^{k}\sum_{n=1}^{k}\sum_{p=1}^{k}\sum_{i=1}^{k}\sum_{l=1}^{k}\frac{SS_1S_4}{2\pi j\frac{T_b}{F}(C_i-C_p)}e^{2\pi j\frac{T_b}{F}(5C_m-3C_p-C_i-2C_l)\frac{1}{T_c}}e^{2\pi j\frac{T_b}{F}(2C_n-2C_p)\frac{1}{T_d}}$$

$\times e^{-2\pi j\frac{T_b}{F}C_i\omega} + \frac{SS_1S_4}{2\pi j\frac{T_b}{F}(C_i-C_n)}e^{2\pi j\frac{T_b}{F}(5C_m-2C_n-3C_p-2C_l)\frac{1}{T_c}}e^{2\pi j\frac{T_b}{F}(2C_i-C_n-C_p)\frac{1}{T_d}}e^{-2\pi j\frac{T_b}{F}(2C_n-C_i)\omega}$
$+ \frac{SS_2S_4}{2\pi j\frac{T_b}{F}(C_i+C_n-2C_p)}e^{2\pi j\frac{T_b}{F}(C_i+2C_n-C_m-2C_p)\frac{1}{T_c}}e^{2\pi j\frac{T_b}{F}(2C_i+3C_n-5C_p)\frac{1}{T_d}}e^{-2\pi j\frac{T_b}{F}(C_i+2C_n-4C_p)\omega}$
$+ \frac{SS_1S_3}{2\pi j\frac{T_b}{F}(C_n+2C_p+C_i-4C_m)}e^{2\pi j\frac{T_b}{F}(2C_p+2C_n+C_i-3C_m-2C_l)\frac{1}{T_c}}e^{2\pi j\frac{T_b}{F}(3C_n+5C_p+2C_i-10C_m)\frac{1}{T_d}}$
$\times e^{-2\pi j\frac{T_b}{F}(8C_m-4C_p-2C_n-C_i)\omega}$

$(10) For \quad \frac{-1}{T_c}-\frac{2}{T_d}<\omega<\frac{-3}{T_c}+\frac{2}{T_d}$

$$X_{o_2}(\omega,z)=E_2\sum_{m=1}^{k}\sum_{n=1}^{k}\sum_{p=1}^{k}\sum_{i=1}^{k}\sum_{l=1}^{k}\Bigg\{\frac{SS_1S_4}{2\pi j\frac{T_b}{F}(C_n+C_i-2C_p)}e^{2\pi j\frac{T_b}{F}(5C_m-3C_i-2C_l)\frac{1}{T_c}}$$
$\times e^{2\pi j\frac{T_b}{F}(2C_i+3C_n-5C_p)\frac{1}{T_d}}e^{-2\pi j\frac{T_b}{F}C_i\omega} + \frac{SS_1S_4}{2\pi j\frac{T_b}{F}(C_i-C_p)}e^{2\pi j\frac{T_b}{F}(5C_m+2C_i-5C_p-2C_l)\frac{1}{T_c}}e^{2\pi j\frac{T_b}{F}(2C_n-2C_i)\frac{1}{T_d}}$
$\times e^{-2\pi j\frac{T_b}{F}C_p\omega} + \frac{SS_1S_4}{2\pi j\frac{T_b}{F}(C_i-C_n)}e^{2\pi j\frac{T_b}{F}(5C_m+C_i-3C_p-2C_n-2C_l)\frac{1}{T_c}}e^{2\pi j\frac{T_b}{F}(2C_i-C_n-C_p)\frac{1}{T_d}}e^{-2\pi j\frac{T_b}{F}(2C_n-C_i)\omega}$
$+ \frac{SS_2S_4}{2\pi j\frac{T_b}{F}(C_i-C_n-2C_p)}e^{2\pi j\frac{T_b}{F}(2C_n-2C_p-C_m+C_i)\frac{1}{T_c}}e^{2\pi j\frac{T_b}{F}(2C_i+3C_n-5C_p)\frac{1}{T_d}}e^{-2\pi j\frac{T_b}{F}(C_i+2C_n-4C_p)\omega}$
$+ \frac{SS_1S_3}{2\pi j\frac{T_b}{F}(C_i+C_n+2C_p-4C_m)}e^{2\pi j\frac{T_b}{F}(2C_p+2C_n+C_i-2C_l-3C_m)\frac{1}{T_c}}e^{2\pi j\frac{T_b}{F}(2C_i+3C_n+5C_p-10C_m)\frac{1}{T_d}}$
$\times e^{-2\pi j\frac{T_b}{F}(8C_m-C_i-2C_n-4C_p)\omega}$

$(11) For \quad \frac{-3}{T_c}<\omega<\frac{-1}{T_c}+\frac{-2}{T_d}$

$X_{o_2}(\omega,z)=E_2\sum_{m=1}^{k}\sum_{n=1}^{k}\sum_{p=1}^{k}\sum_{i=1}^{k}\sum_{l=1}^{k}\frac{SS_1S_4}{2\pi j\frac{T_b}{F}(C_i+C_n-2C_p)}e^{2\pi j\frac{T_b}{F}(5C_m-2C_l-3C_i)\frac{1}{T_c}}$
$\times e^{2\pi j\frac{T_b}{F}(2C_i+3C_n-5C_p)\frac{1}{T_d}}e^{-2\pi j\frac{T_b}{F}C_i\omega} + \frac{SS_1S_4}{2\pi j\frac{T_b}{F}(C_i-C_n)}e^{2\pi j\frac{T_b}{F}(5C_m-6C_n-2C_l+3C_i)\frac{1}{T_c}}$
$\times e^{2\pi j\frac{T_b}{F}(2C_n-2C_p)\frac{1}{T_d}}e^{-2\pi j\frac{T_b}{F}(C_i-2C_p)\omega}$

$$(12) For \quad \frac{-3}{T_c}+\frac{-2}{T_d}<\omega<\frac{-3}{T_c}$$
$$X_{o_2}(\omega,z)=E_2\sum_{m=1}^{k}\sum_{n=1}^{k}\sum_{p=1}^{k}\sum_{i=1}^{k}\sum_{l=1}^{k}\frac{SS_1S_4}{2\pi j\frac{T_b}{F}(C_i+C_n-2C_p)}$$
$$e^{2\pi j\frac{T_b}{F}(5C_m+6C_n+3C_i-2C_l-12C_p)\frac{1}{T_c}}e^{2\pi j\frac{T_b}{F}(2C_i+3C_n-5C_p)\frac{1}{T_d}}e^{-2\pi j\frac{T_b}{F}(C_i+2C_n-4C_p\omega} \tag{D.18}$$

When the pulse-width of the data is smaller than the pulse-width of clock ( $T_d < T_c$ ), $X_{o_2}$ becomes:

$(1) For \quad \omega>\frac{3}{T_c}+\frac{2}{T_d}, \quad \omega<-\frac{3}{T_c}-\frac{2}{T_d} \quad \Rightarrow \quad X_{o_2}(\omega,z)=0$

$(2) For \quad \frac{1}{T_c}+\frac{2}{T_d}<\omega<\frac{3}{T_c}+\frac{2}{T_d}$

$X_{o_2}(\omega,z)=E_2\sum_{m=1}^{k}\sum_{n=1}^{k}\sum_{p=1}^{k}\sum_{i=1}^{k}\sum_{l=1}^{k}\frac{SS_1S_3}{2\pi j\frac{T_b}{F}(C_i-C_n)}e^{2\pi j\frac{T_b}{F}(3C_i-2C_l-C_m)\frac{1}{T_c}}e^{2\pi j\frac{T_b}{F}(2C_i-C_n+C_p-2C_m)\frac{1}{T_d}}$
$e^{-2\pi j\frac{T_b}{F}C_i\omega}$

$(3) For \quad \frac{3}{T_c}<\omega<\frac{1}{T_c}+\frac{2}{T_d}$

$X_{o_2}(\omega,z)=E_2\sum_{m=1}^{k}\sum_{n=1}^{k}\sum_{p=1}^{k}\sum_{i=1}^{k}\sum_{l=1}^{k}\frac{SS_2S_4}{2\pi j\frac{T_b}{F}(C_i-C_n)}e^{2\pi j\frac{T_b}{F}(C_i-C_m)\frac{1}{T_c}}e^{2\pi j\frac{T_b}{F}(2C_i-C_n-C_p)\frac{1}{T_d}}$

$$\times e^{-2\pi j\frac{T_b}{F}C_i\omega}+\frac{SS_1S_3}{2\pi j\frac{T_b}{F}(C_i-C_n)}e^{2\pi j\frac{T_b}{F}(C_i+C_m-2C_l)\frac{1}{T_c}}e^{2\pi j\frac{T_b}{F}(2C_i-C_n+C_p-2C_m)\frac{1}{T_d}}e^{-2\pi j\frac{T_b}{F}C_i\omega}$$
$$+\frac{SS_1S_3}{2\pi j\frac{T_b}{F}(C_i+C_p-2C_m)}e^{2\pi j\frac{T_b}{F}(2C_n+C_i-C_m-2C_l)\frac{1}{T_c}}e^{2\pi j\frac{T_b}{F}(2C_i+2C_p-4C_m)\frac{1}{T_d}}e^{-2\pi j\frac{T_b}{F}C_i\omega}$$
$$+\frac{SS_1S_3}{2\pi j\frac{T_b}{F}(C_i-C_n)}e^{2\pi j\frac{T_b}{F}(2C_i+C_n-C_m-2C_l)\frac{1}{T_c}}e^{2\pi j\frac{T_b}{F}(C_n+C_p-2C_m)\frac{1}{T_d}}e^{-2\pi j\frac{T_b}{F}C_i\omega}$$

(4)$For\quad \frac{3}{T_c}+\frac{2}{T_d}<\omega<\frac{1}{T_c}+\frac{2}{T_d}$

$$X_{o_2}(\omega,z)=E_2\sum_{m=1}^{k}\sum_{n=1}^{k}\sum_{p=1}^{k}\sum_{i=1}^{k}\sum_{l=1}^{k}SS_2S_4\frac{1}{2\pi j\frac{T_b}{F}(C_i-C_n)}e^{2\pi j\frac{T_b}{F}(3C_i--2C_nC_m)\frac{1}{T_c}}e^{2\pi j\frac{T_b}{F}(C_n-C_p)\frac{1}{T_d}}$$
$$\times e^{-2\pi j\frac{T_b}{F}C_i\omega}+\frac{SS_1S_3}{2\pi j\frac{T_b}{F}(C_i-C_n)}e^{2\pi j\frac{T_b}{F}(3C_i+C_m-2C_n-2C_l)\frac{1}{T_c}}e^{2\pi j\frac{T_b}{F}(C_n+C_p-2C_m)\frac{1}{T_d}}e^{-2\pi j\frac{T_b}{F}C_i\omega}$$
$$+\frac{SS_1S_3}{2\pi j\frac{T_b}{F}(C_i+C_n+2C_p-4C_m)}e^{2\pi j\frac{T_b}{F}(3C_i+2C_n-5C_m-2C_l+2C_p)\frac{1}{T_c}}e^{2\pi j\frac{T_b}{F}(C_n+C_p-2C_m)\frac{1}{T_d}}e^{-2\pi j\frac{T_b}{F}C_i\omega}$$
$$+\frac{SS_2S_4}{2\pi j\frac{T_b}{F}(C_i-C_n)}e^{2\pi j\frac{T_b}{F}(3C_n-2C_i-C_m)\frac{1}{T_c}}e^{2\pi j\frac{T_b}{F}(2C_i-C_n-C_p)\frac{1}{T_d}}e^{-2\pi j\frac{T_b}{F}C_n\omega}$$
$$+\frac{SS_1S_3}{2\pi j\frac{T_b}{F}(C_i-C_n)}e^{2\pi j\frac{T_b}{F}(3C_n+C_m-2C_i-2C_l)\frac{1}{T_c}}e^{2\pi j\frac{T_b}{F}(2C_i-C_n+C_p-2C_m)\frac{1}{T_d}}e^{-2\pi j\frac{T_b}{F}C_n\omega}$$
$$+\frac{SS_1S_3}{2\pi j\frac{T_b}{F}(C_i+C_p-2C_m)}e^{2\pi j\frac{T_b}{F}(2C_n+5C_m-3C_p-2C_i-2C_l)\frac{1}{T_c}}e^{2\pi j\frac{T_b}{F}(2C_i+2C_p-4C_m)\frac{1}{T_d}}e^{-2\pi j\frac{T_b}{F}(2C_m-C_p)\omega}$$
$$+\frac{SS_1S_3}{2\pi j\frac{T_b}{F}(C_i-C_n)}e^{2\pi j\frac{T_b}{F}(4C_n-C_m-C_i-2C_l)\frac{1}{T_c}}e^{2\pi j\frac{T_b}{F}(C_n+C_p-2C_m)\frac{1}{T_d}}e^{-2\pi j\frac{T_b}{F}(2C_n-C_i)\omega}$$

(5)$For\quad \frac{1}{T_c}<\omega<\frac{-1}{T_c}+\frac{2}{T_d}$

$$X_{o_2}(\omega,z)=E_2\sum_{m=1}^{k}\sum_{n=1}^{k}\sum_{p=1}^{k}\sum_{i=1}^{k}\sum_{l=1}^{k}SS_1S_4\frac{1}{2\pi j\frac{T_b}{F}(C_i-C_n)}e^{2\pi j\frac{T_b}{F}(5C_m-C_i-3C_p-2C_l)\frac{1}{T_c}}$$
$$\times e^{2\pi j\frac{T_b}{F}(2C_i-C_n-C_p)\frac{1}{T_d}}e^{-2\pi j\frac{T_b}{F}C_i\omega}+\frac{SS_2S_4}{2\pi j\frac{T_b}{F}(C_i-C_p)}e^{2\pi j\frac{T_b}{F}(2C_n-C_i-2C_m)\frac{1}{T_c}}e^{2\pi j\frac{T_b}{F}(2C_i-2C_p)\frac{1}{T_d}}$$
$$\times e^{-2\pi j\frac{T_b}{F}C_i\omega}+\frac{SS_1S_3}{2\pi j\frac{T_b}{F}(C_i+C_p-2C_m)}e^{2\pi j\frac{T_b}{F}(C_m+4C_n-2C_l-C_i)\frac{1}{T_c}}e^{2\pi j\frac{T_b}{F}(2C_i+2C_p-4C_m)\frac{1}{T_d}}e^{-2\pi j\frac{T_b}{F}C_i\omega}$$
$$+\frac{SS_1S_3}{2\pi j\frac{T_b}{F}(C_i+C_n+2C_p-4C_m)}e^{2\pi j\frac{T_b}{F}(11C_m-6C_p-C_i-2C_l-2C_n)\frac{1}{T_c}}e^{2\pi j\frac{T_b}{F}(2C_i+3C_n+5C_p-10C_m)\frac{1}{T_d}}$$
$$\times e^{-2\pi j\frac{T_b}{F}C_i\omega}+\frac{SS_2S_4}{2\pi j\frac{T_b}{F}(C_i-C_n)}e^{2\pi j\frac{T_b}{F}(4C_i-3C_n-C_m)\frac{1}{T_c}}e^{2\pi j\frac{T_b}{F}(3C_n-2C_i-C_m)\frac{1}{T_d}}e^{-2\pi j\frac{T_b}{F}C_n\omega}$$
$$+\frac{SS_1S_3}{2\pi j\frac{T_b}{F}(C_i-C_n)}e^{2\pi j\frac{T_b}{F}(4C_i-3C_n+C_m-2C_l)\frac{1}{T_c}}e^{2\pi j\frac{T_b}{F}(3C_n-2C_l+C_p-2C_m)\frac{1}{T_d}}e^{-2\pi j\frac{T_b}{F}C_n\omega}$$
$$+\frac{SS_1S_3}{2\pi j\frac{T_b}{F}(C_i+C_n+2C_p-4C_m)}e^{2\pi j\frac{T_b}{F}(4C_i+4C_p-9C_m-2C_l+3C_n)\frac{1}{T_c}}e^{2\pi j\frac{T_b}{F}(6C_m-2C_i-3C_p-C_n)\frac{1}{T_d}}$$
$$\times e^{-2\pi j\frac{T_b}{F}(C_n+2C_p-4C_m)\omega}+\frac{SS_2S_4}{2\pi j\frac{T_b}{F}(C_i-C_n)}e^{2\pi j\frac{T_b}{F}(3C_n-2C_i-C_m)\frac{1}{T_c}}e^{2\pi j\frac{T_b}{F}(2C_i-C_n-C_p)\frac{1}{T_d}}e^{-2\pi j\frac{T_b}{F}C_n\omega}$$
$$+\frac{SS_1S_3}{2\pi j\frac{T_b}{F}(C_i-C_n)}e^{2\pi j\frac{T_b}{F}(4C_i-3C_n+C_m-2C_l)\frac{1}{T_c}}e^{2\pi j\frac{T_b}{F}(3C_n-2C_i+C_p-2C_m)\frac{1}{T_d}}e^{-2\pi j\frac{T_b}{F}C_n\omega}$$
$$+\frac{SS_1S_3}{2\pi j\frac{T_b}{F}(C_i+C_p-2C_m)}e^{2\pi j\frac{T_b}{F}(5C_m-3C_p-2C_i-2C_l+2C_n)\frac{1}{T_c}}e^{2\pi j\frac{T_b}{F}(2C_i+2C_p-4C_m)\frac{1}{T_d}}$$
$$\times e^{-2\pi j\frac{T_b}{F}(C_p-2C_m)\omega}+\frac{SS_1S_3}{2\pi j\frac{T_b}{F}(C_i-C_n)}e^{2\pi j\frac{T_b}{F}(4C_n-C_i-C_m-2C_l)\frac{1}{T_c}}e^{2\pi j\frac{T_b}{F}(C_n+C_p-2C_m)\frac{1}{T_d}}e^{-2\pi j\frac{T_b}{F}(2C_n-C_i)\omega}$$

(6)$For\quad \frac{3}{T_c}+\frac{-2}{T_d}<\omega<\frac{1}{T_c}$

$$X_{o_2}(\omega,z)=E_2\sum_{m=1}^{k}\sum_{n=1}^{k}\sum_{p=1}^{k}\sum_{i=1}^{k}\sum_{l=1}^{k}\frac{SS_1S_4}{2\pi j\frac{T_b}{F}(C_i-C_n)}e^{2\pi j\frac{T_b}{F}(C_i+5C_m-2C_n-2C_l-3C_p)\frac{1}{T_c}}e^{2\pi j\frac{T_b}{F}(C_n-C_p)\frac{1}{T_d}}$$
$$\times e^{-2\pi j\frac{T_b}{F}C_i\omega}+\frac{SS_2S_4}{2\pi j\frac{T_b}{F}(C_i+C_n)-2C_p}e^{2\pi j\frac{T_b}{F}(2C_n-C_m-2C_p+C_i)\frac{1}{T_c}}e^{2\pi j\frac{T_b}{F}(2C_n-2C_p)\frac{1}{T_d}}e^{-2\pi j\frac{T_b}{F}C_i\omega}$$
$$+\frac{SS_1S_3}{2\pi j\frac{T_b}{F}(C_i+C_n+C_p-4C_m)}e^{2\pi j\frac{T_b}{F}(2C_n-3C_m+2C_p+C_i-2C_l)\frac{1}{T_c}}e^{2\pi j\frac{T_b}{F}(C_p+C_n-2C_m)\frac{1}{T_d}}e^{-2\pi j\frac{T_b}{F}C_i\omega}$$
$$+\frac{SS_1S_4}{2\pi j\frac{T_b}{F}(C_i-C_n)}e^{2\pi j\frac{T_b}{F}(5C_m+C_n-2C_i-3C_p-2C_l)\frac{1}{T_c}}e^{2\pi j\frac{T_b}{F}(2C_i+3C_n-C_p)\frac{1}{T_d}}e^{-2\pi j\frac{T_b}{F}(C_i-2C_n)\omega}$$
$$+\frac{SS_2S_4}{2\pi j\frac{T_b}{F}(C_i-C_p)}e^{2\pi j\frac{T_b}{F}(C_p+2C_n-2C_i-2C_m)\frac{1}{T_c}}e^{2\pi j\frac{T_b}{F}(2C_i-2C_p)\frac{1}{T_d}}e^{-2\pi j\frac{T_b}{F}C_p\omega}$$
$$+\frac{SS_1S_3}{2\pi j\frac{T_b}{F}(C_i+C_p-2C_m)}e^{2\pi j\frac{T_b}{F}(2C_n+3C_m-C_p-2C_i-2C_l)\frac{1}{T_c}}e^{2\pi j\frac{T_b}{F}(2C_p+2C_i-4C_m)\frac{1}{T_d}}e^{-2\pi j\frac{T_b}{F}(C_p-2C_m)\omega}$$

$$+\frac{SS_1S_3}{2\pi j\frac{T_b}{F}(C_i+C_n+2C_p-4C_m)}e^{2\pi j\frac{T_b}{F}(15C_m-3C_n-8C_p-2C_i-2C_l)\frac{1}{T_c}}e^{2\pi j\frac{T_b}{F}(2C_i+5C_p+3C_n-10C_m)\frac{1}{T_d}}$$
$$\times e^{-2\pi j\frac{T_b}{F}(C_n+2C_p-4C_m)\omega}+\frac{SS_2S_4}{2\pi j\frac{T_b}{F}(C_i-C_n)}e^{2\pi j\frac{T_b}{F}(4C_i-3C_n-C_m)\frac{1}{T_c}}e^{2\pi j\frac{T_b}{F}(3C_n-2C_i-C_m)\frac{1}{T_d}}e^{-2\pi j\frac{T_b}{F}C_n\omega}$$
$$+\frac{SS_1S_3}{2\pi j\frac{T_b}{F}(C_i-C_n)}e^{2\pi j\frac{T_b}{F}(4C_i-3C_n+C_m-2C_l)\frac{1}{T_c}}e^{2\pi j\frac{T_b}{F}(3C_n-2C_i+C_p-2C_m)\frac{1}{T_d}}e^{-2\pi j\frac{T_b}{F}C_n\omega}$$
$$+\frac{SS_1S_3}{2\pi j\frac{T_b}{F}(C_i+C_n+2C_p-4C_m)}e^{2\pi j\frac{T_b}{F}(4C_i+3C_n+4C_p-9C_m-2C_l)\frac{1}{T_c}}e^{2\pi j\frac{T_b}{F}(6C_m-3C_p-C_n-2C_i)\frac{1}{T_d}}$$
$$\times e^{-2\pi j\frac{T_b}{F}(C_n+2C_p-4C_m)\omega}+\frac{SS_2S_4}{2\pi j\frac{T_b}{F}(C_i-C_n)}e^{2\pi j\frac{T_b}{F}(4C_n-3C_i-C_m)\frac{1}{T_c}}e^{2\pi j\frac{T_b}{F}(2C_i-C_n-C_p)\frac{1}{T_d}}e^{-2\pi j\frac{T_b}{F}(C_i-2C_n)\omega}$$
$$+\frac{SS_1S_3}{2\pi j\frac{T_b}{F}(C_i-C_n)}e^{2\pi j\frac{T_b}{F}(4C_n-3C_i+C_m-2C_l)\frac{1}{T_c}}e^{2\pi j\frac{T_b}{F}(2C_i-C_n+C_p-2C_m)\frac{1}{T_d}}e^{-2\pi j\frac{T_b}{F}(C_i-2C_n)\omega}$$
$$+\frac{SS_1S_3}{2\pi j\frac{T_b}{F}(C_i+C_p-2C_m)}e^{2\pi j\frac{T_b}{F}(2C_n+7C_m-4C_p-3C_i-2C_l)\frac{1}{T_c}}e^{2\pi j\frac{T_b}{F}(2C_p+2C_i-4C_m)\frac{1}{T_d}}e^{-2\pi j\frac{T_b}{F}(C_i+C_p-4C_m)\omega}$$

(7) $For \quad \frac{-3}{T_c}+\frac{2}{T_d}<\omega<\frac{3}{T_c}+\frac{-2}{T_d}$

$$X_{o_2}(\omega,z)=E_2\sum_{m=1}^{k}\sum_{n=1}^{k}\sum_{p=1}^{k}\sum_{i=1}^{k}\sum_{l=1}^{k}\frac{SS_1S_4}{2\pi j\frac{T_b}{F}(C_i-C_n)}e^{2\pi j\frac{T_b}{F}(5C_m+C_i-2C_n-3C_p-2C_l)\frac{1}{T_c}}e^{2\pi j\frac{T_b}{F}(C_n-C_p)\frac{1}{T_d}}$$
$$\times e^{-2\pi j\frac{T_b}{F}C_i\omega}+\frac{SS_2S_4}{2\pi j\frac{T_b}{F}(C_i+C_n-2C_p)}e^{2\pi j\frac{T_b}{F}(2C_n+C_i-C_m-2C_p)\frac{1}{T_c}}e^{2\pi j\frac{T_b}{F}(2C_n-2C_p)\frac{1}{T_d}}e^{-2\pi j\frac{T_b}{F}C_i\omega}$$
$$+\frac{SS_1S_3}{2\pi j\frac{T_b}{F}(C_i+C_n+2C_p-4C_m)}e^{2\pi j\frac{T_b}{F}(2C_n+C_i+2C_p-3C_m-2C_l)\frac{1}{T_c}}e^{2\pi j\frac{T_b}{F}(C_p+C_n-2C_m)\frac{1}{T_d}}e^{-2\pi j\frac{T_b}{F}C_i\omega}$$
$$\frac{SS_1S_4}{2\pi j\frac{T_b}{F}(C_i-C_n)}e^{2\pi j\frac{T_b}{F}(5C_m+C_n-2C_i-3C_p-2C_l)\frac{1}{T_c}}e^{2\pi j\frac{T_b}{F}(2C_i+3C_n-C_p)\frac{1}{T_d}}e^{-2\pi j\frac{T_b}{F}C_n\omega}$$
$$+\frac{SS_2S_4}{2\pi j\frac{T_b}{F}(C_i-C_p)}e^{2\pi j\frac{T_b}{F}(2C_n-2C_m+C_p-2C_i)\frac{1}{T_c}}e^{2\pi j\frac{T_b}{F}(2C_i-2C_p)\frac{1}{T_d}}e^{-2\pi j\frac{T_b}{F}C_p\omega}$$
$$+\frac{SS_1S_3}{2\pi j\frac{T_b}{F}(C_i+C_p-2C_m)}e^{2\pi j\frac{T_b}{F}(2C_n-C_p+3C_m-2C_i-2C_l)\frac{1}{T_c}}e^{2\pi j\frac{T_b}{F}(2C_i+2C_p-4C_m)\frac{1}{T_d}}e^{-2\pi j\frac{T_b}{F}(2C_m-C_p)\omega}$$
$$+\frac{SS_1S_3}{2\pi j\frac{T_b}{F}(C_i+C_n+2C_p-4C_m)}e^{2\pi j\frac{T_b}{F}(15C_m-2C_i-8C_p-3C_n-2C_l)\frac{1}{T_c}}e^{2\pi j\frac{T_b}{F}(2C_i+5C_p+3C_n-10C_m)\frac{1}{T_d}}$$
$$\times e^{-2\pi j\frac{T_b}{F}(C_n+2C_p-4C_m)\omega}+\frac{SS_2S_4}{2\pi j\frac{T_b}{F}(C_i-C_n)}e^{2\pi j\frac{T_b}{F}(C_i-C_m)\frac{1}{T_c}}e^{2\pi j\frac{T_b}{F}(C_n-C_p)\frac{1}{T_d}}e^{-2\pi j\frac{T_b}{F}(C_i-2C_n)\omega}$$
$$+\frac{SS_1S_3}{2\pi j\frac{T_b}{F}(C_i-C_n)}e^{2\pi j\frac{T_b}{F}(C_m+C_i-2C_l)\frac{1}{T_c}}e^{2\pi j\frac{T_b}{F}(C_p+C_n-2C_m)\frac{1}{T_d}}e^{-2\pi j\frac{T_b}{F}(2C_n-C_i)\omega}$$
$$+\frac{SS_1S_3}{2\pi j\frac{T_b}{F}(C_i+2C_p+C_n-4C_m)}e^{2\pi j\frac{T_b}{F}(3C_m-2C_p+C_i-2C_l)\frac{1}{T_c}}e^{2\pi j\frac{T_b}{F}(C_n+C_p-2C_m)\frac{1}{T_d}}$$
$$\times e^{-2\pi j\frac{T_b}{F}(C_i+2C_n+4C_p-8C_m)\omega}$$

(8) $For \quad \frac{-1}{T_c}<\omega<\frac{-3}{T_c}+\frac{2}{T_d}$

$$X_{o_2}(\omega,z)=E_2\sum_{m=1}^{k}\sum_{n=1}^{k}\sum_{p=1}^{k}\sum_{i=1}^{k}\sum_{l=1}^{k}\frac{SS_1S_4}{2\pi j\frac{T_b}{F}(C_i-C_p)}e^{2\pi j\frac{T_b}{F}(5C_m-3C_i-8C_p-2C_n-2C_l)\frac{1}{T_c}}e^{2\pi j\frac{T_b}{F}(2C_i-2C_p)\frac{1}{T_d}}$$
$$\times e^{-2\pi j\frac{T_b}{F}C_i\omega}+\frac{SS_2S_4}{2\pi j\frac{T_b}{F}(C_i+C_n-2C_p)}e^{2\pi j\frac{T_b}{F}(6C_p-3C_i-C_m-2C_n)\frac{1}{T_c}}e^{2\pi j\frac{T_b}{F}(2C_i+3C_n-5C_p)\frac{1}{T_d}}e^{-2\pi j\frac{T_b}{F}C_i\omega}$$
$$+\frac{SS_1S_3}{2\pi j\frac{T_b}{F}(C_i+2C_p+C_n-4C_m)}e^{2\pi j\frac{T_b}{F}(13C_m-3C_i-6C_p-2C_n-2C_l)\frac{1}{T_c}}e^{2\pi j\frac{T_b}{F}(2C_i+3C_n+5C_p-10C_m)\frac{1}{T_d}}e^{-2\pi j\frac{T_b}{F}C_i\omega}$$
$$\frac{SS_1S_4}{2\pi j\frac{T_b}{F}(C_i-C_n)}e^{2\pi j\frac{T_b}{F}(5C_m+4C_i-3C_p-5C_n-2C_l)\frac{1}{T_c}}e^{2\pi j\frac{T_b}{F}(3C_n-2C_i-C_p)\frac{1}{T_d}}e^{-2\pi j\frac{T_b}{F}C_n\omega}$$
$$+\frac{SS_2S_4}{2\pi j\frac{T_b}{F}(C_i+C_n-2C_p)}e^{2\pi j\frac{T_b}{F}(5C_n+4C_i-C_m-8C_p)\frac{1}{T_c}}e^{2\pi j\frac{T_b}{F}(3C_p-2C_i-C_n)\frac{1}{T_d}}e^{-2\pi j\frac{T_b}{F}(2C_p-C_n)\omega}$$
$$+\frac{SS_1S_3}{2\pi j\frac{T_b}{F}(C_i+2C_p+C_n-4C_m)}e^{2\pi j\frac{T_b}{F}(5C_n+4C_i+8C_p-15C_m-2C_l)\frac{1}{T_c}}e^{2\pi j\frac{T_b}{F}(6C_m-C_n-3C_p-2C_i)\frac{1}{T_d}}$$
$$\times e^{-2\pi j\frac{T_b}{F}(-2C_p-C_n+4C_m)\omega}+\frac{SS_1S_4}{2\pi j\frac{T_b}{F}(C_i-C_n)}e^{2\pi j\frac{T_b}{F}(5C_m-2C_i-3C_p+C_n-2C_l)\frac{1}{T_c}}e^{2\pi j\frac{T_b}{F}(3C_n+2C_i-C_p)\frac{1}{T_d}}$$
$$\times e^{-2\pi j\frac{T_b}{F}C_n\omega}+\frac{SS_2S_4}{2\pi j\frac{T_b}{F}(C_i-C_p)}e^{2\pi j\frac{T_b}{F}(2C_n+C_p-2C_i-2C_m)\frac{1}{T_c}}e^{2\pi j\frac{T_b}{F}(2C_i-2C_p)\frac{1}{T_d}}e^{-2\pi j\frac{T_b}{F}C_p\omega}$$
$$+\frac{SS_1S_3}{2\pi j\frac{T_b}{F}(C_i+C_p-2C_m)}e^{2\pi j\frac{T_b}{F}(3C_m+2C_n-2C_i-C_p-2C_l)\frac{1}{T_c}}e^{2\pi j\frac{T_b}{F}(2C_p+2C_i-4C_m)\frac{1}{T_d}}e^{-2\pi j\frac{T_b}{F}(C_p-2C_m)\omega}$$

$$+\frac{SS_1S_3}{2\pi j\frac{T_b}{F}(C_i+2C_p+C_n-4C_m)}e^{2\pi j\frac{T_b}{F}(15C_m-3C_n-2C_i-8C_p-2C_l)\frac{1}{T_c}}e^{2\pi j\frac{T_b}{F}(2C_i+3C_n+5C_p-10C_m)\frac{1}{T_d}}$$
$$\times e^{-2\pi j\frac{T_b}{F}(2C_p+C_n-4C_m)\omega}+\frac{SS_2S_4}{2\pi j\frac{T_b}{F}(C_i-C_m)}e^{2\pi j\frac{T_b}{F}(C_i-C_m)\frac{1}{T_c}}e^{2\pi j\frac{T_b}{F}(C_n-C_p)\frac{1}{T_d}}e^{-2\pi j\frac{T_b}{F}(2C_n-C_i)\omega}$$
$$+\frac{SS_1S_3}{2\pi j\frac{T_b}{F}(C_i-C_n)}e^{2\pi j\frac{T_b}{F}(C_i+C_m-2C_l)\frac{1}{T_c}}e^{2\pi j\frac{T_b}{F}(C_n+C_p-2C_m)\frac{1}{T_d}}e^{-2\pi j\frac{T_b}{F}(2C_n-C_i)\omega}$$
$$+\frac{SS_1S_3}{2\pi j\frac{T_b}{F}(C_i+2C_p+C_n-4C_m)}e^{2\pi j\frac{T_b}{F}(3C_m+C_i-2C_p-2C_l)\frac{1}{T_c}}e^{2\pi j\frac{T_b}{F}(C_n+C_p-2C_m)\frac{1}{T_d}}$$
$$\times e^{-2\pi j\frac{T_b}{F}(8C_m-4C_p-2C_n-C_i)\omega}$$

(9)$For\quad \frac{1}{T_c}+\frac{-2}{T_d}<\omega<\frac{-1}{T_c}$

$$X_{o_2}(\omega,z)=E_2\sum_{m=1}^{k}\sum_{n=1}^{k}\sum_{p=1}^{k}\sum_{i=1}^{k}\sum_{l=1}^{k}\frac{SS_1S_4}{2\pi j\frac{T_b}{F}(C_i+C_n-2C_p)}e^{2\pi j\frac{T_b}{F}(5C_m-C_i-4C_p+2C_n-2C_l)\frac{1}{T_c}}$$
$$\times e^{2\pi j\frac{T_b}{F}(C_n-C_p)\frac{1}{T_d}}e^{-2\pi j\frac{T_b}{F}C_i\omega}+\frac{SS_1S_4}{2\pi j\frac{T_b}{F}(C_i-C_p)}e^{2\pi j\frac{T_b}{F}(5C_m+2C_n-3C_p-2C_i-2C_l)\frac{1}{T_c}}e^{2\pi j\frac{T_b}{F}(2C_p-2C_i)\frac{1}{T_d}}$$
$$\times e^{-2\pi j\frac{T_b}{F}C_p\omega}+\frac{SS_2S_4}{2\pi j\frac{T_b}{F}(C_i+C_n-2C_p)}e^{2\pi j\frac{T_b}{F}(4C_p-2C_i-C_n-C_m)\frac{1}{T_c}}e^{2\pi j\frac{T_b}{F}(3C_p-C_n-2C_i)\frac{1}{T_d}}e^{-2\pi j\frac{T_b}{F}(C_n-2C_p)\omega}$$
$$+\frac{SS_1S_3}{2\pi j\frac{T_b}{F}(C_n+2C_p+C_i-4C_m)}e^{2\pi j\frac{T_b}{F}(9C_m-C_n-2C_i-4C_p-2C_l)\frac{1}{T_c}}e^{2\pi j\frac{T_b}{F}(6C_m-3C_p-2C_i-C_n)\frac{1}{T_d}}$$
$$\times e^{-2\pi j\frac{T_b}{F}(2C_p+C_n-4C_m)\omega}+\frac{SS_1S_4}{2\pi j\frac{T_b}{F}(C_i-C_n)}e^{2\pi j\frac{T_b}{F}(5C_m-5C_n-3C_p+4C_i-2C_l)\frac{1}{T_c}}e^{2\pi j\frac{T_b}{F}(3C_n-2C_i-C_p)\frac{1}{T_d}}$$
$$\times e^{-2\pi j\frac{T_b}{F}C_n\omega}+\frac{SS_2S_4}{2\pi j\frac{T_b}{F}(C_i+C_n-2C_p)}e^{2\pi j\frac{T_b}{F}(4C_i-8C_p+5C_n-C_m)\frac{1}{T_c}}e^{2\pi j\frac{T_b}{F}(3C_p-C_n-2C_i)\frac{1}{T_d}}e^{-2\pi j\frac{T_b}{F}(2C_p-C_n)\omega}$$
$$+\frac{SS_1S_3}{2\pi j\frac{T_b}{F}(C_n+2C_p+C_i-4C_m)}e^{2\pi j\frac{T_b}{F}(5C_n-15C_m+4C_i+8C_p-2C_l)\frac{1}{T_c}}e^{2\pi j\frac{T_b}{F}(6C_m-3C_p-2C_i-C_n)\frac{1}{T_d}}$$
$$\times e^{-2\pi j\frac{T_b}{F}(4C_m-C_n-2C_p)\omega}+\frac{SS_1S_4}{2\pi j\frac{T_b}{F}(C_i-C_n)}e^{2\pi j\frac{T_b}{F}(5C_m-3C_p-C_i-2C_l)\frac{1}{T_c}}e^{2\pi j\frac{T_b}{F}(2C_i-C_n-C_p)\frac{1}{T_d}}$$
$$\times e^{-2\pi j\frac{T_b}{F}(C_n-C_i)\omega}+\frac{SS_2S_4}{2\pi j\frac{T_b}{F}(C_i-C_p)}e^{2\pi j\frac{T_b}{F}(2C_n-C_i-2C_m)\frac{1}{T_c}}e^{2\pi j\frac{T_b}{F}(2C_i-2C_p)\frac{1}{T_d}}e^{-2\pi j\frac{T_b}{F}(2C_p-C_i)\omega}$$
$$+\frac{SS_1S_3}{2\pi j\frac{T_b}{F}(C_i+C_p-2C_m)}e^{2\pi j\frac{T_b}{F}(C_m-2C_l+2C_n-C_i)\frac{1}{T_c}}e^{2\pi j\frac{T_b}{F}(4C_i+4C_p-8C_m)\frac{1}{T_d}}e^{-2\pi j\frac{T_b}{F}(4C_m-2C_p-C_i)\omega}$$
$$+\frac{SS_1S_3}{2\pi j\frac{T_b}{F}(C_n+2C_p+C_i-4C_m)}e^{2\pi j\frac{T_b}{F}(11C_m-2C_n-C_i-6C_p-2C_l)\frac{1}{T_c}}e^{2\pi j\frac{T_b}{F}(2C_i+5C_p-10C_m+3C_n)\frac{1}{T_d}}$$
$$\times e^{-2\pi j\frac{T_b}{F}(C_i+4C_p+2C_n-8C_m)\omega}$$

(10)$For\quad \frac{-3}{T_c}<\omega<\frac{1}{T_c}+\frac{-2}{T_d}$

$$X_{o_2}(\omega,z)=E_2\sum_{m=1}^{k}\sum_{n=1}^{k}\sum_{p=1}^{k}\sum_{i=1}^{k}\sum_{l=1}^{k}\frac{SS_1S_4}{2\pi j\frac{T_b}{F}(C_n+C_i-2C_p)}e^{2\pi j\frac{T_b}{F}(5C_m+2C_n-4C_p-C_i-2C_l)\frac{1}{T_c}}$$
$$\times e^{2\pi j\frac{T_b}{F}(C_n-C_p)\frac{1}{T_d}}e^{-2\pi j\frac{T_b}{F}C_i\omega}+\frac{SS_1S_4}{2\pi j\frac{T_b}{F}(C_i-C_p)}e^{2\pi j\frac{T_b}{F}(5C_m+2C_n-3C_p-C_i-2C_l)\frac{1}{T_c}}e^{2\pi j\frac{T_b}{F}(2C_p-2C_i)\frac{1}{T_d}}$$
$$\times e^{-2\pi j\frac{T_b}{F}C_p\omega}+\frac{SS_1S_4}{2\pi j\frac{T_b}{F}(C_n+C_i-2C_p)}e^{2\pi j\frac{T_b}{F}(4C_p-C_m-C_n-2C_i)\frac{1}{T_c}}e^{2\pi j\frac{T_b}{F}(3C_p-2C_i-C_n)\frac{1}{T_d}}$$
$$\times e^{-2\pi j\frac{T_b}{F}(2C_p-C_n)\omega}+\frac{SS_1S_3}{2\pi j\frac{T_b}{F}(C_n+2C_p+C_i-4C_m)}e^{2\pi j\frac{T_b}{F}(9C_m-4C_p-2C_i-C_n-2C_l)\frac{1}{T_c}}$$
$$\times e^{2\pi j\frac{T_b}{F}(6C_m-3C_p-2C_i-C_n)\frac{1}{T_d}}e^{-2\pi j\frac{T_b}{F}(4C_m-C_n-2C_p)\omega}+\frac{SS_1S_4}{2\pi j\frac{T_b}{F}(C_i-C_n)}e^{2\pi j\frac{T_b}{F}(5C_m+3C_i-3C_p-4C_n-2C_l)\frac{1}{T_c}}$$
$$\times e^{2\pi j\frac{T_b}{F}(C_n-C_p)\frac{1}{T_d}}e^{-2\pi j\frac{T_b}{F}(2C_n-C_i)\omega}+\frac{SS_2S_4}{2\pi j\frac{T_b}{F}(C_i+C_n-2C_p)}e^{2\pi j\frac{T_b}{F}(4C_n-2C_p-C_m+3C_i)\frac{1}{T_c}}$$
$$\times e^{2\pi j\frac{T_b}{F}(C_n-C_p)\frac{1}{T_d}}e^{-2\pi j\frac{T_b}{F}(4C_p-C_i-2C_n)\omega}+\frac{SS_1S_3}{2\pi j\frac{T_b}{F}(C_i+C_n+2C_p-4C_m)}$$
$$\times e^{2\pi j\frac{T_b}{F}(6C_p+4C_n+3C_i-2C_l-11C_m)\frac{1}{T_c}}e^{2\pi j\frac{T_b}{F}(C_n+C_p-2C_m)\frac{1}{T_d}}e^{-2\pi j\frac{T_b}{F}(8C_m-C_i-2C_n-4C_p)\omega}$$

(11)$For\quad \frac{-1}{T_c}+\frac{-2}{T_d}<\omega<\frac{-3}{T_c}$

$$X_{o_2}(\omega,z)=E_2\sum_{m=1}^{k}\sum_{n=1}^{k}\sum_{p=1}^{k}\sum_{i=1}^{k}\sum_{l=1}^{k}\frac{SS_1S_4}{2\pi j\frac{T_b}{F}(C_i+C_n-2C_p)}e^{2\pi j\frac{T_b}{F}(5C_m+5C_n-2C_l+2C_i-10C_p)\frac{1}{T_c}}$$
$$\times e^{2\pi j\frac{T_b}{F}(C_n-C_p)\frac{1}{T_d}}e^{-2\pi j\frac{T_b}{F}(C_n-2C_p)\omega}+\frac{SS_1S_4}{2\pi j\frac{T_b}{F}(C_i-C_p)}e^{2\pi j\frac{T_b}{F}(5C_m+C_i+2C_n-6C_p-2C_l)\frac{1}{T_c}}$$
$$\times e^{2\pi j\frac{T_b}{F}(2C_i-2C_p)\frac{1}{T_d}}e^{-2\pi j\frac{T_b}{F}(2C_p-C_i)\omega}+\frac{SS_2S_4}{2\pi j\frac{T_b}{F}(C_i+C_n-2C_p)}e^{2\pi j\frac{T_b}{F}(2C_n-2C_p-C_m+C_i)\frac{1}{T_c}}$$

$\times e^{2\pi j\frac{T_b}{F}(2C_i+3C_n-5C_p)\frac{1}{T_d}}e^{-2\pi j\frac{T_b}{F}(4C_p-C_i-2C_n)\omega}+\frac{SS_1S_3}{2\pi j\frac{T_b}{F}(C_i+C_n+2C_p-4C_m)}$
$\times e^{2\pi j\frac{T_b}{F}(2C_p+2C_n+C_i-2C_l-4C_m)\frac{1}{T_c}}e^{2\pi j\frac{T_b}{F}(3C_n+5C_p+2C_i-10C_m)\frac{1}{T_d}}e^{-2\pi j\frac{T_b}{F}(8C_m-C_i-2C_n-4C_p)\omega}$

$$(12)For\quad \frac{-3}{T_c}+\frac{-2}{T_d}<\omega<\frac{-3}{T_c}$$
$$X_{o_2}(\omega,z)=E_2\sum_{m=1}^{k}\sum_{n=1}^{k}\sum_{p=1}^{k}\sum_{i=1}^{k}\sum_{l=1}^{k}\frac{SS_1S_4}{2\pi j\frac{T_b}{F}(C_i+C_n-2C_p)}$$
$$e^{2\pi j\frac{T_b}{F}(5C_m+6C_n+3C_i-2C_l-12C_p)\frac{1}{T_c}}e^{2\pi j\frac{T_b}{F}(2C_i+3C_n-5C_p)\frac{1}{T_d}}e^{-2\pi j\frac{T_b}{F}(4C_p-2C_n-C_i\omega} \tag{D.19}$$

In order to calculate $X_{o_3}$ and in regarding to parameters $S$, $S_1$, $S_2$,$S_3$, $S_4$ and by defining $E_3$ as follow:

$$E_3=64\pi^5A_c^4A_dT_c^4T_d\gamma_{osc}(\gamma_{sc}+2\gamma_{oc})e^{G_1(\omega)z}\left(\frac{1-e^{-2\alpha z}}{2\alpha}\right)^2$$

for $T_d>T_c$ we would have:

$$(1)For\quad \omega>\frac{4}{T_c}+\frac{1}{T_d},\quad \omega<\frac{-4}{T_c}+\frac{-1}{T_d}\quad\Rightarrow\quad X_{o_3}(\omega,z)=0$$

$$(2)For\quad \frac{2}{T_c}+\frac{1}{T_d}<\omega<\frac{4}{T_c}+\frac{1}{T_d}$$
$X_{o_3}(\omega,z)=E_3\sum_{m=1}^{k}\sum_{n=1}^{k}\sum_{p=1}^{k}\sum_{i=1}^{k}\sum_{l=1}^{k}\frac{SS_1S_3}{2\pi j\frac{T_b}{F}(C_i-C_n)}e^{2\pi j\frac{T_b}{F}(4C_i+C_p-2C_l-3C_m)\frac{1}{T_c}}e^{2\pi j\frac{T_b}{F}(C_i-C_n)\frac{1}{T_d}}$
$e^{-2\pi j\frac{T_b}{F}C_i\omega}$

$$(3)For\quad \frac{4}{T_c}+\frac{-1}{T_d}<\omega<\frac{2}{T_c}+\frac{1}{T_d}$$
$X_{o_3}(\omega,z)=E_3\sum_{m=1}^{k}\sum_{n=1}^{k}\sum_{p=1}^{k}\sum_{i=1}^{k}\sum_{l=1}^{k}\frac{SS_2S_4}{2\pi j\frac{T_b}{F}(C_i-C_n)}e^{2\pi j\frac{T_b}{F}(2C_i-C_p-C_m)\frac{1}{T_c}}e^{2\pi j\frac{T_b}{F}(2C_i-C_n)\frac{1}{T_d}}$
$\times e^{-2\pi j\frac{T_b}{F}C_i\omega}+\frac{SS_1S_3}{2\pi j\frac{T_b}{F}(C_i-C_n)}e^{2\pi j\frac{T_b}{F}(2C_i+C_p-C_m-2C_l)\frac{1}{T_c}}e^{2\pi j\frac{T_b}{F}(C_i-C_n)\frac{1}{T_d}}e^{-2\pi j\frac{T_b}{F}C_i\omega}$
$+\frac{SS_1S_3}{2\pi j\frac{T_b}{F}(C_i-C_n)}e^{2\pi j\frac{T_b}{F}(2C_i-2C_n+5C_m-2C_l-3C_p)\frac{1}{T_c}}e^{2\pi j\frac{T_b}{F}(C_i-C_n)\frac{1}{T_d}}e^{-2\pi j\frac{T_b}{F}C_i\omega}$
$+\frac{SS_1S_3}{2\pi j\frac{T_b}{F}(C_i-C_n)}e^{2\pi j\frac{T_b}{F}(2C_i+2C_n+C_p-3C_m-2C_l)\frac{1}{T_c}}e^{-2\pi j\frac{T_b}{F}C_n\omega}$

$$(4)For\quad \frac{1}{T_d}<\omega<\frac{4}{T_c}+\frac{-1}{T_d}$$
$X_{o_3}(\omega,z)=E_3\sum_{m=1}^{k}\sum_{n=1}^{k}\sum_{p=1}^{k}\sum_{i=1}^{k}\sum_{l=1}^{k}SS_2S_4\frac{1}{2\pi j\frac{T_b}{F}(C_i-C_n)}e^{2\pi j\frac{T_b}{F}(2C_i-C_p-C_m)\frac{1}{T_c}}e^{2\pi j\frac{T_b}{F}(C_i-C_n)\frac{1}{T_d}}$
$\times e^{-2\pi j\frac{T_b}{F}C_i\omega}+\frac{SS_1S_3}{2\pi j\frac{T_b}{F}(C_i-C_n)}e^{2\pi j\frac{T_b}{F}(2C_i+C_p-C_m-2C_l)\frac{1}{T_c}}e^{2\pi j\frac{T_b}{F}(C_i-C_n)\frac{1}{T_d}}e^{-2\pi j\frac{T_b}{F}C_i\omega}$
$+\frac{SS_1S_3}{2\pi j\frac{T_b}{F}(C_i-C_n)}e^{2\pi j\frac{T_b}{F}(2C_i-2C_n+5C_m-2C_l+3C_p)\frac{1}{T_c}}e^{2\pi j\frac{T_b}{F}(C_i-C_n)\frac{1}{T_d}}e^{-2\pi j\frac{T_b}{F}C_i\omega}$
$+\frac{SS_1S_3}{2\pi j\frac{T_b}{F}(C_i-C_n)}e^{2\pi j\frac{T_b}{F}(6C_n+C_p-3C_m-2C_i-2C_l)\frac{1}{T_c}}e^{2\pi j\frac{T_b}{F}(C_i-C_n)\frac{1}{T_d}}e^{-2\pi j\frac{T_b}{F}(C_i-2C_n)\omega}$

$$(5)For\quad \frac{2}{T_c}+\frac{-1}{T_d}<\omega<\frac{1}{T_d}$$
$X_{o_3}(\omega,z)=E_3\sum_{m=1}^{k}\sum_{n=1}^{k}\sum_{p=1}^{k}\sum_{i=1}^{k}\sum_{l=1}^{k}SS_1S_4\frac{1}{2\pi j\frac{T_b}{F}(C_i-C_n)}e^{2\pi j\frac{T_b}{F}(5C_m-3C_p-2C_l)\frac{1}{T_c}}$

$$\times e^{2\pi j\frac{T_b}{F}(C_i-C_n)\frac{1}{T_d}}e^{-2\pi j\frac{T_b}{F}C_i\omega}+\frac{SS_2S_4}{2\pi j\frac{T_b}{F}(C_i+C_n+2C_p-4C_m)}e^{2\pi j\frac{T_b}{F}(2C_n-C_p-2C_m)\frac{1}{T_c}}e^{2\pi j\frac{T_b}{F}(2C_i-2C_p)\frac{1}{T_d}}$$
$$\times e^{-2\pi j\frac{T_b}{F}C_i\omega}+\frac{SS_1S_3}{2\pi j\frac{T_b}{F}(C_i-C_n)}e^{2\pi j\frac{T_b}{F}(2C_n+C_p-2C_l-C_m)\frac{1}{T_c}}e^{2\pi j\frac{T_b}{F}(C_i-C_n)\frac{1}{T_d}}e^{-2\pi j\frac{T_b}{F}C_i\omega}$$
$$+\frac{SS_2S_4}{2\pi j\frac{T_b}{F}(C_i-C_n)}e^{2\pi j\frac{T_b}{F}(2C_i-C_p-C_m)\frac{1}{T_c}}e^{-2\pi j\frac{T_b}{F}C_n\omega}$$
$$+\frac{SS_1S_3}{2\pi j\frac{T_b}{F}(C_i-C_n)}e^{2\pi j\frac{T_b}{F}(2C_i+C_p-C_m-2C_l)\frac{1}{T_c}}e^{-2\pi j\frac{T_b}{F}C_n\omega}$$
$$+\frac{SS_1S_3}{2\pi j\frac{T_b}{F}(C_i-C_n)}e^{2\pi j\frac{T_b}{F}(2C_i-3C_p+5C_m-2C_l-2C_n)\frac{1}{T_c}}e^{-2\pi j\frac{T_b}{F}C_n\omega}$$
$$+\frac{SS_1S_3}{2\pi j\frac{T_b}{F}(C_i-C_n)}e^{2\pi j\frac{T_b}{F}(6C_n+C_p-3C_m-2C_l-2C_i)\frac{1}{T_c}}e^{2\pi j\frac{T_b}{F}(C_i-C_n)\frac{1}{T_d}}e^{-2\pi j\frac{T_b}{F}(2C_n-C_i)\omega}$$

(6)$For\quad \frac{-2}{T_c}+\frac{1}{T_d}<\omega<\frac{2}{T_c}++\frac{-1}{T_d}$

$$X_{o_3}(\omega,z)=E_3\sum_{m=1}^{k}\sum_{n=1}^{k}\sum_{p=1}^{k}\sum_{i=1}^{k}\sum_{l=1}^{k}\frac{SS_1S_4}{2\pi j\frac{T_b}{F}(C_i-C_n)}e^{2\pi j\frac{T_b}{F}(5C_m-2C_l-3C_p)\frac{1}{T_c}}e^{2\pi j\frac{T_b}{F}(C_i-C_n)\frac{1}{T_d}}$$
$$\times e^{-2\pi j\frac{T_b}{F}C_i\omega}+\frac{SS_2S_4}{2\pi j\frac{T_b}{F}(C_i+C_n)+2C_p-4C_m}e^{2\pi j\frac{T_b}{F}(2C_n-C_m-C_p)\frac{1}{T_c}}e^{2\pi j\frac{T_b}{F}(C_i+C_n)+2C_p-4C_m)\frac{1}{T_d}}$$
$$\times e^{-2\pi j\frac{T_b}{F}C_i\omega}+\frac{SS_1S_3}{2\pi j\frac{T_b}{F}(C_i-C_n)}e^{2\pi j\frac{T_b}{F}(2C_n-C_m+C_p-2C_l)\frac{1}{T_c}}e^{2\pi j\frac{T_b}{F}(C_i-C_n)\frac{1}{T_d}}e^{-2\pi j\frac{T_b}{F}C_i\omega}$$
$$+\frac{SS_2S_4}{2\pi j\frac{T_b}{F}(C_i-C_n)}e^{2\pi j\frac{T_b}{F}(2C_n-C_p-C_m)\frac{1}{T_c}}e^{2\pi j\frac{T_b}{F}(C_i-C_n)\frac{1}{T_d}}e^{-2\pi j\frac{T_b}{F}(2C_n-C_i)\omega}$$
$$+\frac{SS_1S_3}{2\pi j\frac{T_b}{F}(C_i-C_n)}e^{2\pi j\frac{T_b}{F}(2C_n-C_m+C_p-2C_l)\frac{1}{T_c}}e^{2\pi j\frac{T_b}{F}(C_i-C_n)\frac{1}{T_d}}e^{-2\pi j\frac{T_b}{F}(2C_n-C_i)\omega}$$
$$+\frac{SS_1S_3}{2\pi j\frac{T_b}{F}(C_i-C_n)}e^{2\pi j\frac{T_b}{F}(5C_m-3C_p-2C_l)\frac{1}{T_c}}e^{2\pi j\frac{T_b}{F}(C_i-C_n)\frac{1}{T_d}}e^{-2\pi j\frac{T_b}{F}(2C_n-C_i)\omega}$$

(7)$For\quad \frac{-1}{T_d}<\omega<\frac{-2}{T_c}+\frac{1}{T_d}$

$$X_{o_3}(\omega,z)=E_3\sum_{m=1}^{k}\sum_{n=1}^{k}\sum_{p=1}^{k}\sum_{i=1}^{k}\sum_{l=1}^{k}\frac{SS_1S_4}{2\pi j\frac{T_b}{F}(C_i+C_n-2C_p)}e^{2\pi j\frac{T_b}{F}(5C_m-2C_i+2C_n-3C_p-2C_l)\frac{1}{T_c}}$$
$$\times e^{2\pi j\frac{T_b}{F}(C_i+C_n-2C_p)\frac{1}{T_d}}e^{-2\pi j\frac{T_b}{F}C_i\omega}+\frac{SS_1S_4}{2\pi j\frac{T_b}{F}(C_i-C_n)}e^{2\pi j\frac{T_b}{F}(2C_i-2C_n+5C_m-3C_p-2C_l)\frac{1}{T_c}}e^{-2\pi j\frac{T_b}{F}C_n\omega}$$
$$+\frac{SS_2S_4}{2\pi j\frac{T_b}{F}(C_i+C_n+2C_p-4C_m)}e^{2\pi j\frac{T_b}{F}(4C_n+2C_i+3C_p-9C_m-2C_l)\frac{1}{T_c}}e^{-2\pi j\frac{T_b}{F}(C_n+2C_p-4C_m)\omega}$$
$$\frac{SS_1S_3}{2\pi j\frac{T_b}{F}(C_i-C_n)}e^{2\pi j\frac{T_b}{F}(2C_i+C_p-C_m-2C_l)\frac{1}{T_c}}e^{-2\pi j\frac{T_b}{F}C_n\omega}$$
$$+\frac{SS_2S_4}{2\pi j\frac{T_b}{F}(C_i-C_n)}e^{2\pi j\frac{T_b}{F}(2C_n-C_p-C_m)\frac{1}{T_c}}e^{2\pi j\frac{T_b}{F}(C_i-C_n)\frac{1}{T_d}}e^{-2\pi j\frac{T_b}{F}(2C_n-C_i)\omega}$$
$$+\frac{SS_1S_3}{2\pi j\frac{T_b}{F}(C_i-C_n)}e^{2\pi j\frac{T_b}{F}(2C_n+C_p-C_m-2C_l)\frac{1}{T_c}}e^{2\pi j\frac{T_b}{F}(C_i-C_n)\frac{1}{T_d}}e^{-2\pi j\frac{T_b}{F}(2C_n-C_i)\omega}$$
$$+\frac{SS_1S_3}{2\pi j\frac{T_b}{F}(C_i-C_n)}e^{2\pi j\frac{T_b}{F}(5C_m-3C_p-2C_l)\frac{1}{T_c}}e^{2\pi j\frac{T_b}{F}(C_i-C_n)\frac{1}{T_d}}e^{-2\pi j\frac{T_b}{F}(2C_n-C_i)\omega}$$

(8)$For\quad \frac{-4}{T_c}+\frac{1}{T_d}<\omega<\frac{-1}{T_d}$

$$X_{o_3}(\omega,z)=E_3\sum_{m=1}^{k}\sum_{n=1}^{k}\sum_{p=1}^{k}\sum_{i=1}^{k}\sum_{l=1}^{k}\frac{SS_1S_4}{2\pi j\frac{T_b}{F}(C_i+C_n-2C_p}e^{2\pi j\frac{T_b}{F}(5C_m-2C_i-3C_p+2C_n-2C_l)\frac{1}{T_c}}$$
$$\times e^{2\pi j\frac{T_b}{F}(C_i+C_n-2C_p)\frac{1}{T_d}}e^{-2\pi j\frac{T_b}{F}C_i\omega}+\frac{SS_1S_4}{2\pi j\frac{T_b}{F}(C_i-C_n)}e^{2\pi j\frac{T_b}{F}(2C_i-3C_p+5C_m-2C_n-2C_l)\frac{1}{T_c}}e^{2\pi j\frac{T_b}{F}(C_i-C_n)\frac{1}{T_d}}$$
$$\times e^{-2\pi j\frac{T_b}{F}(2C_n+C_i)\omega}+\frac{SS_2S_4}{2\pi j\frac{T_b}{F}(C_i+2C_p+C_n-4C_m)}e^{2\pi j\frac{T_b}{F}(2C_i-9C_m+3C_p+4C_n)\frac{1}{T_c}}$$
$$\times e^{2\pi j\frac{T_b}{F}(C_i+2C_p+C_n-4C_m)\frac{1}{T_d}}e^{-2\pi j\frac{T_b}{F}(8C_m-4C_p-2C_n-C_i)\omega}+\frac{SS_1S_3}{2\pi j\frac{T_b}{F}(C_i-C_n)}e^{2\pi j\frac{T_b}{F}(2C_i-C_m+C_p-2C_l)\frac{1}{T_c}}$$
$$\times e^{2\pi j\frac{T_b}{F}(C_i-C_n)\frac{1}{T_d}}e^{-2\pi j\frac{T_b}{F}(2C_n-C_i)\omega}$$

(9)$For\quad \frac{-2}{T_c}+\frac{-1}{T_d}<\omega<\frac{-4}{T_c}+\frac{1}{T_d}$

$$X_{o3}(\omega,z)=E_3\sum_{m=1}^{k}\sum_{n=1}^{k}\sum_{p=1}^{k}\sum_{i=1}^{k}\sum_{l=1}^{k}\frac{SS_1S_4}{2\pi j\frac{T_b}{F}(C_i+C_n-2C_p)}e^{2\pi j\frac{T_b}{F}(5C_m+2C_i-11C_p+6C_n-2C_l)\frac{1}{T_c}}$$
$$\times e^{-2\pi j\frac{T_b}{F}(C_n-2C_p)\omega}+\frac{SS_1S_4}{2\pi j\frac{T_b}{F}(C_i-C_n)}e^{2\pi j\frac{T_b}{F}(5C_m-2C_n-3C_p+2C_i-2C_l)\frac{1}{T_c}}e^{2\pi j\frac{T_b}{F}(C_i-C_n)\frac{1}{T_d}}$$
$$\times e^{-2\pi j\frac{T_b}{F}(2C_n-C_i)\omega}+\frac{SS_2S_4}{2\pi j\frac{T_b}{F}(C_n+2C_p+C_i-4C_m)}e^{2\pi j\frac{T_b}{F}(2C_i+4C_n+3C_p-9C_m)\frac{1}{T_c}}$$
$$\times e^{2\pi j\frac{T_b}{F}(C_n+2C_p+C_i-4C_m)\frac{1}{T_d}}e^{-2\pi j\frac{T_b}{F}(8C_m-4C_p-C_i-2C_n)\omega}+\frac{SS_1S_3}{2\pi j\frac{T_b}{F}(C_i-C_n)}e^{2\pi j\frac{T_b}{F}(C_p+2C_i-C_m-2C_l)\frac{1}{T_c}}$$
$$\times e^{2\pi j\frac{T_b}{F}(C_i-C_n)\frac{1}{T_d}}e^{-2\pi j\frac{T_b}{F}(2C_n-C_i)\omega}$$

$$(10)For\quad\frac{-4}{T_c}+\frac{-1}{T_d}<\omega<\frac{-}{T_c}+\frac{-1}{T_d}$$
$$X_{o3}(\omega,z)=E_3\sum_{m=1}^{k}\sum_{n=1}^{k}\sum_{p=1}^{k}\sum_{i=1}^{k}\sum_{l=1}^{k}\frac{SS_1S_4}{2\pi j\frac{T_b}{F}(C_n+C_i-2C_p)}e^{2\pi j\frac{T_b}{F}(5C_m+8C_n-15C_p+4C_i-2C_l)\frac{1}{T_c}}$$
$$\times e^{2\pi j\frac{T_b}{F}(C_n+C_i-2C_p)\frac{1}{T_d}}e^{-2\pi j\frac{T_b}{F}(4C_p-C_i-2C_n)\omega}\tag{D.20}$$

When the pulse-width of the data is smaller than the pulse-width of clock($T_d<T_c$)for $X_{o_3}$ we would have:

$$(1)For\quad\omega>\frac{4}{T_c}+\frac{1}{T_d},\quad\omega<\frac{-4}{T_c}+\frac{-1}{T_d}\quad\Rightarrow\quad X_{o3}(\omega,z)=0$$

$$(2)For\quad\frac{4}{T_c}+\frac{-1}{T_d}<\omega<\frac{4}{T_c}+\frac{1}{T_d}$$
$$X_{o3}(\omega,z)=E_3\sum_{m=1}^{k}\sum_{n=1}^{k}\sum_{p=1}^{k}\sum_{i=1}^{k}\sum_{l=1}^{k}\frac{SS_1S_3}{2\pi j\frac{T_b}{F}(C_i-C_n)}e^{2\pi j\frac{T_b}{F}(4C_i+C_p-2C_l-3C_m)\frac{1}{T_c}}e^{2\pi j\frac{T_b}{F}(C_i-C_n)\frac{1}{T_d}}$$
$$e^{-2\pi j\frac{T_b}{F}C_i\omega}$$

$$(3)For\quad\frac{2}{T_c}+\frac{1}{T_d}<\omega<\frac{4}{T_c}+\frac{-1}{T_d}$$
$$X_{o3}(\omega,z)=E_3\sum_{m=1}^{k}\sum_{n=1}^{k}\sum_{p=1}^{k}\sum_{i=1}^{k}\sum_{l=1}^{k}\frac{SS_1S_3}{2\pi j\frac{T_b}{F}(C_i-C_n)}e^{2\pi j\frac{T_b}{F}(4C_n+C_p-3C_m-2C_l)\frac{1}{T_c}}e^{2\pi j\frac{T_b}{F}(2C_i-2C_n)\frac{1}{T_d}}$$
$$\times e^{-2\pi j\frac{T_b}{F}C_n\omega}$$

$$(4)For\quad\frac{2}{T_c}+\frac{-1}{T_d}<\omega<\frac{2}{T_c}+\frac{1}{T_d}$$
$$X_{o3}(\omega,z)=E_3\sum_{m=1}^{k}\sum_{n=1}^{k}\sum_{p=1}^{k}\sum_{i=1}^{k}\sum_{l=1}^{k}SS_2S_4\frac{1}{2\pi j\frac{T_b}{F}(C_i-C_n)}e^{2\pi j\frac{T_b}{F}(2C_i-C_p-C_m)\frac{1}{T_c}}e^{2\pi j\frac{T_b}{F}(C_i-C_n)\frac{1}{T_d}}$$
$$\times e^{-2\pi j\frac{T_b}{F}C_i\omega}+\frac{SS_1S_3}{2\pi j\frac{T_b}{F}(C_i-C_n)}e^{2\pi j\frac{T_b}{F}(2C_i+C_p-C_m-2C_l)\frac{1}{T_c}}e^{2\pi j\frac{T_b}{F}(C_i-C_n)\frac{1}{T_d}}e^{-2\pi j\frac{T_b}{F}C_i\omega}$$
$$+\frac{SS_1S_3}{2\pi j\frac{T_b}{F}(C_i-C_n)}e^{2\pi j\frac{T_b}{F}(2C_i-2C_n+5C_m-2C_l-3C_p)\frac{1}{T_c}}e^{2\pi j\frac{T_b}{F}(C_i-C_n)\frac{1}{T_d}}e^{-2\pi j\frac{T_b}{F}C_i\omega}$$
$$+\frac{SS_1S_3}{2\pi j\frac{T_b}{F}(C_i-C_n)}e^{2\pi j\frac{T_b}{F}(6C_n+C_p-3C_m-2C_i-2C_l)\frac{1}{T_c}}e^{2\pi j\frac{T_b}{F}(C_i-C_n)\frac{1}{T_d}}e^{-2\pi j\frac{T_b}{F}(2C_n-C_i)\omega}$$

$$(5)For\quad\frac{1}{T_d}<\omega<\frac{2}{T_c}+\frac{-1}{T_d}$$
$$X_{o3}(\omega,z)=E_3\sum_{m=1}^{k}\sum_{n=1}^{k}\sum_{p=1}^{k}\sum_{i=1}^{k}\sum_{l=1}^{k}SS_2S_4\frac{1}{2\pi j\frac{T_b}{F}(C_i-C_n)}e^{2\pi j\frac{T_b}{F}(2C_n-C_p-C_m)\frac{1}{T_c}}$$
$$\times e^{2\pi j\frac{T_b}{F}(2C_i-2C_n)\frac{1}{T_d}}e^{-2\pi j\frac{T_b}{F}C_n\omega}+\frac{SS_1S_3}{2\pi j\frac{T_b}{F}(C_i-C_n}e^{2\pi j\frac{T_b}{F}(2C_n+C_p-C_m-2C_l)\frac{1}{T_c}}e^{2\pi j\frac{T_b}{F}(2C_i-2C_n)\frac{1}{T_d}}$$
$$\times e^{-2\pi j\frac{T_b}{F}C_n\omega}+\frac{SS_1S_3}{2\pi j\frac{T_b}{F}(C_i-C_n)}e^{2\pi j\frac{T_b}{F}(5C_m-3C_p-2C_l)\frac{1}{T_c}}e^{2\pi j\frac{T_b}{F}(2C_i-2C_n)\frac{1}{T_d}}e^{-2\pi j\frac{T_b}{F}C_n\omega}$$

$$(6)For \quad \frac{-1}{T_d} < \omega < \frac{1}{T_d}$$

$$X_{o3}(\omega,z) = E_3 \sum_{m=1}^{k}\sum_{n=1}^{k}\sum_{p=1}^{k}\sum_{i=1}^{k}\sum_{l=1}^{k} \frac{SS_1S_4}{2\pi j\frac{T_b}{F}(C_i-C_n)} e^{2\pi j\frac{T_b}{F}(5C_m-2C_l-3C_p)\frac{1}{T_c}} e^{2\pi j\frac{T_b}{F}(C_i-C_n)\frac{1}{T_d}}$$
$$\times e^{-2\pi j\frac{T_b}{F}C_i\omega} + \frac{SS_2S_4}{2\pi j\frac{T_b}{F}(C_i+C_n)+2C_p-4C_m} e^{2\pi j\frac{T_b}{F}(2C_n-C_m-C_p)\frac{1}{T_c}} e^{2\pi j\frac{T_b}{F}(C_i+C_n)+2C_p-4C_m)\frac{1}{T_d}}$$
$$\times e^{-2\pi j\frac{T_b}{F}C_i\omega} + \frac{SS_1S_3}{2\pi j\frac{T_b}{F}(C_i-C_n)} e^{2\pi j\frac{T_b}{F}(2C_n-C_m+C_p-2C_l)\frac{1}{T_c}} e^{2\pi j\frac{T_b}{F}(C_i-C_n)\frac{1}{T_d}} e^{-2\pi j\frac{T_b}{F}C_i\omega}$$
$$+ \frac{SS_2S_4}{2\pi j\frac{T_b}{F}(C_i-C_n)} e^{2\pi j\frac{T_b}{F}(2C_n-C_p-C_m)\frac{1}{T_c}} e^{2\pi j\frac{T_b}{F}(C_i-C_n)\frac{1}{T_d}} e^{-2\pi j\frac{T_b}{F}(2C_n-C_i)\omega}$$
$$+ \frac{SS_1S_3}{2\pi j\frac{T_b}{F}(C_i-C_n)} e^{2\pi j\frac{T_b}{F}(2C_n-C_m+C_p-2C_l)\frac{1}{T_c}} e^{2\pi j\frac{T_b}{F}(C_i-C_n)\frac{1}{T_d}} e^{-2\pi j\frac{T_b}{F}(2C_n-C_i)\omega}$$
$$+ \frac{SS_1S_3}{2\pi j\frac{T_b}{F}(C_i-C_n)} e^{2\pi j\frac{T_b}{F}(5C_m-3C_p-2C_l)\frac{1}{T_c}} e^{2\pi j\frac{T_b}{F}(C_i-C_n)\frac{1}{T_d}} e^{-2\pi j\frac{T_b}{F}(2C_n-C_i)\omega}$$

$$(7)For \quad \frac{-2}{T_c} + \frac{1}{T_d} < \omega < \frac{-1}{T_d}$$

$$X_{o3}(\omega,z) = E_3 \sum_{m=1}^{k}\sum_{n=1}^{k}\sum_{p=1}^{k}\sum_{i=1}^{k}\sum_{l=1}^{k} \frac{SS_1S_4}{2\pi j\frac{T_b}{F}(C_i-C_n)} e^{2\pi j\frac{T_b}{F}(5C_m-3C_p-2C_l)\frac{1}{T_c}} e^{2\pi j\frac{T_b}{F}(2C_i-2C_n)\frac{1}{T_d}}$$
$$\times e^{-2\pi j\frac{T_b}{F}C_n\omega} + \frac{SS_2S_4}{2\pi j\frac{T_b}{F}(C_i+C_n+2C_p-4C_m)} e^{2\pi j\frac{T_b}{F}(2C_n-C_p-C_m)\frac{1}{T_c}} e^{2\pi j\frac{T_b}{F}(2C_i+2C_n4C_p-8C_m)\frac{1}{T_d}}$$
$$\times e^{-2\pi j\frac{T_b}{F}(C_n+2C_p-4C_m)\omega} + \frac{SS_1S_3}{2\pi j\frac{T_b}{F}(C_i-C_n)} e^{2\pi j\frac{T_b}{F}(2C_n+C_p-C_m-2C_l)\frac{1}{T_c}} e^{2\pi j\frac{T_b}{F}(2C_i-2C_n)\frac{1}{T_d}} e^{-2\pi j\frac{T_b}{F}C_n\omega}$$

$$(8)For \quad \frac{-2}{T_c} + \frac{-1}{T_d} < \frac{-2}{T_c} + \omega < \frac{1}{T_d}$$

$$X_{o3}(\omega,z) = E_3 \sum_{m=1}^{k}\sum_{n=1}^{k}\sum_{p=1}^{k}\sum_{i=1}^{k}\sum_{l=1}^{k} \frac{SS_1S_4}{2\pi j\frac{T_b}{F}(C_i+C_n-2C_p} e^{2\pi j\frac{T_b}{F}(5C_m-2C_i-3C_p+2C_n-2C_l)\frac{1}{T_c}}$$
$$\times e^{2\pi j\frac{T_b}{F}(C_i+C_n-2C_p)\frac{1}{T_d}} e^{-2\pi j\frac{T_b}{F}C_i\omega} + \frac{SS_1S_4}{2\pi j\frac{T_b}{F}(C_i-C_n)} e^{2\pi j\frac{T_b}{F}(2C_i-3C_p+5C_m-2C_n-2C_l)\frac{1}{T_c}} e^{2\pi j\frac{T_b}{F}(C_i-C_n)\frac{1}{T_d}}$$
$$\times e^{-2\pi j\frac{T_b}{F}(2C_n-C_i)\omega} + \frac{SS_2S_4}{2\pi j\frac{T_b}{F}(C_i+2C_p+C_n-4C_m)} e^{2\pi j\frac{T_b}{F}(2C_i-9C_m+3C_p+4C_n)\frac{1}{T_c}}$$
$$\times e^{2\pi j\frac{T_b}{F}(C_i+2C_p+C_n-4C_m)\frac{1}{T_d}} e^{-2\pi j\frac{T_b}{F}(8C_m-4C_p-2C_n-C_i)\omega} + \frac{SS_1S_3}{2\pi j\frac{T_b}{F}(C_i-C_n)} e^{2\pi j\frac{T_b}{F}(2C_i-C_m+C_p-2C_l)\frac{1}{T_c}}$$
$$\times e^{2\pi j\frac{T_b}{F}(C_i-C_n)\frac{1}{T_d}} e^{-2\pi j\frac{T_b}{F}(2C_n-C_i)\omega}$$

$$(9)For \quad \frac{-4}{T_c} + \frac{1}{T_d} < \omega < \frac{-2}{T_c} + \frac{-1}{T_d}$$

$$X_{o3}(\omega,z) = E_3 \sum_{m=1}^{k}\sum_{n=1}^{k}\sum_{p=1}^{k}\sum_{i=1}^{k}\sum_{l=1}^{k} \frac{SS_1S_4}{2\pi j\frac{T_b}{F}(C_i+C_n-2C_p)} e^{2\pi j\frac{T_b}{F}(5C_m-7C_p+4C_n-2C_l)\frac{1}{T_c}}$$
$$\times e^{2\pi j\frac{T_b}{F}(2C_i+2C_n-4C_p)\frac{1}{T_d}} e^{-2\pi j\frac{T_b}{F}(2C_p-C_n)\omega}$$

$$(10)For \quad \frac{-4}{T_c} + \frac{-1}{T_d} < \omega < \frac{-4}{T_c} + \frac{1}{T_d}$$

$$X_{o3}(\omega,z) = E_3 \sum_{m=1}^{k}\sum_{n=1}^{k}\sum_{p=1}^{k}\sum_{i=1}^{k}\sum_{l=1}^{k} \frac{SS_1S_4}{2\pi j\frac{T_b}{F}(C_n+C_i-2C_p)} e^{2\pi j\frac{T_b}{F}(5C_m+8C_n-15C_p+4C_i-2C_l)\frac{1}{T_c}}$$
$$\times e^{2\pi j\frac{T_b}{F}(C_n+C_i-2C_p)\frac{1}{T_d}} e^{-2\pi j\frac{T_b}{F}(4C_p-C_i-2C_n)\omega} \tag{D.21}$$

Appendix E

# Calculation of the Output Signal of a FWM Device in OCDMA Receivers: Mean and Variance of the Output Current

As we have seen, the received signal in OCDMA systems can be decomposed in two parts: the desired user's signal and the interference from other users. After through the FWM device (working as an AND gate) we obtain three signals: the desired's user signal, the signal due to multiuser interference, and noise due to FWM. In this appendix we obtain the components of the output signal separately. The results are used in section of (5.2.5).

## E.1 Calculation of the Mean of the Current in the Output of the Optical Detector

For the case of the main signal (the one associated with the desired user), we can expand the response of the detector by using Volterra series. By using (3.38) and the two first terms of Volterra series, we can obtain a good approximation of the output signal after the AND gate. We obtain:

$$A_o(\omega, z) = \iint H'_{o_{1,2}}(\omega_1, \omega_2, \omega - \omega_1 + \omega_2, z) A_p(\omega_1) A_s^*(\omega_2) A_p(\omega - \omega_1 + \omega_2) d\omega_1 d\omega_2 \tag{E.1}$$

where $A_p(\omega)$ and $A_s(\omega)$ are the Fourier transforms of the pump and input signals. If we suppose that these signals are Sinc-shaped, we obtain:

$A_p(\omega) = \frac{a_p}{2\Omega_p} \prod(\omega/\Omega_p)$

$A_s(\omega) = \frac{\sqrt{P_0}\tau_p}{2} b \prod(\omega\tau_p/2\pi)$

where b is the value of bit "0" or "1". By substituting in (E.1), $A_o(\omega, z)$ can be expressed as:

$$\begin{aligned} A_o(\omega,z) &= \left(\frac{a_p}{2\Omega_p}\right)^2 \frac{\sqrt{P_0}\tau_p}{2} b \int_{-\Omega_p}^{\Omega_p} \int_{max(-\frac{w}{2},-\Omega_p-\omega+\omega_1)}^{min(\frac{w}{2},\Omega_p-\omega+\omega_1)} H'_{o_{1,2}}(\omega_1,\omega_2,\omega-\omega_1+\omega_2,z) d\omega_1 d\omega_2 \\ &= 2j\gamma_{osp} e^{G_1(\omega)z} \frac{1-e^{-2\alpha z}}{2\alpha} \left(\frac{a_p}{2\Omega_p}\right)^2 \frac{\sqrt{P_0}\tau_p}{2} b \int_{-\Omega_p}^{\Omega_p} \int_{max(-\frac{w}{2},-\Omega_p-\omega+\omega_1)}^{min(\frac{w}{2},\Omega_p-\omega+\omega_1)} d\omega_1 d\omega_2 \end{aligned} \tag{E.2}$$

The mean current at the output of optical detector due to the desired user's signal, according to appendix A is:

$$\begin{aligned} E\{I|M\} =& \left(\frac{1}{2\pi}\right)^2 \iint e^{-j(\omega-\upsilon)t} \left[ A_o(\omega)A_o(\upsilon) + R_{A_o}(\omega,\upsilon) + R_{FWM}(\omega,\upsilon) \right] Sinc\left(\frac{(\omega-\upsilon)T}{2\pi}\right) d\omega d\upsilon \\ =& \gamma_{osp}^2 e^{-2\alpha z} \left(\frac{1-e^{-2\alpha z}}{2\alpha}\right)^2 \left(\frac{a_p}{2\Omega_p}\right)^4 \frac{P_0}{W^2} \left(\frac{1}{2\pi}\right)^2 b \\ & \times \iint e^{-j\beta_1(\omega-\upsilon)z} e^{-j\beta_1(\omega-\upsilon)t} \left[ \int_{-\Omega_p}^{\Omega_p} \int_{max(-\frac{w}{2},-\Omega_p-\omega+\omega_1)}^{min(\frac{w}{2},\Omega_p-\omega+\omega_1)} d\omega_1 d\omega_2 \right] \\ & \times \left[ \int_{-\Omega_p}^{\Omega_p} \int_{max(-\frac{w}{2},-\Omega_p-\omega+\omega_1')}^{min(\frac{w}{2},\Omega_p-\omega+\omega_1')} d\omega_1' d\omega_2' \right] Sinc\left(\frac{(\omega-\upsilon)T}{2\pi}\right) \\ & + \iint e^{-j(\omega-\upsilon)t} \left[ R_{A_o}(\omega,\upsilon) + R_{FWM}(\omega,\upsilon) \right] Sinc\left(\frac{(\omega-\upsilon)T}{2\pi}\right) d\omega d\upsilon \end{aligned} \tag{E.3}$$

where

$R_{A_o}(\omega,\upsilon) = E\{A_{MAI}(\omega)A_{MAI}^*(\upsilon)\}$, $R_{FWM}(\omega,\upsilon) = E\{A_{FWM}(\omega)A_{FWM}^*(\upsilon)\}$

Assuming that the time response of the optical detector, $T$, is much bigger than the received pulse time, $\tau_p$, we obtain:

$$\begin{aligned} E\{A_{MAI} =& \gamma_{osp}^2 e^{-2\alpha z} \left(\frac{1-e^{-2\alpha z}}{2\alpha}\right)^2 \left(\frac{a_p}{2\Omega_p}\right)^4 \frac{P_0}{W^2} \left(\frac{1}{2\pi}\right)^2 \frac{b}{T} \int \left[ \int_{-\Omega_p}^{\Omega_p} \int_{max(-\frac{w}{2},-\Omega_p-\omega+\omega_1)}^{min(\frac{w}{2},\Omega_p-\omega+\omega_1)} d\omega_1 d\omega_2 \right]^2 d\omega \\ & + \frac{2\pi}{T} \int \left[ R_{A_o}(\omega,\omega) + R_{FWM}(\omega,\omega) \right] d\omega \end{aligned} \tag{E.4}$$

## E.2 Calculation of the Variance of the Output Current of the Optical Detector due to the Interference Signal

We obtain the signal at output of the AND gate due to interference signal by two methods. In both methods we obtain the variance of the output current from the autocorrelation of the output. According to Appendix A,

$$\sigma^2_{MAI}(z) = T^2 \iint \iint [R_{A_o}(\omega_1, \upsilon_1, z) R_{A_o}(\omega_2, \upsilon_2, z) + R_{A_o}(\omega_1, \upsilon_2, z) R_{A_o}(\omega_2, \upsilon_1, z)] \\ Sinc\left(\frac{(\omega_1 - \upsilon_1)T}{2\pi}\right) Sinc\left(\frac{(\omega_2 - \upsilon_2)T}{2\pi}\right) d\omega_1 d\upsilon_1 d\omega_2 d\upsilon_2 \tag{E.5}$$

We assume that signals are stationary in the nonlinear environment for obtaining the autocorrelation function with the first method, but in the second method we obtain the autocorrelation function without this assumption.

### E.2.1 First Method: Assuming Signals are Stationary

In this method we assume that signals in the nonlinear environment are stationary. As shown in [88], signals due to interference users are stationary random processes. Therefore, obtaining the autocorrelation function at the output of the AND gate from the coupled equations (3.22), (3.23), (3.24) is a complex task. We use the Fourier transform of these equations.

We know that the signal due to multiuser interference after passing through the decoder can be expressed as:

$a_s(t,z) = a_{s_R}(t,z) + j a_{s_I}(t,z)$

where in $z = 0$ the two Gaussian process $a_{s_R}(t,z)$ and $a_{s_I}(t,z)$ are independent and with zero mean [89]. We assume that throughout the nonlinear environment, the signals are gaussian shape and zero mean. Then we can write $A_s(t,z)$ as follows:

$A_s(t,z) = A_{s_R}(t,z) + j A_{s_I}(t,z)$

where $A_{s_R}(t,z)$ and $A_{s_I}(t,z)$ are the Fourier transforms of $a_{s_R}(t,z)$ and $a_{s_I}(t,z)$. We know that the Fourier transform of a Gaussian function is also Gaussian, So both of them are Gaussian processes whose means are zero. We use the same assumption for the output signal of FWM, $A_o(t,z)$. Now we assume that passing throughout the nonlinear environment does not have any effect on the clock signal (pump) and its changes are only due to attenuation, dispersion and also from SPM (self phase modulation). Then, the equation of

the pump signal becomes:

$$\frac{\partial A_p(\omega,z)}{\partial z} = -\frac{\alpha_0(\omega)}{2}A_p(\omega,z) - j\Delta(\omega)A_p(\omega,z) + j2\gamma_{pp}\iint A_p(\omega_1,z)A_p^*(\omega_2,z)A_p(\omega-\omega_1+\omega_2,z)d\omega_1 d\omega_2 \tag{E.6}$$

At the beginning of the nonlinear environment for pump signal we have:

$$a_p(t,0) = a_p Sinc(\frac{t}{\tau_{pump}})A_p(\omega,0) = \frac{a_p}{2\Omega_p}\prod\left(\frac{\omega}{\Omega_p}\right) \tag{E.7}$$

where $A_p(\omega,0)$ is the Fourier transform of $a_p(t,0)$ , $\prod(x) = \{^{1}_{0} \quad ^{-1\le x\le 1}_{|x|>1}$ and $\Omega_p = \frac{2\pi}{\tau_{pump}}$. Then, the coupled equations (3.22), (3.23), (3.24)become:

$$\frac{\partial A_S(\omega,z)}{\partial z} = -\frac{\alpha_0(\omega)}{2}A_S(\omega,z) - j\Delta(\omega)A_S(\omega,z) + j\Big[\gamma_{ss}\iint A_S(\omega_1,z)A_S^*(\omega_2,z)A_S(\omega-\omega_1+\omega_2,z)d\omega_1 d\omega_2$$
$$+ 2\gamma_{so}\iint A_O(\omega_1,z)A_O^*(\omega_2,z)A_S(\omega-\omega_1+\omega_2,z)d\omega_1 d\omega_2 + 4\gamma_{sp}\iint A_P(\omega_1,z)A_P^*(\omega_2,z)A_S(\omega-\omega_1+\omega_2,z)d\omega_1 d\omega_2$$
$$+ 2\gamma_{sop}e^{-j\Delta kz}\iint A_O^*(\omega_2,z)A_P^*(\omega_1,z)A_P(\omega-\omega_1+\omega_2,z)d\omega_1 d\omega_2\Big] \tag{E.8}$$

$$\frac{\partial A_O(\omega,z)}{\partial z} = -\frac{\alpha_0(\omega)}{2}A_O(\omega,z) - j\Delta(\omega)A_O(\omega,z) + j\Big[\gamma_{oo}\iint A_O(\omega_1,z)A_O^*(\omega_2,z)A_O(\omega-\omega_1+\omega_2,z)d\omega_1 d\omega_2$$
$$+2\gamma_{os}\iint A_S(\omega_1,z)A_S^*(\omega_2,z)A_O(\omega-\omega_1+\omega_2,z)d\omega_1 d\omega_2+4\gamma_{op}\iint A_P(\omega_1,z)A_P^*(\omega_2,z)A_O(\omega-\omega_1+\omega_2,z)d\omega_1 d\omega_2$$
$$+ 2\gamma_{osp}e^{-j\Delta kz}\iint A_S^*(\omega_2,z)A_P^*(\omega_1,z)A_P(\omega-\omega_1+\omega_2,z)d\omega_1 d\omega_2\Big] \tag{E.9}$$

Now we can obtain the autocorrelation functions of $A_s(\omega,z)$, $A_o(\omega,z)$ from these equations. For this purpose we multiply equation (E.8) with $A_s^*(\upsilon,z)$, obtaining:

$$A_s^*(\upsilon,z)\frac{\partial A_S(\omega,z)}{\partial z} = -\frac{\alpha_0(\omega)}{2}A_s^*(\upsilon,z)A_S(\omega,z) - j\Delta(\omega)A_s^*(\upsilon,z)A_S(\omega,z) + j\Big[\gamma_{ss}\iint A_s^*(\upsilon,z)A_S(\omega_1,z)A_S^*(\omega_2,z)$$
$$\times A_S(\omega-\omega_1+\omega_2,z)d\omega_1 d\omega_2+2\gamma_{so}\iint A_O(\omega_1,z)A_O^*(\omega_2,z)A_s^*(\upsilon,z)A_S(\omega-\omega_1+\omega_2,z)d\omega_1 d\omega_2+4\gamma_{sp}\iint A_P(\omega_1,z)$$
$$\times A_P^*(\omega_2,z)A_s^*(\upsilon,z)A_S(\omega-\omega_1+\omega_2,z)d\omega_1 d\omega_2 + 2\gamma_{sop}e^{-j\Delta kz}\iint A_s^*(\upsilon,z)A_O^*(\omega_2,z)A_P^*(\omega_1,z)$$
$$\times A_P(\omega-\omega_1+\omega_2,z)d\omega_1 d\omega_2\Big] \tag{E.10}$$

In (E.10) we change $\omega$ to $\upsilon$ and multiply its complex conjugate with $A_s(\omega,z)$, obtaining:

$$A_S(\omega,z)\frac{\partial A_S^*(\omega,z)}{\partial z} = -\frac{\alpha_0^*(\omega)}{2}A_S^*(\omega,z)A_S(\omega,z) - j\Delta^*(\omega)A_S^*(\upsilon,z)A_S(\omega,z) - j\gamma_{ss}\iint A_S(\omega,z)A_S^*(\omega_1,z)$$
$$\times A_S^*(\omega_2,z)A_S^*(\upsilon-\omega_1+\omega_2,z)d\omega_1 d\omega_2 - 2j\gamma_{so}\iint A_O(\omega_2,z)A_O^*(\omega_1,z)A_S(\omega,z)A_S^*(\upsilon-\omega_1+\omega_2,z)d\omega_1 d\omega_2$$

$$- 4j\gamma_{sp}\iint A_P^*(\omega_1,z)A_P(\omega_2,z)A_S(\omega,z)A_S^*(\upsilon-\omega_1+\omega_2,z)d\omega_1 d\omega_2 - j2\gamma_{sop}e^{+j\Delta kz}\iint A_S(\omega,z)A_O(\omega_2,z)$$

$$\times A_P^*(\omega_1,z)A_P^*(\omega-\omega_1+\omega_2,z)d\omega_1 d\omega_2 \tag{E.11}$$

By adding equations (E.10) and (E.11) and applying statistical averages to them we obtain the following equation:

$$\frac{\partial R_{A_s}(\omega,\upsilon,z)}{\partial z} = -\frac{\alpha_0(\omega)+\alpha_0^*(\upsilon)}{2}R_{A_s}(\omega,\upsilon,z) - j(\Delta(\omega)-\Delta^*(\upsilon))R_{A_s}(\omega,\upsilon,z) + j2\gamma_{ss}\Bigg[\iint R_{A_s}(\omega_1,\upsilon,z)$$
$$\times R_{A_s}(\omega-\omega_1+\omega_2,\omega_2,z) + R_{A_s}(\omega_1,\omega_2,z)R_{A_s}(\omega-\omega_1+\omega_2,\upsilon,z) - R_{A_s}(\omega_2,\upsilon-\omega_1+\omega_2,z)R_{A_s}(\omega,\omega_2,z)$$
$$- R_{A_s}(\omega,\upsilon-\omega_1+\omega_2,z)R_{A_s}(\omega_2,\omega_1,z)]d\omega_1 d\omega_2\Bigg] + 2j\gamma_{so}\iint[R_{A_o}(\omega_1,\omega_2,z)R_{A_s}(\omega-\omega_1+\omega_2,\upsilon,z)$$
$$+ R_{A_oA_s}(\omega_1,\upsilon,z)R_{A_sA_o}(\omega-\omega_1+\omega_2,\omega_2,z) - R_{A_o}(\omega,\omega_1,z)R_{A_s}(\omega_2,\upsilon-\omega_1+\omega_2,z) - R_{A_oA_s}(\omega,\upsilon-\omega_1$$
$$+\omega_2,z)R_{A_sA_o}(\omega_2,\omega_1,z)]d\omega_1 d\omega_2 + 2j\gamma_{sp}\iint A_P(\omega_1,z)A_P^*(\omega_2,z)[R_{A_s}(\upsilon,\omega-\omega_1+\omega_2,z)$$
$$- R_{A_s}(\omega,\upsilon-\omega_1+\omega_2,z)]d\omega_1 d\omega_2 + j2\gamma_{sop}\iint A_P(\omega_1,z)A_P(\omega-\omega_1+\omega_2,z)e^{-j\Delta kz}E\{A_s^*(\upsilon,z)A_o^*(\omega_2,z)\}$$
$$- A_P^*(\omega_1,z)A_P^*(\omega-\omega_1+\omega_2,z)e^{+j\Delta kz}E\{A_s(\omega,z)A_o(\omega_2,z)\}d\omega_1 d\omega_2 \tag{E.12}$$

where

$R_{A_s}(\omega,\upsilon,z) = E\{A_s(\omega,z)A_s^*(\upsilon,z)\}$, $R_{A_o}(\omega,\upsilon,z) = E\{A_o(\omega,z)A_o^*(\upsilon,z)\}$, $R_{A_sA_o}(\omega,\upsilon,z) = E\{A_s(\omega,z)A_o^*(\upsilon,z)\}$, $R_{A_oA_s}(\omega,\upsilon,z) = E\{A_o(\omega,z)A_s^*(\upsilon,z)\}$.

We can simplify (E.12) by using: $E\{x_1x_2x_3^*x_4^*\} = E\{x_1x_3^*\}E\{x_2x_4^*\} + E\{x_1x_4^*\}E\{x_2x_3^*\}$

where $x_1$, $x_2$, $x_3$ and $x_4$ are complex Gaussian random variables with zero mean [90]. Similarly, we can express $R_{A_o}(\omega,\upsilon,z)$ as follows:

$$\frac{\partial R_{A_o}(\omega,\upsilon,z)}{\partial z} = -\frac{\alpha_0(\omega)+\alpha_0^*(\upsilon)}{2}R_{A_o}(\omega,\upsilon,z) - j(\Delta(\omega)-\Delta^*(\upsilon))R_{A_o}(\omega,\upsilon,z) + j\gamma_{oo}\Bigg[\iint R_{A_o}(\omega_1,\upsilon,z)$$
$$\times R_{A_o}(\omega-\omega_1+\omega_2,\omega_2,z) + R_{A_o}(\omega_1,\omega_2,z)R_{A_o}(\omega-\omega_1+\omega_2,\upsilon,z) - R_{A_o}(\omega_2,\upsilon-\omega_1+\omega_2,z)R_{A_o}(\omega,\omega_2,z)$$
$$- R_{A_o}(\omega,\upsilon-\omega_1+\omega_2,z)R_{A_o}(\omega_2,\omega_1,z)]d\omega_1 d\omega_2\Bigg] + 2j\gamma_{os}\iint\Bigg[R_{A_s}(\omega_1,\omega_2,z)R_{A_o}(\omega-\omega_1+\omega_2,\upsilon,z)$$
$$+ R_{A_sA_o}(\omega_1,\upsilon,z)R_{A_oA_s}(\omega-\omega_1+\omega_2,\omega_2,z) - R_{A_s}(\omega,\omega_1,z)R_{A_o}(\omega_2,\upsilon-\omega_1+\omega_2,z)$$
$$- R_{A_sA_o}(\omega,\upsilon-\omega_1+\omega_2,z)R_{A_oA_s}(\omega_2,\omega_1,z)\Bigg]d\omega_1 d\omega_2 + 2j\gamma_{op}\iint A_P(\omega_1,z)A_P^*(\omega_2,z)[R_{A_o}(\upsilon,\omega-\omega_1+\omega_2,z)$$
$$- R_{A_o}(\omega,\upsilon-\omega_1+\omega_2,z)]d\omega_1 d\omega_2 + j2\gamma_{osp}\iint A_P(\omega_1,z)A_P(\omega-\omega_1+\omega_2,z)e^{-j\Delta kz}E\{A_o^*(\upsilon,z)A_s^*(\omega_2,z)\}$$
$$- A_P^*(\omega_1,z)A_P^*(\omega-\omega_1+\omega_2,z)e^{+j\Delta kz}\times E\{A_o(\omega,z)A_s(\omega_2,z)\}d\omega_1 d\omega_2 \tag{E.13}$$

Now we assume that the interference signal is stationary throughout the nonlinear environment. Considering Appendix B, we use the following assumptions for solving equations (E.12) and (E.13):

$R_{A_s}(\omega,\upsilon,z) = F_s(\omega,z)\delta(\omega-\upsilon)$, $R_{A_o}(\omega,\upsilon,z) = F_o(\omega,z)\delta(\omega-\upsilon)$, $R_{A_sA_o}(\omega,\upsilon,z) = F_{so}(\omega,z)\delta(\omega-\upsilon)$, $R_{A_oA_s}(\omega,\upsilon,z) = F_{os}(\omega,z)\delta(\omega-\upsilon)$

Then, equations (E.12) and (E.13) become:

$$\begin{aligned}
&\delta(\omega-\upsilon)\tfrac{\partial F_s(\omega,z)}{\partial z} = -\tfrac{\alpha_0(\omega)+\alpha_0^*(\upsilon)}{2}\delta(\omega-\upsilon)F_s(\omega,z) - j(\Delta(\omega)-\Delta^*(\upsilon))\delta(\omega-\upsilon)F_s(\omega,z)\\
&+ j2\gamma_{ss}\Big[\iint \delta(\omega_1-\upsilon)F_s(\omega_1,z)\delta(\omega-\omega_1)F_s(\omega_2,z) + \delta(\omega_1-\omega_2)F_s(\omega_1,z)\delta(\omega-\omega_1+\omega_2-\upsilon)F_s(\upsilon,z)\\
&- \delta(\upsilon-\omega_1)F_s(\omega_2,z)\delta(\omega-\omega_1)F_s(\omega_1,z)\delta(\omega+\omega_1-\omega_2-\upsilon)F_s(\omega,z)\delta(\omega_1-\omega_2)F_s(\omega_1,z)d\omega_1 d\omega_2\Big]\\
&+ 2j\gamma_{so}\iint[\delta(\omega_1-\omega_2)F_o(\omega_1,z)\delta(\omega-\omega_1+\omega_2-\upsilon)F_s(\upsilon,z) + \delta(\omega_1-\upsilon)F_{os}(\omega_1,z)\delta(\omega-\omega_1)F_{so}(\omega_2,z)\\
&- \delta(\omega-\omega_1)F_o(\omega_1,z)\delta(\upsilon-\omega_1)F_s(\omega_2,z)\delta(\omega+\omega_1-\omega_2-\upsilon)F_{os}(\omega,z)\delta(\omega_1-\omega_2)F_{so}(\omega_1,z)]d\omega_1 d\omega_2\\
&+ 2j\gamma_{sp}\iint A_P(\omega_1,z)A_P^*(\omega_2,z)[\delta(\upsilon-\omega+\omega_1-\omega_2)F_s(\upsilon,z) - \delta(\omega-\upsilon+\omega_2-\omega_1)F_s(\omega,z)]d\omega_1 d\omega_2\\
&+ j2\gamma_{sop}\iint A_P(\omega_1,z)A_P(\omega-\omega_1+\omega_2,z)e^{-j\Delta kz}E\{A_s^*(\upsilon,z)A_o^*(\omega_2,z)\} - A_P^*(\omega_1,z)A_P^*(\omega-\omega_1+\omega_2,z)e^{+j\Delta kz}\\
&\times E\{A_s(\omega,z)A_o(\omega_2,z)\}d\omega_1 d\omega_2
\end{aligned} \tag{E.14}$$

$$\begin{aligned}
&\delta(\omega-\upsilon)\tfrac{\partial F_o(\omega,z)}{\partial z} = -\tfrac{\alpha_0(\omega)+\alpha_0^*(\upsilon)}{2}\delta(\omega-\upsilon)F_o(\omega,z) - j(\Delta(\omega)-\Delta^*(\upsilon))\delta(\omega-\upsilon)F_o(\omega,z)\\
&+ j2\gamma_{oo}\Big[\iint \delta(\omega_1-\upsilon)F_o(\omega_1,z)\delta(\omega-\omega_1)F_o(\omega_2,z) + \delta(\omega_1-\omega_2)F_o(\omega_1,z)\delta(\omega-\omega_1+\omega_2-\upsilon)F_o(\upsilon,z)\\
&- \delta(\upsilon-\omega_1)F_o(\omega_2,z)\delta(\omega-\omega_1)F_o(\omega_1,z)\delta(\omega+\omega_1-\omega_2-\upsilon)F_o(\omega,z)\delta(\omega_1-\omega_2)F_o(\omega_1,z)d\omega_1 d\omega_2\Big]\\
&+ 2j\gamma_{os}\iint[\delta(\omega_1-\omega_2)F_s(\omega_1,z)\delta(\omega-\omega_1+\omega_2-\upsilon)F_o(\upsilon,z) + \delta(\omega_1-\upsilon)F_{so}(\omega_1,z)\delta(\omega-\omega_1)F_{os}(\omega_2,z) -\\
&\delta(\omega-\omega_1)F_s(\omega_1,z)\delta(\upsilon-\omega_1)F_o(\omega_2,z)\delta(\omega+\omega_1-\omega_2-\upsilon)F_{so}(\omega,z)\delta(\omega_1-\omega_2)F_{os}(\omega_1,z)]d\omega_1 d\omega_2\\
&+ 2j\gamma_{op}\iint A_P(\omega_1,z)A_P^*(\omega_2,z)[\delta(\upsilon-\omega+\omega_1-\omega_2)F_o(\upsilon,z) - \delta(\omega-\upsilon+\omega_2-\omega_1)F_o(\omega,z)]d\omega_1 d\omega_2\\
&+ j2\gamma_{osp}\iint A_P(\omega_1,z)A_P(\omega-\omega_1+\omega_2,z)e^{-j\Delta kz}E\{A_o^*(\upsilon,z)A_s^*(\omega_2,z)\} - A_P^*(\omega_1,z)A_P^*(\omega-\omega_1+\omega_2,z)e^{+j\Delta kz}\\
&\times E\{A_o(\omega,z)A_s(\omega_2,z)\}d\omega_1 d\omega_2
\end{aligned} \tag{E.15}$$

Simplifying the two previous equations we obtain:

$$\delta(\omega-\upsilon)\frac{\partial F_s(\omega,z)}{\partial z} = -\frac{\alpha_0(\omega)+\alpha_0^*(\upsilon)}{2}\delta(\omega-\upsilon)F_s(\omega,z) - j(\Delta(\omega)-\Delta^*(\upsilon))\delta(\omega-\upsilon)F_s(\omega,z) + j2\gamma_{ss}\Big[\delta(\omega-\upsilon)$$
$$\times F_s(\omega,z)\int F_s(\omega_2,z)d\omega_2 + \delta(\omega-\upsilon)F_s(\upsilon,z)\int F_s(\omega_2,z)d\omega_2 - \delta(\omega-\upsilon)F_s(\omega,z)\int F_s(\omega_2,z)d\omega_2 - \delta(\omega-\upsilon)$$
$$\times F_s(\upsilon,z)\int F_s(\omega_2,z)d\omega_2\Big] + 2j\gamma_{so}\Big[\delta(\omega-\upsilon)F_s(\omega,z)\int F_o(\omega_2,z)d\omega_2 + \delta(\omega-\upsilon)F_{os}(\upsilon,z)\int F_{so}(\omega_2,z)d\omega_2$$
$$-\delta(\omega-\upsilon)F_o(\omega,z)\int F_s(\omega_2,z)d\omega_2 - \delta(\omega-\upsilon)F_{os}(\upsilon,z)\int F_{so}(\omega_2,z)d\omega_2\Big] + 2j\gamma_{sp}\int A_P(\omega_1,z)A_P^*(\upsilon-\omega+\omega_1,z)$$
$$\times[F_s(\upsilon,z)-F_s(\omega,z)]d\omega_1 \tag{E.16}$$

$$\delta(\omega-\upsilon)\frac{\partial F_o(\omega,z)}{\partial z} = -\frac{\alpha_0(\omega)+\alpha_0^*(\upsilon)}{2}\delta(\omega-\upsilon)F_o(\omega,z) - j(\Delta(\omega)-\Delta^*(\upsilon))\delta(\omega-\upsilon)F_o(\omega,z) + j2\gamma_{oo}\Big[\delta(\omega-\upsilon)$$
$$\times F_o(\omega,z)\int F_o(\omega_2,z)d\omega_2 + \delta(\omega-\upsilon)F_o(\upsilon,z)\int F_o(\omega_2,z)d\omega_2 - \delta(\omega-\upsilon)F_o(\omega,z)\int F_o(\omega_2,z)d\omega_2 - \delta(\omega-\upsilon)$$
$$\times F_o(\upsilon,z)\int F_o(\omega_2,z)d\omega_2\Big] + 2j\gamma_{os}\Big[\delta(\omega-\upsilon)F_o(\omega,z)\int F_s(\omega_2,z)d\omega_2 + \delta(\omega-\upsilon)F_{so}(\upsilon,z)\int F_{os}(\omega_2,z)d\omega_2$$
$$-\delta(\omega-\upsilon)F_s(\omega,z)\int F_o(\omega_2,z)d\omega_2 - \delta(\omega-\upsilon)F_{so}(\upsilon,z)\int F_{os}(\omega_2,z)d\omega_2\Big] + 2j\gamma_{op}\int A_P(\omega_1,z)A_P^*(\upsilon-\omega+\omega_1,z)$$
$$\times[F_o(\upsilon,z)-F_o(\omega,z)]d\omega_1 \tag{E.17}$$

Finally, we can rewrite (E.16) and (E.17) as follows:

$$\delta(\omega-\upsilon)\frac{\partial F_s(\omega,z)}{\partial z} = -\frac{\alpha_0(\omega)+\alpha_0^*(\upsilon)}{2}\delta(\omega-\upsilon)F_s(\omega,z) - j(\Delta(\omega)-\Delta^*(\upsilon))\delta(\omega-\upsilon)F_s(\omega,z) + 2j\gamma_{so}\Big[\delta(\omega-\upsilon)$$
$$\times F_s(\omega,z)\int F_o(\omega_2,z)d\omega_2 - \delta(\omega-\upsilon)F_o(\upsilon,z)\int F_s(\omega_2,z)d\omega_2 + 2j\gamma_{sp}[F_s(\upsilon,z)-F_s(\omega,z)]\Big]\int A_P(\omega_1,z)$$
$$\times A_P^*(\upsilon-\omega+\omega_1,z)d\omega_1 \tag{E.18}$$

$$\delta(\omega-\upsilon)\frac{\partial F_o(\omega,z)}{\partial z} = -\frac{\alpha_0(\omega)+\alpha_0^*(\upsilon)}{2}\delta(\omega-\upsilon)F_o(\omega,z) - j(\Delta(\omega)-\Delta^*(\upsilon))\delta(\omega-\upsilon)F_o(\omega,z) + 2j\gamma_{os}\Big[\delta(\omega-\upsilon)$$
$$\times F_o(\omega,z)\int F_s(\omega_2,z)d\omega_2 - \delta(\omega-\upsilon)F_s(\upsilon,z)\int F_o(\omega_2,z)d\omega_2 + 2j\gamma_{op}[F_o(\upsilon,z)-F_o(\omega,z)]\Big]\int A_P(\omega_1,z)$$
$$\times A_P^*(\upsilon-\omega+\omega_1,z)d\omega_1 \tag{E.19}$$

We observe that all terms except last term in equations (E.18) and (E.19) include the Dirac function in $\omega=\upsilon$ due to the assumption that signals are stationary. If this assumption holds, the last term should include

the Dirac function. None of the functions $A_P(\omega, z)$ and $F_o(\omega, z)$ include Dirac functions, and therefore these equations are not correct. In this method, as we show, assumption of stationarity of signals throughout the nonlinear environment is not correct, and the two last terms of equations (3.26) and (3.27)include the effect of the pump signal on the output signal. They are important in the FWM process but in fact, in final results do not have any effect. We conclude that the stationary assumption throughout the nonlinear environment is not correct and we should solve the nonlinear FWM equations without the stationary assumption.

### E.2.2 Second Method: Using Volterra Series

In this method we solve the equations without assumption the stationarity of the interference signal throughout the nonlinear media. First we express the output system by input signal using Volterra series. According to Appendix B we have:

$$
\begin{aligned}
&A_O(\omega,z) = \iint H'_{O_{1,2}}(\omega_1,\omega_2,\omega-\omega_1+\omega_2,z)A_p(\omega_1)A_s^*(\omega_2)A_p(\omega-\omega_1+\omega_2)d\omega_1 d\omega_2 \\
&+ \iint\iint H'_{O_{3,2}}(\omega_1,\omega_2,\omega_3,\omega_4,\omega-\omega_1+\omega_2-\omega_3+\omega_4,z)A_p(\omega_1)A_s^*(\omega_2)A_s(\omega_3)A_s^*(\omega_4) \\
&\times A_p(\omega-\omega_1+\omega_2-\omega_3+\omega_4)d\omega_1 d\omega_2 + \iint\iint H'_{O_{1,4}}(\omega_1,\omega_2,\omega_3,\omega_4,\omega-\omega_1+\omega_2-\omega_3+\omega_4,z)A_p(\omega_1)A_p^*(\omega_2) \\
&\times A_p(\omega_3)A_s^*(\omega_4)A_p(\omega-\omega_1+\omega_2-\omega_3+\omega_4)d\omega_1 d\omega_2 \qquad \text{(E.20)}
\end{aligned}
$$

Considering equation (E.20) we can express the autocorrelation function of $A_O(\omega, z)$ as follows:

$$
\begin{aligned}
&R_{A_o}(\omega,\upsilon,z) = E\{A_O(\omega,z)A_O^*(\upsilon,z)\} \\
&= \iint\iint H'_{O_{1,2}}(\omega_1,\omega_2,\omega-\omega_1+\omega_2,z)H'^*_{O_{1,2}}(\upsilon_1,\upsilon_2,\upsilon-\upsilon_1+\upsilon_2,z)A_p^*(\upsilon_1)A_p^*(\upsilon-\upsilon_1+\upsilon_2) \\
&\times A_p(\omega_1)A_p(\omega-\omega_1+\omega_2)E\Big\{A_s^*(\omega_2)A_s^*(\upsilon_2)\Big\}d\omega_1 d\omega_2 d\upsilon_1 d\upsilon_2
\end{aligned}
$$

$$
\begin{aligned}
&+ \int\ldots\int H'_{O_{3,2}}(\omega_1,\omega_2,\omega_3,\omega_4,\omega-\omega_1+\omega_2-\omega_3+\omega_4,z) \\
&\times H'^*_{O_{3,2}}(\upsilon_1,\upsilon_2,\upsilon_3,\upsilon_4,\upsilon-\upsilon_1+\upsilon_2-\upsilon_3+\upsilon_4,z)A_p^*(\upsilon_1) \\
&\times A_p^*(\upsilon-\upsilon_1+\upsilon_2-\upsilon_3+\upsilon_4)A_p(\omega_1)A_p(\omega-\omega_1+\omega_2-\omega_3+\omega_4) \\
&\times E\Big\{A_s^*(\omega_2)A_s(\omega_3)A_s^*(\omega_4)A_s(\upsilon_2)A_s^*(\upsilon_3)A_s(\upsilon_4)\Big\}d\omega_1\ldots d\omega_4 d\upsilon_1\ldots d\upsilon_4
\end{aligned}
$$

$$
\begin{aligned}
&+ \int\ldots\int H'_{O_{1,4}}(\omega_1,\omega_2,\omega_3,\omega_4,\omega-\omega_1+\omega_2-\omega_3+\omega_4,z) \\
&\times H'^*_{O_{1,4}}(\upsilon_1,\upsilon_2,\upsilon_3,\upsilon_4,\upsilon-\upsilon_1+\upsilon_2-\upsilon_3+\upsilon_4,z)A_p^*(\upsilon_1)A_p(\upsilon_2)A_p^*(\upsilon_3) \\
&\times A_p^*(\upsilon-\upsilon_1+\upsilon_2-\upsilon_3+\upsilon_4)A_p(\omega_1)A_p^*(\omega_2)A_p(\omega_3)A_p(\omega-\omega_1+\omega_2-\omega_3+\omega_4) \\
&\times E\Big\{A_s^*(\omega_4)A_s(\upsilon_4)\Big\}d\omega_1\ldots d\omega_4 d\upsilon_1\ldots d\upsilon_4
\end{aligned}
$$

$$
\begin{aligned}
&+\int\dots\int H'_{O_{1,2}}(\omega_1,\omega_2,\omega-\omega_1+\omega_2,z)H'^{*}_{O_{3,2}}(\upsilon_1,\upsilon_2,\upsilon_3,\upsilon_4,\upsilon-\upsilon_1+\upsilon_2-\upsilon_3+\upsilon_4,z)\\
&\times A_p(\omega_1)A_p(\omega-\omega_1+\omega_2)A^*_p(\upsilon_1)A^*_p(\upsilon-\upsilon_1+\upsilon_2-\upsilon_3+\upsilon_4)\\
&\times E\Big\{A^*_s(\omega_2)A_s(\upsilon_2)A^*_s(\upsilon_3)A_s(\upsilon_4)\Big\}d\omega_1 d\omega_2 d\upsilon_1\dots d\upsilon_4\\
&+\int\dots\int H'^{*}_{O_{1,2}}(\upsilon_1,\upsilon_2,\upsilon-\upsilon_1+\upsilon_2,z)H'_{O_{3,2}}(\omega_1,\omega_2,\omega_3,\omega_4,\omega-\omega_1+\omega_2-\omega_3+\omega_4,z)\\
&\times A^*_p(\upsilon_1)A^*_p(\upsilon-\upsilon_1+\upsilon_2)A_p(\omega_1)A_p(\omega-\omega_1+\omega_2-\omega_3+\omega_4)\\
&\times E\Big\{A^*_s(\upsilon_2)A_s(\omega_2)A^*_s(\omega_3)A_s(\omega_4)\Big\}d\omega_1 d\omega_2 d\upsilon_1\dots d\upsilon_4\\
&+\int\dots\int H'_{O_{1,2}}(\omega_1,\omega_2,\omega-\omega_1+\omega_2,z)H'^{*}_{O_{1,4}}(\upsilon_1,\upsilon_2,\upsilon_3,\upsilon_4,\upsilon-\upsilon_1+\upsilon_2-\upsilon_3+\upsilon_4,z)\\
&\times A_p(\omega_1)A_p(\omega-\omega_1+\omega_2)A^*_p(\upsilon_1)A_p(\upsilon_2)A^*_p(\upsilon_3)A^*_p(\upsilon-\upsilon_1+\upsilon_2-\upsilon_3+\upsilon_4)\\
&\times E\Big\{A^*_s(\omega_2)A_s(\upsilon_4)\Big\}d\omega_1 d\omega_2 d\upsilon_1\dots d\upsilon_4\\
&+\int\dots\int H'^{*}_{O_{1,2}}(\upsilon_1,\upsilon_2,\upsilon-\upsilon_1+\upsilon_2,z)H'_{O_{1,4}}(\omega_1,\omega_2,\omega_3,\omega_4,\omega-\omega_1+\omega_2-\omega_3+\omega_4,z)\\
&\times A^*_p(\upsilon_1)A^*_p(\upsilon-\upsilon_1+\upsilon_2)A_p(\omega_1)A^*_p(\omega_2)A_p(\omega_3)A_p(\omega-\omega_1+\omega_2-\omega_3+\omega_4)\\
&\times E\Big\{A^*_s(\upsilon_2)A_s(\omega_4)\Big\}d\omega_1 d\omega_2 d\upsilon_1\dots d\upsilon_4\\
&+\int\dots\int H'_{O_{3,2}}(\omega_1,\omega_2,\omega_3,\omega_4,\omega-\omega_1+\omega_2-\omega_3+\omega_4,z)\\
&\times H'^{*}_{O_{1,4}}(\upsilon_1,\upsilon_2,\upsilon_3,\upsilon_4,\upsilon-\upsilon_1+\upsilon_2-\upsilon_3+\upsilon_4,z)\\
&\times A_p(\omega_1)A_p(\omega-\omega_1+\omega_2-\omega_3+\omega_4)A^*_p(\upsilon_1)A_p(\upsilon_2)A^*_p(\upsilon_3)A^*_p(\upsilon-\upsilon_1+\upsilon_2-\upsilon_3+\upsilon_4)\\
&\times E\Big\{A_s(\omega_2)A^*_s(\omega_3)A_s(\omega_4)A_s(\upsilon_4)\Big\}d\omega_1\dots d\omega_4 d\upsilon_1\dots d\upsilon_4\\
&+\int\dots\int H'^{*}_{O_{3,2}}(\upsilon_1,\upsilon_2,\upsilon_3,\upsilon_4,\upsilon-\upsilon_1+\upsilon_2-\upsilon_3+\upsilon_4,z)\\
&\times H'_{O_{1,4}}(\omega_1,\omega_2,\omega_3,\omega_4,\omega-\omega_1+\omega_2-\omega_3+\omega_4,z)\\
&\times A^*_p(\upsilon_1)A^*_p(\upsilon-\upsilon_1+\upsilon_2-\upsilon_3+\upsilon_4)A_p(\omega_1)A^*_p(\omega_2)A_p(\omega_3)A_p(\omega-\omega_1+\omega_2-\omega_3+\omega_4)\\
&\times E\Big\{A^*_s(\upsilon_2)A_s(\upsilon_3)A^*_s(\upsilon_4)A_s(\omega_4)\Big\}d\omega_1\dots d\omega_4 d\upsilon_1\dots d\upsilon_4
\end{aligned}
\tag{E.21}
$$

According to [78], $A_s(\omega)$ is white noise, and therefore:

$$
E\Big\{A_s(\Omega_1)\dots A_s(\Omega_k)A^*_s(\Omega_{k+1})\dots A^*_s(\Omega_{k+l})\Big\}=\begin{cases}\sum_{i,j}\prod_{i\le k,j>k}E\Big\{A_s(\Omega_i)A^*_s(\Omega_j)\Big\} & k=l\\ 0 & k\neq l\end{cases}
\tag{E.22}
$$

Also we know the value of $E\Big\{A_s(\Omega_i)A^*_s(\Omega_j)\Big\}$, where $S_{a_s}(\Omega)=\sqrt{\frac{MP_0}{W^2N_0}}\prod(\tau_p\Omega)$. So (E.21) can be writ-

ten as follows:

$$R_{A_o}(\omega,\upsilon,z) = \iint\iint H'_{O_{1,2}}(\omega_1,\omega_2,\omega-\omega_1+\omega_2,z)H'^{*}_{O_{1,2}}(\upsilon_1,\upsilon_2,\upsilon-\upsilon_1+\upsilon_2,z)A^{*}_{p}(\upsilon_1)$$
$$\times A^{*}_{p}(\upsilon-\upsilon_1+\upsilon_2)A_p(\omega_1)A_p(\omega-\omega_1+\omega_2)E\Big\{A^{*}_{s}(\omega_2)A^{*}_{s}(\upsilon_2)\Big\}d\omega_1 d\omega_2 d\upsilon_1 d\upsilon_2$$

$$+\int\ldots\int H'_{O_{3,2}}(\omega_1,\omega_2,\omega_3,\omega_4,\omega-\omega_1+\omega_2-\omega_3+\omega_4,z)$$
$$\times H'^{*}_{O_{3,2}}(\upsilon_1,\upsilon_2,\upsilon_3,\upsilon_4,\upsilon-\upsilon_1+\upsilon_2-\upsilon_3+\upsilon_4,z)A^{*}_{p}(\upsilon_1)$$
$$\times A^{*}_{p}(\upsilon-\upsilon_1+\upsilon_2-\upsilon_3+\upsilon_4)A_p(\omega_1)A_p(\omega-\omega_1+\omega_2-\omega_3+\omega_4)$$
$$\times\Bigg[\Sigma E\Big\{A^{*}_{s}(\omega_{k_1})A_s(\omega_{k_2})\Big\}E\Big\{A^{*}_{s}(\omega_{k_3})A_s(\upsilon_{l_1})\Big\}E\Big\{A^{*}_{s}(\upsilon_{l_2})A_s(\upsilon_{l_3})\Big\}$$
$$+\sum E\Big\{A^{*}_{s}(\omega_{k_1})A_s(\upsilon_{l_1})\Big\}E\Big\{A^{*}_{s}(\upsilon_{l_2})A_s(\omega_{k_2})\Big\}E\Big\{A^{*}_{s}(\omega_{k_3})A_s(\upsilon_{l_3})\Big\}\Bigg]d\omega_1\ldots d\omega_4 d\upsilon_1\ldots d\upsilon_4$$

$$+\int\ldots\int H'_{O_{1,4}}(\omega_1,\omega_2,\omega_3,\omega_4,\omega-\omega_1+\omega_2-\omega_3+\omega_4,z)$$
$$\times H'^{*}_{O_{1,4}}(\upsilon_1,\upsilon_2,\upsilon_3,\upsilon_4,\upsilon-\upsilon_1+\upsilon_2-\upsilon_3+\upsilon_4,z)A^{*}_{p}(\upsilon_1)A_p(\upsilon_2)A^{*}_{p}(\upsilon_3)$$
$$\times A^{*}_{p}(\upsilon-\upsilon_1+\upsilon_2-\upsilon_3+\upsilon_4)A_p(\omega_1)A^{*}_{p}(\omega_2)A_p(\omega_3)A_p(\omega-\omega_1+\omega_2-\omega_3+\omega_4)$$
$$\times E\Big\{A^{*}_{s}(\omega_4)A_s(\upsilon_4)\Big\}d\omega_1\ldots d\omega_4 d\upsilon_1\ldots d\upsilon_4$$

$$+\int\ldots\int H'_{O_{1,2}}(\omega_1,\omega_2,\omega-\omega_1+\omega_2,z)H'^{*}_{O_{3,2}}(\upsilon_1,\upsilon_2,\upsilon_3,\upsilon_4,\upsilon-\upsilon_1+\upsilon_2-\upsilon_3+\upsilon_4,z)$$
$$\times A_p(\omega_1)A_p(\omega-\omega_1+\omega_2)A^{*}_{p}(\upsilon_1)A^{*}_{p}(\upsilon-\upsilon_1+\upsilon_2-\upsilon_3+\upsilon_4)$$
$$\times\Bigg[E\Big\{A^{*}_{s}(\omega_2)A_s(\upsilon_2)\Big\}E\Big\{A^{*}_{s}(\upsilon_3)A_s(\upsilon_4)\Big\}+E\Big\{A^{*}_{s}(\omega_2)A_s(\upsilon_4)\Big\}E\Big\{A^{*}_{s}(\upsilon_3)A_s(\upsilon_2)\Big\}\Bigg]d\omega_1 d\omega_2 d\upsilon_1\ldots d\upsilon_4$$

$$+\int\ldots\int H'^{*}_{O_{1,2}}(\upsilon_1,\upsilon_2,\upsilon-\upsilon_1+\upsilon_2,z)H'_{O_{3,2}}(\omega_1,\omega_2,\omega_3,\omega_4,\omega-\omega_1+\omega_2-\omega_3+\omega_4,z)$$
$$\times A^{*}_{p}(\upsilon_1)A^{*}_{p}(\upsilon-\upsilon_1+\upsilon_2)A_p(\omega_1)A_p(\omega-\omega_1+\omega_2-\omega_3+\omega_4)$$
$$\times\Bigg[E\Big\{A^{*}_{s}(\omega_2)A_s(\upsilon_2)\Big\}E\Big\{A^{*}_{s}(\omega_4)A_s(\omega_3)\Big\}+E\Big\{A^{*}_{s}(\omega_4)A_s(\upsilon_2)\Big\}E\Big\{A^{*}_{s}(\omega_2)A_s(\omega_3)\Big\}\Bigg]d\upsilon_1 d\upsilon_2 d\omega_1\ldots d\omega_4$$

$$+\int\ldots\int H'_{O_{1,2}}(\omega_1,\omega_2,\omega-\omega_1+\omega_2,z)H'^{*}_{O_{1,4}}(\upsilon_1,\upsilon_2,\upsilon_3,\upsilon_4,\upsilon-\upsilon_1+\upsilon_2-\upsilon_3+\upsilon_4,z)$$
$$\times A_p(\omega_1)A_p(\omega-\omega_1+\omega_2)A^{*}_{p}(\upsilon_1)A_p(\upsilon_2)A^{*}_{p}(\upsilon_3)A^{*}_{p}(\upsilon-\upsilon_1+\upsilon_2-\upsilon_3+\upsilon_4)$$
$$\times E\Big\{A^{*}_{s}(\omega_2)A_s(\upsilon_4)\Big\}d\omega_1 d\omega_2 d\upsilon_1\ldots d\upsilon_4$$

$$+\int\ldots\int H'^{*}_{O_{1,2}}(\upsilon_1,\upsilon_2,\upsilon-\upsilon_1+\upsilon_2,z)H'_{O_{1,4}}(\omega_1,\omega_2,\omega_3,\omega_4,\omega-\omega_1+\omega_2-\omega_3+\omega_4,z)$$
$$\times A^{*}_{p}(\upsilon_1)A^{*}_{p}(\upsilon-\upsilon_1+\upsilon_2)A_p(\omega_1)A^{*}_{p}(\omega_2)A_p(\omega_3)A_p(\omega-\omega_1+\omega_2-\omega_3+\omega_4)$$
$$\times E\Big\{A^{*}_{s}(\upsilon_2)A_s(\omega_4)\Big\}d\upsilon_1 d\upsilon_2 d\omega_1\ldots d\omega_4$$

$$
\begin{aligned}
&+\int\ldots\int H'_{O_{3,2}}(\omega_1,\omega_2,\omega_3,\omega_4,\omega-\omega_1+\omega_2-\omega_3+\omega_4,z)\\
&\times H'^{*}_{O_{1,4}}(\upsilon_1,\upsilon_2,\upsilon_3,\upsilon_4,\upsilon-\upsilon_1+\upsilon_2-\upsilon_3+\upsilon_4,z)\\
&\times A_p(\omega_1)A_p(\omega-\omega_1+\omega_2-\omega_3+\omega_4)A_p^*(\upsilon_1)A_p(\upsilon_2)A_p^*(\upsilon_3)A_p^*(\upsilon-\upsilon_1+\upsilon_2-\upsilon_3+\upsilon_4)\\
&\times E\Big\{A_s(\omega_2)A_s^*(\omega_3)A_s(\omega_4)A_s(\upsilon_4)\Big\}d\omega_1\ldots d\omega_4 d\upsilon_1\ldots d\upsilon_4\\
&+\int\ldots\int H'^{*}_{O_{3,2}}(\upsilon_1,\upsilon_2,\upsilon_3,\upsilon_4,\upsilon-\upsilon_1+\upsilon_2-\upsilon_3+\upsilon_4,z)\\
&\times H'_{O_{1,4}}(\omega_1,\omega_2,\omega_3,\omega_4,\omega-\omega_1+\omega_2-\omega_3+\omega_4,z)\\
&\times A_p^*(\upsilon_1)A_p^*(\upsilon-\upsilon_1+\upsilon_2-\upsilon_3+\upsilon_4)A_p(\omega_1)A_p^*(\omega_2)A_p(\omega_3)A_p(\omega-\omega_1+\omega_2-\omega_3+\omega_4)\\
&\times E\Big\{A_s^*(\upsilon_2)A_s(\upsilon_3)A_s^*(\upsilon_4)A_s(\omega_4)\Big\}d\omega_1\ldots d\omega_4 d\upsilon_1\ldots d\upsilon_4
\end{aligned}
\tag{E.23}
$$

Now we can simplify (E.23) according to Appendix B. For simplicity, we assume that the wave vector mismatch,$\Delta k=0$. Then, the first term of equation (E.23) becomes:

$$
\begin{aligned}
R_{A_{o_1}}(\omega,\upsilon,z)&=4\left(\frac{\gamma_{osp}}{2\alpha}\right)^2(1-e^{-2\alpha z})^2\iint\iint H'_{O_{1,2}}(\omega_1,\omega_2,\omega-\omega_1+\omega_2,z)H'^{*}_{O_{1,2}}(\upsilon_1,\upsilon_2,\upsilon-\upsilon_1+\upsilon_2,z)\\
&\times\sqrt{\frac{Mp_0}{W^2N_0}}\prod\left(\frac{2\omega_2}{W}\right)\delta(\omega_2-\upsilon_2)\left(\frac{a_p}{2\Omega_p}\right)^4\prod\left(\frac{\upsilon_1}{\Omega_p}\right)\prod\left(\frac{(\upsilon-\upsilon_1+\upsilon_2)}{\Omega_p}\right)\prod\left(\frac{\omega_1}{\Omega_p}\right)\\
&\times\prod\left(\frac{(\omega-\omega_1+\omega_2)}{\Omega_p}\right)d\omega_1 d\upsilon_1 d\omega_2
\end{aligned}
\tag{E.24}
$$

and we have:

$$
\begin{aligned}
R_{A_{o_1}}(\omega,\upsilon,z)&=4\left(\frac{\gamma_{osp}}{2\alpha}\right)^2(1-e^{-2\alpha z})^2\sqrt{\frac{Mp_0}{W^2N_0}}\left(\frac{a_p}{2\Omega_p}\right)^4\int_{-\frac{w}{2}}^{\frac{w}{2}}\int_{-\infty}^{\infty}\int_{-\infty}^{\infty}e^{G_1(\omega)z}e^{G_1^*(\upsilon)z}\left(\frac{1-e^{-2\alpha z}e^{j\beta_2(\omega_1-\omega)(\omega_2-\omega_1)z}}{2\alpha-j\beta_2(\omega_1-\omega)(\omega_2-\omega_1)}\right)\\
&\times\left(\frac{1-e^{-2\alpha z}e^{j\beta_2(\upsilon_1-\upsilon)(\upsilon_2-\upsilon_1)z}}{2\alpha-j\beta_2(\upsilon_1-\upsilon)(\upsilon_2-\upsilon_1)}\right)\prod\left(\frac{\upsilon_1}{\Omega_p}\right)\prod\left(\frac{(\upsilon-\upsilon_1+\omega_2)}{\Omega_p}\right)\prod\left(\frac{\omega_1}{\Omega_p}\right)\prod\left(\frac{(\omega-\omega_1+\omega_2)}{\Omega_p}\right)d\omega_1 d\upsilon_1 d\omega_2
\end{aligned}
\tag{E.25}
$$

After separating integrations regarding (E.25) to $\omega_1$ and $\upsilon_1$, we have:

$$R_{A_{o_1}}(\omega,\upsilon,z) = 4\left(\frac{\gamma_{osp}}{2\alpha}\right)^2(1-e^{-2\alpha z})^2\sqrt{\frac{Mp_0}{W^2N_0}}\left(\frac{a_p}{2\Omega_p}\right)^4 e^{-2\alpha z}e^{-j\beta_1(\omega-\upsilon)z}$$
$$\times\int_{-\frac{w}{2}}^{\frac{w}{2}}\left[\int_{-\infty}^{\infty}\left(\frac{1-e^{-2\alpha z}e^{j\beta_2(\omega_1-\omega)(\omega_2-\omega_1)z}}{2\alpha-j\beta_2(\omega_1-\omega)(\omega_2-\omega_1)}\right)\prod\left(\frac{\omega_1}{\Omega_p}\right)\prod\left(\frac{(\omega-\omega_1+\omega_2)}{\Omega_p}\right)d\omega_1\right]$$
$$\times\left[\int_{-\infty}^{\infty}\left(\frac{1-e^{-2\alpha z}e^{j\beta_2(\upsilon_1-\upsilon)(\upsilon_2-\upsilon_1)z}}{2\alpha-j\beta_2(\upsilon_1-\upsilon)(\upsilon_2-\upsilon_1)}\right)\prod\left(\frac{\upsilon_1}{\Omega_p}\right)\prod\left(\frac{(\upsilon-\upsilon_1+\omega_2)}{\Omega_p}\right)d\upsilon_1\right]d\omega_2 \tag{E.26}$$

We observe that the calculation of (E.26) is not simple, and also the calculation of the next terms of (E.23) according to the values for $H'_{O_{1,4}}$ and $H'_{O_{3,2}}$ found in Appendix B, are difficult. In order to simplify the calculation we assume that the value of dispersion is low, so we can say $\beta_1 \gg \beta_2$. Then, by substituting $\beta_2 = 0$, (E.26) become:

$$R_{A_{o_1}}(\omega,\upsilon,z) = 4\left(\frac{\gamma_{osp}}{2\alpha}\right)^2(1-e^{-2\alpha z})^2\sqrt{\frac{Mp_0}{W^2N_0}}\left(\frac{a_p}{2\Omega_p}\right)^4 e^{-2\alpha z}e^{-j\beta_1(\omega-\upsilon)z}$$
$$\times\int_{-\frac{w}{2}}^{\frac{w}{2}}\int_{-\infty}^{\infty}\int_{-\infty}^{\infty}\prod\left(\frac{\omega_1}{\Omega_p}\right)\prod\left(\frac{(\omega-\omega_1+\omega_2)}{\Omega_p}\right)\prod\left(\frac{\upsilon_1}{\Omega_p}\right)\prod\left(\frac{(\upsilon-\upsilon_1+\omega_2)}{\Omega_p}\right)d\omega_1 d\upsilon_1 d\omega_2 \tag{E.27}$$

Simplifying further we obtain:

$$R_{A_{o_1}}(\omega,\upsilon,z) = 4\left(\frac{\gamma_{osp}}{2\alpha}\right)^2(1-e^{-2\alpha z})^2\sqrt{\frac{Mp_0}{W^2N_0}}\left(\frac{a_p}{2\Omega_p}\right)^4 e^{-2\alpha z}e^{-j\beta_1(\omega-\upsilon)z}$$
$$\times\int_{max\{-\frac{w}{2},(-2\Omega_p-\omega),(-2\Omega_p-\upsilon)\}}^{min\{-\frac{w}{2},(2\Omega_p-\omega),(2\Omega_p-\upsilon)\}}(2\Omega_p-|\omega+\omega_2|)(2\Omega_p-|\upsilon+\omega_2|)d\omega_2 \tag{E.28}$$

We can simplify the terms of (E.23) in a similar way than the one used (E.28), so $R_{A_{o_2}}(\omega,\upsilon,z)$ becomes:

$$R_{A_{o_2}}(\omega,\upsilon,z) = 4\gamma_{osp}^2\left(\frac{\gamma_{ss}}{2\alpha}\left[\frac{(1-e^{-2\alpha z})}{2\alpha}-\frac{(1-e^{-4\alpha z})}{4\alpha}\right]+2\frac{\gamma_{os}}{2\alpha}\left[\frac{(1-e^{-2\alpha z})}{2\alpha}-\frac{(1-e^{-4\alpha z})}{4\alpha}\right]\right)^2$$
$$\times\int\cdots\int e^{G_1(\omega)z}e^{G_1^*(\upsilon)z}\left(\frac{Mp_0}{W^2N_0}\right)^{\frac{3}{2}}\Big[2\delta(\omega_2-\upsilon_2)\delta(\omega_3-\upsilon_3)+4\delta(\omega_2-\upsilon_3)\delta(\omega_2-\upsilon_3)\Big]\delta(\omega_4-\upsilon_4)$$
$$\times\prod\left(\frac{2\omega_2}{W}\right)\prod\left(\frac{2\upsilon_3}{W}\right)\prod\left(\frac{2\omega_4}{W}\right)\left(\frac{a_p}{2\Omega_p}\right)^4\prod\left(\frac{\omega_1}{\Omega_p}\right)\prod\left(\frac{\upsilon_1}{\Omega_p}\right)\prod\left(\frac{\omega-\omega_1+\omega_2-\omega_3+\omega_4}{\Omega_p}\right)$$
$$\times\prod\left(\frac{\upsilon-\upsilon_1+\upsilon_2-\upsilon_3+\upsilon_4}{\Omega_p}\right)d\omega_1 d\omega_2 d\omega_3 d\omega_4 d\upsilon_1 d\upsilon_2 d\upsilon_3 d\upsilon_4 \tag{E.29}$$

Simplifying further we obtain:

$$R_{A_{o_2}}(\omega,\upsilon,z)=8\gamma_{osp}^2\left(\frac{a_p}{2\Omega_p}\right)^4\left(\frac{Mp_0}{W^2N_0}\right)^{\frac{3}{2}}e^{-2\alpha z}e^{-j\beta_1(\omega-\upsilon)z}\left(\frac{\gamma_{ss}+2\gamma_{os}}{2\alpha}\left[\frac{(1-e^{-2\alpha z})}{2\alpha}-\frac{(1-e^{-4\alpha z})}{4\alpha}\right]\right)^2$$
$$\times\int\cdots\int\prod\left(\frac{2\omega_2}{W}\right)\prod\left(\frac{2\omega_3}{W}\right)\prod\left(\frac{2\omega_4}{W}\right)\prod\left(\frac{\omega_1}{\Omega_p}\right)\prod\left(\frac{\upsilon_1}{\Omega_p}\right)\prod\left(\frac{\omega-\omega_1+\omega_2-\omega_3+\omega_4}{\Omega_p}\right)$$
$$\times\prod\left(\frac{\upsilon-\upsilon_1+\upsilon_2-\upsilon_3+\upsilon_4}{\Omega_p}\right)d\omega_1d\omega_2d\omega_3d\omega_4d\upsilon_1+16\gamma_{osp}^2\left(\frac{a_p}{2\Omega_p}\right)^4\left(\frac{Mp_0}{W^2N_0}\right)^{\frac{3}{2}}e^{-2\alpha z}e^{-j\beta_1(\omega-\upsilon)z}$$
$$\times\left(\frac{\gamma_{ss}+2\gamma_{os}}{2\alpha}\left[\frac{(1-e^{-2\alpha z})}{2\alpha}-\frac{(1-e^{-4\alpha z})}{4\alpha}\right]\right)^2\int\cdots\int\prod\left(\frac{2\omega_2}{W}\right)\prod\left(\frac{2\upsilon_2}{W}\right)\prod\left(\frac{2\omega_4}{W}\right)\prod\left(\frac{\omega_1}{\Omega_p}\right)\prod\left(\frac{\upsilon_1}{\Omega_p}\right)$$
$$\times\prod\left(\frac{\omega-\omega_1+\omega_4}{\Omega_p}\right)\prod\left(\frac{\upsilon-\upsilon_1+\upsilon_4}{\Omega_p}\right)d\omega_1d\omega_2d\upsilon_2d\omega_4d\upsilon_1 \tag{E.30}$$

By changing the variation $\xi=\omega_2-\omega_3+\omega_4$ in the first term of (E.30) we obtain:

$$R_{A_{o_2}}(\omega,\upsilon,z)=8\gamma_{osp}^2\left(\frac{a_p}{2\Omega_p}\right)^4\left(\frac{Mp_0}{W^2N_0}\right)^{\frac{3}{2}}e^{-2\alpha z}e^{-j\beta_1(\omega-\upsilon)z}\left(\frac{\gamma_{ss}+2\gamma_{os}}{2\alpha}\left[\frac{(1-e^{-2\alpha z})}{2\alpha}-\frac{(1-e^{-4\alpha z})}{4\alpha}\right]\right)^2$$
$$\times\int_{-2\Omega_p-min\{\omega,\upsilon\}}^{2\Omega_p-max\{\omega,\upsilon\}}R(\xi)(2\Omega_p-|\omega+\xi|)(2\Omega_p-|\upsilon+\xi|)d\xi+16\gamma_{osp}^2\left(\frac{a_p}{2\Omega_p}\right)^4\left(\frac{Mp_0}{W^2N_0}\right)^{\frac{3}{2}}e^{-2\alpha z}e^{-j\beta_1(\omega-\upsilon)z}$$
$$\left(\frac{\gamma_{ss}+2\gamma_{os}}{2\alpha}\left[\frac{(1-e^{-2\alpha z})}{2\alpha}-\frac{(1-e^{-4\alpha z})}{4\alpha}\right]\right)^2W^2\int_{-2\Omega_p-min\{\omega,\upsilon\}}^{2\Omega_p-max\{\omega,\upsilon\}}\prod\left(\frac{2\omega_4}{W}\right)(2\Omega_p-|\omega+\omega_4|)(2\Omega_p-|\upsilon+\omega_4|)d\omega_4 \tag{E.31}$$

where $R(\xi)=\begin{cases}\frac{1}{2}\left(\frac{3W}{2}-|\xi|\right)^2 & \frac{W}{2}<|\xi|<\frac{3W}{2}\\ \\ \frac{W}{2}\left(\frac{3W}{2}-|\xi|\right) & |\xi|<\frac{W}{2}\end{cases}$ and combining with (E.31) we obtain:

$$R_{A_{o_2}}(\omega,\upsilon,z)=\left(\frac{\gamma_{osp}}{8\alpha^2}(\gamma_{ss}+2\gamma_{os})\right)^2\left(\frac{a_p}{2\Omega_p}\right)^4\left(\frac{Mp_0}{W^2N_0}\right)^{\frac{3}{2}}e^{-2\alpha z}e^{-j\beta_1(\omega-\upsilon)z}(1-e^{-2\alpha z})^4$$
$$\times\int_{-2\Omega_p-min\{\omega,\upsilon\}}^{2\Omega_p-max\{\omega,\upsilon\}}R^{'}(\xi)(2\Omega_p-|\omega+\xi|)(2\Omega_p-|\upsilon+\xi|)d\xi \tag{E.32}$$

where $R^{'}(\xi)=\begin{cases}\frac{1}{2}\left(\frac{3W}{2}-|\xi|\right)^2 & \frac{W}{2}<|\xi|<\frac{3W}{2}\\ \\ \frac{W}{2}\left(\frac{3W}{2}-|\xi|\right)+2W^2 & |\xi|<\frac{W}{2}\end{cases}$. For the third term of (E.23) we obtain:

$$R_{A_{o_3}}(\omega,\upsilon,z)=8\gamma_{osp}^2\left(\frac{\gamma_{sp}}{2\alpha}\left[\frac{(1-e^{-2\alpha z})}{2\alpha}-\frac{(1-e^{-4\alpha z})}{4\alpha}\right]+2\frac{\gamma_{op}}{2\alpha}\left[\frac{(1-e^{-2\alpha z})}{2\alpha}-\frac{(1-e^{-4\alpha z})}{4\alpha}\right]\right)^2$$
$$\times\int\dots\int e^{G_1(\omega)z}e^{G_1^*(\upsilon)z}\left(\frac{a_p}{2\Omega_p}\right)^4\prod\left(\frac{\omega_1}{\Omega_p}\right)\prod\left(\frac{\omega_2}{\Omega_p}\right)\prod\left(\frac{\omega_3}{\Omega_p}\right)\prod\left(\frac{\upsilon_1}{\Omega_p}\right)\prod\left(\frac{\upsilon_2}{\Omega_p}\right)\prod\left(\frac{\upsilon_3}{\Omega_p}\right)$$
$$\times\prod\left(\frac{\omega-\omega_1+\omega_2-\omega_3+\omega_4}{\Omega_p}\right)\prod\left(\frac{\upsilon-\upsilon_1+\upsilon_2-\upsilon_3+\upsilon_4}{\Omega_p}\right)$$
$$\times\left(\frac{Mp_0}{W^2N_0}\right)^{\frac{1}{2}}\delta(\omega_4-\upsilon_4)\prod\left(\frac{2\omega_4}{\Omega_p}\right)d\omega_1d\omega_2d\omega_3d\omega_4d\upsilon_1d\upsilon_2d\upsilon_3d\upsilon_4 \tag{E.33}$$

Simplifying further, we obtain:

$$R_{A_{o_3}}(\omega,\upsilon,z)=8\gamma_{osp}^2\left(\frac{a_p}{2\Omega_p}\right)^8\left(\frac{Mp_0}{W^2N_0}\right)^{\frac{1}{2}}e^{-2\alpha z}e^{-j\beta_1(\omega-\upsilon)z}\left(\frac{\gamma_{sp}+\gamma_{op}}{2\alpha}\left[\frac{(1-e^{-2\alpha z})}{2\alpha}-\frac{(1-e^{-4\alpha z})}{4\alpha}\right]\right)^2$$
$$\times\int\dots\int(2\Omega_p-|\omega+\omega_2-\omega_3+\omega_4|)(2\Omega_p-|\upsilon+\upsilon_2-\upsilon_3+\omega_4|)\prod\left(\frac{\omega_2}{\Omega_p}\right)\prod\left(\frac{\omega_3}{\Omega_p}\right)\prod\left(\frac{\upsilon_2}{\Omega_p}\right)\prod\left(\frac{\upsilon_3}{\Omega_p}\right)$$
$$\times\prod\left(\frac{2\omega_4}{\Omega_p}\right)d\omega_2d\omega_3d\omega_4d\upsilon_2d\upsilon_3 \tag{E.34}$$

By substituting to two variables $\varphi=\omega_2-\omega_3$ and $\phi=\upsilon_2-\upsilon_3$ in (E.34) we have:

$$R_{A_{o_3}}(\omega,\upsilon,z)=8\gamma_{osp}^2\left(\frac{a_p}{2\Omega_p}\right)^8\left(\frac{Mp_0}{W^2N_0}\right)^{\frac{1}{2}}e^{-2\alpha z}e^{-j\beta_1(\omega-\upsilon)z}\left(\frac{\gamma_{sp}+\gamma_{op}}{2\alpha}\left[\frac{(1-e^{-2\alpha z})}{2\alpha}-\frac{(1-e^{-4\alpha z})}{4\alpha}\right]\right)^2$$
$$\times\iiint(2\Omega_p-|\omega+\varphi+\omega_4|)(2\Omega_p-|\upsilon+\phi+\omega_4|)(2\Omega_p-|\varphi|)(2\Omega_p-\phi|)\prod\left(\frac{2\omega_4}{\Omega_p}\right)d\varphi d\omega_4d\phi \tag{E.35}$$

By separating the two integrations with respect of variables $\varphi$ and $\phi$ we obtain:

$$R_{A_{o_3}}(\omega,\upsilon,z)=\left(\frac{\gamma_{osp}}{8\alpha^2}(\gamma_{sp}+2\gamma_{op})\right)^2\left(\frac{a_p}{2\Omega_p}\right)^8\left(\frac{Mp_0}{W^2N_0}\right)^{\frac{1}{2}}e^{-2\alpha z}e^{-j\beta_1(\omega-\upsilon)z}(1-e^{-2\alpha z})^4$$
$$\times\int\left[\int_{-2\Omega_p-min\{0,\omega+\omega_4\}}^{2\Omega_p-max\{0,\omega+\omega_4\}}(2\Omega_p-|\omega+\varphi+\omega_4|)(2\Omega_p-|\varphi|)d\varphi\right]$$
$$\times\left[\int_{-2\Omega_p-min\{0,\upsilon+\omega_4\}}^{2\Omega_p-max\{0,\upsilon+\omega_4\}}(2\Omega_p-|\upsilon+\phi+\omega_4|)(2\Omega_p-|\phi|)d\phi\right]\prod\left(\frac{2\omega_4}{\Omega_p}\right)d\omega_4 \tag{E.36}$$

By simplifying further in (E.36) we obtain:

$$R_{A_{o_3}}(\omega,\upsilon,z)=\left(\frac{\gamma_{osp}}{8\alpha^2}(\gamma_{sp}+2\gamma_{op})\right)^2\left(\frac{a_p}{2\Omega_p}\right)^8\left(\frac{Mp_0}{W^2N_0}\right)^{\frac{1}{2}}e^{-2\alpha z}e^{-j\beta_1(\omega-\upsilon)z}(1-e^{-2\alpha z})^4$$
$$\times\int_{-4\Omega_p-min\{\omega,\upsilon\}}^{4\Omega_p-max\{\omega,\upsilon\}}\left(2\Omega_p-|\frac{\omega+\omega_4}{2}|\right)^2\left(2\Omega_p-|\frac{\upsilon+\omega_4}{2}|\right)^2\prod\left(\frac{2\omega_4}{\Omega_p}\right)d\omega_4 \tag{E.37}$$

Now by simplifying fourth term of (E.23), we can write $R_{A_{o_4}}(\omega,\upsilon,z)$ as follows:

$$R_{A_{o_4}}(\omega,\upsilon,z)=j4\gamma_{osp}^2\frac{(1-e^{-2\alpha z})}{2\alpha}\left(\frac{(\gamma_{ss}+2\gamma_{os})}{2\alpha}\left[\frac{(1-e^{-2\alpha z})}{2\alpha}-\frac{(1-e^{-4\alpha z})}{4\alpha}\right]\right)$$
$$\times\int\dots\int e^{G_1(\omega)z}e^{G_1^*(\upsilon)z}\left(\frac{Mp_0}{W^2N_0}\right)2\delta(\omega_2-\upsilon_2)\delta(\omega_3-\omega_4)\prod\left(\frac{2\omega_2}{W}\right)\prod\left(\frac{2\omega_3}{W}\right)\left(\frac{a_p}{2\Omega_p}\right)^4\prod\left(\frac{\omega_1}{\Omega_p}\right)$$
$$\prod\left(\frac{\upsilon_1}{\Omega_p}\right)\prod\left(\frac{\upsilon-\upsilon_1+\upsilon_2}{\Omega_p}\right)\prod\left(\frac{\omega-\omega_1+\omega_2-\omega_3+\omega_4}{\Omega_p}\right)d\omega_1\dots d\omega_4 d\upsilon_1 d\upsilon_2 \tag{E.38}$$

By sieving property of the Dirac function and integrating with respect to $\omega_4$ and $\upsilon_2$ we have:

$$R_{A_{o_4}}(\omega,\upsilon,z)=j4\gamma_{osp}^2\left(\frac{Mp_0}{W^2N_0}\right)\left(\frac{a_p}{2\Omega_p}\right)^4e^{-2\alpha z}e^{-\beta_1(\omega-\upsilon)z}\frac{(1-e^{-2\alpha z})}{2\alpha}\left(\frac{(\gamma_{ss}+2\gamma_{os})}{2\alpha}\left[\frac{(1-e^{-2\alpha z})}{2\alpha}-\frac{(1-e^{-4\alpha z})}{4\alpha}\right]\right)$$
$$\times\int\dots\int\prod\left(\frac{2\omega_2}{W}\right)\prod\left(\frac{2\omega_3}{W}\right)\prod\left(\frac{\omega_1}{\Omega_p}\right)\prod\left(\frac{\upsilon_1}{\Omega_p}\right)\prod\left(\frac{\upsilon-\upsilon_1+\omega_2}{\Omega_p}\right)\prod\left(\frac{\omega-\omega_1+\omega_2}{\Omega_p}\right)d\omega_1 d\omega_2 d\omega_3 d\upsilon_1 \tag{E.39}$$

Where by integrating with respect to $\omega_3$ we have:

$$R_{A_{o_4}}(\omega,\upsilon,z)=j\frac{\gamma_{osp}^2}{4\alpha^3}(\gamma_{ss}+\gamma_{os})\left(\frac{Mp_0}{W^2N_0}\right)\left(\frac{a_p}{2\Omega_p}\right)^4(1-e^{-2\alpha z})^3e^{-2\alpha z}e^{-\beta_1(\omega-\upsilon)z}$$
$$\times W\iiint\prod\left(\frac{2\omega_2}{W}\right)\prod\left(\frac{\omega_1}{\Omega_p}\right)\prod\left(\frac{\upsilon_1}{\Omega_p}\right)\prod\left(\frac{\upsilon-\upsilon_1+\omega_2}{\Omega_p}\right)\prod\left(\frac{\omega-\omega_1+\omega_2}{\Omega_p}\right)d\omega_1 d\omega_2 d\upsilon_1 \tag{E.40}$$

By calculating the integral and simplifying further we obtain:

$$R_{A_{o_4}}(\omega,\upsilon,z)=j\frac{\gamma_{osp}^2}{4\alpha^3}(\gamma_{ss}+\gamma_{os})\left(\frac{Mp_0}{WN_0}\right)\left(\frac{a_p}{2\Omega_p}\right)^4(1-e^{-2\alpha z})^3e^{-2\alpha z}e^{-\beta_1(\omega-\upsilon)z}$$
$$\int_{max\{-\frac{w}{2},(-2\Omega_p-\omega),(-2\Omega_p-\upsilon)\}}^{min\{-\frac{w}{2},(2\Omega_p-\omega),(2\Omega_p-\upsilon)\}}(2\Omega_p-|\omega+\omega_2|)(2\Omega_p-|\upsilon+\omega_2|)d\omega_2 \tag{E.41}$$

Regarding the fifth term, using a similar approach to that used for the fourth term, we can write:

$$R_{A_{o_5}}(\omega,\upsilon,z) = -j\frac{\gamma_{osp}^2}{4\alpha^3}(\gamma_{ss}+\gamma_{os})\left(\frac{Mp_0}{WN_0}\right)\left(\frac{a_p}{2\Omega_p}\right)^4(1-e^{-2\alpha z})^3e^{-2\alpha z}e^{-\beta_1(\omega-\upsilon)z}$$
$$\int_{max\{-\frac{w}{2},(-2\Omega_p-\omega),(-2\Omega_p-\upsilon)\}}^{min\{-\frac{w}{2},(2\Omega_p-\omega),(2\Omega_p-\upsilon)\}}(2\Omega_p-|\omega+\omega_2|)(2\Omega_p-|\upsilon+\omega_2|)d\omega_2 \tag{E.42}$$

We observe that the fifth and fourth terms cancel mutually. Similarly $R_{A_{o_6}}(\omega,\upsilon,z)$ and $R_{A_{o_7}}(\omega,\upsilon,z)$ are inverses of each other. Furthermore the eighth term of (E.23) can be simplified as follows:

$$R_{A_{o_8}}(\omega,\upsilon,z) = 16(\gamma_{osp})^2\left(\frac{(\gamma_{ss}+2\gamma_{os})}{2\alpha}\left[\frac{(1-e^{-2\alpha z})}{2\alpha}-\frac{(1-e^{-4\alpha z})}{4\alpha}\right]\right)\left(\frac{(\gamma_{sp}+\gamma_{op})}{2\alpha}\left[\frac{(1-e^{-2\alpha z})}{2\alpha}\right.\right.$$
$$\left.\left.-\frac{(1-e^{-4\alpha z})}{4\alpha}\right]\right)\int\dots\int e^{G_1(\omega)z}e^{G_1^*(\upsilon)z}\left(\frac{Mp_0}{W^2N_0}\right)\prod\left(\frac{2\omega_2}{W}\right)\prod\left(\frac{2\omega_4}{W}\right)\delta(\omega_2-\omega_3)\delta(\omega_4-\upsilon_4)$$
$$\times\left(\frac{a_p}{2\Omega_p}\right)^6\prod\left(\frac{\omega_1}{\Omega_p}\right)\prod\left(\frac{\upsilon_1}{\Omega_p}\right)\prod\left(\frac{\upsilon_2}{\Omega_p}\right)\prod\left(\frac{\upsilon_3}{\Omega_p}\right)\prod\left(\frac{\omega-\omega_1+\omega_2-\omega_3+\omega_4}{\Omega_p}\right)$$
$$\prod\left(\frac{\upsilon-\upsilon_1+\upsilon_2-\upsilon_3+\upsilon_4}{\Omega_p}\right)d\omega_1\dots d\omega_4 d\upsilon_1\dots d\upsilon_4 \tag{E.43}$$

By changing variables $\omega^{'}=\omega_1-\omega_2$ and $\upsilon^{'}=\upsilon_1-\upsilon_2$ we have:

$$R_{A_{o_8}}(\omega,\upsilon,z) = (\frac{\gamma_{osp}}{2\alpha^2})^2(\gamma_{ss}+2\gamma_{os})(\gamma_{sp}+\gamma_{op})\left(\frac{a_p}{2\Omega_p}\right)^6\left(\frac{Mp_0}{W^2N_0}\right)(1-e^{-2\alpha z})^2e^{-2\alpha z}e^{-\beta_1(\omega-\upsilon)z}$$
$$\times\int\dots\int\prod\left(\frac{2\omega_2}{W}\right)\prod\left(\frac{2\omega_4}{W}\right)\prod\left(\frac{\omega_1}{\Omega_p}\right)\prod\left(\frac{\upsilon_1}{\Omega_p}\right)\prod\left(\frac{\upsilon_2}{\Omega_p}\right)\prod\left(\frac{\upsilon_3}{\Omega_p}\right)\prod\left(\frac{\omega-\omega_1+\omega_4}{\Omega_p}\right)$$
$$\prod\left(\frac{\upsilon-\upsilon_1+\upsilon_2-\upsilon_3+\upsilon_4}{\Omega_p}\right)d\omega_1 d\omega_2 d\omega_4 d\upsilon_1 d\upsilon_2 d\upsilon_3 \tag{E.44}$$

By changing variable $\xi=\upsilon_1-\upsilon_2+\upsilon_3$ in (E.44), $R_{A_{o_8}}(\omega,\upsilon,z)$ becomes:

$$R_{A_{o_8}}(\omega,\upsilon,z) = (\frac{\gamma_{osp}}{2\alpha^2})^2(\gamma_{ss}+2\gamma_{os})(\gamma_{sp}+\gamma_{op})\left(\frac{a_p}{2\Omega_p}\right)^6\left(\frac{Mp_0}{W^2N_0}\right)(1-e^{-2\alpha z})^2e^{-2\alpha z}e^{-j\beta_1(\omega-\upsilon)z}$$
$$\times W\iint\prod\left(\frac{2\omega_4}{W}\right)R(\xi)(2\Omega_p-|\omega+\omega_4|)\prod\left(\frac{\upsilon-\xi+omega_4}{\Omega_p}\right)d\omega_4 d\xi \tag{E.45}$$

We solve the integral in (E.45) as follows:

$$R_{A_{o_8}}(\omega,\upsilon,z)=(\frac{\gamma_{osp}}{2\alpha^2})^2(\gamma_{ss}+2\gamma_{os})(\gamma_{sp}+\gamma_{op})\left(\frac{a_p}{2\Omega_p}\right)^6\left(\frac{Mp_0}{WN_0}\right)(1-e^{-2\alpha z})^2e^{-2\alpha z}e^{-\beta_1(\omega-\upsilon)z}$$
$$\times\int\prod\left(\frac{2\omega_4}{W}\right)(2\Omega_p-|\omega+\omega_4|)\int_{-\Omega_p-(\upsilon+\omega_4)}^{\Omega_p-(\upsilon+\omega_4)}R(\xi)d\xi d\omega_4 \tag{E.46}$$

The last term of (E.23) is similar to $R_{A_{o_8}}(\omega,\upsilon,z)$ , so we have:

$$R_{A_{o_9}}(\omega,\upsilon,z)=(\frac{\gamma_{osp}}{2\alpha^2})^2(\gamma_{ss}+2\gamma_{os})(\gamma_{sp}+\gamma_{op})\left(\frac{a_p}{2\Omega_p}\right)^6\left(\frac{Mp_0}{WN_0}\right)(1-e^{-2\alpha z})^2e^{-2\alpha z}e^{-\beta_1(\omega-\upsilon)z}$$
$$\times\int\prod\left(\frac{2\omega_4}{W}\right)(2\Omega_p-|\omega+\omega_4|)\int_{-\Omega_p-(\upsilon+\omega_4)}^{\Omega_p-(\upsilon+\omega_4)}R(\xi)d\xi d\omega_4 \tag{E.47}$$

Finally we obtain:

$$R_{A_o}(\omega,\upsilon,z)=R_{A_{o_1}}(\omega,\upsilon,z)+R_{A_{o_2}}(\omega,\upsilon,z)+\ldots+R_{A_{o_9}}(\omega,\upsilon,z) \tag{E.48}$$

Using (E.4) we can calculate the variance of the output signal. Since $R_{A_{o_1}}(\omega,\upsilon,z)$ is very big compared to the other terms, we can approximate $R_{A_o}(\omega,\upsilon,z)=R_{A_{o_1}}(\omega,\upsilon,z)$. Then, we obtain:

$$\sigma^2_{MAI,M}(z)=\left(\frac{1}{2\pi}\right)^4\iint\iint[R_{A_{o_1}}(\omega_a,\upsilon_b,z)R_{A_{o_1}}(\omega_b,\upsilon_a,z)]$$
$$\times Sinc\left(\frac{(\omega_a-\upsilon_a)T}{2\pi}\right)Sinc\left(\frac{(\omega_b-\upsilon_b)T}{2\pi}\right)d\omega_a d\upsilon_a d\omega_b d\upsilon_b \tag{E.49}$$

Now the value of the variance due to (E.23) can be calculated using (E.49):

$$\sigma^2_{MAI,M}(z)=\left[4\left(\frac{\gamma_{osp}}{2\alpha}\right)^2(1-e^{-2\alpha z})^2\sqrt{\frac{Mp_0}{W^2N_0}}\left(\frac{a_p}{2\Omega_p}\right)^4e^{-2\alpha z}\left(\frac{1}{2\pi}\right)^2\right]^2$$
$$\times\int_{-\frac{w}{2}}^{-\frac{w}{2}}\int_{-\frac{w}{2}}^{-\frac{w}{2}}\left[\iint\iint e^{-j\beta_1(\omega_a-\upsilon_a)z}e^{-j\beta_1(\omega_b-\upsilon_b)z}(2\Omega_p-|\omega_a+\omega_2|)(2\Omega_p-|\upsilon_b+\omega_2|)\right.$$
$$\left.\times(2\Omega_p-|\omega_b+\omega_2^{'}|)(2\Omega_p-|\upsilon_a+\omega_2^{'}|)Sinc\left(\frac{(\omega_a-\upsilon_a)T}{2\pi}\right)Sinc\left(\frac{(\omega_b-\upsilon_b)T}{2\pi}\right)d\omega_a d\upsilon_a d\omega_b d\upsilon_b\right]d\omega_2 d\omega_2^{'} \tag{E.50}$$

By separating the integrals we have:

$$\sigma^2_{MAI,M}(z) = \left[4\left(\frac{\gamma_{osp}}{2\alpha}\right)^2(1-e^{-2\alpha z})^2\sqrt{\frac{Mp_0}{W^2N_0}}\left(\frac{a_p}{2\Omega_p}\right)^4 e^{-2\alpha z}\left(\frac{1}{2\pi}\right)^2\right]^2$$
$$\times\left[\int_{-\frac{w}{2}}^{-\frac{w}{2}}\int_{-\frac{w}{2}}^{-\frac{w}{2}}\left[\iint e^{-j\beta_1(\omega_a-\upsilon_a)z}(2\Omega_p-|\omega_a+\omega_2|)(2\Omega_p-|\upsilon_a+\omega_2^{'}|)Sinc\left(\frac{(\omega_a-\upsilon_a)T}{2\pi}\right)d\omega_a d\upsilon_a\right]\right.$$
$$\left.\times\left[\iint e^{-j\beta_1(\omega_b-\upsilon_b)z}(2\Omega_p-|\upsilon_b+\omega_2|)(2\Omega_p-|\omega_b+\omega_2^{'}|)Sinc\left(\frac{(\omega_b-\upsilon_b)T}{2\pi}\right)d\omega_b d\upsilon_b\right]d\omega_2 d\omega_2^{'}\right] \quad \text{(E.51)}$$

Since the two first integrals are equal and the two second integrals are complex conjugated, we can write:

$$\sigma^2_{MAI,M}(z) = \left[4\left(\frac{\gamma_{osp}}{2\alpha}\right)^2(1-e^{-2\alpha z})^2\sqrt{\frac{Mp_0}{W^2N_0}}\left(\frac{a_p}{2\Omega_p}\right)^4 e^{-2\alpha z}\left(\frac{1}{2\pi}\right)^2\right]^2\left[\int_{-\frac{w}{2}}^{-\frac{w}{2}}\int_{-\frac{w}{2}}^{-\frac{w}{2}}\left|\iint e^{-j\beta_1(\omega_a-\upsilon_a)z}\right.\right.$$
$$\left.\left.\times(2\Omega_p-|\omega_a+\omega_2|)(2\Omega_p-|\upsilon_a+\omega_2^{'}|)Sinc\left(\frac{(\omega_a-\upsilon_a)T}{2\pi}\right)d\omega_a d\upsilon_a\right|^2 d\omega_2 d\omega_2^{'}\right] \quad \text{(E.52)}$$

By changing variable $u=\omega_a-\upsilon_a$ we obtain:

$$\sigma^2_{MAI,M}(z) = \left[4\left(\frac{\gamma_{osp}}{2\alpha}\right)^2(1-e^{-2\alpha z})^2\sqrt{\frac{Mp_0}{W^2N_0}}\left(\frac{a_p}{2\Omega_p}\right)^4 e^{-2\alpha z}\left(\frac{1}{2\pi}\right)^2\right]^2$$
$$\times\left[\int_{-\frac{w}{2}}^{-\frac{w}{2}}\int_{-\frac{w}{2}}^{-\frac{w}{2}}\left|\iint e^{-j\beta_1 uz}(2\Omega_p-|u+\upsilon_a+\omega_2|)(2\Omega_p-|\upsilon_a+\omega_2^{'}|)Sinc\left(\frac{uT}{2\pi}\right)d\omega_a d\upsilon_a\right|^2 d\omega_2 d\omega_2^{'}\right] \quad \text{(E.53)}$$

We can rewrite (E.53) as

$$\sigma^2_{MAI,M}(z) = \left[4\left(\frac{\gamma_{osp}}{2\alpha}\right)^2(1-e^{-2\alpha z})^2\sqrt{\frac{Mp_0}{W^2N_0}}\left(\frac{a_p}{2\Omega_p}\right)^4 e^{-2\alpha z}\left(\frac{1}{2\pi}\right)^2\right]^2$$
$$\times\left[\int_{-\frac{w}{2}}^{-\frac{w}{2}}\int_{-\frac{w}{2}}^{-\frac{w}{2}}\left|\int e^{-j\beta_1 uz}\left(\int(2\Omega_p-|u+\upsilon_a+\omega_2|)(2\Omega_p-|\upsilon_a+\omega_2^{'}|)d\upsilon_a\right)Sinc\left(\frac{uT}{2\pi}\right)du\right|^2 d\omega_2 d\omega_2^{'}\right] \quad \text{(E.54)}$$

By integrating with respect to $\upsilon_a$ we obtain following integral:

$$\sigma^2_{MAI,M}(z) = \left[4\left(\frac{\gamma_{osp}}{2\alpha}\right)^2(1-e^{-2\alpha z})^2\sqrt{\frac{Mp_0}{W^2N_0}}\left(\frac{a_p}{2\Omega_p}\right)^4 e^{-2\alpha z}\left(\frac{1}{2\pi}\right)^2\right]^2$$
$$\times\left[\int_{-\frac{w}{2}}^{-\frac{w}{2}}\int_{-\frac{w}{2}}^{-\frac{w}{2}}\left|\int e^{-j\beta_1 uz}\left(2\Omega_p-\frac{|u+\omega_2-\omega_2^{'}|}{2}\right)^2 Sinc\left(\frac{uT}{2\pi}\right)du\right|^2 d\omega_2 d\omega_2^{'}\right] \tag{E.55}$$

By integrating with respect to $\omega_2$ in the first term and substituting $x=\omega_2-\omega_2^{'}$ in the second term we obtain:

$$\sigma^2_{MAI,M}(z) = \left[4\left(\frac{\gamma_{osp}}{2\alpha}\right)^2(1-e^{-2\alpha z})^2\sqrt{\frac{Mp_0}{W^2N_0}}\left(\frac{a_p}{2\Omega_p}\right)^4 e^{-2\alpha z}\left(\frac{1}{2\pi}\right)^2\right]^2$$
$$\times\left[\int_{-w}^{w}(W-|x|)\left|\int e^{-j\beta_1 uz}\left(2\Omega_p-\frac{|u+x|}{2}\right)^2 Sinc\left(\frac{uT}{2\pi}\right)du\right|^2 dx\right] \tag{E.56}$$

We can (E.56) rewrite as follows:

$$\sigma^2_{MAI,M}(z) = \left[4\left(\frac{\gamma_{osp}}{2\alpha}\right)^2(1-e^{-2\alpha z})^2\sqrt{\frac{Mp_0}{W^2N_0}}\left(\frac{a_p}{2\Omega_p}\right)^4 e^{-2\alpha z}\left(\frac{1}{2\pi}\right)^2\right]^2\left[\int_{-w}^{w}\frac{2(W-|x|)}{T}\left[\int\frac{\cos(\beta_1 uz)\sin(uT/2)}{u}\right.\right.$$
$$\left.\left.\times\left(2\Omega_p-\frac{|u+x|}{2}\right)^2 du\right]^2 dx+\int_{-w}^{w}\frac{2(W-|x|)}{T}\left[\int\frac{\sin(\beta_1 uz)\sin(uT/2)}{u}\left(2\Omega_p-\frac{|u+x|}{2}\right)^2 du\right]^2 dx\right] \tag{E.57}$$

If we assume that $T\gg\tau_p$ we obtain:

$$\sigma^2_{MAI,M}(z) = 2\left[\left(\frac{\gamma_{osp}}{\alpha}\right)^2(1-e^{-2\alpha z})^2\sqrt{\frac{Mp_0}{W^2N_0}}\left(\frac{a_p}{2\Omega_p}\right)^4 e^{-2\alpha z}\left(\frac{1}{2\pi}\right)^2\frac{1}{T}\right]^2\left[\int_0^w(W-x)\left(2\Omega_p-\frac{x}{2}\right)^4 dx\right] \tag{E.58}$$

## E.3 Calculation of the Noise due to FWM

The spectral density of FWM, $\rho_{N,C}$ can be obtained as follows [91]:

$$\rho_{N,C} = \sum_{j=s,p,c} \tilde{\eta}_{c,j} \rho_{ASE}(\omega_j) \tag{E.59}$$

where $\rho_{ASE}$ is the power spectral density of the amplified spontaneous emission noise. In other words we have:

$\tilde{\eta}_{c,s} = \frac{\eta_{FWM}}{G_s}$, $\tilde{\eta}_{c,p} = \frac{\eta_{FWM}}{G_p}\frac{P_s(0)}{P_p(0)}$, $\tilde{\eta}_{c,s} = 1$ where $\eta_{FWM}$ is the FWM gain, which can be calculated employing the ratio between the output power signal and the input power signal. We assume that $\tilde{\eta}_{c,p}$ and $\tilde{\eta}_{c,s}$ are much smaller than one, and we can neglect them. Then we obtain:

$$\rho_{N,C} = \rho_{ASE}(2\omega_p, z) \tag{E.60}$$

We can express the amplified spontaneous emission as follows [92]:

$$\rho_{ASE}(\omega, z) = \hbar\omega (b_g z)^{a_g} \left[ a_{sp} \Gamma(-a_g, b_g z_0, b_g z) + \frac{b_{sp}}{b_g} \Gamma(1 - a_g, b_g z_0, b_g z) \right] \tag{E.61}$$

where $a_g(\lambda) = a_2(\lambda - \lambda_p)^2 + a_2(\lambda - \lambda_p) + 1$, $b_g(\lambda) = b_2(\lambda - \lambda_p)^2 + b_2(\lambda - \lambda_p)$ and the values of $a_{sp}$ and $b_{sp}$ are related to parameter $a_g$ and $b_g$ as follows:

$a_{sp} = a_g \left[ 1 - \frac{exp(\hbar\omega - \Delta\bar{\varepsilon}_f)}{k_B T} \right]^{-1}$, $b_{sp} = a_{sp} \left[ \frac{b_g}{a_g} - \left( 1 - \frac{a_{sp}}{a_g} \right) \frac{\hbar\omega - \Delta\bar{\varepsilon}_f}{k_B T} \right]$

where $k_B$ is the Boltzmann constant ($k_B = 1.38 \times 10^{-23}$), T is the absolute temperature and $\Delta\bar{\varepsilon}_f$ denotes the difference of the quasi-Fermi levels. Also $\Gamma(a, x_1, x_2)$ denotes the incomplete Gamma function, which is defined as:

$\Gamma(a, x_1, x_2) = \int_{x_1}^{x_2} x^{a-1} exp(-x) dx$

In (E.60), $z_0$ is equal to zero. Considering Appendix C, the autocorrelation of the ASE noise in FWM becomes:

$$R_{FWM}(\omega - \upsilon, z) = \rho_{ASE}(\omega, z)\delta(\omega - \upsilon) \tag{E.62}$$

## E.4 Calculation of the Variance of the Output Current in the Optical Detector and Error Probability

According to the results obtained in sections (E.2), (E.3) and (A.10), the variance of the output of the detector is:

$$\sigma^2_{I,M,b}(z) = \sigma^2_{MAI,M}(z) + \left(\frac{1}{2\pi}\right)^4 \iint\iint \rho_{ASE}(\omega_1,z)\delta(\omega_1-\upsilon_2)\rho_{ASE}(\omega_2,z)\delta(\omega_2-\upsilon_1)$$
$$\times Sinc\left(\frac{(\omega_1-\upsilon_1)T}{2\pi}\right)Sinc\left(\frac{(\omega_2-\upsilon_2)T}{2\pi}\right)d\omega_1 d\upsilon_1 d\omega_2 d\upsilon_2 + 2\left(\frac{1}{2\pi}\right)^4 \iint\iint R_{A_o}(\omega_1,\upsilon_2,z)\rho_{ASE}(\omega_2,z)\delta(\omega_2-\upsilon_1)$$
$$\times Sinc\left(\frac{(\omega_1-\upsilon_1)T}{2\pi}\right)Sinc\left(\frac{(\omega_2-\upsilon_2)T}{2\pi}\right)d\omega_1 d\upsilon_1 d\omega_2 d\upsilon_2 + 2\left(\frac{1}{2\pi}\right)^4 \iint\iint R_{A_o}(\omega_1,\upsilon_2,z)A_o(\omega_2)A_o^*(\upsilon_1)$$
$$\times Sinc\left(\frac{(\omega_1-\upsilon_1)T}{2\pi}\right)Sinc\left(\frac{(\omega_2-\upsilon_2)T}{2\pi}\right)d\omega_1 d\upsilon_1 d\omega_2 d\upsilon_2 + 2\left(\frac{1}{2\pi}\right)^4 \iint\iint \rho_{ASE}(\omega_1,z)\delta(\omega_1-\upsilon_2)A_o(\omega_2)A_o^*(\upsilon_1)$$
$$\times Sinc\left(\frac{(\omega_1-\upsilon_1)T}{2\pi}\right)Sinc\left(\frac{(\omega_2-\upsilon_2)T}{2\pi}\right)d\omega_1 \tag{E.63}$$

By simplifying further, we obtain:

$$\sigma^2_{I,M,b}(z) = \sigma^2_{MAI,M}(z) + \left(\frac{1}{2\pi}\right)^4 \iint\iint \rho_{ASE}(\omega_1,z)\rho_{ASE}(\omega_2,z)Sinc\left(\frac{(\omega_1-\omega_2)T}{2\pi}\right)d\omega_1 d\omega_2$$
$$+ 2\left(\frac{1}{2\pi}\right)^4 4\left(\frac{\gamma_{osp}}{2\alpha}\right)^2(1-e^{-2\alpha z})^2\sqrt{\frac{Mp_0}{W^2N_0}}\left(\frac{a_p}{2\Omega_p}\right)^4 e^{-2\alpha z}\int\left[\int_{-\frac{W}{2}}^{\frac{W}{2}}\left|\int e^{-j\beta_1\omega_1 z}(2\Omega_p-|\omega_1+x|)\right.\right.$$
$$\left.\left.\times Sinc\left(\frac{(\omega_1-\omega_2)T}{2\pi}\right)d\omega_1\right|^2 dx\right]\rho_{ASE}(\omega_2,z)d\omega_2 + 8b\left(\frac{1}{2\pi}\right)^4\left(\frac{\gamma_{osp}}{2\alpha}\right)^2(1-e^{-2\alpha z})^2\sqrt{\frac{Mp_0}{W^2N_0}}\left(\frac{a_p}{2\Omega_p}\right)^4 e^{-2\alpha z}$$
$$\times\int_{-\frac{W}{2}}^{\frac{W}{2}}\left|\iint e^{-j\beta_1\omega_1 z}(2\Omega_p-|\omega_1+x|)A_o^*(\upsilon_1)Sinc\left(\frac{(\omega_1-\upsilon_1)T}{2\pi}\right)d\omega_1 d\upsilon_1\right|^2 dx$$
$$+ 2b\left(\frac{1}{2\pi}\right)^4\int\rho_{ASE}(\omega_1,z)\left|\int A_o(\omega_2)Sinc\left(\frac{(\omega_2-\omega_1)T}{2\pi}\right)d\omega_2\right|^2 d\omega_1 \tag{E.64}$$

Assuming that the response time of optical detector, $T$, is bigger than the duration of the received pulse, $\tau_p$, we can simplify (E.64) as follows:

$$\sigma^2_{I,M,b}(z) = \sigma^2_{MAI,M}(z) + \left(\frac{1}{2\pi}\right)^3 \frac{1}{T}\left[\int \rho_{ASE}(\omega_1, z)d\omega_1\right]^2 + 8\left(\frac{1}{2\pi}\right)^2 \frac{1}{T^2}\left(\frac{\gamma_{osp}}{2\alpha}\right)^2 (1-e^{-2\alpha z})^2$$
$$\times \sqrt{\frac{Mp_0}{W^2N_0}}\left(\frac{a_p}{2\Omega_p}\right)^4 e^{-2\alpha z}\int\left[\int_{max\{-\frac{W}{2},-2\Omega_p-\omega_2\}}^{min\{\frac{W}{2},2\Omega_p-\omega_2\}} (2\Omega_p - |\omega_2+x|)^2 dx\right]\rho_{ASE}(\omega_2,z)d\omega_2 + 8b\left(\frac{1}{2\pi}\right)^2$$
$$\times \frac{1}{T^2}\left(\frac{\gamma_{osp}}{2\alpha}\right)^2 (1-e^{-2\alpha z})^2 \sqrt{\frac{Mp_0}{W^2N_0}}\left(\frac{a_p}{2\Omega_p}\right)^4 e^{-2\alpha z}\int_{-\frac{W}{2}}^{\frac{W}{2}}\left|\int e^{-j\beta_1\omega_1 z}(2\Omega_p - |\omega_1+x|)A^*_o(\omega_1)d\omega_1\right|^2 dx$$
$$+ 2b\left(\frac{1}{2\pi}\right)^2 \frac{1}{T^2}\int \rho_{ASE}(\omega_1,z)\left|A_o(\omega_1)\right|^2 d\omega_1 \tag{E.65}$$

Finally, the error probability is:

$$P(Error) = \sum_{l=1}^{M}\binom{M}{l}\left(\frac{1}{2k}\right)^l\left(1-\frac{1}{2k}\right)^{M-l}$$
$$\times \frac{1}{2}\left[Q\left(\frac{Th - E\{I_0|m\}}{\sigma^2_{I,M,0}(z)}\right) + Q\left(\frac{E\{I_1|m\} - Th}{\sigma^2_{I,M,1}(z)}\right)\right] \tag{E.66}$$

# Bibliography


[1] T.Miki, "The potential of photonic networks," *IEEE Comm. Magazine,*, vol. 32, no. 12, Dec. 1994.

[2] S. Hamilton. and B. Robinson., "100 Gbit/s synchronous all-optical time-division multiplexing multi-access network testbed," *J. Lightw. Tech.*, vol. 20, no. 12, Dec. 2002.

[3] I. Kang and M. Yan, "Simple setup for simultaneous optical clock recovery and ultra-short sampling pulse generation," *Elec. Lett.*, vol. 38, no. 20, pp. 1199–1201, Sep. 2002.

[4] J. Salehi, "Code division multiple-access techniques in optical fiber networks-part I: Fundamental principles," *IEEE Trans. On Comm*, vol. 37, no. 8, Aug. 1989.

[5] I. E. Mansouri, J. Fatome, C. Finot, M. Lintz, and S. Pitois, "All-fibered high-quality stable 20- and 40-GHz picosecond pulse generators for 160-Gb/s OTDM applications," *Photonics Technology Letters*, vol. 23, no. 20, Oct. 2011.

[6] J. Turkiewicz and et al, "160 Gb/s OTDM networking using deployed fiber," *IEEE J. of Lightwave Technology*, vol. 23, no. 1, pp. 225–235, Jan 2005.

[7] H. Dutton, *Understanding Optical Communications, First Edition*. IBM, Sep. 1998.

[8] M. Nakazawa, "Solitons for breaking barriers to terabit/second WDM and OTDM transmission in the next millennium," *IEEE J. on Selected Topics In Quantum Electronics*, vol. 6, no. 6, Dec. 2000.

[9] F. M. Abbou, *Optical Transmission and Networks for Next Generation Internet Traffic Highways*. IGI Global, 2014.

[10] ITU-T, *Spectral grids for WDM applications: DWDM frequency grid*. Recomendation ITU-T G.694.1, 2012 Feb.

[11] H. Yin and D. Richardson, *Optical code division multiple access communication networks*. chap, 2008.

[12] L. Couch, "Modern communication systems principles and applications," *Prentice Hall*, Jan. 1994.

[13] J. Salehi and C. Brackett, "Code division multiple-access techniques in optical fiber networks-part II: Systems performance analysis," *IEEE Trans. On Comm*, vol. 37, no. 8, Aug. 1989.

[14] P. Prucnal, M. Santoro, and T. Fan, "Spread spectrum fiber-optic local area network using optical processing," *J. Lightwave Technol*, vol. 4, no. 5, pp. 547–554, May. 1986.

[15] W. Kwong, P. Perrier, and P. Prucnal, "Performance comparison of asynchronous and synchronous code-division multiple-access techniques for fiberoptic local area networks," *IEEE Trans. Commun*, vol. 39, no. 11, Nov. 1991.

[16] T. Miyazawa, "Multirate spectral phase-encoded time-spreading O-CDMA system using orthogonal variable spreading factor code sequences," *Photonics Technology Letters*, vol. 19, no. 19, Oct. 2007.

[17] P. R. Prucnal, *Optical code division multiple access: fundamentals and applications.* CRC Press, 2006.

[18] D. Zaccarin and M. Kavehrad, "An optical CDMA system based on spectral encoding of LED," *IEEE Photon. Technol. Lett*, vol. 5, no. 4, April. 1993.

[19] E. Park, A. Mendez, and E. Garmire, "Temporal/spatial optical CDMA networks: Design, demonstration, and comparison with temporal networks," *IEEE Photonics Technology Letters*, vol. 4, no. 10, Oct. 1992.

[20] L. Galdino, J. Maranhao, M. Furtado, E. Moschim, L. Bonani, and F. Durand, "Impact of MAI on the performance of WDM/OCDM OBS networks using 2D wavelength-hopping and time spreading optical codes," *Sarnoff Symposium*, May. 2011.

[21] P. R. Prucnal, M. A. Santoro, and T. R. Fan., "Spread spectrum fiber-optic local area network using optical processing." *Journal of Lightwave Technology.*, vol. 4, no. 5, May. 1986.

[22] J. Zhang and G. Picchi., "Tunable prime code encoder/decoder for all-optical CDMA applications." *Elect. Letters.*, vol. 29, no. 13, June. 1993.

[23] E. Ip, P. Ji, E. Mateo, Y.-K. Huang, L. Xu, D. Qian, N. Bai, and T. Wang, "100G and beyond transmission technologies for evolving optical networks and relevant physical-layer issues," *Proceedings of the IEEE.*, vol. 100, no. 5, May 2012.

[24] J. Sokoloff., P. Prucnal, I. Glesk, and M. Kane., "A terahertz optical asymmetric demultiplexer (TOAD)." *IEEE Photonics Technology Letters*, vol. 5, no. 7, July. 1993.

[25] R. Runser., D. Zhou., C. Coldwell., B. Wang., P. Toliver., K. Deng., L. Glesk., and P.R.Prucnal., "Interferometric ultrafast SOA based optical switches: From devices to application." *Optical and Quant. Electron.*, vol. 33, no. 7-10, 2001.

[26] K. Kitayama., H. Sotobayashi., and N. Wada., "Optical code division multiplexing (OCDM) and its applications to photonic networks." *IEICE*, vol. 149, no. 1-3, Jan 2003.

[27] J. Lee., P. Teh., P. Petropoulos., M. Ibsen., and D. Richardson., "Reduction of interchannel interference noise in a two-channel grating-based OCDMA system using a nonlinear optical loop mirror." *IEEE Photonics Technology Letters*, vol. 13, no. 5, May. 2001.

[28] H. Sotobayashi, W. Chujo, and K. Kitayama, "1.6-b/s/Hz 6.4 Tb/s QPSK-OCDM/WDM (40CDM x 40WDM x 40Gb/s) transmission experiment using optical hard thresholding." *IEEE Photonics Technology Letters*, vol. 14, no. 4, April. 2002.

[29] Z. Jiang., D. Seo., S. Yang., D. Leaird., A. Weiner., R. Roussev., C. Langrock., and M. Fejer., "Four user, 2.5 Gb/s. spectrally coded O-CDMA system demonstration using low power nonlinear processing." *Lightwave Technology*, vol. 23, no. 1, Jan. 2005.

[30] P. N. Butcher and D. Cotter, *The Elements of Nonlinear Optics.* Cambridge, UK: Cambridge University Press, 1990.

[31] B. Ni, J. S. Lehnert, and A. M. Weiner, "Performance of nonlinear receivers in asynchronous spectral-phase-encoding optical CDMA systems," *J. Lightw. Tech.*, vol. 25, no. 8, pp. 2069–2080, Aug. 2007.

[32] Z. Zheng and A. M. Weiner, "Spectral phase correlation of coded femtosecond pulses by second-harmonic generation in thick nonlinear crystals," *Optics Letters,*, vol. 25, no. 13, pp. 984–986, 2000.

[33] K. Jamshidi and J. A. Salehi, "Statistical characterization and bit-error rate analysis of lightwave systems with optical amplification using two-photon-absorption receiver structures," *J. Lightw. Tech.*, vol. 24, no. 3, pp. 1302–1316, Mar. 2006.

[34] ——, "Performance analysis of spectral-phase-encoded optical cdma system using two-photon-absorption receiver structure for asynchronous and slot-level synchronous transmitters," *Journal of Lightwave Technology*, vol. 25, no. 6, pp. 1638–1645, 2007.

[35] G. P. Agrawal, *Nonlinear Fiber Optics, Fourth edition.* Academic Press, 2007.

[36] M. Cvijetic and I. B. Djordjevic, *Advanced optical communication systems and networks.* Artech House,, 2013.

[37] R. Sabella and P. Lugli, *High speed optical communications.* Springer Science and Business Media, 2012.

[38] N. Bloembergen, *Nonlinear optics.* World Scientific, 1996.

[39] M. Noshad, M. Noshad, S. M. Alavirad, and S. Sallent, "Performance analysis of AND gates based on four-wave-mixing for application in optical-code division multiple access systems," *IET Optoelectronics Journal*, vol. 6, no. 1, pp. 13–25, 2012.

[40] W. J. Rugh, *Nonlinear System Theory: The Volterra/Wiener Approach.* Johns Hopkins University Press,, 1981.

[41] K. V. Peddanarappagari and M. Brandt-Pearce, "Nonlinear system theory: The volterra/wiener approach," *submitted to IEEE Transactions on Communications*, 2012.

[42] W. J. Rugh, *Nonlinear system theory:The Volterra/Weiner Approach.* Baltimore: Johns Hopkins University Press, 1981.

[43] K. V. Peddanarappagari and M. Brandt-Pearce, "Volterra series transfer function of single mode fibers," *J. Lightw. Tech.*, vol. 15, no. 12, pp. 2232–2241, Dec. 1997.

[44] S. A. Hamilton, B. S. Robinson, T. E. Murphy, S. J. Savage, and E. P. Ippen, "100 Gb/s optical time-division multiplexed networks," *J. Lightw. Tech.*, vol. 20, no. 12, pp. 2086–2100, Dec. 2002.

[45] H. Zarkoob and J. Salehi., "Performance limits of optical clock recovery systems based on two-photon absorption detection scheme," *IEEE J. Sel. Top. Quantum Elec.*, vol. 14, no. 3, pp. 963–971, May/Jun. 2008.

[46] V. Roncin, S. Lobo, M. Ngo, L. Bramerie, A. O'Hare, M. Joindot, and J.-C. Simon, "Patterning effects in all-optical clock recovery: Novel analysis using a clock remodulation technique," *IEEE J. Sel. Topics Quantum Elec.*, vol. 16, no. 5, pp. 1495–1502, 2010.

[47] F. G. Agis, C. Ware, D. Erasme, R. Ricken, V. Quiring, and W. Sohler, "10-GHz clock recovery using an optoelectronic phase-locked loop based on three-wave mixing in periodically poled lithium niobate," *IEEE Photon. Techn. Lett.*, vol. 18, no. 13, pp. 1460–1462, 2006.

[48] C. Kouloumentas, A. Tzanakaki, and I. Tomkos, "Clock recovery at 160 Gb/s and beyond, using a fiber-based optical power limiter," *IEEE Photon. Techn. Lett.*, vol. 18, no. 22, pp. 2365–2367, 2006.

[49] R. Salem, A. A. Ahmadi, G. E. Tudury, G. M. Carter, and T. E. Murphy, "Two-photon absorption for optical clock recovery in OTDM networks," *J. Lightw. Tech.*, vol. 24, no. 9, pp. 3353–3362, Sep. 2006.

[50] M. Noshad, M. Noshad, S. M. Alavirad, and S. Sallent, "Performance analysis of AND gates based on four-wave-mixing for application in optical-code division multiple access systems," *IET Optoelectronics Journal*, vol. 6, no. 1, pp. 13–25, 2012.

[51] I. P. Gorwn and H. A. Haus, "Random walk of coherently ampli- fied solitons in optical fiber transmission," *Opt. Lett.*, vol. 11, pp. 665–667, 1986.

[52] R. J. J. S. T. C. J. Y. Darren D. Hudson, Kevin W. Holman and D. J. Jones, "Mode-locked fiber laser frequency-controlled with an intracavity electro-optic modulator," *Optics Letters.*, vol. 20, no. 21, pp. 2948–2950, 2005.

[53] J. Mulet, M. Kroh, and J. Mrk, "Pulse properties of external-cavity mode-locked semiconductor lasers," *Optics express*, vol. 14, no. 3, pp. 1119–1124, 2006.

[54] G. P. Agrawal, *Nonlinear Fiber Optics, Third edition.* Academic Press, 2001.

[55] ——, *Applications of Nonlinear Fiber Optics.* Academic Press, 2010.

[56] A. Vizzino, M. Gioannini, and I. Montrosset, "Dynamic simulation of clock recovery with self-pulsating three-section distributed-feedback lasers," *IEEE J. Quantum Elec.*, vol. 38, no. 12, pp. 1580–1586, Dec. 2002.

[57] J. Proakis and M. Salehi, *Digital Communications, 5th Ed.,.* McGraw-Hill, 2007.

[58] C. C. K. Chan, *Optical Performance Monitoring: Advanced Techniques for Next-Generation Photonic Networks.* Academic Press, 2010.

[59] G. A. Hussein, A. A. Mohamed, O. A. Oraby, E. S. Hassan, I. M. Eldokany, E.-S. M. El-Rabaie, M. I. Dessouky, S. A. Alshebeili, and F. E. A. El-Samie, "Multiple access interference cancelation technique in optical CDMA systems." *Photonic Network Communications*, vol. 26, no. 2-3, pp. 74–83, 2013.

[60] C. M. Negi, A. Pandey, G. G. Soni, S. K. Gupta, and J. Kumar, "Optical CDMA networks using different detection techniques and coding schemes." *Intl Journal of Future Generation Communication and Networking*, vol. 4, no. 3, pp. 25–34, 2011.

[61] I. A. Ashour, S. Shaari, P. Menon, and H. A. Bakarman, "Optical code-division multiple-access and wavelength division multiplexing: Hybrid scheme review." *J. of Comp. Sc.*, vol. 8, no. 10, pp. 1718–1729, 2012.

[62] B.-C. Yeh, C.-H. Lin, and J. Wu., "Noncoherent spectral/spatial OCDMA system using two-dimensional hybrid codes," *Journal of Optical Comm. and Networking.*, vol. 2, no. 9, pp. 653–661, 2010.

[63] H.-H. Chen, *The next generation CDMA technologies.* John Wiley & Sons, 2007.

[64] J. Anaman and S. Prince, "Correlation properties and performance evaluation of 1-dimensional OOC's for OCDMA," *In Devices, Circuits and Systems (ICDCS), 2012 Intl Conf on*, pp. 167–171, 2012.

[65] S. Idris, S. Shaukat, and I. Glesk, "All-optical clock recovery for OCDMA systems with optical time gating," *In Telecommunications Forum (TELFOR)*, no. 20 th, pp. 903–906, 2012.

[66] D. Singh and J. Singh, "Performance evaluation of OCDMA communication system under the effect of jitter," *Intl Journal of Engineering Research and Applications*, vol. 2, no. 5, pp. 204–209, 2012.

[67] S. Sharma and Preeti, "BER analysis of incoherent SAC-OCDMA system using ZVCC in a noisy environment," *Advanced Computing and Communication Technologies (ACCT), 2012 Second International Conference on*, no. 2, pp. 208–210, 2012.

[68] Z. Jiang, D. S. Seo, S. D. Yang, D. E. Leaird, R. V. Roussev, C. Langrock, M. M. Fejer, and A. M. Weiner., "Low-power high-contrast coded waveform discrimination at 10 GHz via nonlinear processing," *IEEE Photonics Technology Letters*, vol. 16, no. 7, pp. 1778–1780, 2004.

[69] A. M. Alhassan, N. Badruddin, N. M. Saad, and S. A. Aljunid, "Beat noise mitigation through spatial multiplexing in spectral amplitude coding OCDMA networks," *In Photonics (ICP), 2013 IEEE 4th International Conference on*, pp. 169–171, 2013.

[70] A. Borude and S. Krishnan., "Simulation of optical CDMA using OOC code," *Intl Journal of Scientific and Research Publications*, vol. 2, pp. 139–143, 2012.

[71] M. Noshad, M. Noshad, S. M. Alavirad, and S. Sallent, "Performance analysis of AND gates based on four-wave-mixing for application in optical-code division multiple access systems," *IET Optoelectronics Journal*, vol. 6, no. 1, pp. 13–25, 2012.

[72] J. Wu, F.-R. Gu, and H.-W. Tsao, "Jitter performance analysis of SOCDMA-based EPON using perfect difference codes," *Journal of Lightwave Technology*, vol. 22, no. 5, pp. 1309–1318, 2004.

[73] K. S. Kim, D. M. Marom, L. B. Milstein, and Y. Fainman, "Hybrid pulse position modulation/ultrashort light pulse code-division multiple-access systems-part i: Fundamental analysis." *Communications, IEEE Transactions*, vol. 50, no. 12, pp. 2018–2031, 2002.

[74] ——, "Hybrid pulse position modulation/ultrashort light pulse code-division multiple-access systems-part ii: Time-space processor and modified schemes." *Communications, IEEE Transactions*, vol. 51, no. 7, pp. 1135–1148, 2003.

[75] R. Salem and T. Murphy, "Broad-band optical clock recovery system using two-photon absorption," *IEEE Photonic Technology Letters*, vol. 16, no. 9, pp. 2141–2143, 2004.

[76] A. Yazdani, D. Rincón, and S. Sallent., "Efficient time gating in ultrafast optical TDM networks," *Photonic Network Communications*, vol. 28, no. 3, pp. 218–224, 2014.

[77] B. Moslehi, "Analysis of optical phase noise in fiber-optic systems employing a laser source with arbitrary coherence time," *Lightwave Technology*, vol. 4, no. 9, pp. 1334–1351, 1986.

[78] D. Middleton, *An Introduction to Statistical Communication Theory.* IEEE Press,, 2009.

[79] X. Liu, "Analytical and numerical results for some classes of nonlinear schrdinger equations." *Doctoral dissertation, University of Toronto*, 2013.

[80] J. Weideman and B. M. Herbst., "Split-step methods for the solution of the nonlinear schrodinger equation." *SIAM Journal on Numerical Analysis*, vol. 23, no. 3, pp. 485–507, 1986.

[81] W. Bao, "Numerical methods for the nonlinear schrodinger equation with nonzero far-field conditions." *Methods and Applications of Analysis*, vol. 1, no. 3, pp. 367–388, 2004.

[82] M. M. Alem-Karladani, "A survey on optical orthogonal codes," *http://alum.sharif.edu/ malem/Optical-Orthogonal-Codes.pdf*, 2010.

[83] S. Bottacchi, *Theory and Design of Terabit Optical Fiber Transmission Systems.* Cambridge University Press, 2014.

[84] F. Boccardi and H. Howard, "Zero-forcing precoding for the MIMO broadcast channel under per-antenna power constraints," *In Signal Processing Advances in Wireless Communications*, vol. IEEE 7th Workshop, no. 06, pp. 1–5, 2006.

[85] P. Sadeghi, A. K. Rodney, and K. Zubair, "Minimum mean square error equalization on the 2-sphere." *InStatistical Signal Processing (SSP)*, vol. IEEE Workshop on 2014 Jun 29, pp. 101–104, 2014.

[86] A. E. Loulou, S. A. Gorgani, and M. Renfors, "Enhanced ofdm techniques for fragmented spectrum use." *In Future Network and Mobile Summit (Future Network Summit)*, vol. IEEE, pp. 1–10, 2013.

[87] R. Davey and J. Kani, "Options for future optical access networks." *IEEE Communications Magazine*, vol. 51, 2006.

[88] J. Salehi, A. Weiner, and J. Heritage., "Coherent ultrashort light pulse code division multiple access communication systems," *J. Lightwave Technol*, vol. 8, no. 3, pp. 478–491, Mar. 1990.

[89] B. Ni, J. S. Lehnert, and A. M. Weiner, "Performance of nonlinear receivers in asynchronous spectral-phase-encoding optical cdma systems," *Journal of lightwave technology*, vol. 25, no. 8, pp. 2069–2080, 2007.

[90] J. W. Goodman, *Statistical Optics.* New York: Wiley, 2000.

[91] K. Obermann, I. Koltchanov, K. Petermann, S. Diez, R. Ludwig, and H. G. Weber, "Noise analysis of frequency converters utilizing semiconductor-laser amplifiers," *IEEE Journal of Quantum Electronics*, vol. 33, no. 1, pp. 81–88, 1997.

[92] I. Koltchanov, S. Kindt, K. Petermann, S. Diez, R. Ludwig, R. Schnabel, and H. G. Weber, "Gain dispersion and saturation effects in four-wave mixing in semiconductor laser amplifiers," *IEEE Journal of Quantum Electronics*, vol. 32, no. 4, pp. 712–720, 1996.